BIOOXIDATION OF REFRACTORY ARSENIC-BEARING GOLD ORES

by

Ridge Mukorera Nyashanu

A thesis submitted for the degree of ***Doctor of Philosophy*** of the University of London and for the ***Diploma*** of Imperial College of Science, Technology and Medicine.

T.H. Huxley School of Environment, Earth Science & Engineering
Royal School of Mines
Imperial College of Science, Technology and Medicine
University of London

August 1998

To the memory of my late mother -Tadzei Zorodzai Mudita

To my family

ABSTRACT

During recent years bacterial oxidation has gained popularity as a pre-treatment process for refractory gold-bearing arsenical ores. Research and development has been focused on various aspects of bacterial oxidation of refractory arsenical gold ores because the majority of these ores are ones in which gold is locked in mineral sulphides pyrite and arsenopyrite. However bioleaching of these ores produce a mixture of arsenic(III) and arsenic(V). Salts of the latter are much more stable for subsequent disposal of the waste residues and therefore it is important that all the arsenic reports as arsenic(V) at the end of the oxidation stage.

The bacterial leaching and mineralogy of refractory arsenic-bearing gold ores from different deposits were investigated to determine the fate of arsenic during processing and to assess the effect of biological pre-treatment on gold extraction. Experiments were conducted using a mixed culture of iron and sulphur oxidising bacteria dominated by *Thiobacillus ferrooxidans*. The speciation of arsenic during bioleaching of arsenopyrite-rich concentrates was studied using polarography. Leaching of a concentrate which was predominantly arsenopyrite resulted in 78% of the leached arsenic reporting in solution as arsenic(III) at the end of the bacterial oxidation stage. It has been found that adding pyrite and iron(III) to arsenopyrite concentrates promotes the formation of arsenic(V) leaving less than 1% of the extracted arsenic as arsenic(III). Study of the oxidation of concentrates from different ore deposits with various ratios of pyrite to arsenopyrite showed that the amount of pyrite was an important factor in determining the dominating arsenic oxidation state in the leach solutions at the end of the oxidation stage. These results demonstrate the importance of ore composition in terms of pyrite to arsenopyrite ratio in the production of environmentally acceptable biooxidation residues containing arsenic(V). Iron(III) alone was found not to be able to oxidise arsenic(III), instead pyrite was needed as a catalyst. Furthermore a strong dependence of pyrite leaching and arsenic(III) oxidation was demonstrated.

Actual mineral degradation during the oxidation process has been studied using optical microscopy and a scanning electron microscope (SEM). SEM and optical microscopy

examination of the biooxidation residues revealed the development of corrosion patterns and pores oriented along the crystallographic planes in some of the pyrite grain. A study of the stability of the arsenical solid residues emanating from the bacterial oxidation of these arsenical concentrates has also been incorporated. The composition of the residues was examined with acid treatment of the bioresidues, chemical, and x-ray diffraction (XRD) analysis. Arsenic solubility of the solid under study were evaluated using the standard United States Environmental Protection Agency (U.S. EPA) Toxicity Characteristic Leaching Procedure (TCLP) test. The stability of the solid bacterial oxidation residues was found to be directly related to the mineralogical composition of the feed concentrate, in particular the ratio of pyrite to arsenopyrite and also the extent of arsenic extraction and oxidation during the bacterial oxidation stage. The potential of biooxidation for the production of environmental acceptable residues from arsenical gold ores has been shown.

CONTENTS

TITLE 1

DEDICATION 2

ABSTRACT 3

LIST OF FIGURES 9

LIST OF TABLES 15

ACKNOWLEDGEMENTS 17

PROLOGUE 18

CHAPTER ONE: GENERAL INTRODUCTION 19

1.1 General overview 19

1.2 Environmental aspects of biooxidation treatment of refractory gold ores 22

1.3 Objectives of the research 27

1.4 Structure of thesis 28

CHAPTER TWO: LITERATURE REVIEW 29

2.1 Mineralogy of refractory gold ores 29

2.1.1 Introduction 29

2.1.2 Refractoriness of certain gold ores to cyanidation 30

2.1.3 Characterisation of visible gold 34

2.1.4 Characterisation of 'invisible gold' 35

2.1.5 Structure and composition of pyrite and arsenopyrite 37

2.2 Processing of refractory gold ores 40

2.3 Biooxidation 43

2.3.1 Introduction 43

2.3.2 Bacterial cultures involved in oxidation of minerals 44

2.3.3 The chemistry of bacterial oxidation of minerals 46

2.3.4 Mechanisms of bacterial oxidation 53

2.3.5 Kinetic factors important for elucidation of bacterial oxidation mechanisms 55

2.3.6 Toxicity effects of metals and resistance mechanism..... 66
2.4 Conclusion..... 70

CHAPTER THREE: MATERIALS AND EXPERIMENTAL METHODS.... 71
3.1 Introduction..... 71
3.2 Mineralogical study..... 72
3.2.1 Optical microscopy..... 72
3.2.2 Scanning electron microscopy (SEM)-microprobe analyses..... 73
3.2.3 Laser ablation-ICP-AES..... 73
3.2.4 X-ray diffraction analyses..... 74
3.3 Bacterial oxidation studies..... 75
3.3.1 Maintenance of bacterial culture and production of cell suspensions..... 75
3.3.2 Shake flask experiments..... 78
3.3.3 Batch stirred flasks reactors..... 79
3.3.4 Metal/metalloid analyses..... 80
3.4 Cyanidation tests..... 86
3.5 Solubility testing..... 87
3.6 Oxidised precipitates..... 87
3.7 pH, redox potential, dissolved oxygen measurements..... 87
3.8 Decomposition of solids for chemical analysis..... 88

CHAPTER FOUR: MINERALOGY OF THE ORES..... 89
4.1 Introduction..... 89
4.2 Indarama deposit..... 92
4.2.1 Indarama 1..... 92
4.2.2 Indarama 2 to Indarama 5..... 96
4.2.3 Arsenopyrite crystals..... 96
4.2.4 Pyrite crystals..... 100
4.2.5 Refractory gold..... 100
4.3 Akbakai deposit..... 100
4.3.1 Arsenopyrite crystals..... 101

4.3.2 Pyrite crystals..... 102
4.3.3 Refractory gold..... 103
4.4 Riverlea deposit..... 103
4.4.1 Arsenopyrite crystals..... 103
4.4.2 Pyrite crystals..... 104
4.4.3 Refractory gold..... 105
4.5 Olympias and Fairview deposits..... 105
4.6 Pyrite and arsenopyrite ratios in the concentrates..... 105
4.7 Cyanidation tests..... 107

CHAPTER FIVE: SPECIATION OF ARSENIC IN BACTERIAL OXIDATION OF ARSENICAL ORES..... 109
5.1 Introduction..... 109
5.2 Results..... 110
5.2.1 Release of arsenic into solution..... 110
5.2.2 Release of iron into solution during bacterial oxidation..... 117
5.2.3 Effect of adding pyrite on the speciation of arsenic..... 120
5.2.4 Effect of ferric iron on the speciation of arsenic..... 125
5.2.5 Effect of controlling pH on the speciation of arsenic..... 133
5.2.6 Effect of pulp density on the speciation of arsenic..... 138
5.2.7 Effect of stibnite on the speciation of arsenic..... 141
5.2.8 Oxidation of arsenic(III) synthetic solutions by iron(III), pyrite and bacteria..... 145
5.3 Discussion..... 147
5.3.1 Introduction..... 147
5.3.2 Bacterial oxidation of different concentrates..... 148
5.3.3 Effect of concentrate grade..... 150
5.3.4 Oxidation of iron(II) in the presence of arsenic(III)..... 150
5.3.5 Effect of pyrite leaching on the oxidation of arsenic(III)..... 152
5.3.6 The effect of iron(III) additions..... 153
5.3.7 Effect of controlling pH..... 155

5.3.8 Effect of pulp density and stibnite..... 156
5.3.9 Oxidation of arsenic(III) during bacterial oxidation..... 157
5.3.10 Mechanisms of bacterial leaching of pyrite and arsenopyrite..... 161

CHAPTER SIX: MINERALOGICAL CHANGES AND STABILITY OF BACTERIAL OXIDATION RESIDUES..... 163
6.1 Introduction..... 163
6.2 Gold liberation..... 164
6.3 Microscopic examination of the biooxidation residues..... 166
6.4 Environmental stability of the biooxidation residues..... 173
6.5 Discussion..... 178
CHAPTER SEVEN: GENERAL DISCUSSION AND CONCLUSIONS..... 182
7.1 General discussion..... 182
7.2 Conclusions..... 185
7.3 Further work..... 188

CHAPTER EIGHT: REFERENCES..... 189

APPENDICES..... 209

LIST OF FIGURES

Figure		Page
Figure 2.1:	Mössbauer spectrum of Au-bearing arsenopyrite. The vertical lines indicates the position of pure metallic gold absorption peak	37
Figure 2.2:	The structure of (a)pyrite and (b) arsenopyrite	39
Figure 2.3:	Block diagram of the two-stage roasting process	41
Figure 2.4:	Block diagram of acid pressure leach process	42
Figure 2.5:	Speciation of major iron(III) components in a solution containing 0.3 M Fe(III), 0.45 M S(VI) and 0.2 M As(V)	48
Figure 2.6:	E_h-pH diagram for pyrite for the stable Fe-S-H_2O system at 298 K, activity of iron = 10^{-3} and of sulphur = 10^{-1}	51
Figure 2.7:	Eh-pH diagram for the system As-Fe-O-H-S, if $\Delta G°_{298}$ ($FeAsO_4$) is taken to be -199.1 kcal/gfw	52
Figure 2.8:	Typical growth curve for batch cultivation of bacterial population showing the various phases	57
Figure 2.9:	A diagrammatic representation of Thiobacillus ferrooxidans in the native environment (leaching pyritic ore)	61
Figure 2.10:	A diagrammatic representation of the secondary oxidation of arsenic(III) during bacterial leaching	62
Figure 2.11:	Cyclic degradation of pyrite showing different pathways of sulphur oxidation	65
Figure 3.1:	Schematic representation of laser-ICP system showing the ablation chamber and pathway of Argon gas into the ICP	74
Figure 3.2:	Diagrammatic representation of the air-stirred Pachuca reactor and the ancillary equipment	77
Figure 3.3:	Schematic diagram of the mechanically stirred flask reactor vessel used for the biooxidation experiments	79
Figure 3.4:	Calibration line used for iron(II) determinations	81
Figure 3.5:	Schematic diagram of electrode assembly and cell for modern polarographic technique	84

Figure 3.6: Typical polarograms obtained during the determination of As(III) concentrations by differential pulse polarography..... 85

Figure 3.7: A plot of the peak current versus As(III) concentration obtained for different concentrations using the standard addition method during a run..... 86

Figure 4.1: The geology and location of the Indarama and the Riverlea mines and the area around Kwekwe..... 90

Figure 4.2: The geometry of the vein system of the Akbakai deposit..... 91

Figure 4.3: Optical microscopy photomicrograph showing small gold particle as an inclusion in gudmundite. Stibnite also present (Indarama 1)..... 94

Figure 4.4: Optical microscopy photomicrograph showing small gold inclusions in gudmundite particles (Indarama 1)..... 94

Figure 4.5: Optical microscopy photomicrograph showing free gold and aurostibite associated with gudmundite and gangue matrix (Indarama 1)..... 95

Figure 4.6: Optical microscopy photomicrograph showing free gold and aurostibite associated with gudmundite..... 95

Figure 4.7: Optical microscopy photomicrograph showing euhedral to anhedral arsenopyrite particles with some zoned crystals..... 97

Figure 4.8: Gold concentration against atomic arsenic content within the arsenopyrite crystals from the Indarama deposit..... 97

Figure 4.9: Gold concentration against sulphur content within the arsenopyrite crystals from the Indarama deposit..... 98

Figure 4.10: Gold concentration against arsenic content within the arsenopyrite crystals from the Indarama deposit using laser ablation..... 99

Figure 4.11: Sulphur content of the pyrite against arsenic content of the Indarama deposit..... 101

Figure 4.12: Optical microscopy photomicrograph showing native gold and overgrowth on arsenopyrite..... 102

Figure 4.13: Arsenic concentration of the pyrite crystals from the Akbakai deposit..... 104

Figure 4.14: Sulphur against the arsenic content within the pyrite crystals from the Riverlea deposit..... 106

Figure 5.1: Percentage total arsenic extraction and percentage of arsenic(III) formed during bioleaching for Runs 1-3 (see Table 5.1 for composition of solids)..... 113

Figure 5.2: Variation in arsenic(III) and arsenic(V) concentrations of the bioleaching slurry for Runs 1-3 (see Table 5.1 for composition of solids)..... 113

Figure 5.3: Percentage total arsenic extraction and percentage of arsenic(III) formed during bioleaching for Runs 4-6 (see Table 5.1 for composition of solids)..... 114

Figure 5.4: Variation in arsenic(III) and arsenic(V) concentrations of the bioleaching slurry for Runs 4-6 (see Table 5.1 for composition of solids)..... 114

Figure 5.5: Plot of arsenopyrite and pyrite oxidation against time for Runs 1-3 (see Table 5.1 for composition of solids)..... 116

Figure 5.6: Plot of arsenopyrite and pyrite oxidation against time for Runs 4-6 (see Table 5.1 for composition of solids)..... 116

Figure 5.7: Concentrations of iron(II) and iron(III) in the bioleaching slurry for Runs 1-3 (see Table 5.1 for composition of solids).... 118

Figure 5.8: Concentrations of iron(II) and iron(III) in the bioleaching slurry for Runs 4-6 (see Table 5.1 for composition of solids).... 118

Figure 5.9 Percentage total arsenic extraction and percentage of arsenic(III) during bioleaching for Runs 1 and 7-9 (see Table 5.2 for composition of solids)..... 122

Figure 5.10: Variation in arsenic(III) and arsenic(V) concentrations of the bioleaching slurry for Runs 1 and 7-9 (see Table 5.2 for composition of solids)..... 122

Figure 5.11: Plot of arsenopyrite and pyrite oxidation against time for Runs

1 and 7-9 (see Table 5.2 for composition of solids)..... 124

Figure 5.12: Concentrations of iron(II) and iron(III) in the bioleaching slurry for Runs 1 and 7-9 (see Table 5.2 for composition of solids)..... 124

Figure 5.13: Percentage total arsenic extraction and percentage arsenic(III) during bioleaching for Runs 10-13 (see Table 5.3 for composition of solids) 127

Figure 5.14 Variation in arsenic(III) and arsenic(V) concentrations of the bioleaching slurry for Runs 10-13 (see Table 5.3 for composition of solids)..... 127

Figure 5.15 Plot of arsenopyrite and pyrite oxidation against time for Runs 10-13 (see Table 5.3 for composition of solids)..... 129

Figure 5.16: Concentrations of iron(II) and iron(III) in the bioleaching slurry for Runs 10-13 (see Table 5.3 for composition of solids) 129

Figure 5.17 Variation in the percentage of arsenic(III) formed during bioleaching for Runs 2 and 14-18 (see Table 5.4 for composition of solids) 131

Figure 5.18: Variation in arsenic(III) concentrations of the bioleaching slurry for Runs 2 and 14-18 (see Table 5.4 for composition of solids)..... 131

Figure 5.19: Speciation of arsenic in the bioleaching slurry for the Indarama C concentrate (see Table 5.5 for leaching conditions) 132

Figure 5.20: Speciation of arsenic in the bioleaching slurry for the Akbakai D concentrate (see Table 5.5 for leaching conditions)..... 133

Figure 5.21: Speciation of arsenic in the bioleaching slurry of the Indarama C concentrate with pH being controlled around 1.5..... 135

Figure 5.22: Speciation of arsenic in the bioleaching slurry of the Indarama C concentrate with pH being controlled around 1.8..... 135

Figure 5.23: Speciation of arsenic in the bioleaching slurry of the Indarama C concentrate with pH being controlled around 2.5..... 136

Figure 5.24: Speciation of iron in the bioleaching slurry of the Indarama C

with pH being controlled around 1.5 136

Figure 5.25: Speciation of iron in the bioleaching slurry of the Indarama C with pH being controlled around 1.8 137

Figure 5.26: Speciation of iron in the bioleaching slurry of the Indarama C with pH being controlled around 2.5 137

Figure 5.27: Percentage total arsenic extraction and percentage of arsenic(III) during bioleaching for Runs 9 and 23-25 (see Table 5.6 for pulp densities) 139

Figure 5.28: Variation in arsenic(III) and arsenic(V) concentrations of the bioleaching slurry for Runs 9 and 23-25 (see Table 5.6 for pulp densities) 139

Figure 5.29: Plot of arsenopyrite and pyrite oxidation for Runs 9 and 23-25 (see Table 5.6 for pulp densities). 140

Figure 5.30: Concentrations of iron(III) in the bioleaching slurry for Runs 9 and 23-25 (see Table 5.6 for pulp densities) 140

Figure 5.31: Percentage total arsenic extraction and percentage of arsenic(III) for Runs 14 and 26-27 (see Table 5.7 for composition of solids) 143

Figure 5.32: Variation in arsenic(III) and arsenic(V) concentrations of the bioleaching slurry for Runs 14 and 26-28 (see Table 5.7 for composition of solids) 143

Figure 5.33: Concentrations of iron(III) in the bioleaching slurry for Runs 14 and 26-28 (see Table 5.7 for composition of solids) 144

Figure 5.34: Concentration of antimony in the bioleaching slurry for Runs 14 and 26-28 (see Table 5.7 for composition of solids) 144

Figure 5.35: Oxidation of arsenic(III) under different leaching conditions as described in Table 5.7 146

Figure 5.36: Oxidation of arsenic(III) under different leaching conditions as described in Table 5.7 147

Figure 6.1: Gold release versus arsenic extraction during bacterial of the Indarama C concentrate 164

Figure 6.2: Gold release versus arsenic extraction during bacterial of the Riverlea concentrate..... 165

Figure 6.3: Gold release versus arsenic extraction during bacterial of the Akbakai D concentrate..... 165

Figure 6.4: Optical microscopy photomicrograph showing a gold grain which has been liberated from an antimony sulphide..... 166

Figure 6.5: Optical microscopy photomicrograph showing preferential attack of the arsenopyrite crystal in relation to pyrite..... 167

Figure 6.6: Optical microscopy photomicrograph showing penetrating pores in the pyrite crystals during bacterial leaching..... 167

Figure 6.7: Secondary electron image showing the crystals in the concentrate before bacterial attack..... 168

Figure 6.8: Secondary electron image of an arsenopyrite grain after 6 days of bacterial leaching (the Indarama C concentrate)..... 169

Figure 6.9 Secondary electron image of arsenopyrite grain after 8 days of bacterial leaching..... 169

Figure 6.10: Secondary electron image of a pyrite crystal after 5 days of bacterial leaching (the Akbakai concentrate)..... 170

Figure 6.11: Secondary electron image of pyrite grains after 8 days of bacterial leaching (the Indarama C concentrate)..... 170

Figure 6.12: Secondary electron image of a pyrite crystal after 8 days of bacterial leaching (the Indarama concentrate)..... 171

Figure 6.13: Secondary electron image of a pyrite grain after 10 days of bacterial leaching (the Indarama c concentrate)..... 171

Figure 6.14: Secondary electron image of a pyrite crystal after 10 days of bacterial leaching (the Olympias concentrate)..... 172

Figure 6.15: Secondary electron image of a pyrite grain after 10 days of bacterial leaching..... 172

Figure 6.16: Secondary electron image of the residues after 14 days of bacterial leaching..... 173

LIST OF TABLES

Table		Page
Table 1.1:	Common arsenic minerals and compounds.....	23
Table 2.1:	Extraction of arsenic and antimony minerals in cyanide solutions.	31
Table 2.2:	The standard reduction potential with respect to iron(II), of some iron(III) complexes.....	49
Table 2.3:	Summary of the evolution of bacterial populations, superficial and precipitated species, chemical reactions and corrosion patterns during oxidation of arsenopyrite by *Thiobacillus ferrooxidans*.....	59
Table 3.1:	Chemical analyses of the flotation concentrates used in the study.	72
Table 3.2:	Composition of the Silverman and Lundgren nutrient medium.....	76
Table 4.1:	Microprobe analyses results of some arsenopyrite crystals from the Akbakai concentrate.....	103
Table 4.2:	Mineralogical composition of the concentrates in terms of pyrite to arsenopyrite ratios.....	107
Table 4.3:	Summary of cyanidation results before bacterial oxidation of the different concentrates.....	108
Table 5.1:	The origins and compositions of the concentrates used in Runs 1-6.....	111
Table 5.2:	The origins and compositions of concentrates used in Runs 7-9....	121
Table 5.3:	Compositions and origins of the concentrates used in Runs 10-13 to investigate the effect of iron(III) additions.....	126
Table 5.4:	Leaching conditions used to further investigate the effect of initial iron(III) concentrations on the speciation of arsenic.....	130
Table 5.5:	Leaching conditions used in experiments to investigate the effect of recycling the bioliquor.....	132
Table 5.6:	Descriptions of the experimental Runs at different pulp densities.	138
Table 5.7:	Compositions of the arsenopyrite/pyrite/stibnite concentrates used in Runs 14, 26-28.....	142
Table 5.8:	Leaching conditions for the oxidation of arsenic(III) synthetic	

solutions..... 146

Table 6.1: EPA test results for the feed concentrates before bacterial leaching..... 174

Table 6.2: EPA test results of the biooxidation concentrates..... 175

Table 6.3: EPA test results of partially oxidised arsenopyrite..... 176

Table 6.4: EPA results of cyanidation tailings..... 177

ACKNOWLEDGEMENTS

I wish to thank my supervisors, Prof. A.J. Monhemius and Prof. D.L. Buchanan, for their advice, assistance, encouragement and constructive criticism throughout the course of my work on this research. Most of all I appreciate the amount of dialogue that they allowed among us during which I was able to profit from their experience and knowledge.

I also wish to extent my sincere gratitude to Prof. J. Lester (T.H. Huxley School for Environment, Earth Science and Engineering) for lending me his polarographic apparatus and Prof. F.D. Pooley (University College Cardiff, Wales) for donating the bacterial culture used in the work. Thanks are also due to Dr. C. Halls (T.H. Huxley School), Dr. C.J. Stanley (Department of Mineralogy at the Natural History Museum) Dr. J. Barrett (Department of Chemistry, Imperial College), for useful discussions about the work.

I am indebted to all those who helped me in my efforts to get valuable reference material and also in discussion of my work during the course of the experiments. In particular I would like to account the assistance of the following people: Drs. R. Foster, O. Chinyamakobvu, F. Gudyanga, R. Perry, A. Narayanan, I. Tarasova, J. Mangwiro, T. Williams, M. Diaz, J. Teer, P. Swash. The technical support of J. Burgess, R. Walker, G. Nash, B. Coles, R. Giddens, J. Spratt, C. Jones is greatly appreciated.

Special thanks also go to the Institution of Mining and Metallurgy for awarding me the Stanley Elmore Fellowship, the ORS award committee for their financial support and the Authur Bensusan Memorial Trust.

I would like to say thank you to my fellow countrymen for their moral support and continual communication in particular F. Mupavaenda and O. Munodawafa.

Last but not least my gratitude go to my family for their encouragement throughout my studies.

"Certainly, if mining is a shameful and discreditable employment for a gentleman because slaves once worked mines, then agriculture also will not be a creditable employment, because slaves once cultivated the field, and even to-day do so among the Turks, nor architecture be considered honest, because some slaves have been found skilful in that profession; nor medicine, because not a few doctors have been slaves; nor any other worthy craft because men captured by force of arms have practised it. Yet agriculture, architecture and medicine are none the less counted amongst the number of honourable professions; therefore mining ought not for this reason to be excluded from them."

[Agricola, 1555, Book I, p. 23]

CHAPTER ONE

GENERAL INTRODUCTION

1.1 General overview

Due to the depletion of free-milling gold ores, mining companies are increasingly looking at various methods for processing sulphidic gold ores. The principal process route for gold extraction is alkaline cyanidation in which dissolved oxygen and cyanide ions participate according to the following equation:

$$4Au(s) + 8CN^-(aq) + O_2 + 2H_2O = 4Au(CN)_2^-(aq) + 4OH^-(aq) \qquad \text{(Eq.1.1)}$$

For effective gold dissolution to take place, the gold particles in the ore must be accessible to both cyanide ions and oxygen. However certain gold ores do not respond well to this process because the gold is encapsulated by sulphide minerals as submicroscopic inclusions or in solid solution. These ores are called refractory gold ores. A gold ore is termed refractory when poor gold recovery (<80%) is obtained by the standard cyanidation process **[1, 2]**. The definition is, however, arbitrary since the scale of an operation and the profits are normally the most important factors considered by most operating companies for the exploitation of any given gold ore deposit.

To improve the gold recovery from refractory ores, a pre-treatment process is necessary to liberate the gold from the sulphides for the subsequent cyanide dissolution of gold. The most widely used and known pre-treatment process is roasting. This process is carried out at temperatures between 600-800°C and can be represented by the equations below for the roasting of pyrite and arsenopyrite:

$$3FeS_2(s) + 8O_2(g) = Fe_3O_4(s) + 6SO_2\,(g) \qquad \text{(Eq. 1.2)}$$

$$12FeAsS(s) + 29O_2(g) = 4Fe_3O_4(s) + 6As_2O_3(g) + 12SO_2(g) \qquad \text{(Eq. 1.3)}$$

$$4Fe_3O_4(s) + O_2(g) = 6Fe_2O_3(s) \qquad \text{(Eq. 1.4)}$$

The emissions from this process require the building of gas and dust cleaning equipment and also subsequent treatment of the arsenic trioxide to stabilise it before disposal. In light of the current tightening up of environmental legislation, mining companies are increasingly looking to environmentally friendly processes for the extraction of gold from refractory ores. This has led to the development of the pressure oxidation and bio-oxidation pre-treatment processes. These processes convert the sulphur to soluble sulphate and the arsenic is oxidised to arsenate which can be precipitated as stable ferric arsenate. The overall reactions taking place during these processes can be summarised by the following equations:

$$4\,FeS_2 + 15\,O_2 + 10\,H_2O = 4\,FeOOH + 8\,SO_4^{2-} + 16\,H^+ \qquad \text{(Eq. 1.5)}$$

$$2\,FeAsS + 7\,O_2 + 2\,H_2O = 2\,FeAsO_4 + 2\,SO_4^{2-} + 4\,H^+ \qquad \text{(Eq. 1.6)}$$

Pressure oxidation is carried out in autoclaves at high temperatures (180-210°C) and pressures (1800-2200 kPa). These conditions allow complete oxidation of the sulphides within 1-3 hours. Bio-oxidation has been considered to be the process with the most potential from an economic and environmental point of view. In this process bacteria, mainly *Thiobacillus ferrooxidans,* are used to oxidise the sulphide matrix at temperatures of 35-45°C in 3-6 days at atmospheric pressure, subsequently exposing the gold to cyanide and oxygen in the subsequent cyanidation step. The reactions are carried out in mechanically agitated tanks which are supplied with nutrients and air to provide

the oxygen needed for the oxidation reactions and the carbon dioxide for growth of the bacteria. The bacteria derive their energy for growth from the oxidation of ferrous iron and reduced sulphur compounds from the mineral sulphides. The main advantages of bacterial oxidation compared with pressure oxidation have been found to be: low temperature and low pressure process, low degree of process control is required and the process is simple and requires relatively unskilled manpower.

Processing of any gold ore requires mineralogical data, but when it comes to refractory gold ores a detailed mineralogical investigation has to be carried out. Although the mineralogy of gold looks simple due to the fact that there are few gold-bearing minerals, the mineralogical investigations are normally made difficult by low grade ores, uneven distribution of gold in the sample and the nature of the mineralisation. As a result of the above factors, the examination typically requires special techniques. Recent years have seen a number of significant developments in gold process mineralogy. The trend has been to move from purely mineralogical approaches towards combining metallurgical and mineralogical techniques to give more meaningful results in terms of gold extraction metallurgy.

There is an increasing realisation of the tremendous variability of refractory gold ores in their mineralogical association and metallurgical behaviour rendering selection of any one "universally best" process impossible. Generic studies which have been done by several authors only produce valid conclusions to suit a specific type of ore. A comparative study which would attempt to cover all possible situations would be very useful.

At the present time there is little agreement on which of the three methods of oxidation of refractory sulphidic ores is the best. In a recent survey it has been shown that pressure oxidation is the leading technology. An analysis based on the financial rates of return for the three processes applied to the same hypothetical situation showed that plant capacity was the key factor, with bacterial oxidation showing the best returns for smaller

capacity plants (less than 1000 tonnes per day), while pressure oxidation was optimal for larger plants **[3]**.

Despite the general agreement that bacterial oxidation is a promising method from an economic and environmental point of view, however there is evidence that bioleaching of pyrite/arsenopyrite refractory gold concentrates produce a mixture of arsenic(III) and arsenic(V). Salts of the later are much more stable for subsequent environmental disposal of the waste residues, therefore it is important that all the solubilised arsenic reports as arsenic(V) at the end of the bacterial oxidation stage.

1.2 Environmental aspects of biooxidation treatment of refractory gold ores

Arsenic is found in minerals either as a primary constituent of the crystal structure or in small amounts in arsenic carrier minerals. A list of the most common primary arsenic minerals and some arsenic compounds is given in Table 1.1. The primary minerals are found in four oxidation states, (-III), (0), (III) and (V). Arsenic also occurs in both inorganic and organic compounds with major differences in metabolism and toxicity. Exposure to arsenic compounds takes place in certain occupations, e.g. among smelter workers, workers engaged in manufacture and use of arsenic containing pesticides. High levels of arsenic may also be found in drinking water in some areas, often of natural origin but in some cases as a result of unstable mining wastes. Arsenic is absorbed through the respiratory and gastrointestinal tract and an oral consumption of 70-180 mg/L is sufficient to cause fatal poisoning to human life **[4]**. Chronic effects may also result from exposure to inorganic arsenic compounds. Among the noncarcinogenic effects may be mentioned hyperkeratosis, portal hypertension and disturbances of the peripheral vascular and nervous system. These effects have been encountered following exposure to inorganic arsenic, either in drinking water or in drugs. Arsenic is in trivalent form in drugs, however, the valency in drinking water is not known in the areas where effects have been reported **[4]**.

The health and environmental concerns over the use of arsenic has lead to restrictions and reduction in consumption of arsenic as used in: wood preservatives, fungicides,

Table 1.1: Common arsenic minerals and compounds **[5]**.

Mineral or Compound		**Formula**
Arsenides:	Allemontite	$AsSb$
	Safflorite	$(Co,FeNi)As_2$
	Skutterudite	$(Co,Ni)As_3$
	Domeykite	Cu_3As
	Loellingite	$FeAs_2$
	Niccolite	$NiAs$
	Rammelsbergite	$NiAs_2$
	Para-rammelsbergite	$NiAs_2$
	Maucherite	$Ni_{11}As_8$
	Arsenopalladinite	Pd_3As
	Sperrylite	$PtAs_2$
Sulphides and Sulphosalts:		
	Orpiment	As_2S_3
	Realgar	AsS
	Proustite	Ag_3AsS_3
	Cobaltite	$CoAsS$
	Glaucodot	$(Co,Fe)AsS$
	Tennantite	$(Cu,Fe)_{12}As_4S_{13}$
	Enargite	Cu_3AsS_4
	Arsenopyrite	$FeAsS$
	Gersdorffite	$NiAsS$
	Sartorite	$PbAs_2S_4$
	Rathite	$Pb_7As_9S_{20}$
Oxides:	Arsenic trioxide	As_2O_3
	Arsenic pentoxide	As_2O_5
Arsenites:	Armangite	$Mn(AsO_3)_2$
	Ekdemite	$Pb_3(AsO_3)C_{12}$
	Finnemanite	$Pb_5[Cl(AsO_3)_3]$
	Reinerite	$Zn_3(AsO_3)_2$

Arsenates:	Olivenite	$Cu_2(AsO_4)OH$
	Erythrite	$Co_3(AsO_4)_2.8H_2O$
	Scorodite	$FeAsO_4.2H_2O$
	Pharmacosiderite	$(K,H_3O)Fe_4(AsO_4)_3(OH).6H_2O$
	Annabergite	$Ni_3(AsO_4)_2.8H_2O$
	Beudantite	$PbFe_3(AsO_4)(SO_4)(OH)_6$
Acids:	Arseneuos acid	$HAsO_2$
	Arsenic acid	H_3AsO_4

glass, ceramics, non-ferrous alloys and electronics. This will further exacerbate the oversupply of arsenic on the market which is already overloaded. Environmental constraints may prove costly to mining operations and influence the choice of metallurgical process routes. It is important that the arsenic from metallurgical processing of arsenical ores remains stable in the tailings dam to avoid environmental contamination.

Biooxidation of refractory gold ores does not only aim at recovering the precious metals but is also believed to take care of the by-products, to make them suitable for disposal. Biooxidation is followed by neutralisation and it is important to consider the stability of the precipitates before disposal to the tailings dam. Bacterial oxidation of some refractory arsenical ores has been shown to produce the pentavalent state of arsenic, whereas unstable trivalent arsenic is produced during roasting (arsenic trioxide). Although arsenates are known to be the most stable form of arsenic compounds and provide a viable route for the removal of arsenic from process solutions, there is still a lot of controversy with regards to optimum precipitating conditions, the structures of the solids and their long term stability **[6-8]**.

The biooxidation liquors are usually neutralised in a two-stage process whereby arsenic precipitates as ferric arsenate, the sulphates as calcium sulphate and the metals as hydroxides **[9]**. Limestone ($CaCO_3$) is used in the first stage to raise the pH to 5.0 and then lime (CaO) in the second stage to further increase the pH to 8.0. The use of

limestone was found to be cost saving because it is cheaper. The process chemistry during the neutralisation can be simplified as follows:

Stage I: Neutralisation to pH 5.0

$$Fe_2(SO_4)_3 + 3\ CaCO_3 + 3\ H_2O = 2\ Fe(OH)_3 + 3\ CaSO_4 + 3\ CO_2 \quad \text{(Eq. 1.7)}$$

$$H_2SO_4 + CaCO_3 = CaSO_4 + CO_2 + H_2O \quad \text{(Eq. 1.8)}$$

$$Fe_2(SO_4)_3 + 2\ H_3AsO_4 + 3\ CaCO_3 = 2\ FeAsO_4 + 3\ CaSO_4 + CO_2 + 3\ H_2O \quad \text{(Eq. 1.9)}$$

Stage II: Neutralisation to pH 8.0

$$H_2SO_4 + CaO = CaSO_4 + H_2O \quad \text{(Eq. 1.10)}$$

Neutralisation of BIOX liquors from Wiluna and Harbour Lights in Australia produced environmentally acceptable effluent concentrations of arsenic (<0.04mg/L), and produced residues which were stable for disposal on slimes dams, over a wide range of pH (5 to 11) **[6]**. Plant data on the first commercial application of bioleaching on a concentrate consisting of 70 % pyrite and 30 % arsenopyrite at Fairview mine, showed that neutralisation of acidic bioliquor with a Fe^{3+}/As molar ratio greater than 4 resulted in the precipitation of stable ferric arsenates **[10]**. These findings are in accordance with the results of comprehensive studies reported in the literature on the stability of amorphous ferric arsenates. These compounds were produced by neutralisation of purely chemical aqueous acidic systems at atmospheric conditions. A number of factors have been reported to affect the stability of ferric arsenates precipitates, these include Fe/As ratio; pH; temperature and co-precipitation of other compounds **[8, 11, 12]**. Harris and Monette **[12]** showed that the pH stability range of amorphous ferric arsenates is expanded from 3-7 to 4-10, with the coprecipitation of gypsum and base metals such as copper, zinc and cadmium. Fe/As ratio appears to be the most critical factor for the stability of arsenate precipitates. An Fe/As mole ratio equal or greater than 3/1 has been generally accepted to be a pre-requisite for the formation of stable ferric arsenate precipitates **[13-14]**. However Barrett et al., **[15]** reported that the neutralisation of As(V)-Fe(III) sulphate solutions with lime, in the pH range 2-7, produced ferric arsenates only, even at a Fe/As mole ratio as low as 1.7/1.

It is important that all the arsenic be oxidised to arsenic(V) for stable precipitates to be formed during neutralisation. The sludges that were produced during solution neutralisation carried out by Langhans et al., **[16]** did not pass the Toxicity Characteristic Leach Procedure (TCLP) test **[17-18]**, with arsenic concentrations in the TCLP leachate averaging 160 mg/L. The high instability of the sludges was attributed to the low iron:arsenic ratio and more importantly to the existence of the trivalent arsenic species in the liquors. In separate reports **[19-20]**, it was shown that the arsenical sludges and solid residues did not pass the EPA TCLP test because of the presence of the arsenite ions despite the high Fe/As molar ratio of the bioliquor, ranging between 2.7-3.1. The cyanidation tailings from the same work were found to be highly unstable.

Most data refer to neutralisation sludge, very little information is available on the stability of biooxidation residues and cyanidation tailings. In an attempt to cover this area, Adam et al., **[19]** reported that the stability of arsenical pyrites was directly related to the occurrence of iron-arsenic oxidised products reporting on the surface of unoxidised sulphides. The arsenic should be in the pentavalent state. The arsenic stability of the mixed neutralisation/cyanidation tailings from the pilot plant treatment of the Salmita ore assaying Fe: 2.9 wt %, As: 0.8 wt % was reported **[21]**. The molar ratio of Fe/As of the oxidised iron-arsenic precipitates was 2.2, a value below that recommended for optimum stability of amorphous ferric arsenates. At pH 10.5 the concentration of soluble arsenic of the tailings was 6.0 mg/L and this value further reduced to 0.2 mg/L as the pH reached 7.5. While it can be argued that the low concentration of arsenic in the residues was responsible for the stability, the difference in the soluble arsenic at the different pH indicates that there was enough arsenic to exceed the EPA limit for soluble arsenic in an environmentally unstable residue.

The application of hydrothermal precipitation for the immobilisation of arsenic as ferric arsenate has been studied and demonstrated **[22-25]**. Over 90 % of arsenic was found to be precipitated from solutions of pH<1, Fe:As molar ratio ≥ 1, at temperatures above 150 °C. The solids formed were crystalline and consisted of well-defined compounds or mixtures of compounds. The precipitated arsenical compounds included scorodite and

two previously unknown compounds which were designated as Type-1 ($Fe_2(HAsO_4)_3.zH_2O$) and Type-2 ($Fe_4(AsO_4)_3(OH)_x(SO_4)_y$). Based on the arsenic solubility, the stability of Type-2 compound was found to be equivalent to that of scorodite. Although these compounds passed the EPA TCLP test, their long term stability remains a question to be answered and for further testing. These crystalline compounds may be considered better options for arsenic disposal when compared to amorphous ferric arsenates precipitated from neutralisation of arsenical liquor, because the latter compounds may suffer from ageing. This may lead to dehydration and recrystallisation, which consequently may release adsorbed arsenic due to reductions in surface area and active sites **[22]**.

Testing methods for evaluating the stability of hazardous waste residues have been defined in the United States by the Environmental Protection Agency (EPA) **[17]**. According to the U.S. EPA standards, a solid cannot be disposed with respect to arsenic if the toxicity characteristic leach procedure (TCLP) produces a liquid extract greater or equal to 5 mg/L arsenic **[18]**. There has been much concern within the metallurgical industry that the TCLP method of the U.S EPA does not give a realistic indication as to the long term stability of arsenic bearing wastes. As a result many researchers have developed modified versions of the TCLP, which allow the stability of the sludges and residues to be tested over a wider range of pH, utilising sulphuric acid and sodium hydroxide, instead of acetic acid, as extractants **[26-27]**. Even with all these modifications, the long term stability of arsenical residues still remains an area of research.

1.3 Objectives of the research

The objectives of this research were:

(a) to study the effect of different ore genesis, and consequently differing mineralogies on bacterial oxidation,

(b) to study the speciation of arsenic during bacterial oxidation and identify the mineralogical factors that may be controlling this speciation,

(c) to study mineralogical changes taking place during bacterial leaching, and

(d) to study the environmental stability of bio-oxidation residues.

1.4 Structure of thesis

A literature review is presented in **Chapter Two**, discussing the mineralogy of refractory gold ores. The chemistry of bacterial oxidation of pyrite and arsenopyrite is also presented together with the mechanisms of arsenic(III) oxidation which have been suggested by various researchers. **Chapter Three** gives the methodology and equipment used in the mineralogical and bacterial oxidation studies. Attention is drawn to the polarographic technique for speciating arsenic. The solubility testing method used to assess the relative solubilities of the bio-oxidation residues is also discussed. **Chapter Four** describes the mineralogy of the ores used. The mineralogical composition of the concentrates in terms of pyrite to arsenopyrite ratios is also estimated. In **Chapter Five** the speciation of arsenic during bacterial leaching of pyrite/arsenopyrite concentrates with different ratios of pyrite to arsenopyrite is reported. The influence of pyrite on the oxidation of arsenic(III) were investigated, and the relationship between speciation of arsenic and mineralogical composition during bacterial leaching is assessed. A discussion of the findings of the present study compared to the work already reported on speciation of arsenic in bacterial oxidation of arsenical ores is also presented. The mineralogical changes taking place during bacterial oxidation and the environmental stability of the resulting residues is presented in **Chapter Six**. The increase in surface area of the pyrite is also evident on the SEM photomicrographs. Implications of the porous structure of bacterially leached pyrite are discussed. **Chapter Seven** is a general discussion of the results and the environmental implications of the work. Major conclusions from this work are presented and suggestions for further work discussed.

CHAPTER TWO

LITERATURE REVIEW

2.1 Mineralogy of refractory gold ores

2.1.1 Introduction

Concern about the nature of gold in sulphide minerals is not a new problem, it came about when metallurgists discovered that certain gold ores were not amenable to direct cyanidation. Mineralogical studies of refractory gold ores has revealed that a number of factors are responsible for the refractory behaviour of these ores **[2, 28]** and the development of an economic process for a particular gold ore requires a detailed knowledge of its mineralogy.

Mineral deposits generally have a heterogeneous mineralogy and have formed from metalliferous hydrothermal fluids precipitating minerals in favourable locations under varying physio-chemical conditions. The mineralogy and locking characteristics of the gangue minerals and sulphides can be altered by metamorphic and deformational processes**[29]**.

By combining a sound mineralogical knowledge and understanding of ore forming processes with access to analytical techniques, the mineralogical data for the successful exploitation of any gold ore deposit can be provided. Metallurgical recovery is very much dependent on factors such as efficiency of the processing plant. The original design and commercial operation of a processing plant are dependent on mineralogical characteristics of the plant feed.

2.1.2 Refractoriness of certain gold ores to cyanidation

Jha **[30]** classified refractory gold ores into three broad categories: sulphide ores, carbonaceous ores and telluride ores. In some cases an ore may contain more than one of these classes, as a result compounding the problem. The refractoriness can be directly related to a variety and combination of different mineralogical changes which have been recognised by a number of authors **[31-35]**. These changes have been classified and are summarised below.

Presence of submicroscopic or chemically bound gold

There is evidence that gold occurs as submicroscopic inclusions or in solid solution with certain sulphide minerals particularly arsenopyrite and arsenian pyrite **[36-39]**. The term ''invisible'' gold has been used to describe such gold occurrences and also encompasses colloidal size gold in the range 0.1 μm to 1 nm **[28]**. As regards to the milling practice, it may be of no significance whether submicroscopic gold occurs as finely disseminated, colloidal or solid solution because the lower limit of visible gold falls below the lower limit of gold which can be extracted by direct cyanidation because of incomplete exposure during milling. However the distinction between gold in solid solution and colloidal gold becomes important when considering concentration by flotation, as the former is normally confined to one or more of the sulphide minerals, whereas colloidal gold can occur in any mineral including silicates **[33].**

The majority of refractory gold occurs in ores related to pyrite and arsenopyrite with the latter sulphide being the major host, because gold is particularly prone to atomic substitution in arsenic associated minerals. Fine grinding has been found not to be effective under such conditions. To recover such gold the only solution is to break down the sulphide lattice and expose the gold to cyanide and oxygen.

Leaching of gangue minerals

During the formation of gold ore deposits, several minerals are also formed at the same time for example pyrite and pyhrrotite. Although pyrite is inert in alkaline cyanide solutions, pyhrrotite, marcasite and other base metal sulphides react with cyanide to

some extent. These minerals consume the cyanide and oxygen which is meant to be available for gold dissolution and as a result adversely affect the extraction process. These minerals are referred to as cyanicides because they consume cyanide. Table 2.1 shows the dissolution of arsenic and antimony minerals in cyanide solution as cited by Henley **[40].** The arsenic and antimony sulphides are particularly deleterious since they do not only consume cyanide but also reduce extraction of gold, probably by the action of their decomposition products in inhibiting the reaction surface of native gold with cyanide and oxygen **[32].** In plant practice their effects are normally reduced by the addition of lead nitrate, but the exact mechanism as to how Pb^{2+} ions enhances the dissolution kinetics of gold is not yet fully understood. Lead ions also react with the sulphide ions to prevent consumption of cyanide.

Table 2.1: Extraction of arsenic and antimony minerals in cyanide solutions **[40]**.

Mineral	Formula	Percentage dissolution of mineral
Arsenopyrite	FeAsS	0.9
Realgar	AsS	9.4
Stibnite	Sb_2S_3	21.1
Orpiment	As_2S_3	73.0

Note: Arsenic and antimony minerals ground to approximately -74 + 43 μm. Leached in alkaline cyanide solution containing 0.05 % NaCN for 6 hours at pH 12.2 (≡ 1g of mineral sample in 1200 mL of NaCN solution).

Insoluble gold bearing minerals

A number of gold bearing minerals have been studied and documented in the literature. Native gold and electrum, which are the most important gold bearing minerals in many ores, are readily soluble in alkaline cyanide solutions. However gold-bearing minerals ores such as the tellurides ($AuTe_2$), the aurostibite ($AuSb_2$) and the maldonite (Au_2Bi) are insoluble or only sparingly soluble in cyanide solutions. Although these minerals are rarely encountered in many gold ores and occur in small quantities, they may result in a significant loss during processing in certain gold ores. In a few gold ores tellurides are

the principal gold bearing mineral as at the Kensington deposit, Alaska, or they account for a significant fraction of the total gold **[31]**.

Encapsulation and coatings on native gold

When gold occurs as small inclusions in sulphides, an oxidation pre-treatment step can be employed for its recovery. The situation becomes complicated when the gold is physically locked up in silicates and the grain sizes of the gold are too small for fine grinding to be economical. There is no commercial method available to recover such gold.

During the roasting process coatings may form on the surface of the gold particles and inhibit access of cyanide and oxygen for the dissolution of gold **[41]**. The coatings may also be formed by supergene alteration **[42]**. Feather and Koen **[41]** documented in detail the nature and occurrence of gold at various stages in the process of its recovery from the Witswatersrand and related ores. These coatings include iron oxides, silver, antimony, manganese and lead compounds. They found that the ore was already coated before processing and further coating occurred during metallurgical processing, mainly as hydrated oxides. Antimony and lead coatings have been found to be mainly associated with the roasting process. These elements form alloys with gold which are insoluble in cyanide solution. Coatings are also deleterious to other processing techniques. In situations where flotation is to be used as a pre-concentration step, oxides may lead to the gold reporting to the tailings.

Presence of carbonaceous material

Certain gold ores contain carbonaceous material. In most cases this material is capable of adsorbing the gold during the cyanide dissolution process. This phenomenon is known as "preg-robbing". The ability of active carbon to adsorb gold in solution forms the basis of carbon in pulp (CIP) and carbon in leach (CIL) technologies. Refractoriness is compounded in carbonaceous ores by the fact that a certain proportion of the gold may be chemically adsorbed into the carbonaceous material and it is well known that to

strip gold from carbon requires severe conditions of temperature and cyanide concentrations **[30]**.

Electrochemical aspects

Studies performed on some gold ores suggest that the refractoriness of many sulphide ores is not only physical or chemical in nature but also electrochemical to some extent. Many researchers have speculated that gold in contact with conductive minerals would passivate as a result of the enhanced magnitude of cathodic current. This passivation is believed to form as a film on gold surface by precipitation **[43]**. The chemical composition of these films and precipitates depends on the mineralogy of the sample. These films may be oxides, sulphides, carbonates and cyanide complexes. Many researchers and staff in the mineral industry believe that such passivation, especially that cause the formation of films on the surface of gold, occurs only in laboratory experiments with clear solutions and rotating disc electrodes. However, this passivating action, which causes a decrease in the extent and rate of gold dissolution, was recently observed with real ores **[44]**.

Lorenzen and van Deventer **[45]** explained the passivating effect by using a rotating disc of gold in galvanic contact with other conducting minerals in both clear solutions and real slurries. An attempt was also made to distinguish between the effect of galvanic interaction and film formation in quantifying the phenomenon of passivation. The details of the experimental equipment are given in the literature **[45]**. They found that passivation is not merely a laboratory curiosity, but it can reduce the efficiency of industrial operations and is thus relevant to practical leaching operations. In all the experiments the gold electrode passivated rapidly so that the rate of dissolution was much slower than that predicted by the mass-transport limiting model. Besides passivation of gold in cyanide, galvanic interaction between gold and conducting minerals was the main cause for further reduction in the rate of gold dissolution. Minerals such as chalcopyrite, pyrite and pyrrhotite caused a significant decrease in the rate of gold dissolution when they were in contact with gold in dilute cyanide solutions, or when they were present in slurries in which a gold electrode was immersed. The

various films that form on the surface of the gold and the minerals, as well as the galvanic interaction, depend largely on the mineralogy of the ore and the treatment route used for extraction of the desired metal and or/ mineral.

2.1.3 Characterization of visible gold

A useful list of gold minerals with crystallographic parameters, density and hardness is given by Harris **[42]**. He noted that there are 26 recognised gold-bearing minerals, plus three unpublished new minerals and thirteen unnamed compounds. Out of all these gold minerals, the most important one is native gold and its alloy varieties as a result of metal substitution, the most common metal substitution being silver. Electrum normally defines a variety of gold found in epithermal genetic type of gold deposits, where the gold alloy exhibits a wide range of silver contents (20-40 wt % silver).

Automated systems for characterising visible gold

A number of automated methods for collecting data of gold minerals in polished sections have been developed and applied. These include the use of an automated optical image analysis system **[46]**, an automated electron microscope and scanning electron microscope **[47-49]**. These systems are capable of automatically searching the surface of a polished section, and recording the coordinates of gold minerals for subsequent examination.

Alternative methods for characterising visible gold

While identities and compositions of gold minerals can be readily determined in polished thin sections under reflected light, assessment of relative abundances, size distribution and liberation characteristics can cause some problems due to low concentrations of gold in ores leading to very low chances of finding gold on the surface of a polished thin section unless several sections are prepared and scanned using automated systems. A number of authors have commented on this aspect of non-representitivity of thin sections **[31-32, 48]**.

Due to the problems associated with polished thin sections and polished blocks, several alternative assessment methods have been developed. These methods aim at determining quantitatively the distribution of gold among mineralogical sites in the ore. Henley **[33]** used the method below for ores and mill products:

(a) Chemical and mineralogical analysis of the head sample

(b) Heavy liquid separation of size fractions and analysis of the product for Au and other selected elements (eg. As, Sb, S, Fe), analysis of separation products for mercury soluble and mercury insoluble gold, x-ray diffraction and electron probe microanalysis of the grain mounts of separation products.

(c) Extended cyanidation (48-72 hours) with monitoring of cyanide, lime consumptions and Au extraction, followed by dissection of cyanide residues grain mounts to determine the nature and location of refractory gold.

Chryssoulis and Cabri **[31]** used a different approach to quantify visible gold. They used cyanidation of pulverised samples (80-90 % passing 10 μm) as a measure of the concentration of visible gold. This method however underestimates the visible gold because according to their definition, visible gold includes all grains coarser than 0.1 μm. At the particle size range they used, most of the particles will be coarser than the size indicated in the definition and any gold which happens to be locked in these particles will not be liberated.

Corrans and Angove **[50]** described the use of fine grinding to liberate gold particles locked in other minerals, particularly sulphides. They used the grind size of 80 % passing 2-3 μm. Commercial application of fine grinding is limited by energy requirements and also the gold should be present as inclusions. In the case of gold being in solid solution the method does not work.

2.1.4 Characterisation of "invisible" gold

Although ultrafine milling or analysis of pulverised mineral samples can give a semi-quantitative measure of the refractory gold content of ores and mill products, it is necessary to use more advanced analytical methods to further characterise the invisible

refractory gold in ores and mill products. These methods essentially allow microchemical analyses of small areas and include electron microprobe analysis, ion microprobe analysis or secondary ion mass spectrometry (SIMS), proton microprobe analysis (proton induced x-ray emission-PIXE), synchrotron x-ray fluorescence analysis (SXRF), high resolution transmission electron microscopy (HR-TEM), laser ablation inductively coupled mass spectrometer and Mössbauer spectroscopy.

Electron microprobe analysis

This is a non-destructive analytical technique which uses a focused electron beam of 1-2 μm diameter to generate secondary x-rays from within 2 μm depth **[51]**. The detection limit for gold in sulphides is normally about 200 ppm **[52-53]**. Graham et al., **[54]** reported a detection limit of 10 ppm by the use of very high currents (500 nA) and accelerating voltage of 40 kV. This method is essential when attempting the identification of particles less than 50 μm and down to 1 μm in diameter, or when determining their grain size, distribution and associated phases. The electron microprobe also assists in the determination of minor and trace elements in grains of similar size **[55]**. The method has been applied successfully to study gold ore mineralogy **[39, 56]**.

Laser-ablation inductively coupled plasma mass spectrometry

This is a newly developed microanalytical technique which uses high energy laser pulses to ablate material from a mineral surface and analyses it by inductively coupled plasma mass spectrometry **[57]**. The beam can be focused down to 10-100 μm and the detection limit ranges from several hundreds to less than 10 ppm. This technique has been successfully applied in analysing fluid inclusions **[58-60]**. As far as gold is concerned, this technique was used by Musket **[61]** and Middleton **[62]** to determine gold in arsenopyrite and pyrite.

Mössbauer spectroscopy

Of all the methods discussed above, none of them provide enough evidence of structurally incorporated gold in sulphide minerals. Wagner et al., **[63]** applied the Mössbauer spectroscopy technique and confirmed the existence of such gold, although

its chemical state (Au^0, Au^+, Au^{3+}) is not known. This technique is applicable at gold levels 100-300 ppm **[46]**. A number of authors have used this method to characterise gold in solid solution in arsenopyrite **[36-38]**. Figure 2.1 shows a Mössbauer spectrum of gold bearing arsenopyrite, clearly distinguishing native gold and chemically bound gold.

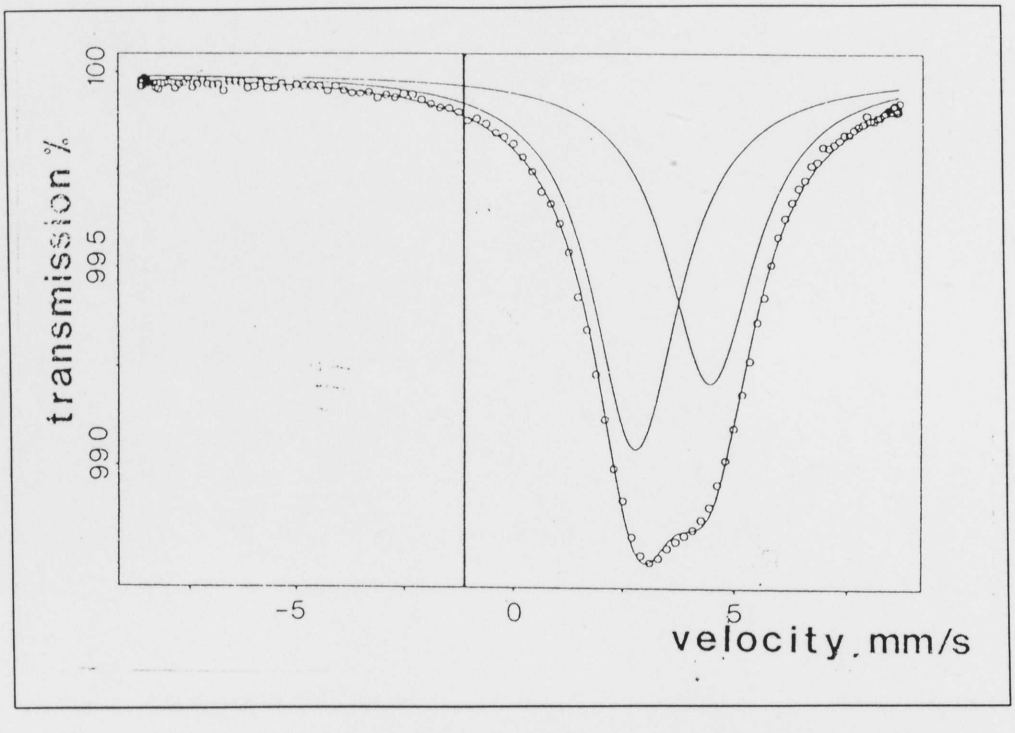


Figure 2.1: Mössbauer spectrum of Au-bearing arsenopyrite. The vertical line indicates the position of pure metallic gold absorption peak **[37]**.

2.1.5 Structure and composition of pyrite and arsenopyrite

Pyrite and arsenopyrite are the most important mineral sulphides which are commonly found associated with the majority of refractory gold ores. They are present in massive hydrothermal sulphide bodies and common in hydrothermal veins, including gold-quartz veins. Arsenopyrite is the most abundant arsenic-bearing mineral while pyrite represents the most abundant sulphide. The association of these minerals with economic mineral deposits has led to numerous investigations regarding their composition, properties, and phase relationships.

Pyrite

Figure 2.2 (a), page 39, shows the structure of pyrite, which can be considered as a halite (NaCl) structure in which the anion sites are taken by S_2 molecules. The Fe atoms and the molecular centres are each on a face-centred cubic lattice of edge length, a. Each sulphur is tetrahedrally coordinated with one S neighbour and three Fe neighbours **[64]**. The typical stoichiometric composition of pyrite in terms of weight percent is considered to be 46.55% Fe and 53.45% S. However Smith **[65]** considered that the S/Fe ratio could be in the range 1.94-2.01, while Kullerud and Yonder **[66]** concluded that this was based on analytical errors and that the ratio was indistinguishable from 2.0. Impurity elements have been found to be associated with pyrite, Fleischer **[67]** summarised these trace elements in pyrite as Co, Ni, and As with Mn being distinctly less common. Zinc and copper have also been frequently abundant in analyses, but they have been attributed to inclusions of sphalerite and chalcopyrite respectively.

Arsenopyrite

The arsenopyrite structure has been reported by Beurger **[68]** as a derivative of the structure of marcasite, the orthorhombic form of FeS_2 resulting in two kinds of structures, one being monoclinic and the other triclinic, closely related to the structure of marcasite. In arsenopyrite the polyanions are As-S pairs. They are arranged so that each Fe has three As and three S neighbours. Figure 2.2 (b) shows the structure of arsenopyrite as reported by Dana **[69]**.

Arsenopyrite can be represented by the formula FeAsS with a theoretical composition by weight of 34.3% Fe, 46.0% As and 19.7% S. However chemical analysis shows variations from this stoichiometric composition especially with regards to As and S. The composition range has been reported to vary between $FeAs_{0.9}S_{1.1}$ and $FeAs_{1.1}S_{0.9}$ **[70]**. Fleischer **[67]** reported that cobalt is the most common impurity in arsenopyrite and its substitution for iron may form a complete solid solution series from arsenopyrite to glaucodot [(Co,Fe)AsS]. Other elements which have been found in association with arsenopyrite are bismuth, nickel, manganese and selenium. Clark **[71]** pointed that the composition of arsenopyrite varies with temperature and the precise limits are not

known and that most naturally occurring arsenopyrites tend to be sulphur-rich according to published results. He also reported that the use of high pressure with arsenopyrite in gold tubes showed that gold diffuses readily into arsenopyrite at temperatures of 600° to 700°C, which suggest a small amount of solid solubility at elevated temperatures. This

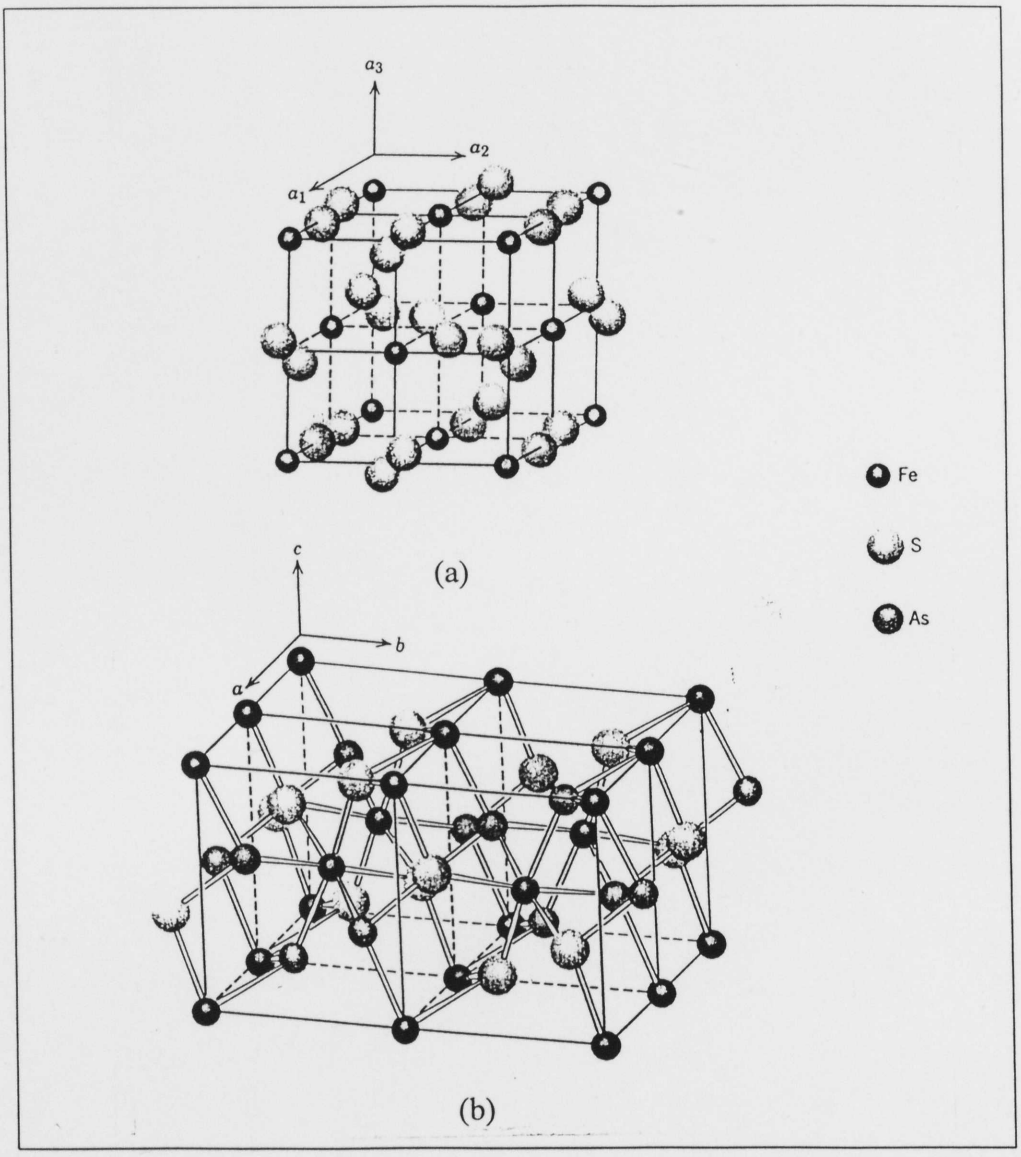


Figure 2.2: The structure of (a) pyrite and (b) arsenopyrite **[69]**.

bears on the frequent association of gold and arsenopyrite in ores, because high pressures and temperatures similar to those reported in the above runs are normally encountered during gold ores formation.

The substitutional mechanism of gold in arsenopyrite is not yet well understood and many mechanisms have been proposed **[72]**. Boyle **[73]** suggested that Au may occupy the As sites in the arsenopyrite structure basing the assumption on the similar radii of these elements when covalently bonded. The covalent radius of Au in aurostibite is 1.40 Å and that of As in arsenopyrite is 1.39 Å. Genkin et al., **[72]** gave a detailed analysis of the mechanisms of gold substitution proposed by different researchers. They also found that gold-bearing arsenopyrite was usually depleted in As with respect to its stoichiometric composition, but correlation of Au enrichment to Fe deficiency has not been found. Gold-bearing pyrites are usually found to contain some arsenic, which is concentrated in the gold-rich zones of the crystals **[74]**. Therefore the sitting of gold in pyrite may not be very different from that of pyrite. The substitution of gold and other elements in the crystal structure of pyrite and arsenopyrite represent structural defects within the crystal lattice. These crystal defects have been considered to be areas of preferential attack in bacterial oxidation of pyrite/arsenopyrite concentrates.

2.2 Processing of refractory gold ores

For effective dissolution of gold to take place, the gold particles in the ore must be accessible to both cyanide ions and oxygen. Although some gold is obtained from ores as free particles of gold by gravity concentration, a greater proportion of gold may remain locked in sulphides as submicroscopic inclusions or in solid solution. The locked gold is not amenable to direct cyanidation and is considered to be refractory gold. In order to recover the refractory gold, the ore has to be pre-treated to break down the sulphide matrix and expose the gold to cyanide and oxygen.

Traditionally roasting (Figure 2.3) has been the dominant pre-treatment process and mainly involve two stages. The objective of the method is the transformation of the iron sulphides to high porosity iron oxides so that cyanide can penetrate the calcine and increase the extraction of gold. In the first stage the supply of oxygen is limited so that the arsenic in the sulphides is oxidised to the trivalent state and removed as volatile arsenic trioxide (As_2O_3). In the second stage of roasting the ore is fully oxidised with excess oxygen to remove sulphur as sulphur dioxide (SO_2). The commonly used furnace

for this process was the "Edwards" hearth, but more morden plants have utilised fluidised-bed furnaces **[75]**. Roasting temperatures must be carefully controlled in order to minimise formation of sulphur trioxide (SO_3) and avoid sulphuric acid condensation with arsenic trioxide. Recovery of gold is typically between 80 and 90 %, furthermore poor temperature control, particular too high temperatures can produce impervious, glassy fluxes that encapsulate the gold **[1]**. Due to environmental constraints, such as control of exit gases (which contain arsenic trioxide and sulphur dioxide), considerable research has been devoted to hydrometallurgical pre-treatments.

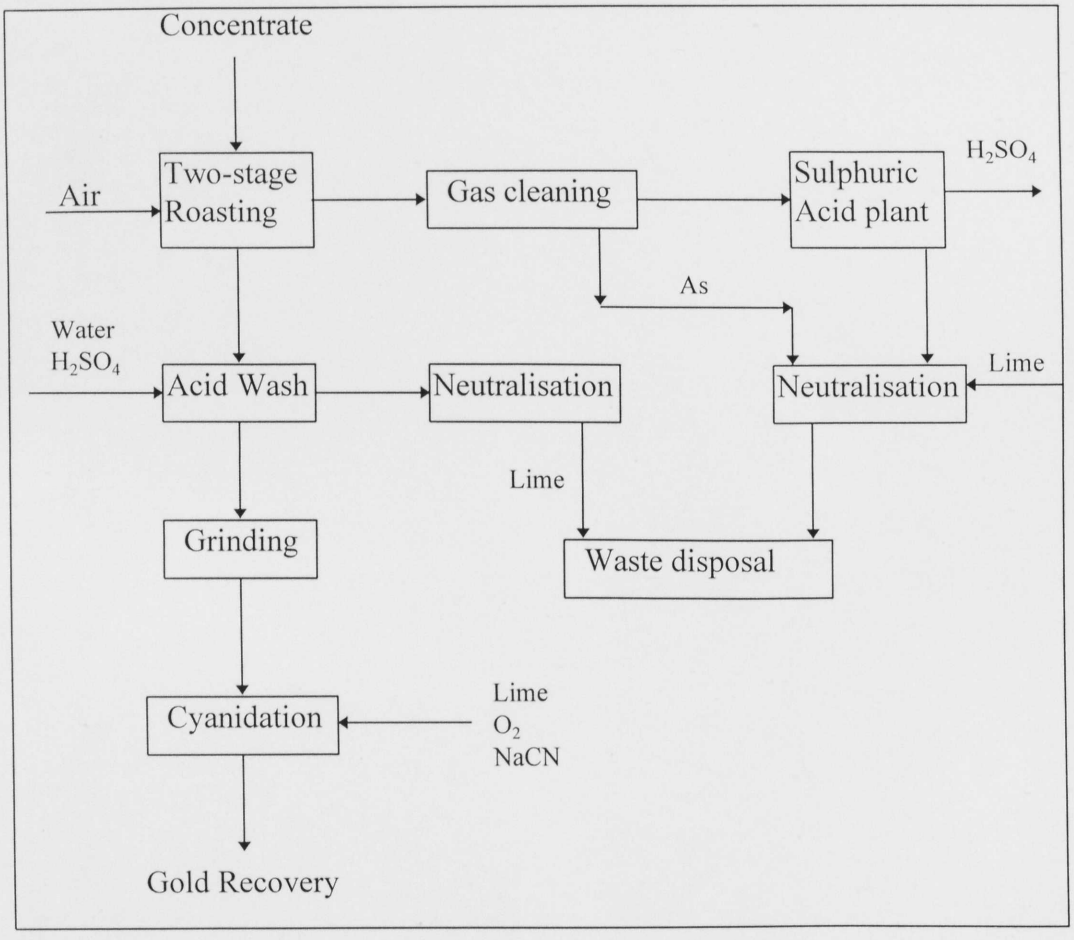


Figure 2.3: Block diagram of the two-stage roasting process.

Pressure oxidation (Figure 2.4) and bio-oxidation have been applied successfully on industrial scales and are gradually replacing roasting **[75-76]**. Pressure oxidation is conducted at relatively high temperatures (180-210°C) and pressures (1800-2200 kPa)

in an oxygen enriched atmosphere achieving an essentially complete oxidation of sulphide minerals in 1-3 hours. During oxidation, compounds and species that render gold refractory to cyanidation are solubilised, resulting in gold liberation. The process is environmentally friendly because the arsenic from arsenopyrite decomposition is oxidised to the arsenate state while the iron is oxidised to ferric. Consumption of the acid by the gangue components, and the elevated temperature of operation promote

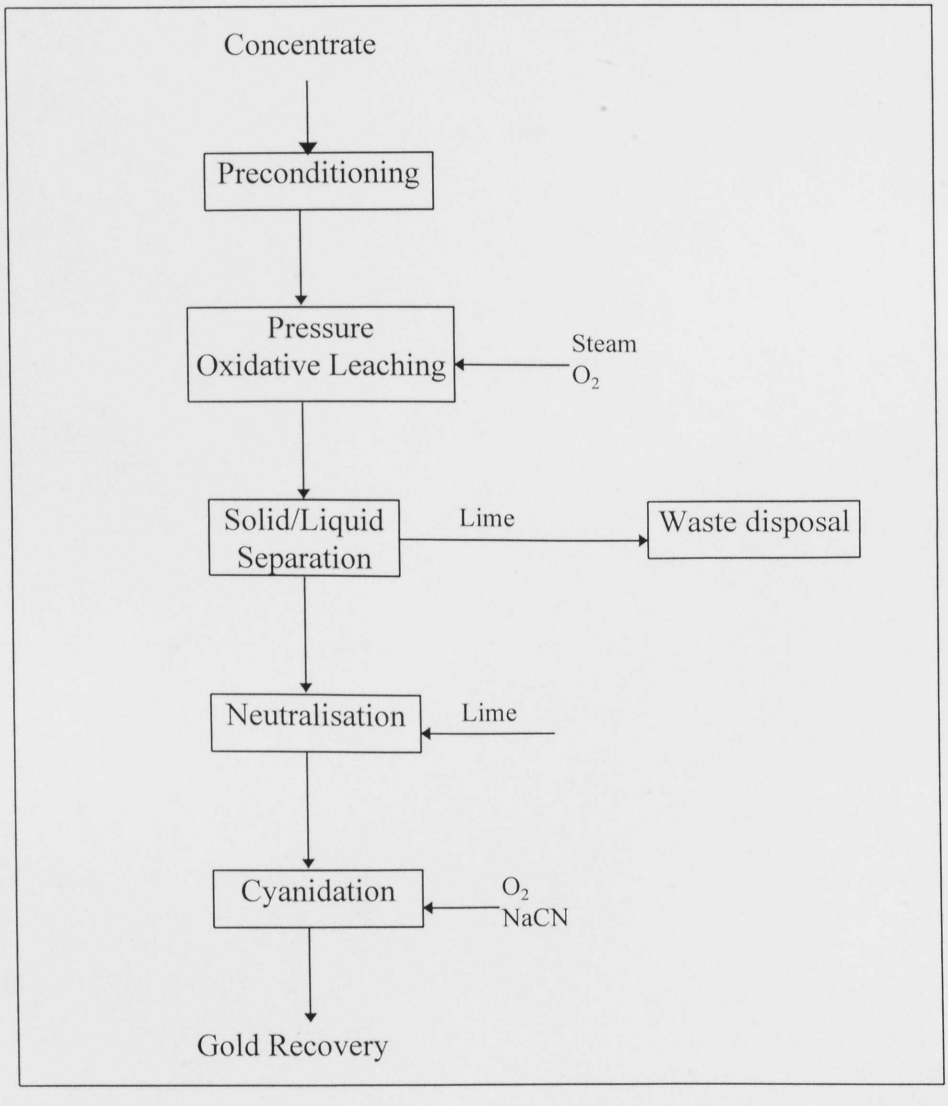


Figure 2.4: Block diagram of the acid pressure leach process.

appreciable hydrolysis and precipitation of arsenate and ferric iron, as ferric arsenate, hematite, basic ferric sulphates, and jarosites. However the process is considered to be

complicated and more expensive than bacterial oxidation because its complex engineering leading to higher capital and operating costs.

2.3 Biooxidation

2.3.1 Introduction

The bacterium usually encountered in metal sulphide oxidation is *Thiobacillus ferrooxidans*. It is versatile and oxidises both iron and sulphur under acidic conditions. It grows readily on mineral sulphides such as chalcopyrite, pyrite and arsenopyrite. Although the knowledge that bacteria attack sulphide minerals is relatively new, observations of the effect of bacterial action date back as early as Roman times, when the presence of copper in mine drainage was described. The earliest recorded copper recovery was in 1670 at the present Rio Tinto mine in Spain. By 1900 dump leaching was practised there, and 20 years later a number of operations were developed in United States as cited by van Aswegen and Haines **[13]**. Originally dump leaching was considered to be the result of chemical reactions only, but in the 1950s it was demonstrated that bacteria were involved.

During bacterial oxidation sulphide minerals are oxidised to soluble species thus breaking down the lattice. The principal advantages of biooxidation over pressure oxidation and roasting are the greatly reduced capital cost for small to medium size plants; it is a flexible and easily controllable process requiring relatively unskilled labour for operation; the process gives improved gold recovery compared with roasting and is assumed to produce environmentally acceptable residues. The process also has some limitations such as slow kinetics compared with pressure oxidation and roasting, bacterial activity is also slow to recover from disruptions such as air supply failure and contamination by toxic species such as cyanide **[77]**.

Due to the potential of biooxidation in the processing of refractory gold ores, much research and pilot plant has been reported world-wide **[78-82]**. The success of the process has seen the installation of commercial biooxidation plants for the pre-treatment of refractory gold ores. These are BIOX plants located in South Africa (Fairview);

Australia (Harbour Lights and Wiluna); Brazil (Sao Bento) and Ghana (Ashanti) and BacTech plant located in Australia (Youanmi mine) **[10, 83-86]**.

2.3.2 Bacterial cultures involved in oxidation of minerals

Various kinds of acidophilic bacteria capable of attacking mineral sulphides have been isolated from industrial leaching operations or from sites of natural leaching such as acid mine drainage. A classification of these bacteria can be made, on the basis of optimum temperature for growth, into mesophiles, moderate thermophiles and thermophiles.

Mesophiles

The dominant species in this group is *Thiobacillus ferrooxidans* with an optimum operation temperature of 25-35°C, although some Canadian isolates had a greater cold tolerance than most strains and an optimum temperature of 20°C **[87]**. Much information has been accumulated on this organism which is capable of chemolithotrophic (meaning that they obtain their energy from inorganic substances such as iron(II) and sulphur compounds) growth in acid environments using energy from the oxidation of ferrous iron and soluble and insoluble sulphides **[88-90]**. *Thiobacillus ferrooxidans* have an optimum pH range of 1.5-2.5 **[51]**. The bacteria can utilise carbon dioxide from air for autotrophic growth.

Other important mesophiles are the chemolithotrophic bacteria *Thiobacillus thiooxidans* and *Leptospirillum ferrooxidans*. These species are highly acidophilic (pH 1.5-2.0), obligatory autotrophic (they obtain carbon for their cells from CO_2). They also need nitrogen and phosphate as main nutrients along with traces of potassium, magnesium calcium and sodium for growing and making their cellular synthesis) and grow optimally at 25-35°C **[91]**. *Thiobacillus thiooxidans* cannot oxidise iron; it is known for its ability to grow on elemental sulphur and some soluble sulphur compounds. *Leptosperillium ferrooxidans* is capable of oxidising ferrous iron but is unable to oxidise reduced sulphur compounds. Because of this, neither organism is able to oxidise

sulphide minerals efficiently on its own. However *Leptospirillium*-like bacteria have been shown to oxidise pyrite **[92]**.

Mixed cultures of the above strains of bacteria have been known to rapidly degrade a number of sulphide ores. The BIOX bacterial culture, isolated by GENCOR Process Research, is a mixed culture of *Thiobacillus ferrooxidans*, *Thiobacillus thiooxidans* and *Leptospirillum ferrooxidans*. The commercial success of the mixed culture has been demonstrated by its use in all the five commercial bio-oxidation plants installed by GENCOR **[93]**. The operating temperature range of all these BIOX plants is 35-50°C. However there is also a cooling problem due to the heat produced during the oxidation of sulphides especially in summer when the temperatures are close to the operating temperature.

Moderate thermophiles

These have been isolated from thermal springs **[94-95]** and they have been shown to be capable of degrading minerals such as pyrite, arsenopyrite and chalcopyrite at temperatures of 45-60°C **[96-97]**. Several strains are now known. These include *TH1* **[94]**, *TH2* **[98]**. Other cultures in this group have been also documented for example *M4* isolated in Australia by Poole **[99]**. Some of the species have been classified as members of the genus *Sulfobacillus* **[100]**. For vigorous autotrophic growth, most moderate thermophiles require carbon dioxide enriched air as well as cysteine or some form of reduced organic sulphur **[91]**. Their role in most industrial leaching processes is still limited. When moderate thermophilic bacteria are used problems of cooling the reactor in hot climates or during the reaction are eliminated. A major problem which has been found with this group is their reduced tolerance to arsenic compared to the mesophile group **[97]**.

Extreme Thermophiles

Like the moderate thermophiles these have also been isolated from hot springs and other environments. Extreme thermophiles belonging to the genus *Sulfolobus* have been shown to be able to grow at temperatures up to 80°C using sulphur or iron for energy.

Such bacteria have demonstrated their ability to leach refractory gold concentrates and ores at much faster rates than mesophilic bacteria **[101-102]**. However it has been noted that further work is required to demonstrate the *Sulfolobus* system metallurgy, especially high pulp density operation, potential for selective sulphide oxidation as demonstrated by the mesophilic system, tolerance to high metal concentration (particularly arsenic) and also equivalent gold recovery **[102]**.

2.3.3 The chemistry of bacterial oxidation of minerals

In order to build a comprehensive understanding of the chemistry of bacterial oxidation of sulphides and to achieve the environmentally acceptable disposal of waste solutions and solids, it is important to look at the measurement of pH, the speciation of elements in the biooxidation residues and liquors, and electrode potential measurement. The results of speciation calculations (or experimental determinations) are usually expressed in terms of alpha (α) values which represent the fractions of the species in which the oxidation state of a particular element exist **[103]**. Speciation in any system is normally highly dependent upon the pH of the solution and it is therefore important to understand the theoretical basis of pH and its practical applications. The standard Gibbs free energy equation provides a convenient way of characterising the thermodynamic feasibility of a redox reaction:

$$E^\circ = -\Delta G^\circ / nF \qquad \text{(Eq. 2.1)}$$

where : E° = standard electrode potential

n = number of electrons transferred from the reducing agent to the oxidising agent and

F = Faraday's constant

To be thermodynamically feasible a reaction must have a negative ΔG° value and, in consequence, the corresponding E° value must be positive. The feasibility of a redox reaction at any potential value can be predicted by the use of the Nernst equation. However these potential values do not yield information about the kinetics or galvanic interactions of the reactions involved.

pH measurement

Hydrogen ions play an important role in the energy supply mechanism of *Thiobacillus ferrooxidans* and this probably holds for other acidophiles. Furthermore, the microbe-mediated oxidation of ferrous iron and of mineral sulphides involve electron transfer and movement of hydrogen ions. Therefore the hydrogen ion concentration of the liquid media where biohydrometallurgical processes are carried out has a definite effect on the microbial life as well as on the hydrometallurgical process. During the oxidation of minerals it is important to measure the pH because it can give an indication as to whether the oxidation is taking place. For example in the oxidation of pyrite, pH of the solution will drop since sulphuric acid is a product of the oxidation. Accordingly, optimum pH ranges and the pH intervals within which microorganisms are active can be identified. Due to the relatively complex nature of the of solutions encountered in bacterial oxidation processes, it is difficult to obtain an accurate value for the hydrogen ion concentration **[103]**. In plant and laboratories it is generally accepted to use standard buffer solutions to calibrate pH electrodes and meters used.

Speciation

The ionic speciation of bacterial oxidation solutions is a very important subject in bioleaching of minerals. Refractory gold ores generally comprise mixtures of pyrite and arsenopyrite and bacterial oxidation of these ores produces solutions with very complex ionic speciation because of the multivalent nature of the elements involved. The important oxidation states of elements in these systems are sulphur(0), sulphur(VI), intermediate sulphur species such as thiosulphate, arsenic(III), arsenic(V), iron(II), iron(III), together with ions of other solubilised sulphides.

The primary oxidation products of bacterial leaching of arsenopyrite and pyrite are iron(II), sulphur(0) and arsenic(III) **[99]**. However it is argued that bacteria will catalyse the reactions for the transformation of iron(II) and arsenic(III) to their higher oxidation states **[99, 104-106]**. In an investigation using *moderately thermophilic* mixed bacterial culture, Ewart **[99]** compared the speciation of arsenic during arsenopyrite oxidation using both sterile and bacterial-rich ferric sulphate solutions. He found that the bacteria

catalysed the formation of arsenic(V) and iron(III). Barrett **[104]** gave a comprehensive review of ion speciation during the bacterial oxidation of refractory gold ores. The values for the formation constants were calculated using data supplied by Robins **[103]**. When arsenic(V) is present in an acidic iron(III) solution there are three complexes which have been identified **[107]** as contributing to the speciation. These are $[FeH_2AsO_4]^+$, $[FeHAsO_4]^{2+}$ and $[FeAsO_4]$, the latter being regarded as an aqueous complex which is a precursor of solid iron(III) arsenate(V) which could be precipitated under appropriate conditions. Figure 2.5 shows the speciation and alpha values at different pH values for the major iron(III) components of a solution which contains 0.3 M iron(III), 0.45 M sulphur(VI) and 0.2 M arsenic(V) (typical of the solutions produced in bacterial oxidation of arsenopyrite/pyrite mixtures).

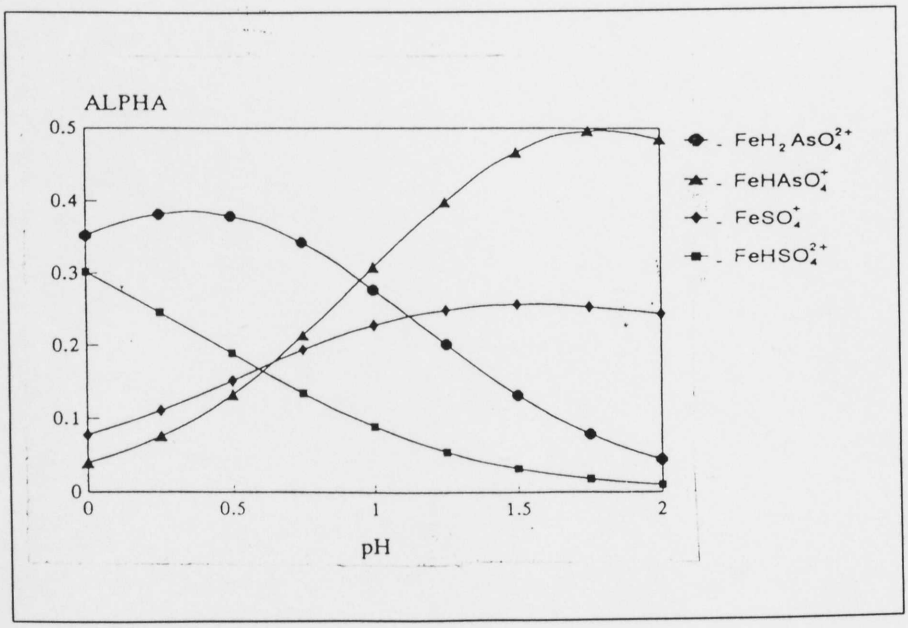


Figure 2.5: Speciation of major iron(III) components in a solution containing 0.3M Fe(III), 0,45M S(VI) and 0.2M As(V) **[104]**.

Electrode potential

The two oxidants of importance in bacterial oxidation of minerals are oxygen and iron(III). The strength of an oxidant is expressed by its standard electrode potential. A higher value of the standard electrode potential indicates that the oxidant is more

powerful. Under non standard conditions the oxidising strength of an oxidant can be predicted by the Nernst equation.

The reduction of oxygen during bacterial oxidation process can be represented by the equation:

$$O_2 + 4H^+ + 4e^- = 2H_2O \qquad \text{(Eq. 2.2)}$$

The standard electrode potential for this reaction is 1.23V **[108]**, the variation of the potential of the above equation with the hydrogen ion activity can be obtained by applying the Nernst equation:

$$E = E° + (RT/4F)\ln(1/P_{O2}a_{H+}{}^4) \qquad \text{(Eq. 2.3)}$$

For standard conditions where the partial pressure of oxygen is unity and T=298K the equation simplifies to:

$$E = 1.23 - 0.0592pH \qquad \text{(Eq. 2.4)}$$

In the metabolism of bacteria, oxygen operates in the cytoplasmic membrane where the local pH value is considered to be 7 **[103]**. Substitution of the pH term into the equation (Eq. 2.4) gives an oxidising potential of 0.816 V and this is the value which is used for predicting the oxidising potential.

Table 2.2 : The standard reduction potential with respect to iron(II), of some iron(III) complexes **[103]**.

Complex	E°/V
$[FeHSO_4]^{2+}$	0.71
$[FeSO_4]^+$	0.68
$[FeHAsO_4]^+$	0.65
$[FeH_2AsO_4]^{2+}$	0.60

The standard redox potential of the system iron(III)/iron(II) is 0.77 V. Because of various iron complexes formed during biooxidation, this value of potential is altered. The calculated values for the standard potentials of the various iron(III) sulphate and iron(III) arsenate complexes are given in Table 2.2. Compared to iron(III) sulphates, iron(III) arsenates have lower oxidation potentials. This may be due to a stronger complexation of the latter complexes.

Thermodynamics of mineral oxidation

In order to make good predictions of the oxidation process likely to take place it is important to consider the thermodynamics of the minerals concerned. Iron(III) has an important role as a primary oxidant for refractory minerals and also as a secondary oxidant during the oxidation of arsenic(III). E_h-pH diagrams are a useful tool in predicting thermodynamically stable species in aqueous systems.

Oxidation of pyrite

Pyrite may be considered to comprise basically of Fe(II) and S(-1), and may be oxidised in aqueous solutions to different species of sulphur with release of iron(II) into the solution; sulphur(VI) with release of iron(II) into solution; or iron(III) and sulphur(VI) according to the equations:

$$Fe^{2+} + 2S + 2e^- = FeS_2 \qquad E° = 0.424\ V \qquad \text{(Eq. 25)}$$

$$Fe^{2+} + 2HSO_4^- + 14H^+ + 14e^- = FeS_2 + 8H_2O \qquad E° = 0.351\ V \qquad \text{(Eq. 2.6)}$$

$$FeSO_4^+ + HSO_4^- + 15H^+ + 15e^- = FeS_2 + 8H_2O \qquad E° = 0.373\ V \qquad \text{(Eq. 2.7)}$$

$$FeHSO_4^{2+} + HSO_4^- + 14H^+ + 15e^- = FeS_2 + 8H_2O \qquad E° = 0.374\ V \qquad \text{(Eq. 2.8)}$$

The overall oxidation of pyrite to the $[FeHSO_4]^{2+}$ or $[FeSO_4]^+$ complexes and sulphur(VI) is feasible with any of the possible oxidants, but the reactions do not take place in a single step. There are four possible primary stages, the oxidation of pyrite to sulphur(0), sulphur(II), sulphur(IV) or sulphur(VI), with the solubilisation of iron(II), which are feasible with any of the iron (III)/sulphate/arsenate complexes. The secondary process of oxidation of iron(II) to iron(III) requires oxygen as an oxidant. The latter

reaction requires bacteria in the bulk solution to catalyse it **[103]**. Although the iron(III) complexes appear to have the potential to oxidise pyrite through to the iron(III) stage, the iron would be produced in the iron(II) state by the reduction of the iron(III) complex. Figure 2.6 shows the E_h-pH diagram for pyrite. Under the conditions used in bacterial oxidation of pyrite (pH < 2 and E_h > 500 mV), it can be predicted that the dissolution of pyrite should produce iron(II), iron(III) and sulphur(VI). However the E_h-pH diagram does not show the intermediate species of sulphur which have been found to exist during bacterial leaching experiments. Furthermore, this diagram assumes equilibrium conditions and standard conditions of temperature and pressure.

Oxidation of arsenopyrite

When arsenopyrite is oxidised the important possible products in bacterial oxidation solutions have been considered to be (i) iron(II), arsenic(III) and sulphur(0); (ii) iron(II), arsenic(III) and sulphur(VI); (iii) iron(II), arsenic(V) and sulphur(VI) and (iv) arsenic(V), iron(III) and sulphur(VI). The half reactions for the possible species are as below:

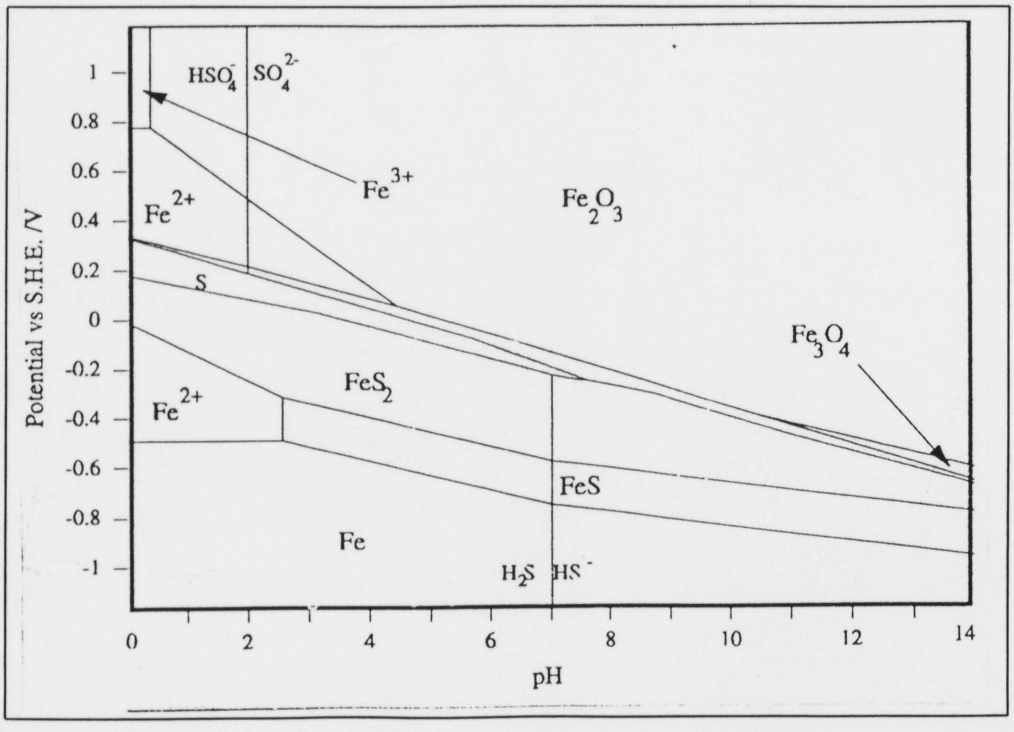


Figure 2.6: Eh-pH diagram for pyrite for the stable Fe-S-H_2O system at 298K, activity of iron = 10^{-3} and activity of sulphur = 10^{-1} **[109].**

$3H^+ + Fe^{2+} + H_3AsO_3 + S + 5e^- = FeAsS + 3H_2O$ $E° = 0.077$ V (Eq. 2.9)

$10H^+ + Fe^{2+} + H_3AsO_3 + HSO_4^- + 11e^- = FeAsS + 7\,H_2O$ $E° = 0.219$ V (Eq. 2.10)

$12H^+ + Fe^{2+} + H_3AsO_4 + HSO_4^- + 13e^- = FeAsS + 8H_2O$ $E° = 0.274$ V (Eq. 2.11)

$13H^+ + [FeH_2AsO_4]^{2+} + HSO_4^- + 14e^- = FeAsS + 8H_2O$ $E° = 0.296$ V (Eq. 2.12)

$14H^+ + [FeHAsO_4]^+ + HSO_4^- + 14e^- = FeAsS + 8H_2O$ $E° = 0.302$ V (Eq. 2.13)

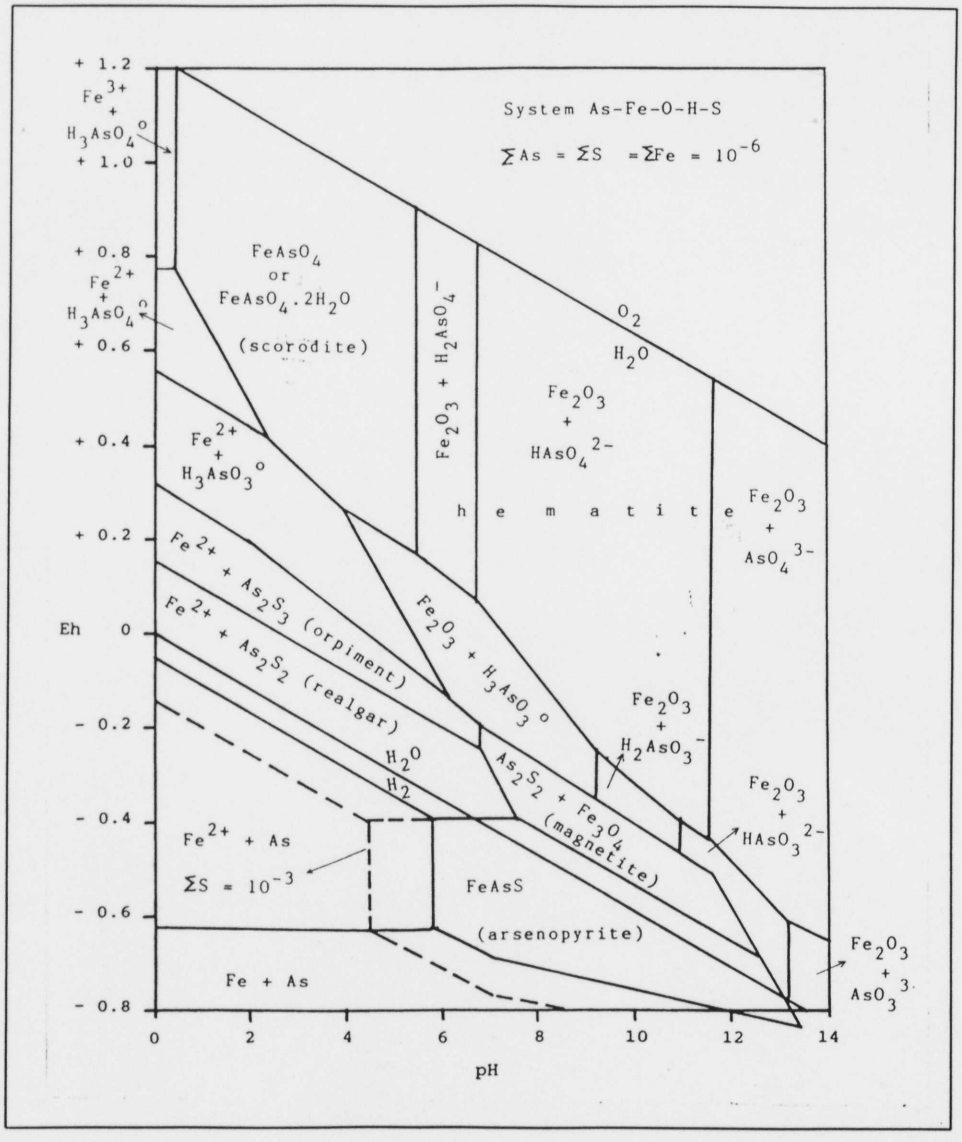


Figure 2.7: E_h-pH diagram for the system As-Fe-O-H-S, if $\Delta G°_{298}(FeAsO_4)$ is taken as -199.1 kcal/gfw **[110]**.

Iron(III) complexes have the potential to oxidise solid arsenopyrite to the iron(II) or sulphur(VI) stage and these processes represent the primary dissolution of the mineral

[103]. The secondary oxidation of iron(II) is catalysed by bacteria. The oxidation of arsenic(III) to arsenic(V) is a complex reaction, the standard reduction potential for the half reaction:

$$H_3AsO_4 + 2H^+ + 2e^- = H_3AsO_3 + H_2O \qquad \text{(Eq. 2.14)}$$

is generally accepted to be 0.56 V **[108]**. Although the potential of oxygen look probable to drive the reaction, it is known to be very slow and bacteria cannot derive energy from it. Barrett et al., **[103]** and Ewart **[99]** have shown that the reaction can be driven by iron(III) in the presence of bacteria and pyrite as a catalyst. Bacterial-rich ferric solutions have also been shown to be more effective in the oxidation of arsenopyrite **[34, 111-112]**. However these researchers did not report the speciation of arsenic in their work. Figure 2.7 shows the E_h-pH diagram for the system As-Fe-O-H-S. The diagram predicts that arsenopyrite is highly unstable under the conditions used in bacterial leaching, i.e. pH < 1.8 and high E_h (> 700 mV). It also includes the ferric arsenate which is one of the most important products of the biooxidation process of arsenical ores. Although thermodynamic data on iron arsenate the natural mineral scorodite ($FeAsO_4.2H_2O$) is limited, an approximation of the Gibbs free energy value for $FeAsO_4$ was made in order to include it on the diagram **[110]**. At lower potentials (200-500 mV) and pH<2 arsenic(III) species(H_3AsO_3) is predicted to form in solution while arsenic(V) species (H_3AsO_4) are predicted at higher potentials.

E_h-pH diagrams are usually constructed at 25°C **[113-114]** because of the unavailability of thermodynamic data of many aqueous species and solid compounds at high temperatures. Despite the fact that these diagrams are constructed at low temperatures and less activity than those normally encountered during experiments, they are very useful tools especially in identifying the species existing at certain E_h-pH conditions and as a result in elucidating the mechanism of reactions.

2.3.4 Mechanisms of bacterial oxidation

The mechanism of bacterial attack is controversial, the main concern is whether the

bacteria have a direct role or an indirect role, whereby in the latter they oxidise Fe(II) generating Fe(III) ions which in turn oxidise the minerals. In view of this, much work on this subject has been reported by a number of authors **[34, 88, 103, 112, 115-122]**. Some authors have divided the mechanism into direct and indirect modes while others have divided it into primary processes and secondary processes.

Direct mechanism

This involves physical contact of the mineral grains and the bacteria. The oxidation is assumed to be independent of other chemical reactions involved in the bacterial leaching such as ferric leaching. The mechanisms can be best represented by considering the oxidation of pyrite and arsenopyrite. The overall equations of bacterial oxidation of pyrite and arsenopyrite are given below:

$$4FeS_2 + 15O_2 + 2H_2O = 2Fe_2(SO_4)_3 + 2H_2SO_4 \quad \text{(Eq. 2.15)}$$

$$4FeAsS + 11O_2 + 16H_2O = 4H_3AsO_4 + 4FeSO_4 \quad \text{(Eq. 2.16)}$$

The direct mechanism of pyrite and arsenopyrite oxidation is assumed to take place according to the equations:

$$2FeS_2 + 7O_2 + 2H_2O = 2FeSO_4 + 2H_2SO_4 \quad \text{(Eq. 2.17)}$$

$$4FeAsS + 11O_2 + 2H_2O = 4FeSO_4 + 4HAsO_2 \quad \text{(Eq. 2.18)}$$

The direct oxidation is assumed to produce ferrous sulphate and arsenious acid. The main species of this oxidation are iron(II), arsenic(III) and sulphur(VI).

Indirect mechanism

The ferrous sulphate produced by the direct attack of the minerals is oxidised to ferric sulphate. The ferric sulphate thus produced by bacteria aids in the rapid dissolution of pyrite and arsenopyrite. Elemental sulphur is also oxidised to sulphuric acid. The equations below summarise these oxidation stages:

$$4FeSO_4 + 2H_2SO_4 + O_2 = 2Fe_2(SO_4)_3 + H_2O \quad \text{(Eq. 2.19)}$$

$$FeS_2 + Fe_2(SO_4)_3 = 3FeSO_4 + S \quad \text{(Eq. 2.20)}$$

$$4FeAsS + 4Fe_2(SO_4)_3 + 6H_2O + 5O_2 = 4H_3AsO_4 + 12FeSO_4 + 4S \quad \text{(Eq. 2.21)}$$

$$2S + 2H_2O + 3O_2 = 2H_2SO_4 \quad \text{(Eq. 2.22)}$$

Similarly the trivalent arsenic species produced by the direct attack is also believed to be oxidised to arsenic(V) as shown below:

$$HAsO_2 + Fe_2(SO_4)_3 + 2H_2O = H_3AsO_4 + FeSO_4 + H_2SO_4 \quad \text{(Eq. 2.23)}$$

The bacterially generated acid ferric sulphate solution not only leaches pyrite and arsenopyrite but also acts as a leachant for other sulphide and non-sulphide minerals whose presence may inhibit gold extraction from ore. As the pyrite and arsenopyrite minerals break down during these reactions the encapsulated gold particles in the mineral phases, no matter how fine, are wholly or partially released and may subsequently be recovered subsequent cyanidation step.

The above mechanisms are important to the understanding of bacterial attack of sulphide minerals because they identify intermediate species. These species are neither initial reactants or final products of bio-oxidation reactions. In this instance the intermediate phases are iron(II), arsenic(III) and intermediate sulphur species are involved as well. It is important to note that in order to arrive at a conclusive mechanism a number of factors should be taken into account in addition to identification of intermediate species.

2.3.5 Factor important to the kinetic of bacterial oxidation mechanisms

The mechanism of any reaction can often be deduced from its rate law. In general terms the order of any reaction in relation to the rate and concentration of the species involved can be expressed by the equation of the type:

$$Rate = [Reactant,\ Product\ or\ Catalyst]^{order} \quad \text{(Eq. 2.24)}$$

The order of the reaction varies from fractional to whole number or even zero (when the rate of the reaction is independent of the concentration of the species). The rate law for any system is essentially empirical and can not be deduced from the stoichiometric equation representing the overall process. Once the rate law of a reaction has been established some mechanistic deductions may be attempted. The crucial part of the deductive process is the interpretation of which molecules (or ions or surface or bacteria) participate in the rate determining step. This is the slowest step of the reaction sometimes referred to as rate limiting in the literature. Like any other chemical reaction bacterial oxidation reactions are far from simple. The various rate processes which contribute to the bacterial oxidation of minerals fall into the following categories **[103]**:

Dissolution of gases in aqueous solution and their aqueous transport

The two most important gases in bio-oxidation are oxygen and carbon dioxide. Oxygen is utilised as an oxidant while carbon dioxide supplies the bacteria with their carbon requirements. The dissolution of these gases into the aqueous phase and their subsequent transportation to the reaction sites is of paramount importance. Gas requirement is one of the most important factors considered in the design of microbiological leaching reactors **[84, 96, 123-125]**. Norris **[96]** investigated the requirements of enriching the air supply of bacterial oxidation process with carbon dioxide. He found that carbon dioxide had very little effect on the activity of the bacteria. This was probably due to the fact that the natural carbon dioxide content of the air was enough for the bacterial requirements. No experiment was done in which carbon dioxide was completely eliminated.

Oxygen transfer to *Thiobaccillus* cultures has been studied **[126-127]**. Lui et al., **[127]** found that dissolved oxygen is rate limiting if its concentration is less than 1.0 mg/L. The gas transfer limitation of a bio-oxidation process dictates the pulp density to be used. The oxygen transfer rate is given by the product of the mass transfer coefficient, K_L, the effective area of the gas-liquid interface surface, a and the concentration difference **[128]**:

$$OTR = K_L.a.(C^* - C) \qquad \text{(Eq. 2.26)}$$

where OTR is the oxygen transfer rate, C^* is the saturated dissolved oxygen concentration and C is the liquor dissolved oxygen concentration. C^* depends on the concentration of oxygen that is being sparged as well as the operating temperature and pressure of the reactor.

Bacterial growth

The growth of bacteria inoculated into a system undergoes some changes as indicated in Figure 2.8. Four distinct stages can be distinguished on the growth curve. Lag phase: several explanations have been given for this period, the need for the presence in the medium of substances excreted by microorganisms, adaptation to the new environment and setting up internal states of molecules (enzymes, RNA, ribosomes) essential for cell growth and maintenance.

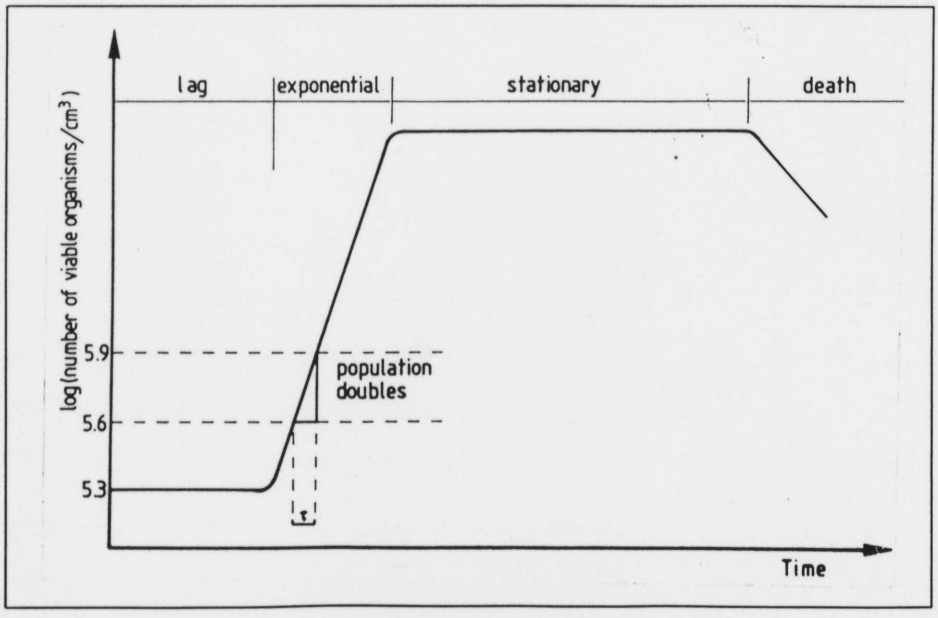


Figure 2.8: Typical growth curve for batch cultivation of bacterial population showing the various phases **[125]**.

During the growth period, the bacterial population increases exponentially as the bacteria multiply by binary division. As the population continues to grow the composition of the culture is modified due to the depletion of nutrients, accumulation of

bacterial metabolism products, change in pH and a decrease in oxygen and carbon dioxide availability. For a period of time the rate of death of bacteria will be equal to the rate of growth and this is called the stationary phase. The last phase is the death period where the population of the bacteria continually decreases. Studies into the growth kinetics of *Thiobacillus ferrooxidans* and other iron and sulphur oxidising bacteria have been carried out **[129-133]**. Failure to maintain the bacterial culture in a growth phase will result in loss of activity.

Bacterial attachment to the mineral surface

It has been shown that during bacterial oxidation of minerals it is essential for the bacteria to attach to the mineral surfaces. Whether the nature of the attachment process is permanent or temporary is still a subject of research. There have been recent publications on this subject **[134-135]**. Monroy-Fernandez et al., **[134]** found that the attachment of bacteria to the mineral surfaces promotes the initial oxidation of arsenopyrite and the release of arsenic(III) and iron(II) into solution. Arsenopyrite surfaces were rapidly coated by the oxidation products, which included elemental sulphur and ferric arsenates.

The attachment/detachment processes of bacteria on the mineral surface are normally dealt with by using the Langmuir approach **[136]** of considering the bacteria populating the mineral surface by an adsorption mechanism. If the fraction of the mineral surface already populated by bacteria is ϑ, the fraction of the available surface is $1-\vartheta$. The rate of attachment of bacteria to the mineral surface depends upon the number of bacteria in solution, B, and the fraction of available surface. The rate of attachment may be expressed as:

$$\textit{Rate of attachment} = k_a B(1-\vartheta) \qquad \text{(Eq. 2.27)}$$

where k_a is the rate constant for the attachment process. The rate of detachment will depend upon the surface covered by bacteria and may be expressed as follows:

$$Rate\ of\ detachment = k_d\vartheta \qquad \text{(Eq. 2.28)}$$

where k_d is the rate constant for the detachment process. At equilibrium the two rates are equal and solving for ϑ, gives:

$$\vartheta = k_aB/(k_aB + k_d) \qquad \text{(Eq. 2.29)}$$

During bacterial oxidation the value of B is sufficiently high such that any new surface will be immediately populated, this is consistent with the value of ϑ tending to unity as the value of B increases. The attachment process during bacterial leaching is normally sufficiently rapid for the process not to be rate determining.

Table 2.3: Summary of the evolution of bacterial populations, superficial and precipitated species, corrosion patterns and chemical reactions during the oxidation of arsenopyrite by *Thiobacillus ferrooxidans*: (0) nil or nondetectable; (-) decrease; (=) stationary or with no significant evolution; (+) increase (++) strong increase **[134]**.

BACTERIAL POPULATIONS	SOLUTION					MINERAL				CHEMICAL REACTIONS
	Fe^{II}	Fe^{III}	As^{III}	As^{V}	pH	surface $FeAsO_4$	S^0	precipited $FeAsO_4$	Corrosion	
• Exponential growth phase of adhering bacteria • Log phase of free bacteria adhering bacteria 80% free bacteria 20%	++	0	++	0	-	+	+	0	Corrosion patterns related to the fragility zones and to the crystallographic orientations	Equation 1 : $4FeAsS + 3O_2 + 2H_2O \rightarrow 4Fe^{2+} + 4HAsO_2 + 4S^0_{(surface)}$ Equation 2 : $2S^0_{(surface)} + 3O_2 + 2H_2O \rightarrow 2SO_4^{2-} + 4H^+$
• Beginning of stationary phase of adhering bacteria • Exponential growth phase of free bacteria adhering bact. 45-75% free bacteria 15-55%	-	++	+	++	++	++	+	+	Isotropic distribution of corrosion patterns related to the crystallographic orientations	Eq. 3 : $4Fe^{2+} + 4H^+ + O_2 \rightarrow 4Fe^{3+} + 2H_2O$ Eq. 4: $FeAsS + 7Fe^{3+} + 4H_2O \rightarrow H_3AsO_4 + 8Fe^{2+} + S^0_{(surf.)} + 5H^+$ Eq. 5 : $HAsO_2 + 2Fe^{3+} + 2H_2O \rightarrow H_3AsO_4 + 2Fe^{2+} + 2H^+$ Equation 6 : $H_3AsO_4 + Fe^{3+} \rightarrow FeAsO_{4(surface)} + 3H^+$
• Stationary phase of adhering and free bacteria adhering bacteria <10% free bacteria > 90%	++	+	++	+	=	+	++	++	Decrease of particle size in reason of isotropic distribution of corrosion	Equation 4 $FeAsS + 7Fe^{3+} + 4H_2O \rightarrow H_3AsO_4 + 8Fe^{2+} + S^0_{(surface)} + 5H^+$ Equation 7 : $H_3AsO_4 + Fe^{3+} \rightarrow FeAsO_{4(precipited)} + 3H^+$

Surface products may control the bio-leaching rate and the evolution of the different stages of biooxidation process, consequently regulating the overall biooxidation

chemical processes on grain surfaces. Table 2.3 gives some of the major steps which were identified during the oxidation of arsenopyrite.

Aqueous transport of inorganic solutes and their integration with bacteria

The important inorganic solutes encountered during bio-oxidation processes are iron(II), arsenic(III), iron(III), arsenic(V), sulphur(VI) and nutrient ions which are essential for bacterial growth and maintenance. Diffusion of reactants and reaction products to and from reaction sites (on the bacteria surface) is an important consideration with regard to the bacterial oxidative activity, growth and maintenance. A build-up of reaction products in sites where the bacteria are attached to the mineral surface may inhibit bacterial oxidation of the minerals.

Bacterially catalysed stages

Chemical oxidation rates of pyrite and arsenopyrite are considerably slower than their bacterial oxidation rate **[103]**. As a result, it appears that the true chemical oxidation during bacterial leaching may be considered to account for a very small percentage of the overall reaction. It is therefore possible to identify the reaction stages in which the bacteria participate as a catalyst. The mechanisms of such stages, i.e. how the bacteria carry out the catalysis, are extremely complicated and not well understood.

Primary processes

Barrett et al. **[103, 137]** have divided the mechanism of pyrite and arsenopyrite oxidation into primary processes and secondary processes. They proposed that the primary processes include the bacterially mediated oxidation of the arsenopyrite/pyrite substrate by oxygen and/or iron(III) to give arsenic(III) and sulphur(VI) as products, with the solubilisation of iron(II). Several models have been proposed for the oxidation of pyrite and arsenopyrite **[103, 134, 138]**. The primary processes of bacterial oxidation of pyrite and arsenopyrite may be represented by the equations:

$$\mathrm{FeAsS} \xrightarrow[\text{Bacteria}]{\text{Oxygen/iron (III)}} \mathrm{Fe\,(II) + As\,(III) + S(VI)} \qquad \text{(Eq. 2.30)}$$

$$FeS_2 \xrightarrow[\text{Bacteria}]{\text{Oxygen/iron (III)}} \text{Fe (II)} + \text{S(VI)} \qquad \text{(Eq. 2.31)}$$

The reaction paths of these processes are far from simple and are considered to occur in several stages. The diagram in Figure 2.9 is a model proposed by Ingledew **[138]**, to explain how the process of electron transport to oxygen is coupled to oxidative phosphorylation (the process of ATP regeneration in the respiratory chain) in *Thiobacillus ferrooxidans*.

Secondary processes

The iron(II) and the arsenic(III) produced in the primary processes are oxidised to iron(III) and arsenic(V) in secondary bacterially catalysed processes. Oxygen must be the oxidant for iron(II). Iron(III) is the oxidant for arsenic(III), with the pyrite surfaces also participating. The secondary processes can be represented by the equations below:

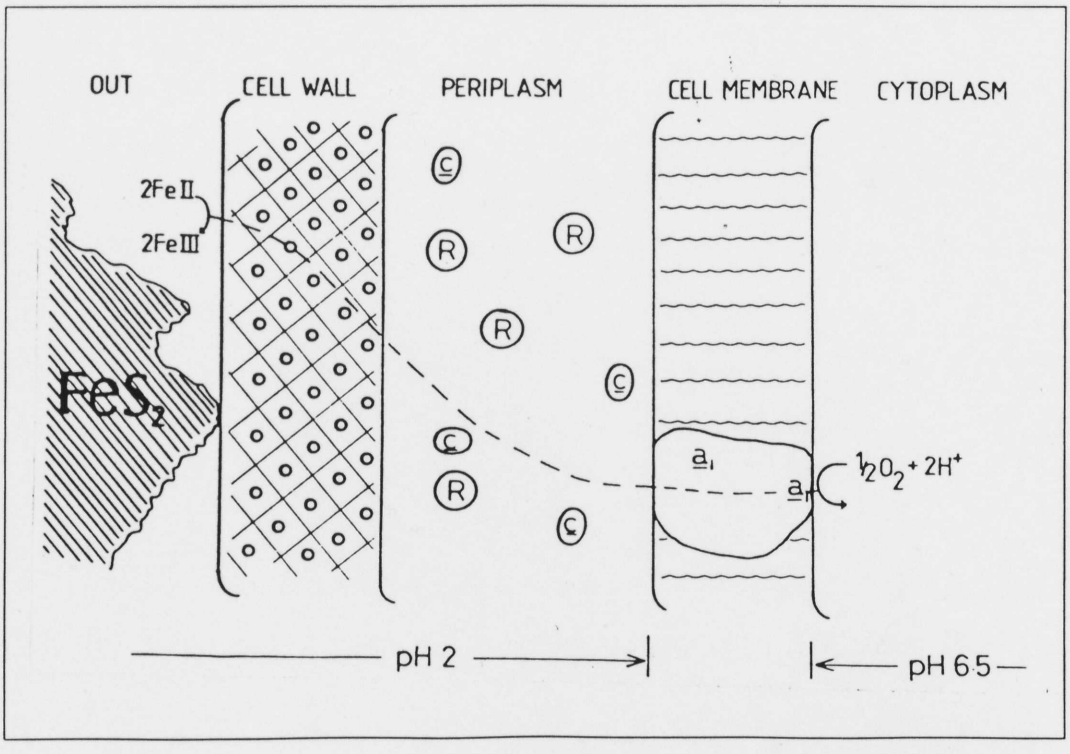


Figure 2.9: A diagrammatic representation of *Thiobacillus ferrooxidans* in the native environment (leaching pyritic ore). R represents rusticyanin; c represents cytochrome, the small circles in the cell wall represent bound Fe(III) **[138]**.

$$Fe(II) \xrightarrow[\text{Bacteria}]{\text{Oxygen}} Fe(III) \qquad \text{(Eq. 2.32)}$$

$$As(III) \xrightarrow[\text{Bacteria}]{\text{Iron (III)/pyrite}} As(V) \qquad \text{(Eq. 2.33)}$$

The oxidation of iron(II) is catalysed by the bacteria and takes place in the bulk solution, while the oxidation of arsenic(III) is catalysed by pyrite and bacterial cells in the presence of iron(III). The diagrammatical representation secondary processes taking place during oxidation of arsenic(III) are shown in Figure 2.10. Modification into mechanisms will take place as further experimental results or evidence become available. While Barrett at al. **[103]** suggested that sulphur is oxidised to sulphur(VI), Monroy-Fernandez et al., **[134]** proposed the formation of elemental sulphur in the bacterial oxidation of arsenopyrite by *Thiobacillus ferrooxidans*.

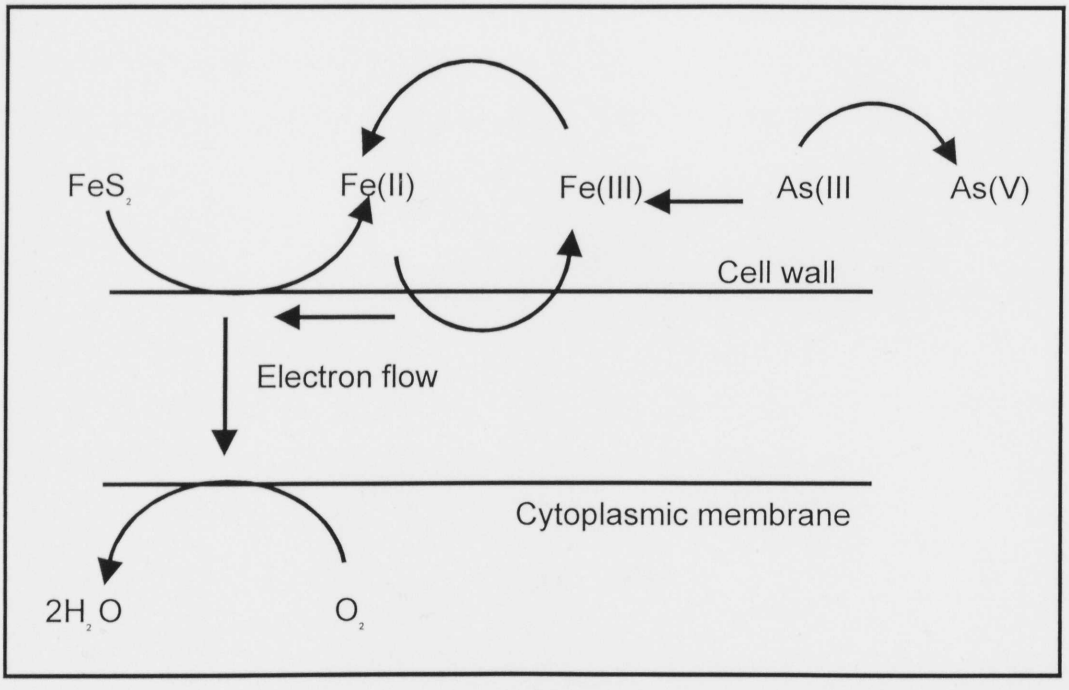


Figure 2.10: A diagrammatic representation of the secondary oxidation of arsenic(III) during bacterial leaching **[103].**

The bacterially generated ferric sulphate acts as a leachant for the arsenopyrite and pyrite, thus generating more ferrous and arsenious acid. In contrast to the above

mechanisms, some authors have proposed that bacterial oxidation of arsenopyrite produces a mixture of all the oxidation states involved in the primary and secondary processes **[139]**, while Iglesias and Carranza **[116]** proposed the direct formation of arsenic acid. According to Panin et al., **[139]** direct bacterial oxidation of arsenopyrite can result in the formation of As(III) and As(V) and ferrous sulphate as shown in equations (Eq. 2.16) and (Eq. 2.18):

Another suggested route for the oxidation of As(III) produced by the direct or indirect oxidation of arsenopyrite is by biologically generated ferric sulphate and oxygen according to the equations (Eq. 2.23) and (Eq. 2.34):

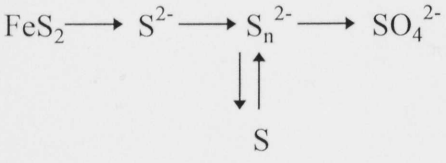
$$2HAsO_2 + O_2 + 2H_2O = 2H_3AsO_4 \qquad \text{(Eq. 2.34)}$$

Despite the modifications to the mechanism of arsenopyrite attack proposed by Barrett at al. **[103]**, some authors continue to consider the mechanism of bacterial attack as direct and indirect **[140-143]**. Examination of the mechanisms proposed shows some similarity in some of the products of oxidation of the minerals for instance the direct mechanism proposes the formation of arsenic(III) and iron(II) which are the same products identified in the primary processes. The major difference is between the indirect mechanism and the secondary processes. Kelly et al., **[88]** suggested that the terms 'direct' and 'indirect' are inadequate in describing pathways in the bacterial oxidation of minerals and their use should be discontinued. In the indirect mechanism it is thought that the bacterially generated iron(III) further oxidises pyrite and arsenopyrite, however Barrett et al., **[103]** have found that the abiotic chemical oxidation of pyrite with iron(III) is a very slow process in comparison to the bacterially catalysed reaction and therefore it must play an insignificant role in the total process. It is also thought that the oxidation of arsenic(III) to arsenic(V) takes place indirectly by bacterially generated iron(III) **[112, 144, 140-143]** and this contradicts the finding of Barrett et al., **[103]** who found that bacteria and pyrite catalysed the oxidation of arsenic(III).

Oxidation of inorganic sulphur

The above mechanisms of bacterial oxidation of pyrite and arsenopyrite generates many of the possible species of iron and arsenic that may be formed with very little information on sulphur species. However the behaviour of inorganic sulphur and its compounds is not clear due to lack of microanalytical techniques for the determination of sulphur compounds and furthermore there is a tendency of many of the species formed to undergo secondary chemical changes especially in acidic conditions that prevail during bioleaching.

The oxidation mechanisms of inorganic sulphur and its compounds by *Thiobacilli* has been reviewed by Kelly **[145-146]** and relatively few enzymes with well-defined functions have been demonstrated in *Thiobacilli* to be positively involved in inorganic sulphur oxidation. Since sulphur is present as sulphide in the minerals pyrite and arsenopyrite, Figure 2.11 show that the oxidation of sulphide can result in the formation of elementary sulphur and thiosulphate. This is a more feasible mechanism because it involves transfer less electrons compared to direct formation of sulphate. Analysis of intermediate sulphur oxidation products during the oxidation of various substrates (elemental sulphur, pyrite and roasted pyrite) by mixed culture dominated by *Thiobacillus ferrooxidans* revealed the presence of polysulphide sulphur in all the three substrates **[147]**. After further experiments were carried out using polysulphide sulphur, it was found that polysulphide sulphur was used as a source of energy for the growth of the bacteria and the pathway for the oxidation of sulphide sulphur was proposed as shown by the equation below:



(Eq. 2.35)

The bacterial degradation of pyrite has been shown to produce thiosulphate **[148]** in the first step according to the equation:

$$FeS_2 + 6\ Fe(H_2O)_6^{3+} + 3\ H_2O = 7\ Fe(H_2O)_6^{2+} + S_2O_3^{2-} + 6\ H^+ \qquad \text{(Eq. 2.36)}$$

It is important to note that thiosulphate will be very unstable in the highly acidic envirnment encountered during bacterial leaching and its determination will be difficult. It was demonstrated that the thiosulphate produced by the above reaction is oxidised to tetrathionate with the concomitant reduction of iron(III) as shown in the equation:

$$2\ S_2O_3^{2-} + 2\ Fe^{3+} = 2\ FeS_2O_3^{+} \longrightarrow 2\ Fe^{2+} + S_4O_6^{2-} \qquad \text{(Eq. 2.37)}$$

The above equation was found to compete with the following equation:

$$S_2O_3^{2-} + H^+ \longrightarrow S^0 + HSO_3^- \qquad \text{(Eq. 2.38)}$$

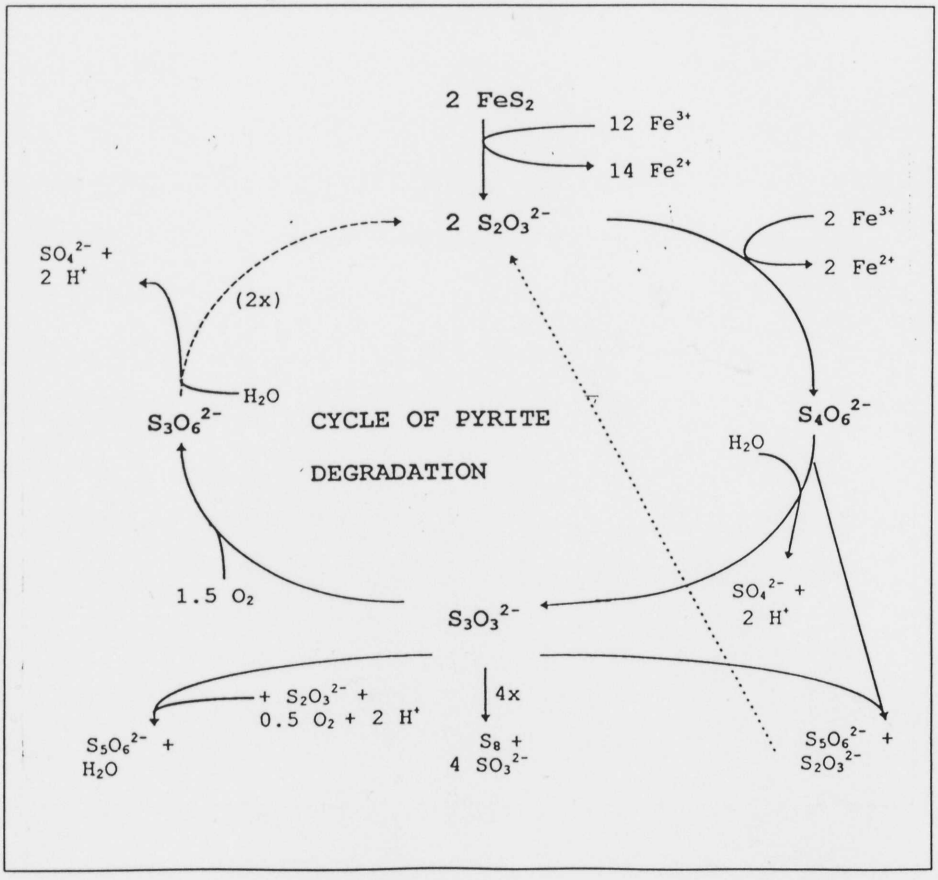


Figure 2.11: Cyclic degradation mechanism of pyrite **[148]**.

Figure 2.11 shows the diagrammatic representation of the degradation of pyrite and the various sulphur intermediate species formed during the process. The dissociation of thiosulphate to produce elemental sulphur makes it difficult to quantify the rate of bacterial oxidation as measured by the oxidation of sulphur. Some researchers **[134]** haveidentified elemental sulphur during bacterial oxidation and concluded that the decomposition of pyrite and arsenopyrite produces elemental sulphur. This sulphur could be a result of the decomposition of the thiosulphate in the highly acidic environment as shown above (Eq. 2.38).

2.3.6 Toxicity effects of metals and resistance mechanism

One of the unusual characteristic of acidophilic chemolithoautotrophic bacteria is their high resistance to toxic metal ions compared to that shown by other bacteria. Norris and Kelly **[149]** outlined the principle underlying the resistance mechanism of bacteria to metal ions. The toxicity of a metal depends upon the physiological state of the bacteria and the speciation of the metal ions which govern their bio-availability. The high resistance of bacteria to metal ions has been explained by physiological or genetic properties of the bacteria **[150-152]**. There is a problem in actually defining the concentrations that distinguish metal-resistant from metal-sensitive bacteria, standard concentrations have not been universally proposed and /or accepted by the scientific community. As a result the metal tolerance of the same species of bacteria have been found to vary when reported by various researchers.

Most metal resistance in bacteria has been attributed to encoding by genes located on the plasmids. The four basic mechanisms by which plasmids encode for metal resistance have been described as **[153]**: inactivation of metals, alteration of the sites of inhibition, impermeability of the metal(s) and metal bypass mechanism. In addition there are many physical, chemical and biological factors that influence metal resistance. It has also been suggested that bacteria may protect themselves from the toxic effect of metals by the production of polysaccharides (slimes) which prevent excess uptake and by the production of low molecular weight binding peptides (phytochelatins) **[154]**.

Barrett et al., **[103]** explained the tolerance of bacteria to high metal ion concentrations in terms of chemical properties associated with their growth. Resistance was attributed to the following factors: the low pH value of their optimal growth media, which results in protonation of anionic sites on cell walls which are then less available for the binding of toxic metal cations; the presence of anions such as phosphate and arsenate which may lead to the precipitation of metal ions or their conversion into less bioavailable complexes; the presence of organic ligands secreted by cells or released from dead cells which may complex metal ions and decrease their bio-availability; and the presence of substances which compete with, and thereby alleviating the toxicity of, toxic metal or metalloid species, for example the phosphate ion decreases toxicity of the arsenate ion **[151]**, and the potassium ion that of the thallium(I) ion.

High concentrations of dissolved arsenic inhibit bacterial growth. In particular arsenic(III) has been found to be more toxic than arsenic(V) to *Thiobacillus ferrooxidans* and *Thiobacillus thiooxidans* **[155]**. Barrett et al., **[156]** reported that major toxic effects to *moderately thermophilic* bacteria were observed at arsenic(III) concentrations of 30 mM, while concentrations up to 90 mM were found in dead cultures. The mixed culture used in commercial BIOX operations has been found to be more resistant to arsenic(V) than arsenic(III) **[157]**. Inoculation of systems containing pyrite and arsenic(III) resulted in a long lag phase in the oxidation of pyrite and it was also suggested that arsenic(III) was approximately two to three times more toxic than arsenic(V). It was however pointed that some of the arsenic(III) was oxidised to arsenic(V) in the experiment reported and as a result the concentration of arsenic(III) may subsequently be diminished towards the later stages of the experiment, consequently underestimating arsenic(III) toxicity. It has been suggested that the lag phase may be due to the period needed during which membrane-associated enzyme-protecting systems develop, or this lag phase may be when the selection of metal-tolerant cells takes place **[158]**. In addition to the observations of the toxicity levels of arsenic(III) and arsenic(V) made by some researchers **[155, 1158]**, Breed et al., **[157]** recently observed that the nature of arsenic(III) and arsenic(V) toxicity was different to a mixed culture of *Thiobacillus ferrooxidans* and *Thiobacillus thiooxidans*. They found

that the addition of a culture to a slurry containing arsenic(III) resulted in a reduced rate of bacterial oxidation while the addition of arsenic(V) resulted in both a lag phase and reduced rate of bacterial oxidation. Their results also suggested that the toxicity of arsenic(III) was not necessarily in the region of two to three times that of arsenic(V) as previously suggested.

Arsenic(III) has been found to inactivate enzymes with thiol (HS) groups at the active centre **[159]**, resulting in carbohydrate depletion and diminished glutathione (GSH) **[160]**. The toxic effect of arsenic(V) arises from its similarity to inorganic phosphate although it has been reported as the least toxic form of inorganic arsenic. Arsenic(V) replaces the phosphate in adenosine tri-phosphate (ATP) to form an unstable ADP-arsenate complex **[159]**. Arsenic resistance in bacteria may be plasmid-borne or located chromosomally **[161-163]**. Chromosomal arsenate resistance reduces the amount of arsenate entering the cell via the phosphate transport system **[151, 159, 164]**. According to Silver et al., **[151]** plasmids in both *Escherichia coli* and *Staphylococcus aureus* contain an 'aperon' that confers resistance to arsenate, arsenite and antimony(III) salts. All three species, arsenate, arsenite and antimony(III) were inducers. Mutants and cloned deoxyribonucleic acid fragments from plasmid (pI258) in *S. aureus* lost arsenate resistance but retained resistances to arsenite and antimony(III), demonstrating that separate genes are involved. There was no mechanism for arsenite resistance but the arsenite was not oxidised to arsenate which is believed to be less toxic.

Some metal ions have been found to act as catalysts especially in the bioleaching of chalcopyrite **[165, 166]**. Mier et al., **[167]** outlined the mechanism of catalysis using silver and bismuth ions. Different modes of catalysis were found, silver reacted with the surface of the chalcopyrite to form a layer of silver sulphide. This layer caused the passivation of the mineral in places with a deposit and promoted anodic behaviour of the surfaces not covered. On the other hand bismuth acted in solution and prevented the formation of phosphate complexes of ferric ion by precipitating a bismuth phosphate, so increasing the oxidising potential of the redox couple Fe^{3+}/Fe^{2+}. These catalysts were not tested on arsenopyritic ore and they might have different effects.

The oxidation of arsenic(III) to arsenic(V) has been suggested to be a resistance mechanism towards the toxicity effects of arsenic(III) **[161-162]** and has been reported to occur in some organisms **[155, 168-169]**. Evidence has been provided for the direct oxidation of arsenic(III) to arsenic(V) by an acidophilic organism isolated from acid mine drainage from a pyritic mine **[168]**. Arsenic(III) in a water sample was almost completely oxidised to arsenic(V) in 5 days when the bacteria were incubated at 30°C. Arsenic(III) was not oxidised in a water sample incubated at 4°C confirming that the oxidation was due to bacterial activity. Further evidence for bacterial activity was provided by the fact that no arsenic(III) oxidation occurred in either the water sample filtered through a 0.2 μm membrane or that containing toluene. However these bacteria could not oxidise ferrous iron and elemental sulphur as a sole energy source. Sehlin and Lindrom **[155]** have provided evidence for the oxidation of arsenic(III) to arsenic(V) by the mineral leaching arcchaebacterium *Sulfolobus acidocaldarius* strain BC. Arsenic(III) oxidation was 8-fold higher for cells grown in the presence of arsenic(III) when compared with cells grown without arsenic(III), they **[155]** also provided evidence for the enzymatic nature of arsenic(III) oxidation by *S. acidocaldarius* strain BC. *Thiobacillus ferrooxidans*, *Thiobacillus thiooxidans* and a mixed culture of *Moderately thermophilic* bacteria **[156, 168, 170]**, were not capable of oxidising arsenic(III) to arsenic(V), nor could they use arsenic(III) as a source of energy. Even the acdidophilic organism which was found to be capable of oxidising arsenic(III) to arsenic(V) could not derive energy for growth from the oxidation of arsenic(III) **[168]**.

To date the mechanism of arsenic resistance in acidophilic chemoautotrophs has not been determined although it has been claimed that arsenic resistance in *Thiobacillus ferrooxidans* is plasmid borne **[171]**.

Thiobacillus ferrooxidans and other iron and sulphur oxidising bacteria have been found to adapt very well to high metal ion concentrations in solution **[75, 172]**. Spencer et al. **[173]** reported a tolerance level of 25 g/L arsenic for a thermophilic bacteria culture during oxidation of a refractory arsenopyrite concentrate. For quantitative conclusions to be made on the level of tolerance of bacteria to metal ions, it is important to obtain

consistent results for the toxicities of metal ions towards the range of bacteria used in biohydrometallurgy. Different authors have reported different levels of tolerance on the same species of bacteria.

2.4 Conclusions

The acceptability of bacterial oxidation processes will be largely determined by long-term stability of the residues. There is evidence that biooxidation of arsenical ores produces a mixture of arsenic(III) and arsenic(V). Salts of the latter are much more stable for subsequent environmental disposal and therefore it is important that all the arsenic reports as arsenic(V) at the end of the oxidation stage. This literature review has shown that there is there are very few reports published which address the problem of arsenic speciation in the bacterial oxidation of arsenic-bearing gold ores.

The influence of mineralogical composition of arsenical ores on the speciation arsenic in bacterial leaching has not been extensively investigated. This area has been further complicated by the controversy in the mechanism of bacterial oxidation of arsenopyrite. The most prevalent mechanism in the literature has been the direct and the indirect mechanism which assumes that ferric ions produced during the process is responsible for the oxidation of arsenic(III) to arsenic(V). However there has been a recent proposed mechanism which divided the mechanisms into primary and secondary processes, this mechanism states that the oxidation of arsenic(III) is occurs in the presence of bacteria and with pyrite acting as a catalyst. There is need to undertake a comparative study of arsenic speciation in bacterial oxidation of different ores in order to understand the effect of mineralogy and the subsequent speciation of arsenic and also to further elucidate the mechanism of bacterial oxidation.

The stability of solid biooxidation residues need to be assessed from a mineralogical composition point of view. The role of bacterial oxidation solution chemistry of arsenic and precipitation needs to be addressed. There has been very little published information on the stability of the resulting bacterial oxidation solid residues, most data refers to the stability of the neutralised bacterial leaching liquors.

CHAPTER THREE

MATERIALS AND EXPERIMENTAL METHODS

3.1 Introduction

Gold ores used

Five gold ores from different deposits which had different mineralogical compositions were used in this study. These were from the Indarama and Riverlea mines in Zimbabwe, the Akbakai mine in Kazakhstan, the Olympias mine in Greece and the Fairview mine in South Africa. Flotation concentrates from these mines were used in bacterial oxidation experiments. Two additional concentrates were also produced, one from the original Akbakai flotation concentrate and the other from composite ore sample from the Indarama mine.

Preparation of the Indarama B and the Akbakai A concentrates

The composite ore from the Indarama mine was concentrated by flotation prior to bioleaching tests. The ore was ground to -200μm, and 25% by weight solids content flotation pulps were prepared. The pH of the pulp was adjusted to 4.0 using sulphuric acid. The flotation was conducted using potassium amyl xanthate (1% solution) as a collector and pine oil as a frother. The flotation pulp was conditioned for 5 minutes and then floated for 1 minute. Part of the sample was preserved for mineralogical studies. For the second concentrate from the Akbakai mine, the received flotation concentrate was reflotated to get a cleaner concentrate using similar conditions as for the Indarama ore. The concentrates were washed to remove most of the flotation reagents before bacterial oxidation. The chemical analyses of the concentrates are given in Table 3.1.

Table 3.1: Chemical analyses of the flotation concentrates used in the study.

Sample Location	Sample Identity	Au (g/t)	wt% Fe	wt% As	wt% S
Akbakai mine	A	237	30.39	13.09	28.23
Akbakai mine	D	79	10.48	4.07	8.54
Indarama mine	B	225	26.55	17.28	20.75
Indarama mine	C	55	36.79	16.60	30.90
Olympias mine	O	32	38.84	7.61	40.77
Riverlea mine	R	67	27.46	9.47	23.23
Fairview mine	F	104	17.80	4.22	15.62

Note: The concentration of gold for the Akbakai concentrate A was estimated from that of the original concentrate (Akbakai D).

3.2 Mineralogical study

The study was effected on run-of-mine ore and the concentrates which were obtained from the commercial plants. Polished thin sections and standard polished sections were prepared for this study. These were subsequently studied under the petrographic microscope and mineral identifications were verified by the aid of scanning electron microprobe analyses. A further study was undertaken using ICP-laser ablation in order to ascertain whether the arsenopyrite contained a significant amount of solid solution or colloidal gold.

3.2.1 Optical microscopy

Optical microscopy was employed to determine the major minerals present and examine the occurrence of visible gold. The instrument used was a Lietz Ortholux Petrographic Microscope. This was also used for preliminary examination of mineralogical changes taking place during bacterial leaching. Polished sections of the pyrite/arsenopyrite concentrates were observed before and after being placed in biooxidation reactors for different periods of time. Polished sections of the biooxidation residues were also prepared and examined by the optical microscope to assess the degradation of the minerals after bacterial attack.

3.2.2 Scanning electron microscopy (SEM)-microprobe analyses

To verify the mineralogical identifications made by the optical microscope and also to locate inclusions of gold in minerals, a scanning microscope coupled with a microprobe (Jeol Superprobe 733 and Cameca SX-50) were used. The operating conditions of the Cameca SX-50 (Natural History Museum) were: accelerating voltage 15-25 kV and beam current 20-100 nA (on the Faraday cup). Standards used were pure metals and arsenopyrite of known composition. The radiations measured were: Fe Kα, S Kα, Au Lα, Sb Lα, Co Kα. The calculated minimum detection limits for trace elements were Au 200 ppm, Sb 100 ppm, Co 150 ppm. Backgrounds levels were carefully placed to avoid slopes, overlapping peaks and in the case of gold, a hole in the background between 31.5 and 31.6 on the LiF crystal used. The Cameca SX-50 was found to have a better detection limit than the Jeol Superprobe, as a result most of the quantitative data reported were measured on the Cameca SX-50. The operating conditions of the Jeol 733 were: accerating voltage 15 kV and beam current of 15-20 nA. Identifications were both qualitative and quantitative using the wavelength and energy dispersive modes.

The surface morphology of pyrite and arsenopyrite minerals before and after bacterial attack were examined with a Hitachi S-800 field emission scanning electron microscope to access the corrosion patterns on the surfaces of the partially leached crystals. The instrument was only used for imaging and the voltage setting was 8 kV. Samples were coated with a very thin gold/palladium coating (about 10 nm) and were not polished.

3.2.3 Laser ablation-ICP-AES

Laser Ablation coupled with Inductively Coupled Plasma Atomic Emission Spectrometer (ICP-AES) was used to characterise the invisible gold in arsenopyrite. The laser ablation ICP-AES system used was a Carl-Ziess Jena LMA 10 ruby laser microprobe coupled to an ARL 34000C simultaneous ICP atomic emission spectrometer (Figure 3.1) **[59]**. A transmitted light microscope was used to focus preselected areas of the sample which was held within a specially constructed perspex ablation chamber. A stream of argon gas was directed over the specimen, through the stage, and into the inlet of an ARL 34000C ICP-AES via a tenport teflon valve **[60]**. The flow of the carrier gas

was carefully controlled so that only small fragments of the ablated material from the sample was transferred to the plasma for analysis. Nebulised aqueous standards were used for calibration.

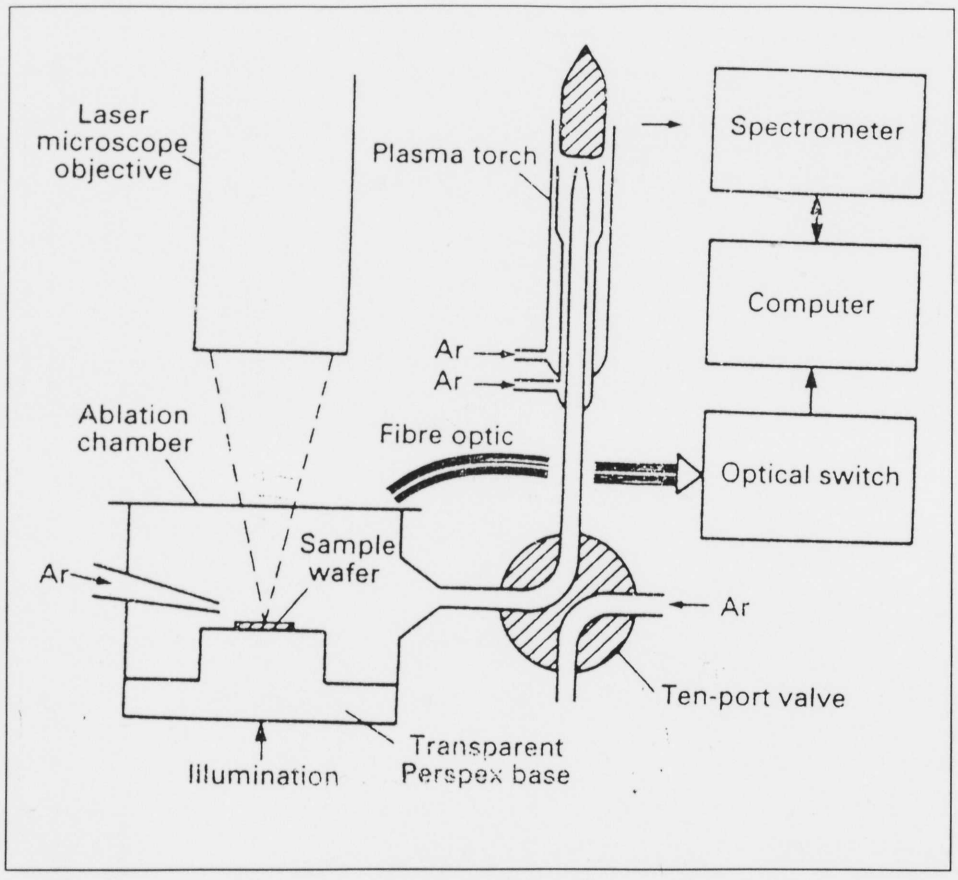


Figure 3.1: Schematic representation of laser-ICP system showing the ablation chamber and pathway of the Argon gas into the ICP **[59]**.

3.2.4 X-ray diffraction analysis

In order to verify whether the biooxidation precipitates in the solid residues were crystalline or amorphous, the mineral concentrates were examined by X-ray diffraction (XRD) before and after bacterial leaching. XRD was also important in identifying some of the gangue phase constituents of the concentrates. The equipment used throughout the work was a Phillips 1710 spectrometer using Cu Kα radiation with a setting of 40 kV and 40 mA.

3.3 Bacterial oxidation

Prior to use all the glassware was washed in concentrated hydrochloric acid before being rinsed in double distilled water. Concentrated hydrochloric acid was used in order to dissolve all residual precipitates adhering to the surfaces of the glassware.

3.3.1 Maintenance of bacterial culture and production of cell suspensions

The mixed culture of bacteria used in this experimental study was originally obtained from Prof. F.D. Pooley, at University College, Cardiff. The culture which is dominated by iron-oxidising *Thiobacillus ferrooxidans* is known to contain small numbers of *Leptosperillum ferrooxidans* [**144**], and has been shown to be adaptable to growth on ferrous sulphate and sulphur with a high tolerance to a range of soluble metals including iron, arsenic, copper and zinc.

The bacterial culture was routinely maintained by sub-culturing in an air-stirred pachuca with the temperature being controlled at 35°C by means of a water jacket. A 5L air-stirred pachuca was used to maintain the stock culture regularly to enable sufficient quantities of cells to be harvested for inoculation into the experiments. The pachuca was manufactured at University College, Cardiff and a schematic diagram of it is shown in Figure 3.2.

The pachuca reactor, which was made of perspex, consisted of a cylindrical outer vessel (A) equipped with an inner cylindrical column (B) whose top was situated just below the liquid level. The culture suspension was stirred and aerated by a stream of air bubbles produced from the sparger assembly (G) situated in the conical section of the reactor (F). The air was passed through a filter on its way into the reactor. The stream of air bubbles which was fed from the bottom of the vessel ensured rapid circulation of the culture suspension, up the inner and down the annular space and allowed transfer of oxygen and carbon dioxide to the leach medium for bacterial growth, as well as increasing the diffusion of leach products from the mineral surface to the bulk solution. The pH of the medium was determined by withdrawing 20 mL of the culture suspension from the reactor and measuring it with a bench pH meter. Water lost due to evaporation

was compensated for by the addition of distilled water. The pachuca was operated at a pulp density of 6-12 % (w/v) using the concentrates from the Olympias and the Indarama mines. The pH of the pachuca was initially adjusted to 1.8 and then allowed to drift to lower values as the oxidation of minerals proceeded (pH range 1.8 to 0.9). The free bacteria cells were harvested after 10-14 days.

Batch growth of the culture was also effected in 1L and 2L mechanically stirred flasks maintained at a temperature of 35°C in a thermostatically controlled water bath. Air was supplied via a sparger arrangement alongside the stirrer. The 9K nutrient medium of Silverman and Lundgren **[131]** with ferrous iron being substituted by pyrite/arsenopyrite concentrate at 6 % pulp density was made up with distilled water and had the composition shown in Table 3.2.

Table 3.2: Composition of the Silverman and Lundgren 9K nutrient medium **[131]**.

Constituent	Mass (g)
$(NH_4)_2SO_4$	3.00
KCl	0.10
$MgSO_4.7H_2O$	0.50
K_2HPO_4	0.50
$Ca(NO_3)_2$	0.01
Distilled water	up to 1L
H_2SO_4	to pH 1.8

Note: The initial pH adjusted to 1.8 prior to the addition of salts.

The contents of the pachuca which comprised of pyrite/arsenopyrite-grown cells was emptied into a 5 litre vessel and then allowed to stand for about 6 hours to enable the precipitates and the unreacted minerals to separate from the supernatant containing the free bacteria. The supernatant solution was carefully decanted into 500 mL polyethylene centrifuge bottles and the cells were recovered by centrifugation at 4800 x g for 30 minutes using a Wifug Laboratory Centrifuge. The resulting cell pellets were then

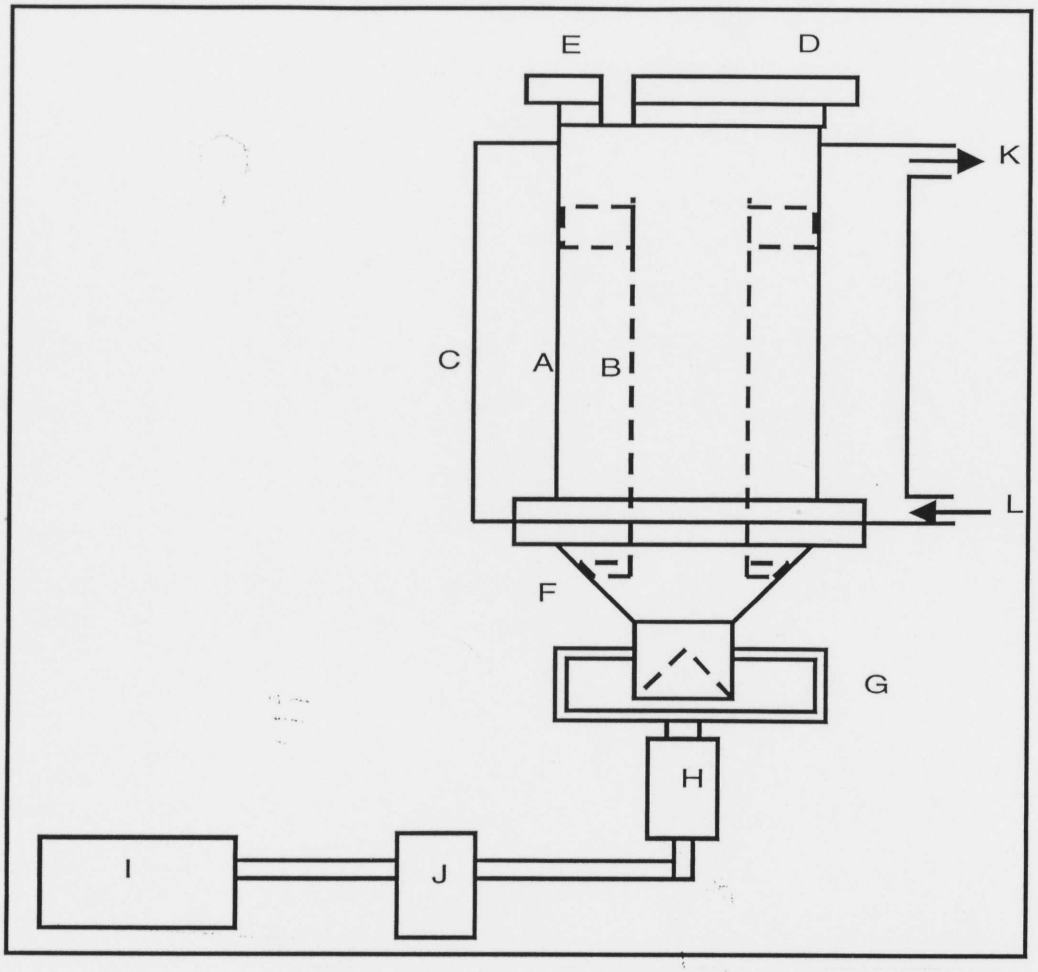


Figure 3.2: Diagrammatic representation of the air-stirred pachuca reactor and the ancillary equipment. A = Reactor vessel, B = Inner column, C = Water jacket, D = Reactor lid, E = Thermometer port, F = Conical lower section of reactor, G = Sparger assembly, H = Airflow rate meter, I = Compressor, J = Air filter, K = Water outlet and L = Water inlet.

suspended in 30-50 mL of 9K salts solution (pH = 1.8). Serial dilutions from this concentrated stock culture were used to inoculate the experimental flasks as soon as possible after harvesting. The cell were not stored for more than 1 week at 4°C. However it was found that the cells remained viable for at least a month when stored at the above temperature. The number of bacterial cells was estimated by direct microscopical counting using a Torma bacteria counting chamber. Serial dilutions of the concentrated cells were made in 9K salts (pH = 1.8) for counting purposes, 20-50 μL of the cell concentrates were diluted in 50-150 mL. A drop of the duluted cells was put on the counting chamber and the number of cells estimated on a phase contrast microscope

using the x1000 magnification objective. The counting chamber had grids of 0.02 mm depth and 1/400 mm^2 area. The number of cells in the grids as counted and the actual number of concentrated cells was calculated using the dilution factor. The final concentrated cell suspensions of the stock culture contained approximately 10^{11}-10^{12} cell/mL.

3.3.2 Shake flasks experiments

All the shake flask leach experiments were carried out in 500 mL Erlenmeyer flasks containing 250 mL of the culture suspension in an orbital incubator which was maintained at a temperature of 35°C and operated at a speed of 160 rpm. No external air was directly bubbled into the flasks, however the shaking action ensured both transfer of oxygen and carbon dioxide to the bacteria and solid-liquid mixing. Low pulp densities (less than 2 % w/v) were also used to ensure sufficient supply of oxygen and carbon dioxide. In the initial bacterial oxidation experiments 1-4 g of pyrite/arsenopyrite concentrates were used corresponding to pulp densities ranging from 0.4-1.6% (w/v). The pH of the pulp was adjusted to the test value during conditioning period prior to inoculation. An inoculum which introduced 1 x10^9 cells per mL of the pulp at the start of the experiment was used throughout this study **[147]**. The rate of water loss by evaporation was determined by measuring the weight loss of the control flask containing 250 mL of 9K salts which was run in conjunction with the leach test flasks. Correction for evaporation was made prior to sampling by using dilute H_2SO_4 (pH = 1.8). Samples (0.4 mL) were pipetted into Eppendorf test tubes (1.5mL) each day, acidified with concentrated hydrochloric acid (0.2 mL 36% w/v) and thoroughly mixed with a vortex type mixer. After centrifugation in an MSE bench top centrifuge (8000 x g, 120 s) the supernatant solution was then separated by pipetting and analysed for iron and arsenic (section 3.3.4).

3.3.3 Batch stirred flasks reactors

The batch leaching tests were carried out in 1-litre glass flasks with overhead stirrers and axial flow impellers (stirring rate 650 rpm) at 5 % pulp density. A schematic diagram of the arrangement is shown in Figure 3.3. Air saturated with water vapour was

sparged through the culture at the rate of 1-1.4 litres/min and temperature of the pulp was maintained at 35°C by means of a thermostatically controlled water bath. Samples of 50 g of the mineral concentrates were added to 900 mL of 9K nutrient medium solution and the pulp was conditioned until the temperature reached 35°C before being inoculated by 100 mL (10 % of the total volume) of the culture suspension, an inoculum which introduced 1 x 10^9 cells per mL of suspension at the start of the experiment. The pH was initially adjusted to 1.8 using sulphuric acid and was then allowed to drift freely to lower values as the oxidation of the minerals proceeded (pH range 1.8 to 0.9). The experiments were run for periods between 240-312 hours. In some experiments the pH was controlled using lithium hydroxide. An initial dissolved iron concentration was used in some experiments to investigate the effect of ferric sulphate additions.

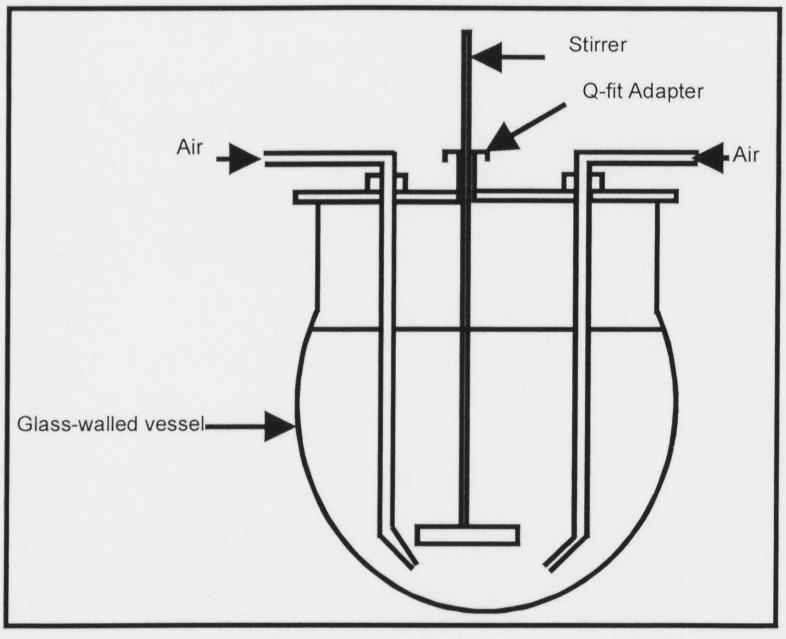


Figure 3.3: Schematic diagram of the mechanically stirred flask reactor vessel used for the biooxidation experiments.

Sampling of the vessel was carried out daily, for metal concentration, pulp potential and pH. A total of 0.8 mL sample of the pulp was removed in duplicate (2 x 0.4 mL) for determination of total metal concentrations and the species of iron and arsenic in the bioleaching slurry. One sample was acidified with concentrated HCl (50 % of the

aliquot volume), the samples were vortex-mixed and allowed to stand for 30 minutes to dissolve all the precipitates **[99]**. The samples were then centrifuged at 8000 rpm for 2 minutes and the supernatant solutions were analysed for total arsenic, total iron, iron(II) and arsenic(III) as detailed in section 3.3.4.

3.3.4 Metal/metalloid analysis

Total iron

The concentration of total iron in the biooxidation solutions was measured using a Perkin-Elmer 1100B Atomic Absorption Spectrophotometer, with an air/acetylene flame. Iron was measured at the absorption wavelength of 248.3, with a slit setting corresponding to a spectral band width of 0.2 nm and a lamp current of 30 mA. The calibration graph was obtained using standards 1-10 mg/L Fe.

Total arsenic

Determination of the total concentration of arsenic was done using the Atomic Absorption Spectrophotometer, with an air/acetylene flame, at an absorption wavelength of 193.8, with the aid of deuterium arc background correction and a slit setting corresponding to a spectral band width of 0.7 nm and lamp current 15 mA. The calibration curve was drawn using standards in the range 5-50 mg/L As.

ICP-AES

Total arsenic, iron, sulphur, antimony and other trace elements (Pb, Zn, Cu) were simultaneously determined by the ICP-AES. During the experiments, 0.2 mL of the supernatant solution after centrifugation of the bioleaching slurry was diluted in 9.8 mL 1M HCl for the above determinations.

Iron (II)

Iron(II) concentration was monitored colorimetrically using 1,10-phenanthroline **[174a]**. Standards were prepared using ferrous ammonium sulphate $[(NH_4)_2SO_4.FeSO_4.6H_2O]$. Acetate buffer was used to raise the pH of the standard to a value between 2 and 4, where the intensity of the iron(II)-phenanthroline complex is independent of acidity. A

solution (1 mL) of 1,10-phenanthroline (0.25 % w/v), prepared by dissolving in 50 mM sulphuric acid, was added to the buffered standard solution and was left to stand for 1 hour. The absorbance of the iron(II)-phenanthroline complex was then read at 515 nm. A linear calibration line was obtained with iron(II) concentrations in the range 1-10 mg/L as shown in Figure 3.4. Samples of the bioleach liquor (50 μL) acidified with concentrated hydrochloric acid were pipetted into sample tubes (20 mL), 10-20 mL acetate buffer was added followed by 1 mL solution of 1,10-phenanthroline. After an hour absorbance at 515 nm was measured using a Unicam UV 2 spectrophotometer.

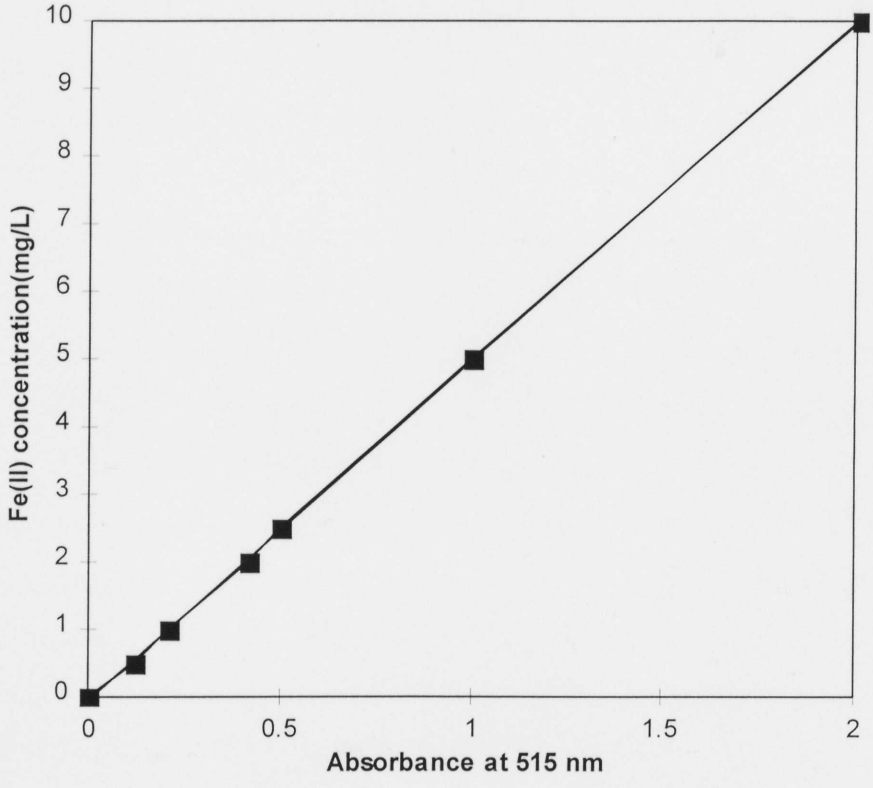


Figure 3.4: Calibration line used for Fe(II) determinations.

Arsenic (III)

The concentration of arsenic(III) during bacterial oxidation was monitored using differential pulse polarography at a dropping mercury electrode. Polarography is the study of current flowing in a conducting solution and the voltage applied to the dropping mercury electrode. Modern apparatus for polarography is shown in Figure 3.5.

The method offers distinct advantages when compared to other techniques for metal speciation determination **[174b]**:

(a) each fresh drop exposes a new mercury surface to the solution, thus preventing the accumulation of any products of electrolysis at the electrode,

(b) mercury forms amalgams with many metals, and it is easier to reduce most metals to their amalgams than to a solid state, and

(c) solid electrodes have surface irregularities and are easily passivated or poisoned but liquid mercury provides a smooth reproducible surface.

Applications of polarography are based on the measurement and interpretation of the current-potential curves as recorded at a dropping mercury electrode. The technique consists of applying a gradual increasing potential difference across the electrodes immersed in the solution under analysis, and measuring the current produced by the reduction of ions at the dropping mercury cathode or oxidation if the electrode is operating anodically. These currents are due to the migration of ions to the cathode in the electrical gradient set up, and to the diffusion of ions in the concentration gradient produced by the removal of ions in the proximity of the cathode. The latter current is proportional to the concentration and is therefore used in the polarographic method, the migration current can be readily suppressed by the supporting electrolyte. The variation of current as function of the continuously changing potential can be recorded by the instrument to give a polarogram. The potential axis is defined with respect to a reference electrode, in this work a Ag/AgCl electrode was used. A sigmoidal curve produced when a substance undergoes oxidation or reduction at the dropping mercury electrode is called a polarographic wave. A characteristic feature of the polarographic wave is the region in which the current after increasing sharply, becomes independent of the applied voltage, this constant current is called the limiting current, and this current is directly proportional to the concentration of the species in solution being reduced at the dropping mercury electrode and this is the reason for the polarographic method being widely applied in quantitative chemical analysis.

The conditions leading to the production of the limiting or diffusion current can be explained as follows. As ions are discharged at the mercury cathode their concentration in the immediate neighbourhood is reduced and this loss is compensated by the diffusion of ions from the bulk of the solution. The rate of this diffusion is governed by the difference in concentration between the ions in the cathode layer and in the remainder of the solution. As the applied voltage increases, the rate of diffusion also increases. Eventually, on increasing the applied voltage further, a condition is reached when the ions are discharged so rapidly that ion concentration in the cathode layer is zero, and the difference in concentration between the cathode layer and the rest of the solution in then simply equal to the concentration of ions in the bulk of the solution. Under these circumstances a steady rate of diffusion is set up giving rise to a steady diffusion current which is practically unaffected by further increases in the applied voltage.

The half wave potential ($E_{1/2}$), is another important parameter, that is, the potential on the polarographic wave at which the current reaches half of its limiting value. Although the wave height depends on the concentration, $E_{1/2}$ is frequently independent of the electroactive species. Differential polarography is the most sensitive and powerful of all the polarographic techniques. The current for each drop is measured twice, once just prior to the imposition of a pulse and once just before each drop is mechanically dislodged. Figure 3.6 shows typical polarograms which were obtained during analyses of As(III) in 1M HCl. The peak height is proportional to the concentration of the analyte as shown in Figure 3.7. The polarography of arsenic has been extensively reviewed **[175]**. Arsenic(III) exhibits two waves by differential pulse polarography in 1M hydrochloric acidic solutions. The first, at about -0.40 V versus a saturated calomel electrode, is due to the reduction of As(III) to elemental arsenic. The second wave, at approximately - 0.85 versus the saturated calomel electrode, arises from the further reduction of elemental arsenic to arsine, AsH_3. Arsenic(V) has been found to be electroactive in only one supporting electrolyte, that being 2M $HClO_4$/0.5M pyrogallol **[175]**.

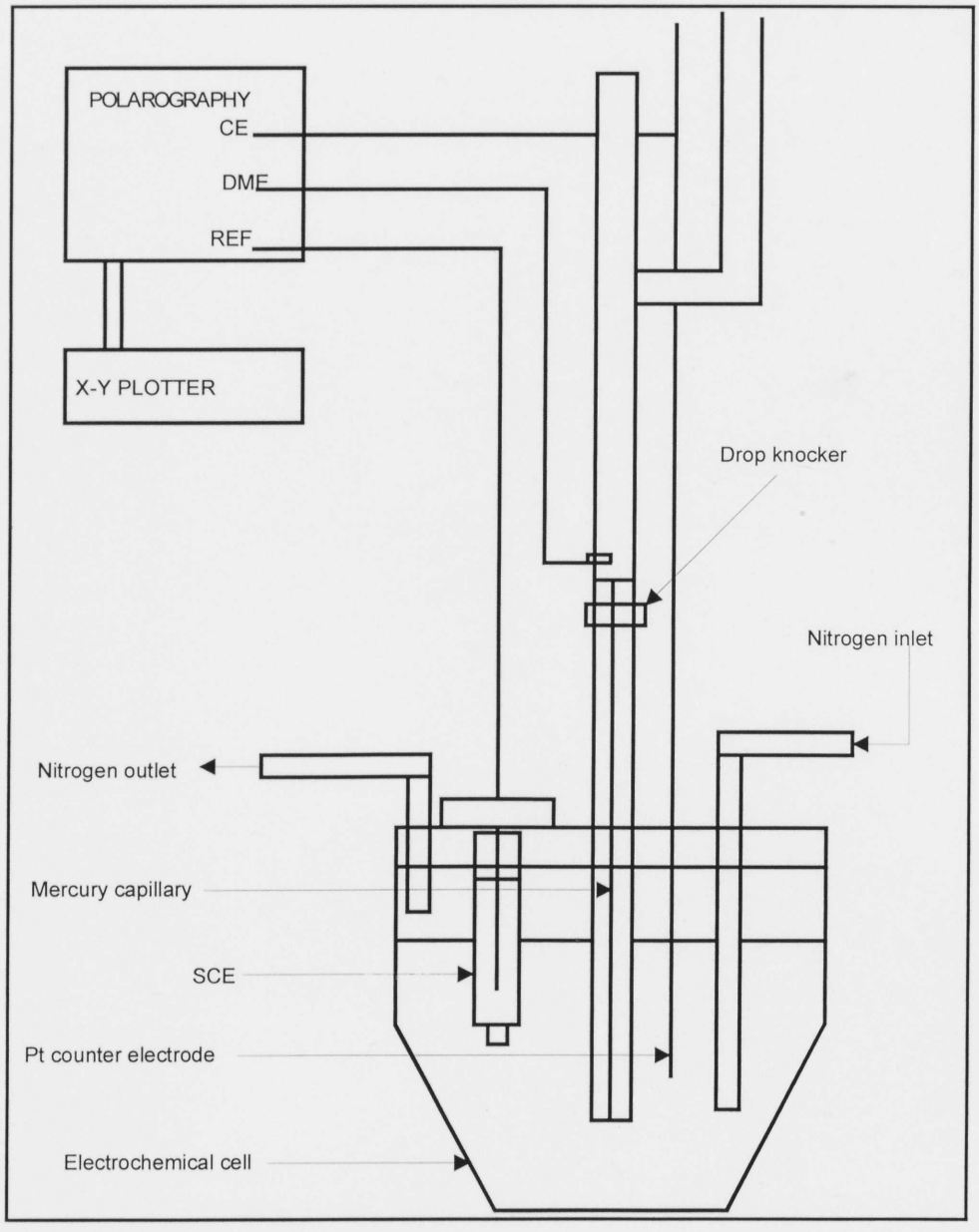


Figure 3.5: Schematic diagram of electrode assembly and cell for modern polarographic technique **[99]**.

The instrument used was an EG & G Princeton Applied Research Polarographic Analyser (Model 384) with a standard dropping mercury electrode (Model 303) and a Houston Digital Plotter.

Hydrochloric acid (10 mL, 1M) was dispensed into the electrolytic cell. After a baseline was drawn, 50-200μL samples from bio-leaching flasks were added. These samples had been acidified with concentrated hydrochloric acid soon after sampling and then

centrifuged. Dissolved oxygen was removed from the 1 M HCl supporting electrolyte by purging with oxygen-free nitrogen for five minutes before sample addition. As(III) gave a characteristic peak at about -0.40V versus Ag/AgCl. In order to confirm that the peaks obtained were as result of arsenic(III), the addition of standard arsenic(III) solution gave peaks of greater height. Additions of cerium sulphate to the sample oxidised the arsenic(III) to arsenic(V) and reduced the peak height.

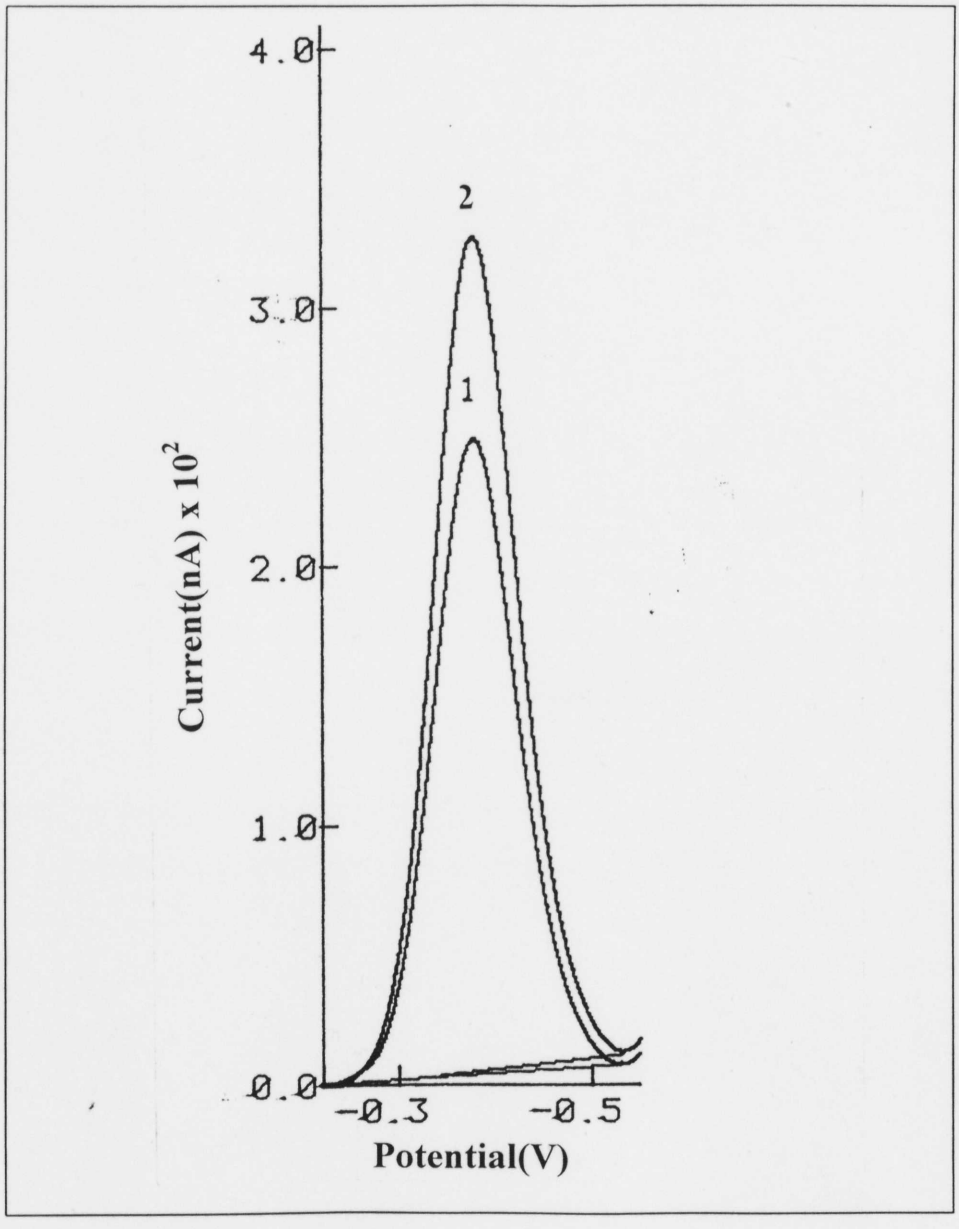


Figure 3.6: Some typical polarograms which were obtained during the determination of As(III) concentration by differential pulse polarography. Polarograms 1 and 2 corresponds to arsenic(III) concentrations of 3.8 mg/L and 4.5 mg/L respectively.

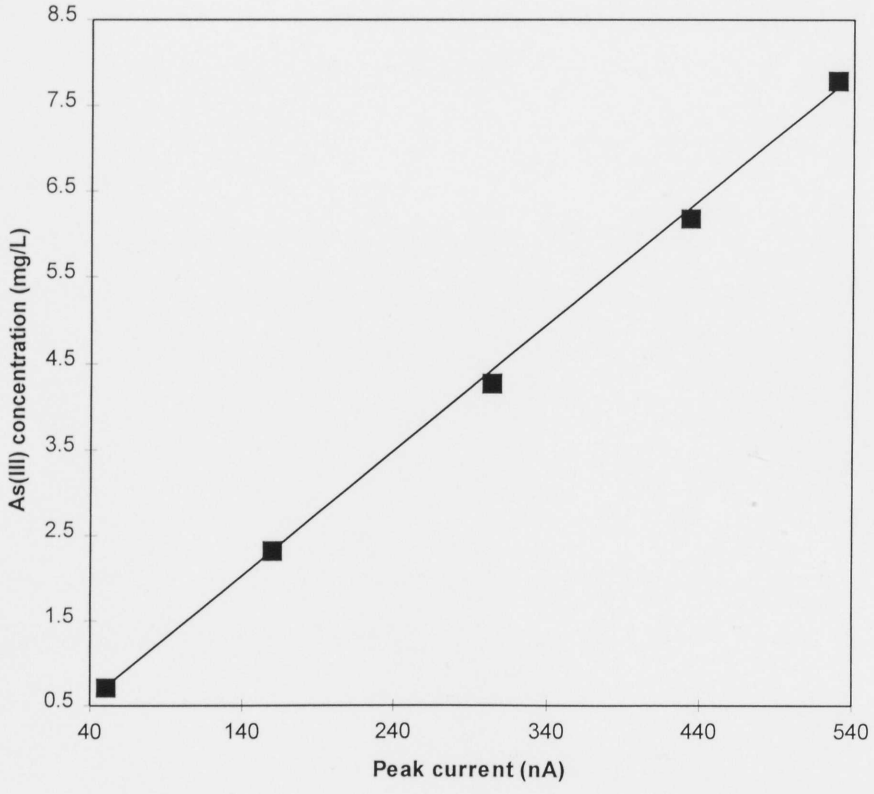


Figure 3.7: A plot of the peak current versus As(III) concentration obtained for different concentrations using the standard addition method during a run.

Gold

The concentration of gold in cyanide solutions was determined using an Atomic Absorption Spectrophotometer, with an air/acetylene flame. Gold was measured at the absorption wavelength of 242.8 nm, with a slit setting corresponding to 0.7 nm and a lamp current of 15 mA. Standards for the calibration line were prepared in the range 1-20 mg/L Au in alkaline sodium cyanide solution (0.4 % NaCN).

3.4 Cyanidation tests

Cyanidation tests were carried at ambient temperature to assess the effect of bio-oxidation on gold extraction. Samples of biooxidised concentrates for cyanide leaching were obtained from batch bacterial leaching tests in mechanically agitated flasks. Reference experiments were carried out on un-pretreated concentrate samples ground to -75 μm. Tests were conducted using magnetically stirred beakers at pulp densities

ranging from 15-25 % solids (w/v), 0.4 % NaCN concentration, ambient temperature, 24 and 48 hours retention time and pH 10-11.

3.5 Solubility testing

To evaluate the arsenic stability of the biooxidation residues before and after leaching of the pyrite/arsenopyrite concentrates, the residues were subjected to the EPA (Environmental Protection Agency), TCLP toxicity test. Before the EPA test all the samples were thoroughly washed and filtered. The test solution (extraction liquid) consists of a buffered acetic acid solution (0.03 M acetic acid and 0.07 M sodium acetate) at pH 5.0 agitated at 30 rpm (end-over-end bottle agitation) for a period of 20 hours. 1 g samples were used in the test procedure, liquid:solid = 20:1. After 20 hours a 10 mL aliquot of the pulp was removed and filtered through a 0.2 μm GFF filter. The filtrate was analysed by ICP-AES for arsenic.

3.6 Oxidised precipitates

To determine the amount and nature of the soluble solids in the biooxidation residues, the residues were acid treated. A sample of 1 g was dispensed into a tube and 25 mL of 5M HCl was added. The contents of the tube were thoroughly mixed and allowed to react for 30 minutes with occasional mixing and then 10 mL of the pulp was filtered through a 0.2 μm filter. The concentrations of Fe, Fe^{2+}, As and As^{3+} were measured in the filtrate and the resulting soluble solids calculated.

3.7 pH, redox potential, dissolved oxygen measurements

The pH and the redox potential of the culture suspension was measured using a JENWAY Microprocessor meter. The electrode for redox measurements was a double junction platinum saturated calomel electrode and pH was monitored using a BDH combination electrode. The meter was calibrated using a buffer of pH 7 and pH 4. The calibration was checked using a buffer of pH 1.68, which was in the region of the operating pH.

Dissolved oxygen measurements of the bacterial oxidation slurry were made using a WTO OXI oxygen meter and probe. The oxygen meter was calibrated according to the manufacturer's specifications.

3.8 Digestion of solids for chemical analyses.

The compositions of the concentrates shown in Table 3.1 was determined by ICP-AES after digestion in aqua regia ($HCl:HNO_3$ = 3:1) and the other methods are detailed in Appendix One.

CHAPTER FOUR

MINERALOGY OF THE ORES

4.1 Introduction

Geological setting

The Indarama and the Riverlea Mines

The Indarama and the Riverlea mines are situated in the central part of the Archaean Midlands greenstone belt near Kwekwe in Zimbabwe. This is one of the largest gold districts in the country and, on a world-wide scale, represents a major province hosting vein deposits of the gold-antimony type **[176]**.

The Indarama mine is 10 km north of Kwekwe. Lithostratigraphically, the Indarama deposit is situated within the Bulawayan Group (2.7-2.9 Ga). Ore-bearing veins are structurally controlled and preferentially dip 25°-45° ENE and WEW. They occur within 600-800 m thick sequence of greenstones, consisting of metabasalts with pillow structures, sulphide-bearing Banded Iron Formations (BIFs), and komatiites. According to Buchholz et al., **[176]** vein formation took place towards the end of the Bulawayan during folding of the greenstone and the intrusion of granitoids. The Riverlea mine is also within the same area as the Indarama mine and Figure 4.1 shows the geology and location of the Indarama and the Riverlea mines and other gold mines in the area. The area around the Riverlea mine is mainly hosted by clastic sediments and hematite slates. The pyrite/arsenopyrite concentrates produced by these mines are processed at the Roasting plant located in Kwekwe. In addition to the pyrite/arsenopyrite concentrate,

the Indarama mine produces an antimony concentrate as well and this is treated at the mine using alkaline leaching of the sulphide.

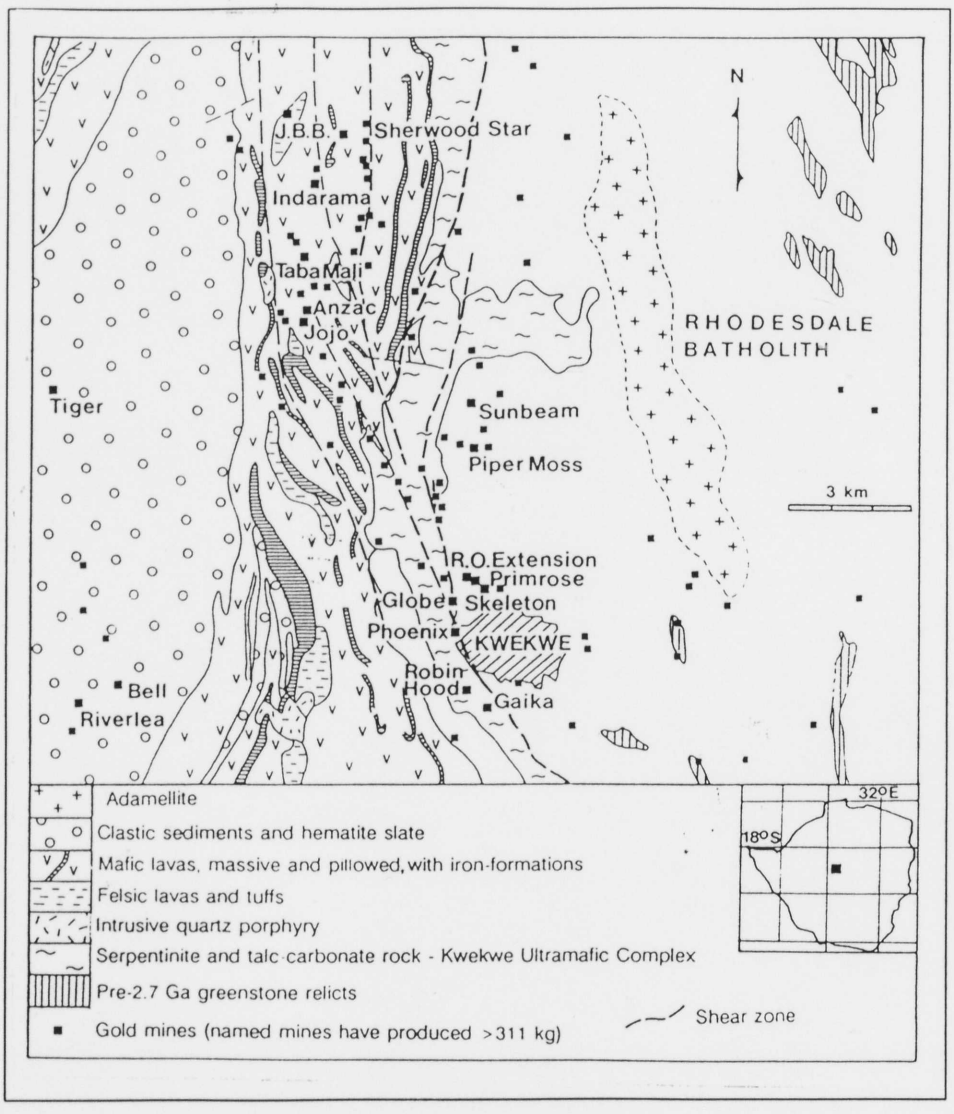


Figure 4.1: The location and geology of the Indarama, the Riverlea mines and area around Kwekwe **[177]**.

The Akbakai Mine

The Akbakai deposit which is 300 km NW of Almaty in Kazakhstan consists of fracture controlled veins hosted mainly by granodiorite. The gold mineralisation is associated with quartz veinlets and sulphides in narrow zones of bracciated and hydrothermally altered rock. The veins are typically 0.5 to 1.5 metres wide and their depth has been traced to about 600 metres. The Akbakai Fault, known as the main vein where it is well

mineralised strikes east-west and dips north at about 70°. A second steep dipping vein (Frolovskaya) is present which has a similar dip to the Main vein, but strikes at about 120°. At least other 10 veins have been recognised which occur in a series of flatter secondary fractures which dip north between 35° and 60°, mostly on the hangingwall side of the main vein **[178]**. Figure 4.2 illustrates the overall geometry of the vein system of the Akbakai deposit.

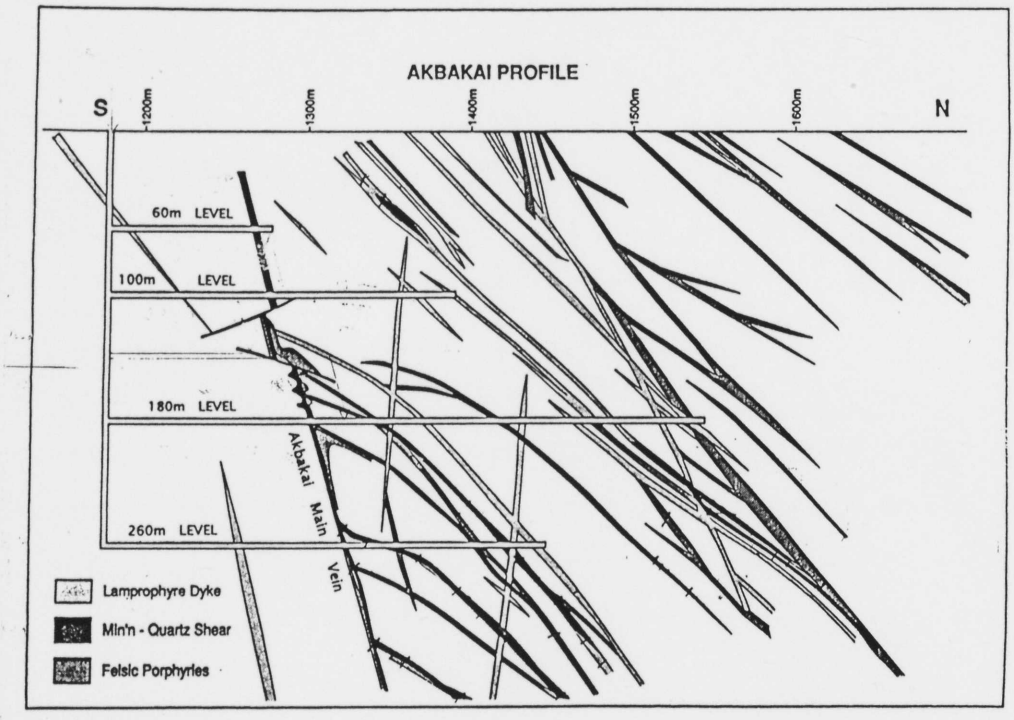


Figure 4.2: The geometry of the vein system of the Akbakai deposit **[178]**.

The Olympias and the Fairview mines

The Olympias mine is situated in the neighbourhood of the village of Olympias, in eastern Chalkidiki, Greece. The economically important geological formation in this area is a marble horizon included within the other rocks of the metamorphic sequence. It can be traced 2500 m north-west of the village of Olympias and has a north-east strike and a dip of 30-35° to the south-east. It consists of a succession of marble lenses with intercalated gneiss bands. The mineralisation is located either at the contact between the marble and the gneiss or within the marble at a small distance from the contact with the

overlying gneiss **[179]**. The vein has a north-south strike, which changes to north-west at levels below 150 m. Its dip is 30-35°E.

The Fairview gold mine is situated 6 km north-east of Barberton in the eastern Transvaal, approximately 280 km east of Johannesburg. The Fairview mine forms part of the metallogenic province of the Barberton greenstone belt, a remnant of Archean volcanic and sedimentary rocks of the Barberton sequence, surrounded by granites, gnesisses and migmatites. The Barberton sequence consists of a lower volcanic succession, the Onverwacht Group, followed by an argillaceous sequence of greywackes, shale and cherts, termed Fig Tree Group, and a predominantly arenaceous quartzite and sandstone succession known as the Moodies Group **[180]**. The most important ore body mined at Fairview is the sulphidic type of ore which is hosted mainly by Fig Tree greywacke and shale. The reef occurs as disseminated to massive pyrite and arsenopyrite concentrated in fractures both concordant and discordant to the host rocks. The fractures are closely clustered and form a complex intermeshed structure approximately 200-300 m in the hanging wall of the Sheba Fault, considered to have resulted from tangential shear movements during the major fold periods **[180]**.

4.2 Indarama deposit

Samples were collected by the author from five different sites in the mine. Sample locations within the mine are shown in Appendix A3.1.1. The samples were identified using the designation IN 1 to IN 5. IN 2 to IN 5 were mixed to form a composite sample. Arsenopyrite (FeAsS), pyrite (FeS_2), stibnite (Sb_2S_3) and gudmundite (FeSbS) are the major sulphides present in the ore, with minor amounts of sphalerite, pyhrrotite, native antimony and berthierite ($FeSb_2S_4$). The minor minerals were found to contain insignificant amount of gold.

4.2.1 Indarama 1

The most abundant sulphide mineral was stibnite with appreciable amounts of gudmundite and arsenopyrite. The stibnite is massive and occurs as lath-like crystals that often exhibit deformation textures (Figure 4.3). Arsenopyrite is present as euhedral

to anhedral crystals. The arsenopyrite is fine grained with most of the crystals being less than 75μm. Gudmundite occurs as euhedral to subhedral particles and is optically homogeneous and zoned (Figure 4.4). The gangue matrix is mainly calcite with some quartz.

Microprobe analysis revealed that arsenopyrite has an arsenic content ranging from 42.6-45.0 wt% (Appendix A3.1.1). Some arsenopyrite grains showed significant amounts of antimony up to 0.2 wt%. Gudmundite was also found to contain some arsenic up to 0.3 wt%.

Native gold was observed by optical microscopy in this sample. The native gold was either associated with the gangue or with gudmundite. Gold was found as inclusions in gudmundite particles, which were typically less than 15 μm. The various associations of gold with the sulphides in the Indarama 1 sample which were observed optically are shown in Figures 4.3 to 4.6.

Microprobe analysis of the native gold inclusions showed pure gold and aurostibite in close association with gudmundite (Figures 4.3 and 4.6). Typical analysis of the aurostibite contained 43.6 wt% Au and 57.6 wt% Sb. To ascertain whether stibnite, which was the main sulphide in this sample, contained significant amount of gold, laser ablation coupled to an inductively coupled plasma mass spectrometer was employed on a section which contained massive stibnite. No gold was detected in the stibnite.

Different forms of refractoriness were observed: native gold inclusions in gudmundite cannot be easily recovered during the cyanidation process because their relative sizes (typically less than 15 μm) fall below the grind size normally employed in milling practice (75 μm). Although fine grinding could liberate some of these particles, many of the gold inclusions will remain locked in the sulphides. In most cases fine grinding is rejected on the grounds that it increases the energy requirements of the milling plant leading to uneconomic recovery.

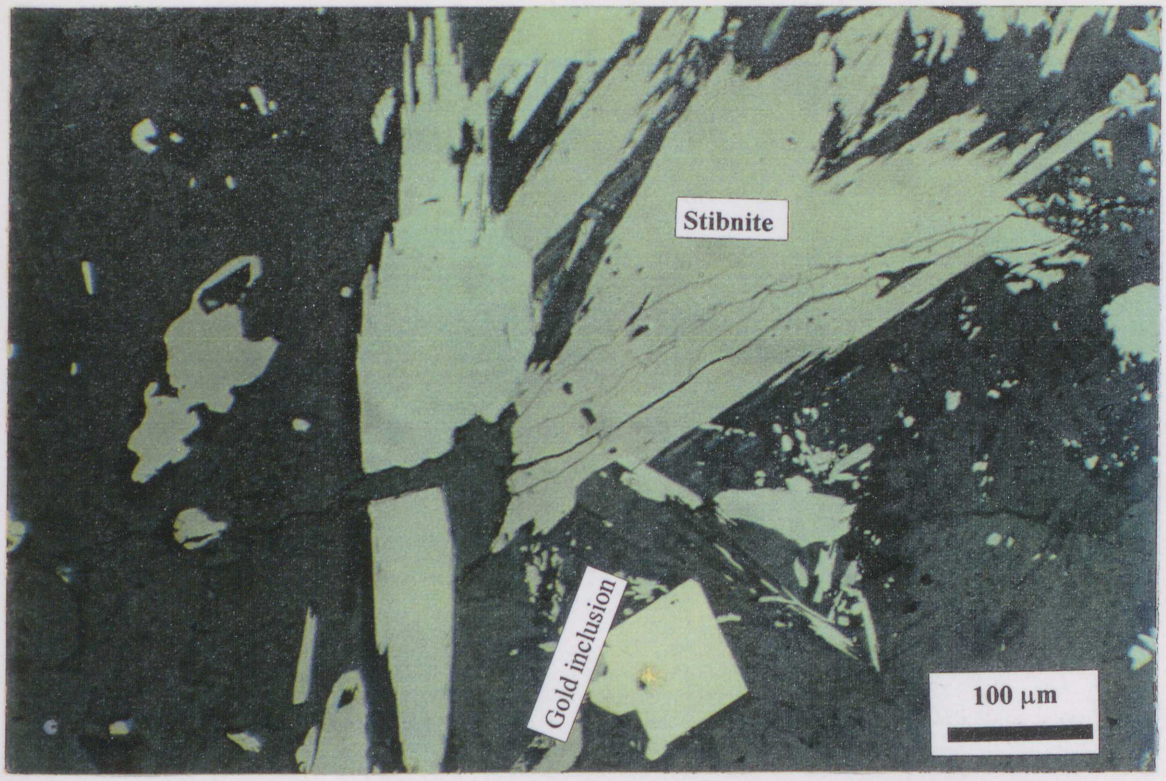


Figure 4.3: Optical microscopy photomicrograph showing small gold particle as an inclusion in gudmundite. Stibnite particles also present (Indarama 1).

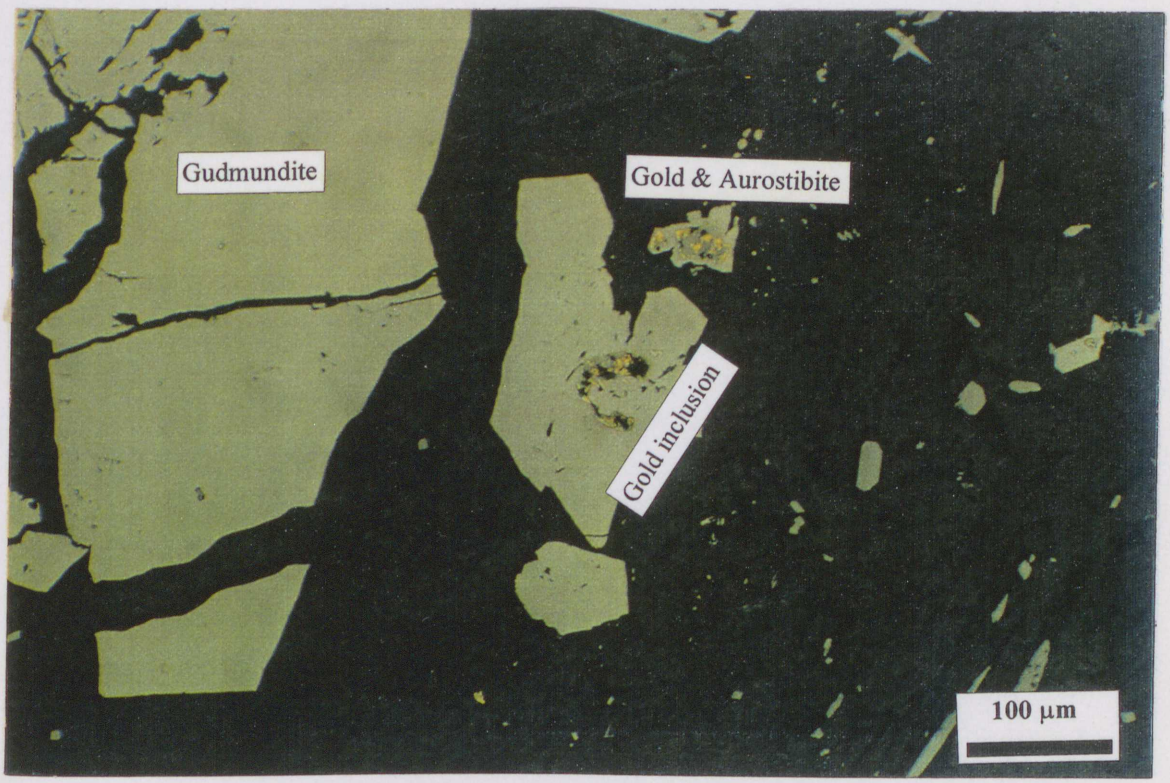


Figure 4.4: Optical microscopy photomicrograph showing gold inclusions in gudmundite particles (Indarama 1).

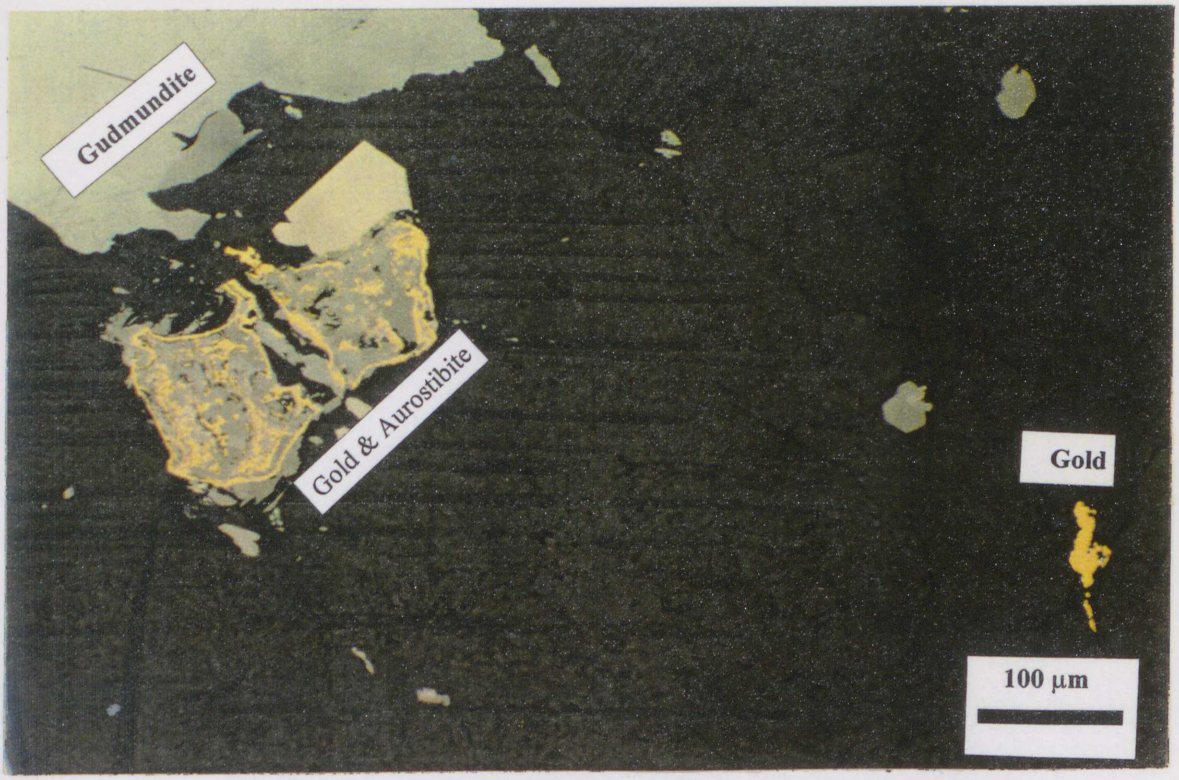


Figure 4.5: Optical microscopy photomicrograph showing free gold and aurostibite associated with gudmundite and gangue matrix (Indarama 1).

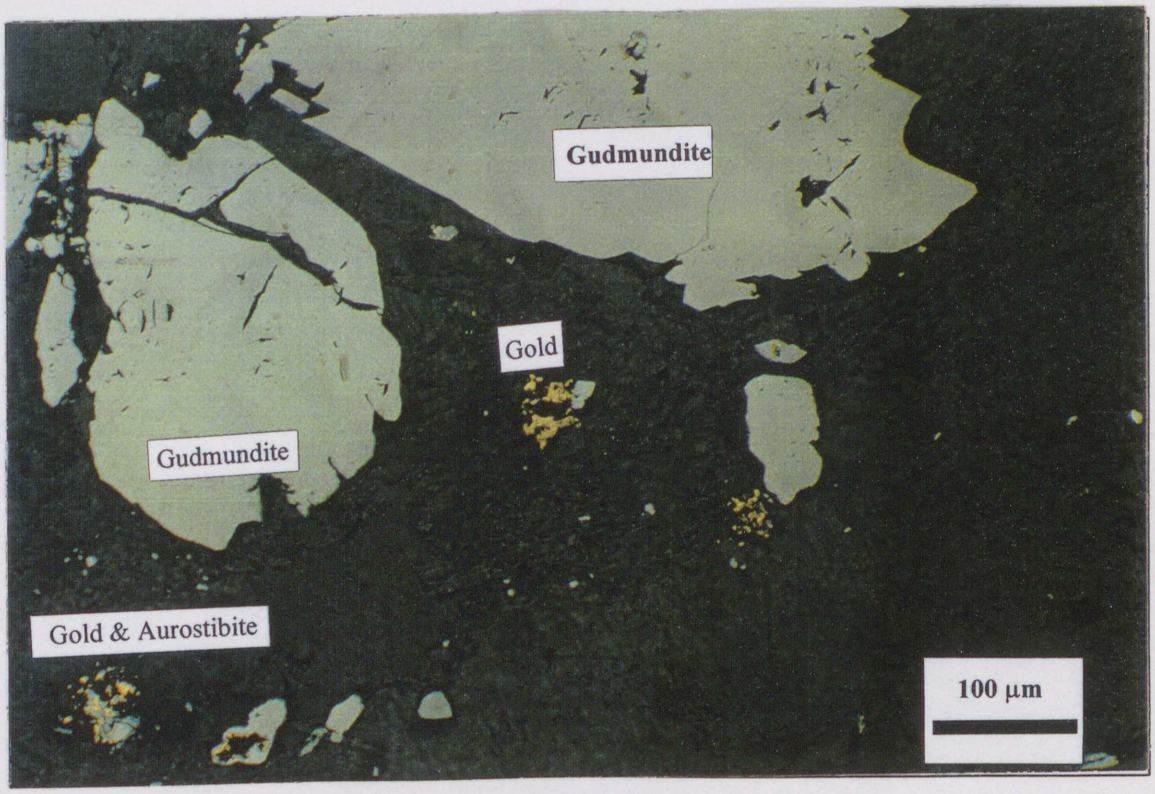


Figure 4.6: Optical microscopy photomicrograph showing free gold and aurostibite associated with gudmundite (Indarama 1).

In close association with native gold, there is also aurostibite. It may be possible to recover some of the gold of the particle shown in Figure 4.5 but the aurostibite parts will be insoluble in cyanide solutions. Stibnite will also react with cyanide to some extent as a result increasing the consumption of cyanide **[40]**, hence the operating costs also increases. The presence of antimony also makes the gold bullion bars brittle.

4.2.2 Indarama 2 to Indarama 5

These samples were mineralogically distinct from Indarama 1. The main sulphide components were arsenopyrite and pyrite (including arsenian pyrite). The gangue matrix consisted of calcite and quartz.

4..2.3 Arsenopyrite crystals

Arsenopyrite occurred as euhedral to anhedral particles. Individual lath-shaped crystals ranged in size between 5-200μm. Both optically homogeneous and zoned arsenopyrite crystals were present (Figure 4.7). Most of the arsenopyrite crystals were chemically zoned. Electron microprobe analyses were done to quantify the compositions of these different zones. Two sets of zones were identified: arsenic-rich and arsenic-poor zones compared to stoichiometric of pure arsenopyrite crystals. The arsenic content of the arsenic rich zones ranged from 33.4-37.7 atomic percent while the arsenic poor zones had 27.1-33.2 atomic percent. The arsenopyrites are sulphur-rich with an As/S atomic ratio below 1 in most cases. Occasionally there was zoning between arsenopyrite and pyrite. The arsenopyrite often contained inclusions of base metal sulphides such as copper, nickel and zinc (Appendix Three refers).

Some of the arsenopyrite contained very high concentrations of refractory gold in solid solution or as colloidal particles (>2000 ppm) in the arsenic-poor zones. A non-linear relationship exists between the atomic percent arsenic and the gold concentration, as evident in Figure 4.8. From this Figure it appears that above 31 atomic percent arsenic gold occurs in high concentrations but below, gold concentrations are in most cases below the detection limit (200 ppm). A similar, but inverse trend exists between the Au-content and the sulphur-content as shown in Figure 4.9. High gold concentrations occur

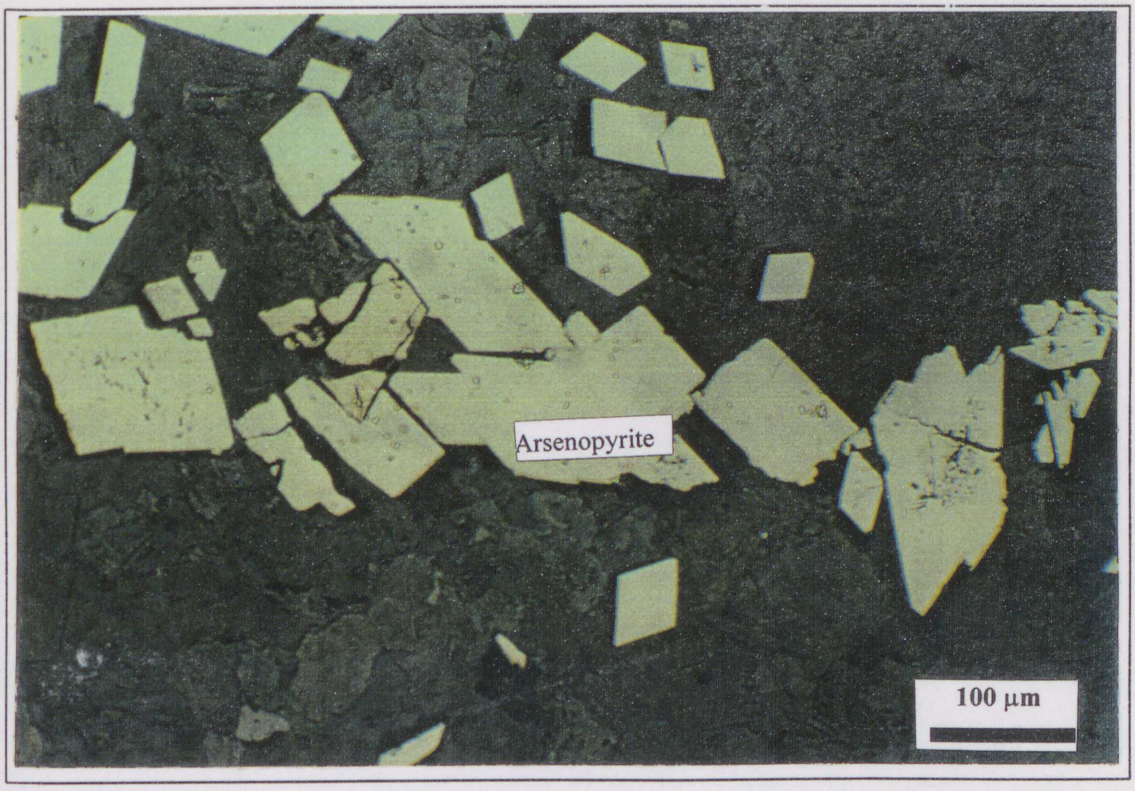


Figure 4.7: Optical microscopy photomicrograph showing euhedral to anhedral arsenopyrite particles with some zoned crystals (Indarama deposit).

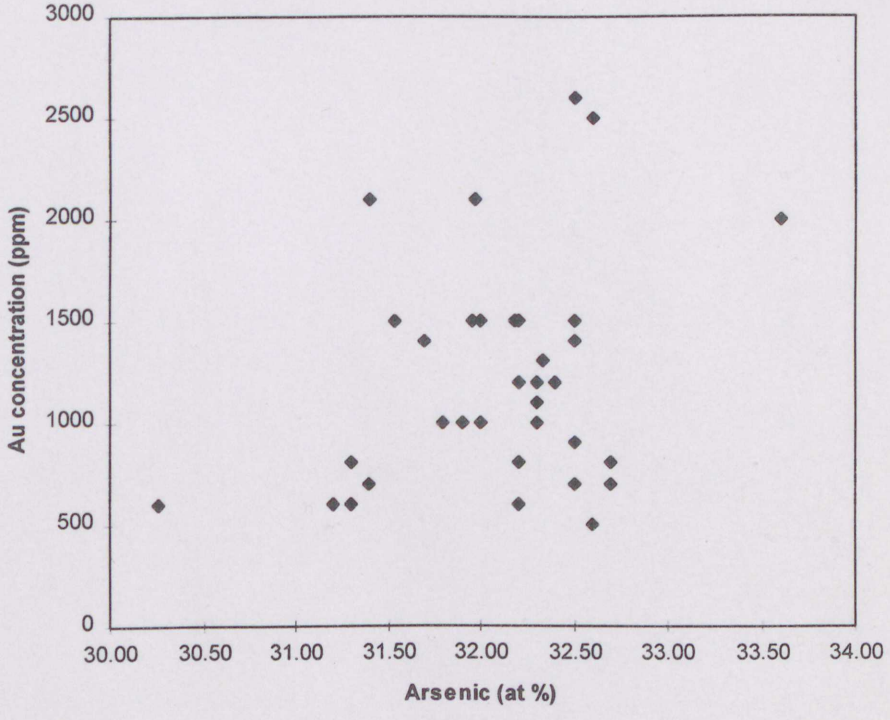


Figure 4.8: Gold concentration against atomic arsenic content within the arsenopyrite crystals from the Indarama deposit.

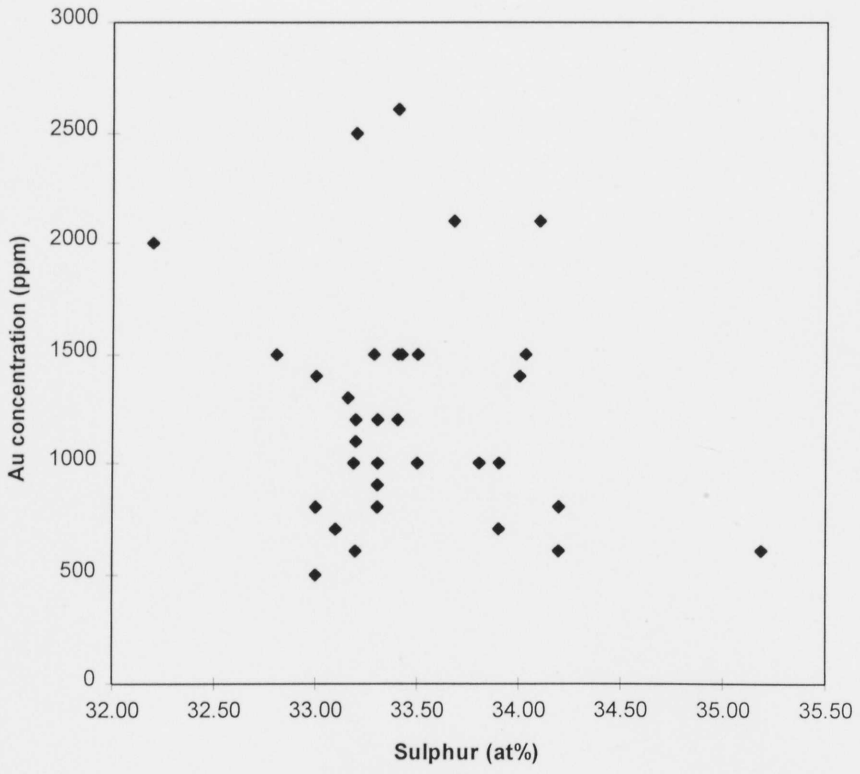


Figure 4.9: Gold concentration against sulphur content within the arsenopyrite crystals from the Indarama deposit.

below a sulphur-content of approximately less than 34.5 atomic percent. However the gold-content varies from one compositional zone to another, but fluctuations also occur within the same zones. The atomic content of the iron and the gold concentration showed no distinct correlation.

Submicroscopic gold is heterogeneously distributed in the arsenopyrite crystals and is particularly enriched in non-stoichiometric arsenopyrite zones (< 33.3 atomic percent), and sulphur-content less than 34 atomic percent. It appears that the distribution of gold is in arsenic-depleted zones of arsenopyrite in most cases. Microprobe analysis revealed gold levels of more than 2000 ppm in some of the arsenopyrite grains. It was interesting to note that submicroscopic gold was heterogeneously distributed in the arsenopyrite grains and was specifically enriched in zones having low arsenic content. In addition to submicroscopic gold present in arsenopyrite, gold particles also occurred as inclusions within arsenopyrite. However this occurrence was very rare and the inclusions were generally less than 1 μm in size. The inclusions were also associated with the contact

between compositional zones.

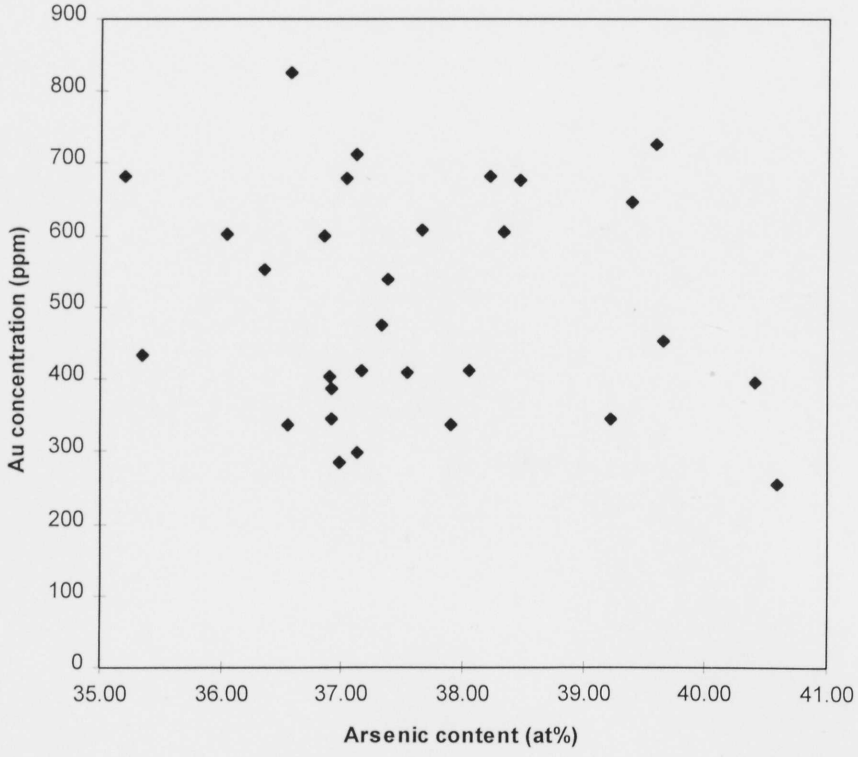


Figure 4.10: Gold concentration against arsenic within arsenopyrite crystals from the Indarama deposit using laser ablation technique.

Laser ablation showed that arsenopyrite contained an appreciable amount of gold possibly in solid solution or as colloidal particles as shown in Figure 4.10 which is a plot of the calculated arsenic-content against the gold concentration. Some of the arsenopyrite crystals were found to contain very high values of refractory gold of over 800 ppm. It was found however that the solid solution or colloidal gold was heterogeneously distributed in the arsenopyrite crystals.

Although laser ablation is a sensitive method with very low detection limits for gold (about 10 ppm), there are some problems associated with the quantitative interpretation of the results. The standards used are aqueous solutions and this does not match the matrix of analysis and it seems that there is preferential ablation of certain elements as shown by the elevated concentrations of arsenic in arsenopyrite calculated from the results of this method. Because of these problems, the results in Figures 4.8 and 4.10 do

not agree. The results of Figure 4.10 seem to suggest that the solid solution gold in arsenopyrite is mostly concentrated in arsenic-rich zones (> 33.4 atomic percent arsenic), however this is due to analytical errors of the method. Laser ablation gives a good indication of the presence of solid solution or colloidal gold in the sulphides.

4.2.4 Pyrite crystals

Pyrite occurred in the Indarama samples in forms ranging from euhedral to anhedral grains. The arsenic content of the pyrite was found to range between 0-5.0 wt% as shown in Figure 4.11. From the figure it is evident that the sulphur-content of the pyrite crystals which contain arsenic lies between 50-52 weight percent. Alternating enrichment of arsenic in pyrite was observed on some grains of pyrite and in some cases inclusions of sphalerite, arsenopyrite, tetrahedrite, nickel and copper sulphides were encountered. Silicate inclusions were also identified in some grains of pyrite. Anhedral pyrite particles were found to exhibit uneven compositional zoning from arsenic-depleted to arsenic-enriched zones.

Gold inclusions were observed in arsenian pyrite in regions enriched in arsenic. At times the gold was associated with arsenopyrite which occurred as inclusions in pyrite. This gold can be said to be refractory because of its nature of occurrence.

4.2.5 Refractory gold

From the above results, two modes of occurrence of gold in the arsenopyrite are: (i) particulate gold inclusions mainly at the contact zones and (ii) gold in solid solution mainly in arsenic depleted zones. From a process point of view it is very difficult if not impossible to recover such invisible gold by the simple cyanidation route. Therefore it is neccessary to liberate the gold possibly by using a pre-treatment step such as bacterial oxidation.

4.3 Akbakai deposit

The major ore minerals of the unweathered primary sulphides are pyrite and arsenopyrite with minor amounts of stibnite, chalcopyrite and sphalerite. The gangue

matrix is mainly composed of quartz and calcite. Native gold was observed as small grains (20-100 μm), usually occurring at the boundary of arsenopyrite and gangue (Figure 4.12) and rarely as inclusions in pyrite or arsenopyrite.

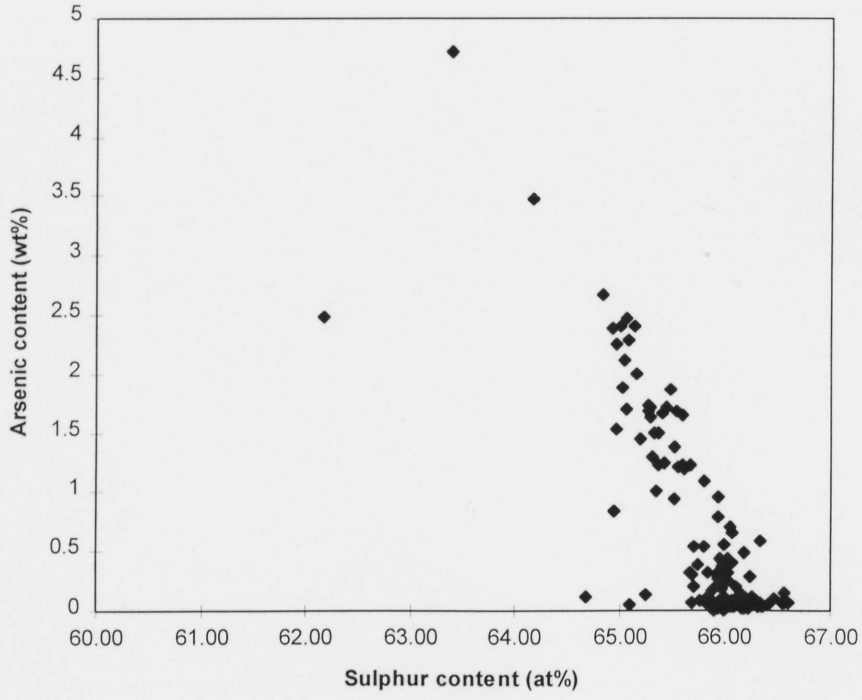


Figure 4.11: Sulphur content of the pyrite against the arsenic content of the Indarama deposit.

4.3.1 Arsenopyrite crystals

Arsenopyrite crystals generally occur as lath-shaped crystals in the range 10-200 μm, and at times they are both optically and chemically zoned. Microprobe analysis revealed that the arsenopyrite is not homogeneous in composition. Zones of arsenic-rich and arsenic-poor concentration were encountered. In addition the arsenopyrite also contained some base metals possibly as inclusions or incorporated into the structure. The arsenic content of the arsenopyrite crystals ranged from 27.54-33.53 atomic percent (39.27-46.23 weight percent).

Most of the gold associated with the arsenopyrite was found to be free gold, however a few arsenopyrite crystals showed a significant amount of gold incorporated into their structure possibly in solid solution or as colloidal particles. A maximum gold

concentration of 6900 ppm was found. Table 4.1 gives a summary of the microprobe analysis (Jeol 733) of the arsenopyrite crystals which were found to contain gold. It is important to note that the gold distribution was not homogeneous within the same crystals.

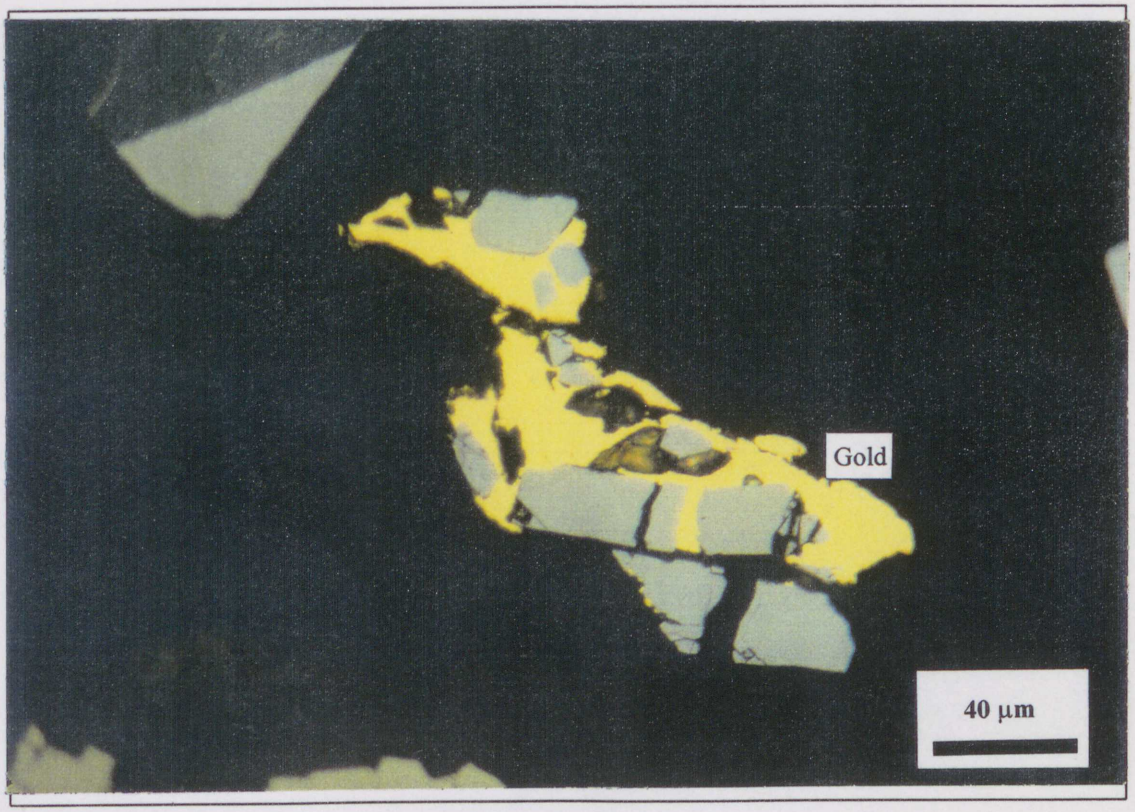


Figure 4.12: Optical microscopy photomicrograph showing native gold overgrowths on arsenopyrite (Akbakai deposit).

4.3.2 Pyrite crystals

Pyrite occurs in forms ranging from euhedral crystals to anhedral grains. Microprobe analysis of the pyrite grains showed that their composition varied from pure pyrite grains to arsenian pyrite. The pyrite also contain base metals, with copper and nickel being the most frequently encountered ones although their concentrations were generally low (< 0.2 weight percent). Microprobe analysis carried revealed no gold in the pyrite crystals. The pyrite crystals from the Akbakai deposit were found to contain low arsenic, in most cases less than 1.5 weight percent as shown in Figure 4.13.

Table 4.1: Microprobe analysis results of some arsenopyrite crystals from the Akbakai concentrate.

Analysis No.	Wt % S	Wt % Fe	Wt% As	Au ppm	Total
1	18.8	34.4	46.1	6900	100.00
2	19.0	34.9	45.9	1800	99.99
4	19.6	35.6	44.6	1600	100.00
5	19.9	35.8	44.0	2400	100.00
6	20.0	33.1	46.8	1500	99.99
7	20.3	33.8	45.6	3100	100.02
8	20.9	35.7	43.3	500	100.00
9	20.7	35.6	43.8	800	100.00
10	20.5	35.6	43.8	900	100.00
11	21.4	35.8	42.6	600	100.00

4.3.3 Refractory gold

The refractory gold in the Akbakai deposit was found to be associated with the arsenopyrite only. The mode of occurrence is possibly in solid solution or colloidal particles. In most cases the gold was detected at the edges of the arsenopyrite grains.

4.4 Riverlea deposit

No native gold was observed on any of the samples examined using the optical microscopy. However the use of the SEM coupled to the microprobe revealed inclusions of gold in the pyrite crystals typically less than 10 μm. Pyrite and arsenopyrite are the main sulphides in this deposit.

4.4.1 Arsenopyrite crystals

Arsenopyrite occurs as euhedral to anhedral particles in the size range between 5-200 μm but at times larger particles were also encountered. Zoning of the pyrite and the arsenopyrite crystals is a common feature. In addition the arsenopyrite crystals are

chemically zoned and some arsenopyrite particles (size range of 5-20 μm) are found as inclusions in the pyrite grains. Microprobe analysis revealed that arsenopyrite has As-content ranging 42.21-45.70 weight percent (30.05-32.91 atomic percent). Some grains of arsenopyrite showed elevated amounts of Ni (up to 0.78 wt %), Sb (up to 1.72 wt %) and Cu (up to 1.27 wt %).

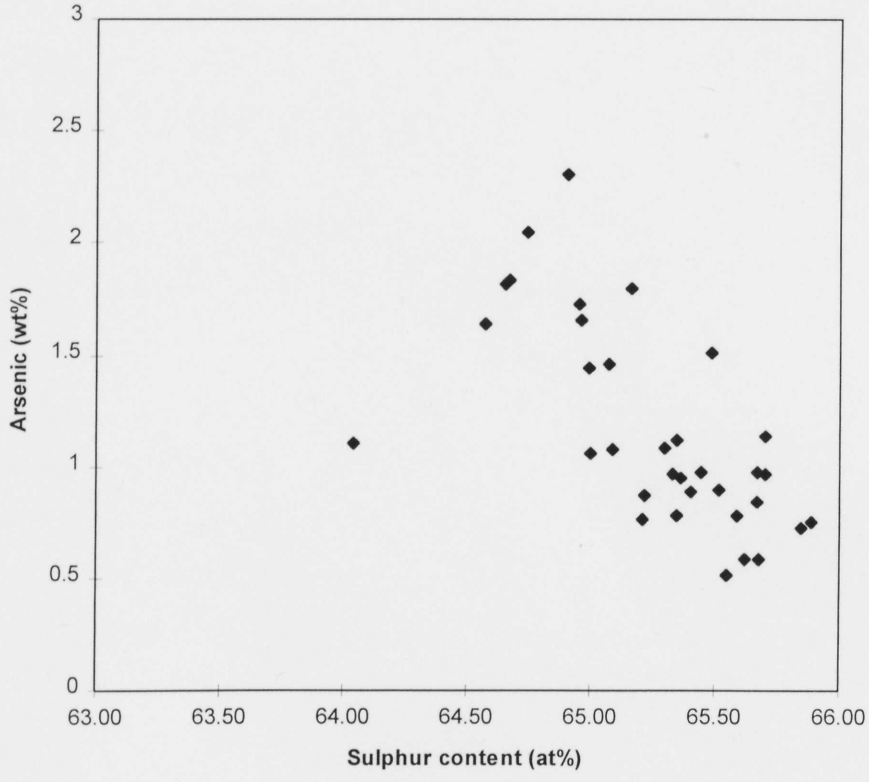


Figure 4.13: Arsenic concentration of the pyrite crystals from the Akbakai deposit.

Microprobe analysis also showed that the arsenopyrite grains contained gold possibly in solid solution or as colloidal particals. Generally lower concentrations of gold were measured compared the values obtained for the Indarama and the Akbakai arsenopyrites. However high concentrations of gold (up to 1700 ppm) were detected in some instances.

4.4.2 Pyrite crystals

Electron microprobe analysis carried out to determine the composition of the pyrite showed that the arsenic content of pyrite ranges from 0-4.89 weight percent. Figure 4.14

shows the sulphur-content plot against the arsenic-content of some of the pyrite grains from the Riverlea deposit. Most of the arsenian pyrite contain 51-54 weight percent sulphur. Like the arsenopyrite grains, Ni, Sb and Cu were also found to be associated with the pyrite grains during microprobe analysis.

4.4.3 Refractory gold

Different forms of refractory gold were observed in the Riverlea deposit. Inclusions of native gold typically less than 10 μm were found in pyrite crystals. Some gold was also found to be associated with arsenopyrite and pyrite, possibly in solid solution.

4.5 Olympias and Fairview deposits

Detailed mineralogical descriptions of the Olympias and the Fairview ore deposits are given in the literature **[36, 93]**. The main mineral sulphides present in the concentrates used in this study were pyrite and arsenopyrite with minor amounts of sphalerite and galena. For this study the concentrate from the Olympias deposit was mainly used to maintain the bacterial culture. The Fairview concentrate was used for the predictions derived from the results obtained from the Indarama, Akbakai and Riverlea concentrates. Further details on the bacterial leaching experiments carried out on this concentrate are given in Chapter Five. The main sulphides present in this concentrate were pyrite and arsenopyrite and the mineralogical composition of the concentrates are given in Table 4.2 (page 107).

4.6 Pyrite and arsenopyrite ratios in the concentrates

The approximate ratios of pyrite to arsenopyrite were calculated from the chemical analysis of the concentrates. The basic assumption made was that all the arsenic was coming from arsenopyrite with the remaining iron being from pyrite. Furthermore the pyrite and the arsenopyrite were assumed to have a stoichiometric composition of FeS_2 and FeAsS. From the mineralogical examination of pyrite it was shown that some of the pyrite particles contained some arsenic and some of the arsenopyrite particles were arsenic depleted. These factors could introduce some errors in the calculated ratios of pyrite to arsenopyrite in the concentrates. However this method was found to give a

better approximation of the mineral composition compared with grain counting using the optical microscope. The mineralogical compositions of the concentrates in terms of pyrite to arsenopyrite is given in the Table 4.2.

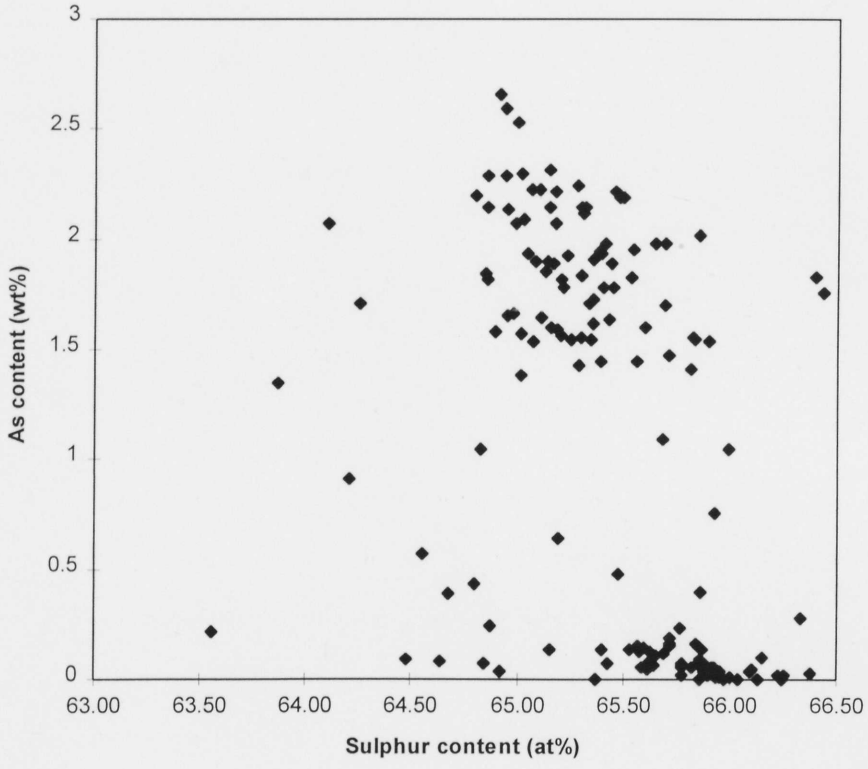


Figure 4.14: Sulphur content against the arsenic content within some of the pyrite crystals from the Riverlea deposit.

A range of pyrite to arsenopyrite ratios were observed in the concentrates from different ore deposits and flotation plants as shown in Table 4.2. It is important to note that the grade of the concentrate in terms of pyrite to arsenopyrite ratio and percentage of sulphides in the concentrates is governed by the flotation efficiency and the mineralogical composition of the initial ore.

The arsenic contents of the pyrite particles differed within the same deposits and also from one deposit to another. Most pyrite crystals in the Riverlea deposit contained arsenic, at concentrations which were higher than those found in the Akbakai and the Indarama concentrates. A large number of pyrite crystals in the Riverlea deposit

contained more than 1 wt% arsenic. Furthermore the pyrite particles in the Riverlea material contained inclusions of arsenopyrite, an occurrence which was less common for the Akbakai and the Indarama deposits.

The Akbakai deposit was found to contain less gold in solid solution with arsenopyrite and the pyrite crystals contained insignificant amount of gold. However both pyrite and arsenopyrite crystals were found to contain gold either in solid solution or as colloidal particles with most of this gold being associated with arsenopyrite and arsenian pyrite.

Table 4.2: Mineralogical composition of the concentrates in terms of pyrite to arsenopyrite ratios.

Sample Location	Wt % FeS_2	Wt % FeAsS	Wt % FeS_2 + FeAsS	Ratio FeS_2/FeAsS
Indarama mine(B)	29.36	37.55	66.91	0.78
Indarama mine(C)	52.45	36.08	88.53	1.45
Akbakai mine(A)	44.32	28.45	72.77	1.56
Akbakai mine(D)	16.00	8.45	24.45	1.89
Riverlea mine(R)	43.82	20.58	64.40	2.13
Fairview mine(F)	31.47	9.17	40.64	3.43
Olympias mine(O)	70.69	17.30	87.99	4.09

4.7 Cyanidation tests

Table 4.3 summarises the results of cyanidation tests on some of the concentrates before any pretreatment. These tests were done to confirm the refractoriness of the ores as observed in the mineralogical study above, as well as to quantify the amount of refractory gold. It is evident that the concentrates range from extremely refractory (Indarama and Riverlea concentrates) to less refractory (Akbakai concentrate). Considering the low gold recovery obtained after direct cyanidation of the Indarama and Riverlea concentrates, it is necessary to have a pretreatment step in order to destroy the sulphide matrix and expose the gold to cyanide and oxygen for subsequent recovery. The mineralogical compositions of the concentrates will also play an important role in

deciding the pretreatment method to be used because of the stringent environmental regulations pertaining to the disposal of waste residues. The main concern in the processing of the above concentrates is their arsenopyrite content. Bio-oxidation is one possibility for improving gold recovery. Employing a pretreatment step in processing the Akbakai concentrate is unlikely to be economically attractive since most of the gold in this ore is free milling gold. However if a concentration step can be used on the cyanide tailings to recover the sulphides with the refractory gold, a pretreatment stage could then be used on the resulting concentrate.

The mineralogical observations reported in this chapter are consistent with the work in the literature on refractory gold ore deposits comprising of pyrite and arsenopyrite **[44, 71-74, 176-177, 181-185]**. Variations in stoichiometry, particularly the ratio As:S, of the arsenopyrite leads to variations in structural parameters. The fact that both pyrite and arsenopyrite were found to contain gold and other elements such as nickel, copper and antimony indicates the presence of major structural defects. These structural defects together with other defects introduced during the mineral processing stages such as crushing and grinding will play an important role if bacterial oxidation is to be used as a pre-treatment step.

Table 4.3: Summary of cyanidation results of the different concentrates before bacterial oxidation.

Sample Location	% Gold Recovery
Indarama mine (B)	25.5
Indarama mine (C)	23.1
Akbakai mine (D)	81.8
Riverlea mine (R)	32.8

Note: Cyanidation conditions: 25 g of sample in 200 mL of cyanide solution (4 g/L NaCN) magnetically stirred for 48 hours. The gold recovery from the Fairview and the Olympias mines before pre-treatment has been reported to be 18% and 13% respectively **[36, 93]**.

CHAPTER FIVE

SPECIATION OF ARSENIC IN BACTERIAL OXIDATION OF ARSENICAL CONCENTRATES

5.1 Introduction

It is important to know the dominant species of arsenic during bacterial oxidation of arsenical ores because arsenic(III) has been shown to be more toxic to bacteria than arsenic(V) **[105]** and also its release into the environment has a more significant impact than arsenic(V). The oxidation of arsenic(III) to arsenic(V) has been suggested as a resistance mechanism by bacteria towards the more toxic arsenic(III) **[145]**. To date there is no published evidence of direct oxidation of arsenic(III) to arsenic(V) by the mixed cultures of *Thiobacillus ferrooxidans*, *Thiobacillus thiooxidans* and *Leptosperillum ferrooxidans* bacteria used in the pre-treatment of refractory gold ores. However there are some soil organisms which have been found to be capable of directly oxidising arsenic(III) to arsenic(V) **[169]**, and Barrett et al., **[105, 156]** have shown that *Moderately thermophilic* bacteria can catalyse the oxidation of arsenic(III) in the presence of ferric ions and pyrite. They suggested that the bacteria possibly provide clean pyrite surfaces which catalyse the oxidation of arsenic. Evidence for the direct oxidation of arsenic(III) to arsenic(V) by an acidophilic organism isolated from acid mine drainage from a pyritic mine has been provided by Wakao et al., **[168]**.

Most reports on bacterial oxidation of arsenical ores give details of high gold recoveries achieved, without addressing arsenic speciation and the long term stability of arsenic tailings and residues. In fact most reports make the assumption that all the arsenic will be present as arsenic(V) and that neutralisation of the bacterial leach solutions will produce stable residues **[6, 86]**. However some researchers have reported the formation of arsenic(III) and that its oxidation requires the presence of very powerful oxidising agents such as ozone, or hydrogen peroxide **[186]**.

The lack of consistent results indicates the need for further research in this area. The aim of the work described in this chapter was to determine the effect of ore composition on the speciation of arsenic during bacterial oxidation of pyrite-arsenopyrite concentrates from different ore deposits.

5.2 RESULTS

5.2.1 Release of arsenic into solution

The species of arsenic released into solution was routinely monitored in the bacterial cultures growing in stirred flasks on different concentrates. The concentrations of total arsenic and arsenic(III) in the figures are expressed as a percentage of the total arsenic in the feed solids. The proportion of arsenic(III) is sometimes quoted as a percentage of the total arsenic solubilised. Duplicate experiments were also run and the reproducibility was 3-6 %.

Pyrite/arsenopyrite concentrates of different mineralogical compositions were subjected to bacterial oxidation. The origin and compositions of the ores used in the first experiments are given in Table 5.1. The experiments reported in this chapter were carried out at 5% pulp density (w/v), except where otherwise stated. A 5% pulp density was chosen to ensure that lack of dissolved oxygen in the bioleaching slurry could not limit the oxidation process. Details of the sampling procedures and analytical techniques used are given in Chapter Three. The bacteria generated in the first runs were harvested and subsequently used for the following inoculations. This could possibly cause a higher oxidation rate of the sulphides due to bacterial adaptation or improvement in the

bacterial culture selection. However the bacterial culture used in this study was already well adapted to high concentrations of arsenic and there was no noticeable difference from one run to another due to further improvement. After sampling the samples were acidified with HCl to dissolve any precipitates or jarosites before analysis (Chapter Three, section 3.3.3).

Table 5.1: The origins and compositions of the concentrates used in Runs 1-6.

Run Number	Sample Location	Sample I.D	wt% As	wt% Fe	Ratio FeS_2/FeAsS
Run 1	Indarama	B	17.28	26.55	0.78
Run 2	Indarama	C	16.60	36.79	1.45
Run 3	Riverlea	R	9.47	27.46	2.13
Run 4	Akbakai	A	13.09	30.39	1.56
Run 5	Akbakai	D	4.07	10.48	1.89
Run 6	Olympias	O	7.96	38.84	4.09

Figure 5.1 shows the percentage of arsenic extraction from the initial concentrates during bioleaching for Runs 1-3. The three concentrates showed different rates of extraction with the Riverlea concentrate showing the fastest rate (Run 3). The Indarama B concentrate showed the slowest initial rate of extraction and it further slowed down with time (Run 1). Complete dissolution of arsenic took place after about 192 hours for the Indarama C and the Riverlea concentrates (Runs 2 and 3 respectively). For the Indarama B concentrate, however only about 86% arsenic was extracted in 288 hours. Although the two Indarama concentrates were from the same deposit, they differed significantly in their mineralogical compositions in terms of pyrite to arsenopyrite ratio.

Figure 5.1 also shows the percentage of arsenic(III) versus time in the bioleaching slurry for the two Indarama concentrates and the Riverlea concentrate and Figure 5.2 shows the corresponding concentrations of arsenic(III) and arsenic(V) in mg/L. Over the oxidation period considered the Indarama B concentrate showed a predominance of

arsenic(III) (Run 1). A maximum proportion of 91% arsenic(III) was measured in the bioleaching slurry within the first 24 hours, this value corresponding to about 350 mg/L arsenic(III). The percentage of arsenic(III) at the end of the oxidation stage was 78% corresponding to about 5800 mg/L as shown in Figures 5.1 and 5.2 (Run 1). Although the oxidation of arsenic(III) to arsenic(V) was taking place, the Indarama B concentrate showed an ever increasing amount of arsenic(III) in the bioleaching slurry as shown in Figure 5.2 (Run 1). The behaviours of the Indarama C and the Riverlea concentrates showed some significant differences from that of the Indarama B concentrate. However there was a predominance of arsenic(III) in the first 100 hours of leaching in all the cases. The maximum proportion of arsenic(III) reached 93% after 72 hours for the Indarama C concentrate and this corresponded to about 3200 mg/L arsenic(III) (Figures 5.1 and 5.2, Run 2). The maximum concentration of arsenic(III) measured for Run 2 occurred after 96 hours (about 4400 mg/L). Figure 5.2 shows that there was significant oxidation of arsenic(III) to arsenic(V) in the bioleaching slurry starting at about 50 % arsenic extraction, leaving about 5% of the solubilised arsenic as arsenic(III) at the end of the oxidation stage (Run 2). The Riverlea concentrate showed a similar trend to the one shown by the Indarama C concentrate but the rate of arsenic(III) oxidation was much faster. After 48 hours 87% of the solubilised arsenic was present as arsenic(III) corresponding to about 1600 mg/L, this was also the maximum concentration of arsenic(III) which was measured in that experiment (Figure 5.1 and 5.2, Run 3). Once the maximum concentration of arsenic(III) was attained, the conversion of arsenic(III) to arsenic(V) was faster than the initial leaching stages and less than 2% arsenic(III) remained in solution at the end of the oxidation stage.

Figure 5.3 shows the percentage of arsenic extracted with time from the other three concentrates (Akbakai A and D and Olympias concentrates). During the first 72 hours, all the three concentrates showed an almost equal rate of extraction of arsenic. More than 75% of arsenic was extracted from the initial concentrates after 72 hours after which the rate of extraction slowed down, with the Akbakai A and D concentrates

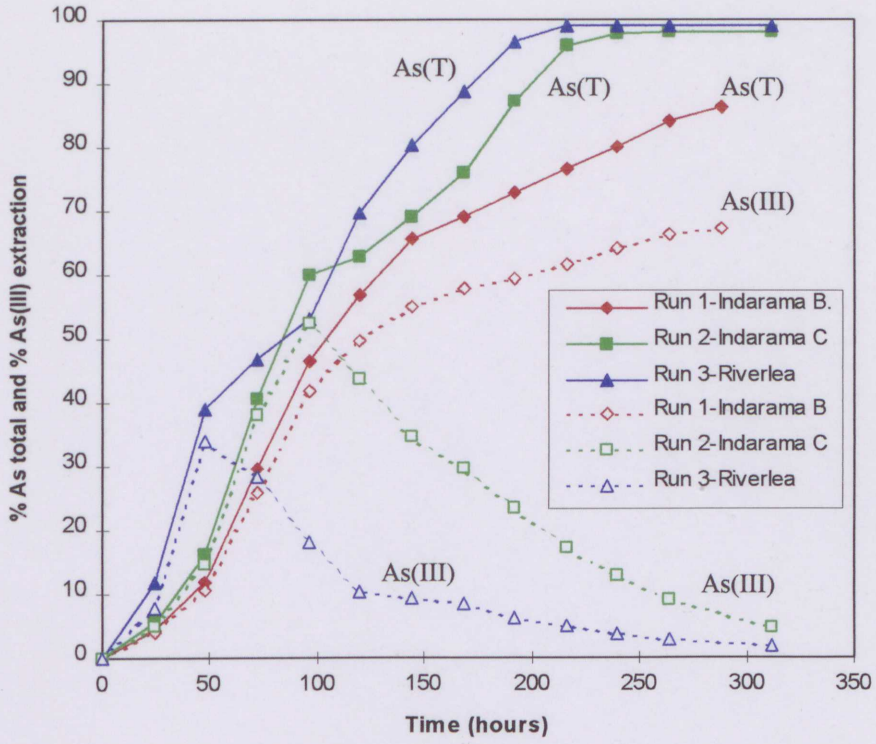


Figure 5.1: Percentage total arsenic extraction and percentage of arsenic(III) formed during bioleaching for Runs 1-3 (see Table 5.1 for composition of solids).

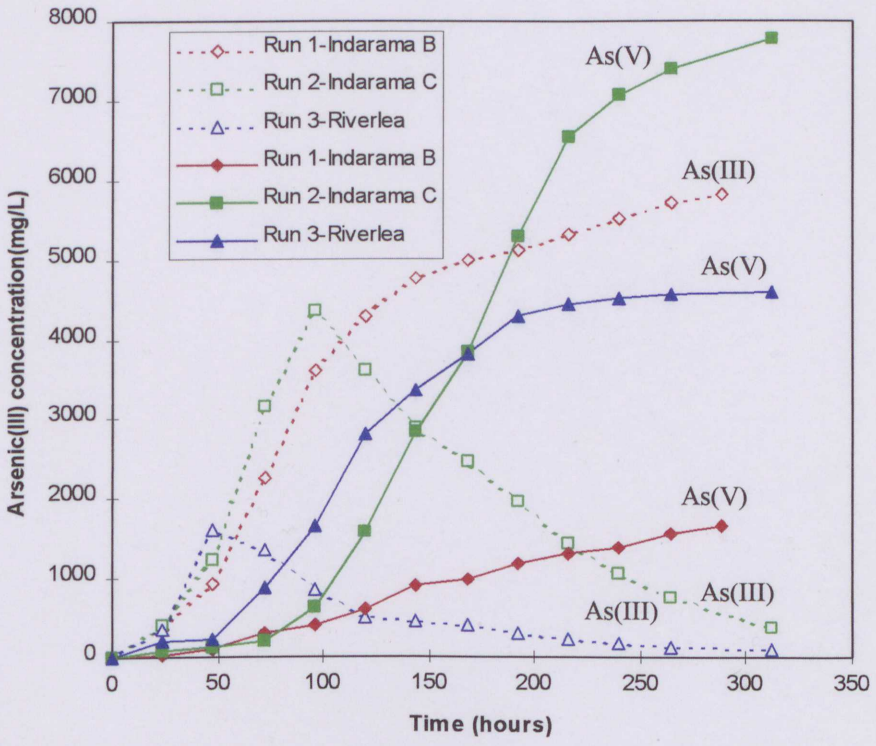


Figure 5.2: Variation in arsenic(III) and arsenic(V) concentrations of the bioleaching slurry for Runs 1-3 (see Table 5.1 for composition of solids).

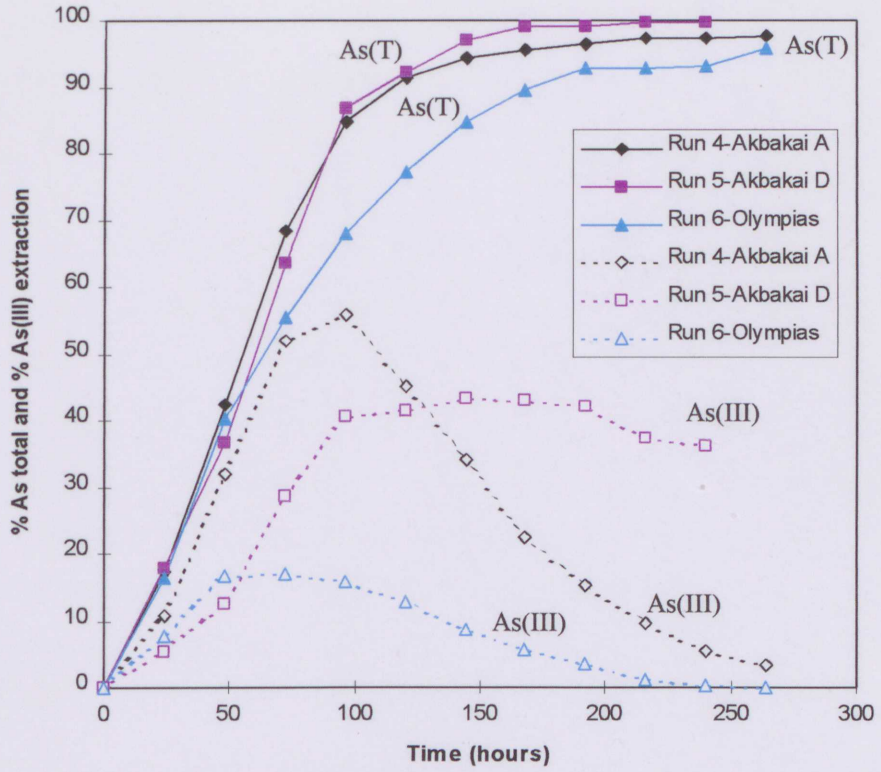


Figure 5.3: Percentage total arsenic extraction and percentage of arsenic(III) formed during bioleaching for Runs 4-6 (see Table 5.1 for composition of solids).

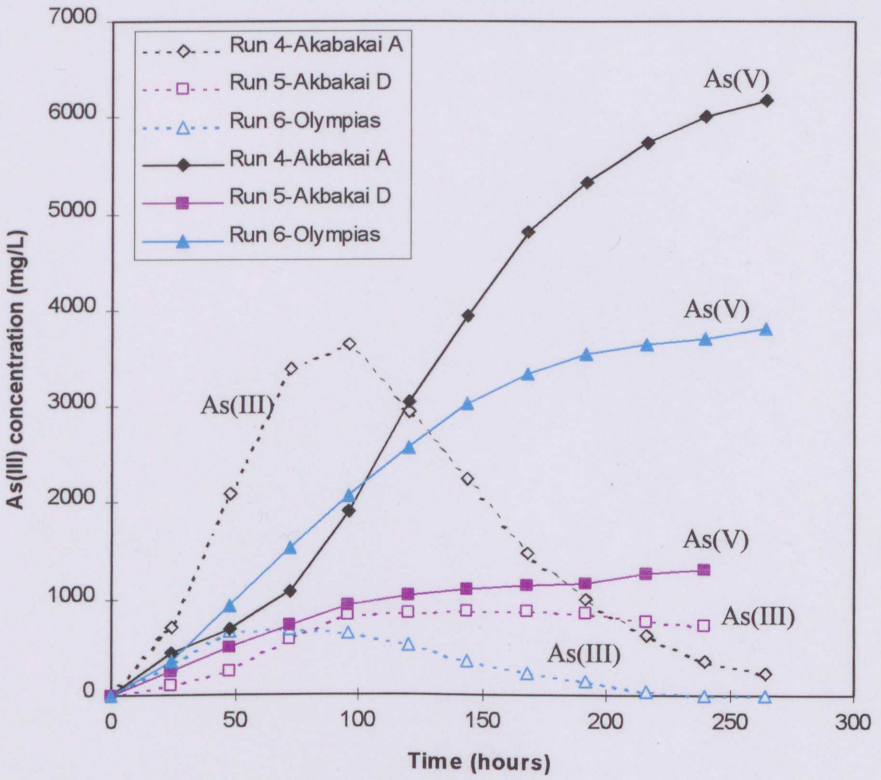


Figure 5.4: Variation in arsenic(III) and arsenic(V) concentrations of the bioleaching slurry for Runs 4-6 (see Table 5.1 for composition of solids).

showing faster rates than the Olympias concentrate. More than 90% arsenic extraction was achieved in all three concentrates after about 144 hours of bioleaching.

Figure 5.3 also shows the percentage of arsenic(III) and Figure 5.4 shows the corresponding concentrations of arsenic(III) and arsenic(V) in mg/L for Runs 4-6. The Akbakai A and D concentrates were from the same deposit but had different mineralogical compositions in terms of pyrite to arsenopyrite ratios as shown in Table 5.1. Runs 4 and 6 showed a similar trends to those of Runs 2 and 3, with arsenic(III) predominating in the leaching slurry during the early stages of the oxidation. The maximum proportion of arsenic(III) for the Akbakai A concentrate was 76% after 72 hours corresponding to about 3400 mg/L (Figures 5.3 and 5.4 respectively, Run 4). The maximum concentration of arsenic(III) in the bioleaching slurry was measured after 96 hours (about 3650 mg/L) for Run 4. Although the Olympias concentrate showed a similar trend, the proportion of arsenic(III) in the leaching slurry never exceeded 50%. The arsenic(III) attained its maximum proportion of 47% after 48 hours, corresponding to about 300 mg/L and the maximum arsenic(III) concentration measured was approximately 680 mg/L after 72 hours. There was almost complete conversion of arsenic(III) to arsenic(V) at the end of the oxidation periods considered for Run 4 and 6. About 3% and 0.2% arsenic(III) remained in the bioleaching slurry after 240 hours for the Akbakai A and the Olympias concentrates respectively. The Akbakai D concentrate showed an almost constant proportion of arsenic(III) after the first 72 hours (Figure 5.4, Run 5). The proportion of arsenic(III) never exceeded 50% as in Run 6. Arsenic(III) reached a maximum proportion of 47% after 96 hours, corresponding to about 830 mg/L (Run 6). More than 36% of the leached arsenic remained as arsenic(III) after 240 hours for Run 5. The results of this run differed significantly from those of Run 4 although the concentrate used in Run 4 was produced from the concentrate used for Run 5. However, there was a difference in the grades of these concentrates (Chapter Four, Table 4.2).

Figure 5.5 and Figure 5.6 show the degree of pyrite and arsenopyrite dissolution during bioleaching for Runs 1-3 and Runs 4-6 respectively. The data shown in these figures were calculated by assuming that all the arsenic in solution was from arsenopyrite

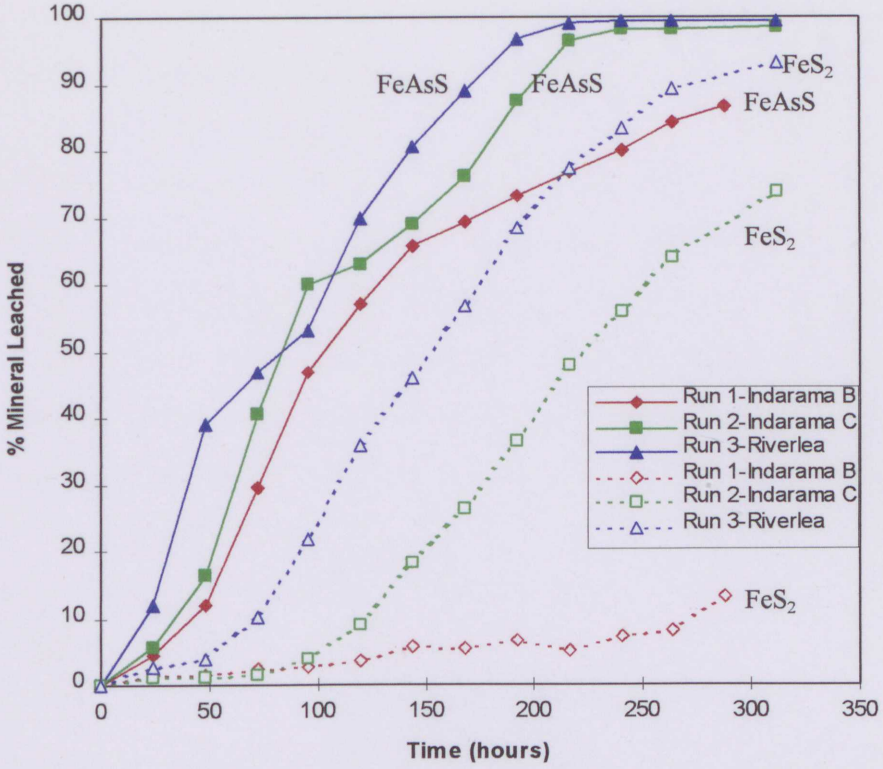


Figure 5.5: Plot of arsenopyrite and pyrite oxidation against time for Runs 1-3 (see Table 5.1 for composition of solids).

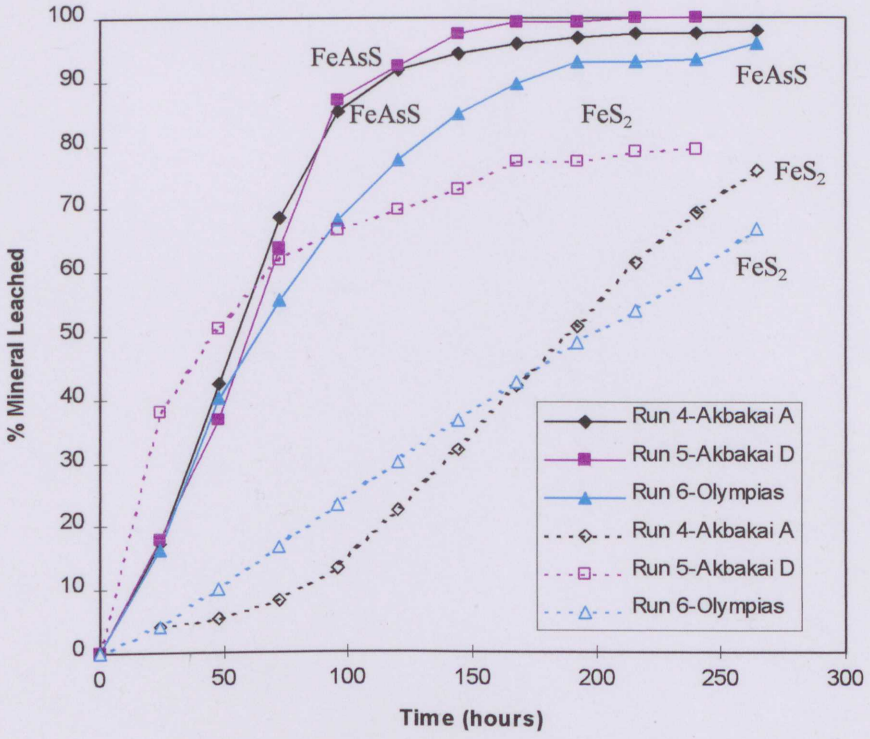


Figure 5.6: Plot of arsenopyrite and pyrite oxidation against time for Runs 4-6 (see Table 5.1 for composition of solids).

dissolution and the excess dissolved iron was used to calculate the amount of pyrite leached. Furthermore stoichiometric mineral compositions were assumed.

In general there is selective leaching of arsenopyrite over pyrite for all the concentrates. The Indarama B concentrate shows the smallest proportion of pyrite and arsenopyrite solubilised (Figure 5.5, Run 1) with time and this concentrate contained more arsenopyrite than pyrite. As the amount of pyrite in the concentrate increases (Table 4.2) more pyrite was solubilised as shown in Figure 5.5 for Runs 2 and 3. There was 86% dissolution of arsenopyrite at the end of the oxidation stage considered for Run 1 and only 13% pyrite dissolution. Comparison of Figure 5.5 (Run 1) to the corresponding Figures of arsenic(III) concentrations (Figures 5.1 and 5.2) it can be seen that most of the arsenic leached remained in the bioleaching slurry as arsenic(III) for Run 1 (about 78%). The dissolution of arsenopyrite was almost complete for Runs 2 and 3 after 216 hours but that of pyrite attained only 47% and 68% respectively. Significant dissolution of pyrite was evident only after most of the arsenopyrite had been leached (more than 60%). There was a correlation between the amount of pyrite leached and the extent of arsenic(III) oxidation in the bioleaching slurry. Significant drops in the arsenic(III) concentration occurred when the leaching of pyrite became the major process taking place in the bioleaching slurry (Comparison of Figures 5.2 and 5.4 with 5.5 and 5.6).

Figure 5.6 shows that the Akbakai D concentrate had the fastest rate of pyrite leaching (Run 5) compared with the other two concentrates, however the amount of arsenic(III) remaining in the bioleaching slurry at the end of the oxidation stage was highest compared with Runs 4 and 5. Run 4 also had more pyrite solubilised compared with Run 6, but the latter had the fastest rate of arsenic(III) oxidation. These differences will be explained in terms of the compositions and the sulphide grades of the concentrates in the discussion section.

5.2.2 Release of iron into solution during bacterial leaching

Figures 5.7 and 5.8 show the concentrations of iron(II) in solution for Runs 1-3 and 4-6 respectively. The concentrations of ferrous iron showed maxima for all the runs within

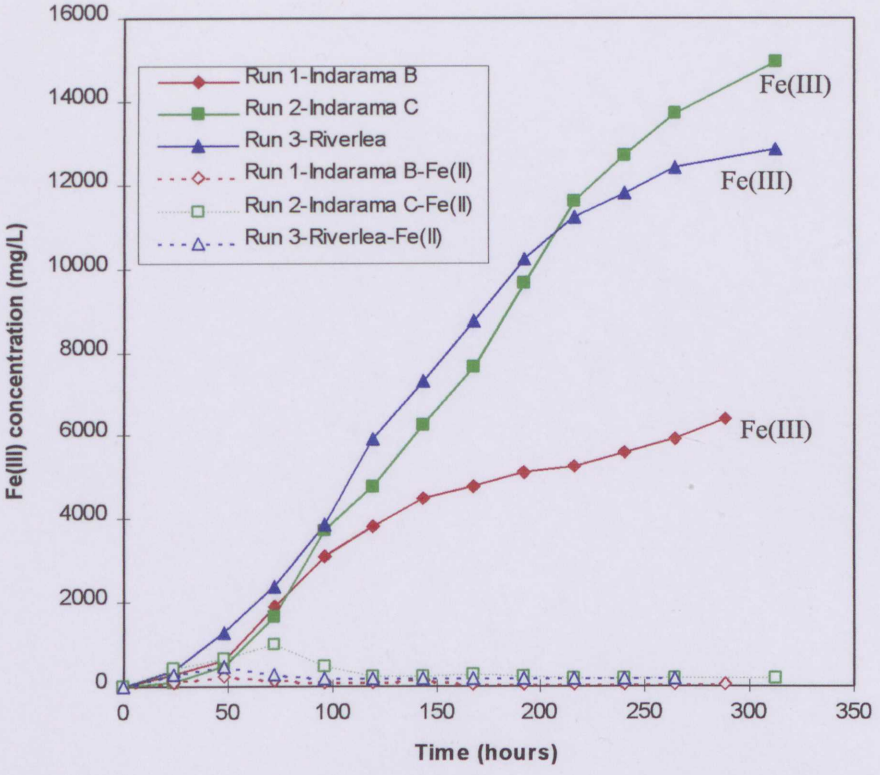


Figure 5.7: Concentrations of iron(II) and iron(III) in the bioleaching slurry for Runs 1-3 (see Table 5.1 for composition of solids).

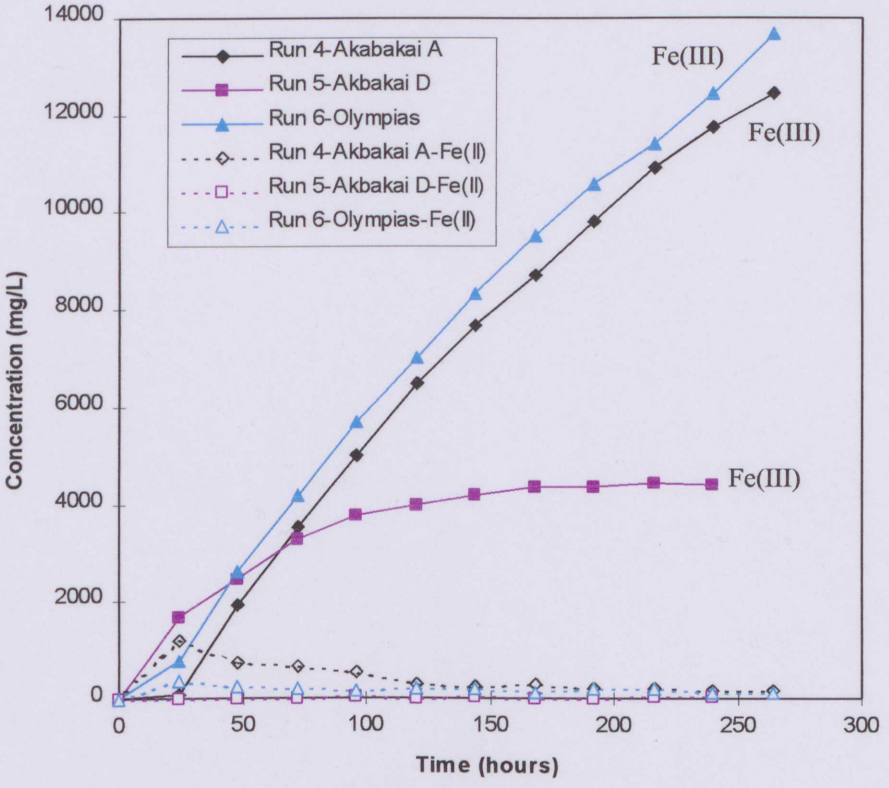


Figure 5.8: Concentrations of iron(II) and iron(III) in the bioleaching slurry for Runs 4-6 (see Table 5.1 for composition of solids).

the first 72 hours. The Indarama C concentrate showed the highest concentration of iron(II) (about 1030 mg/L, Figure 5.7) and the corresponding concentration of arsenic(III) was about 3170 mg/L. Run 1 (the Indarama B concentrate) had about 260 mg/L iron(II) with a corresponding arsenic(III) concentration of about 930 mg/L. The maximum amount of iron(II) for Run 3 (the Riverlea concentrate) was about 480 mg/L, corresponding to about 1600 mg/L arsenic(III) in the bioleaching slurry. The concentrations of iron(II) followed a pattern similar to that of arsenic(III) in the first 72 hours. There seems to be a relationship between the concentrations of arsenic(III) in the bioleaching slurry and the maximum peaks of iron(II) concentrations. Higher concentrations of arsenic(III) corresponded to higher concentrations of iron(II).

In Run 5 the concentration of iron(II) is very low, which means all the ferrous iron formed was immediately oxidised to iron(III). Very low concentrations of iron(II) (maximum of about 23 mg/L) were measured throughout the run (Figure 5.8). The Akbakai A concentrate and the Olympias showed maximum iron(II) concentrations of about 1190 mg/L and 380 mg/L after 24 hours (Figure 5.8) and these values corresponded to about 700 mg/L and 300 mg/L arsenic(III) concentrations in the bioleaching slurries, respectively.

Plots of the iron(III) concentrations versus time for Runs 1-3 and 4-6 are also shown in Figures 5.7 and 5.8 respectively. Comparison of these figures with those of arsenic(III) concentrations showed that iron(III) was produced from the oxidation of iron(II) at the same time as the arsenic(III) began to decrease in the bioleaching slurry and also the rate of arsenic(III) oxidation increased with increasing iron(III) concentrations. An increase in the iron(III) concentrations also coincides with an increase in the arsenic extraction rate. Almost all the iron(II) was oxidised to iron(III) by the end of the oxidation stage. Run 1 which had the highest amount of arsenic(III) at the end of the oxidation stage had an iron(III) concentration which was at least 2-fold less than the iron(III) concentrations of Run 2 and 3 (Figure 5.7).

The concentrations of ferric iron started increasing significantly after 72 hours approaching total values of about 6410 mg/L, 14900 mg/L and 12800 mg/L for Runs 1, 2 and 3 respectively (Figure 5.7). The increase in ferric iron concentrations is due to the increase in free bacteria in solution which oxidised the iron(II) to iron(III) ions for their energy requirements as was shown by counting the free bacteria in solution. Different concentrations of iron(III) were measured in the bioleaching slurry for Run 4-6, and the iron(III) concentrations for these runs were about 12500 mg/L, 4400 mg/L and 13700 mg/L (Figure 5.8). The amount of iron(III) in the bioleaching slurry varied from one concentrate to another depending on their initial compositions.

5.2.3 Effect of adding pyrite on the speciation of arsenic

Due to the variation in the arsenic species existing in the bioleaching slurries for different concentrates which were studied in Runs 1-6 (Figures 5.1-5.8), it was decided to investigate the effect of changing the composition of the highly arsenical concentrate from the Indarama mine (the Indarama B concentrate) by adding pyrite from the Stratoni mine (Table 5.2). Arsenic(III) dominated in the bioleaching slurry of the Indarama B concentrate throughout the oxidation period which was considered in these experiments (Figures 5.1 and 5.2, Run 1). Comparison of the bioleaching results from this concentrate with the other concentrates which contained more pyrite suggested that pyrite promoted the formation of arsenic(V) in the bioleaching slurry.

The compositions of the different mixtures which were used to investigate the effect of pyrite are given in Table 5.2. In addition to the mixtures used, a concentrate from the Fairview mine was also used to compare its arsenic speciation with that of the mixtures and the original concentrate (the Indarama B concentrate). By considering the mineralogical composition of the Fairview concentrate it was predicted that this concentrate would promote the formation of arsenic(V) faster than the mixtures because of its high ratio of pyrite to arsenopyrite.

Figure 5.9 shows the percentage of arsenic extraction from the initial concentrates during bioleaching for Runs 1 and 7-9 whose compositions are given in Table 5.2. Runs

7-9 showed almost the same rate of arsenic extraction. The Fairview concentrate showed the fastest rate of arsenic extraction in the early stages of leaching with more than 80% extraction after 72 hours. More than 97% arsenic extraction was achieved at the end of the oxidation stage in Runs 7-9. Comparison of these results with those for Run 1 show that the pyrite promoted the extraction of arsenic from the Indarama concentrate (Figure 5.9).

Table 5.2: The origins and composition of the concentrates used in Runs 7-9.

Run Number	Sample Location	Sample I.D	wt% As	wt% Fe	Ratio FeS_2/FeAsS
Run 1	Indarama	B	17.28	26.55	0.78
Run 7	Indarama/Stratoni	M 1	12.48	31.47	1.76
Run 8	Indarama/Stratoni	M 2	10.88	33.11	2.27
Run 9	Fairview	F	4.22	17.80	3.43
-	Stratoni	P	1.28	42.95	32.45

Figures 5.9 also shows the percentage and Figure 5.10 corresponding concentrations (mg/L) of arsenic(III) and arsenic(V) in the bioleaching slurry for Runs 1 and 7-9. The two mixtures produced from the Indarama B and the Stratoni P concentrates showed different trends in the behaviour of the arsenic(III) reporting in the bioleaching slurry (Run 7 and 8) compared with the original concentrate (the Indarama B concentrate) (Run 1, Figures 5.9 and 5.10). However the mixtures (M1 and M2) showed the same trends as for the Fairview concentrate but with different rates of arsenic(III) to arsenic(V) oxidation. Arsenic(III) predominated in the bioleaching slurry in the early stages in all the cases. Run 7 showed maximum proportion of 66% arsenic(III) after 48 hours, corresponding to about 2190 mg/L, while that for Run 8 was 71% after 24 hours and corresponding to about 1000 mg/L (Figures 5.9 and 5.10). The maximum concentrations of arsenic(III) which were measured in the bioleaching slurry for Runs 7 and 8 were about 2210 mg/L and 2590 mg/L respectively after 72 hours. The percentage

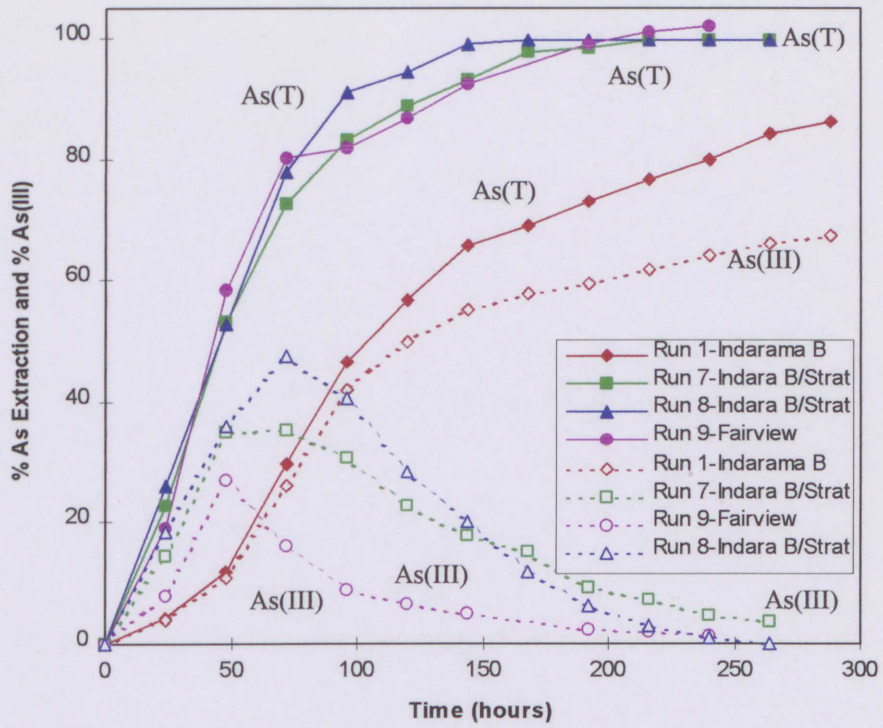


Figure 5.9: Percentage total arsenic extraction and percentage of arsenic(III) during bioleaching for Runs 1 and 7-9 (see Table 5.2 for composition of solids).

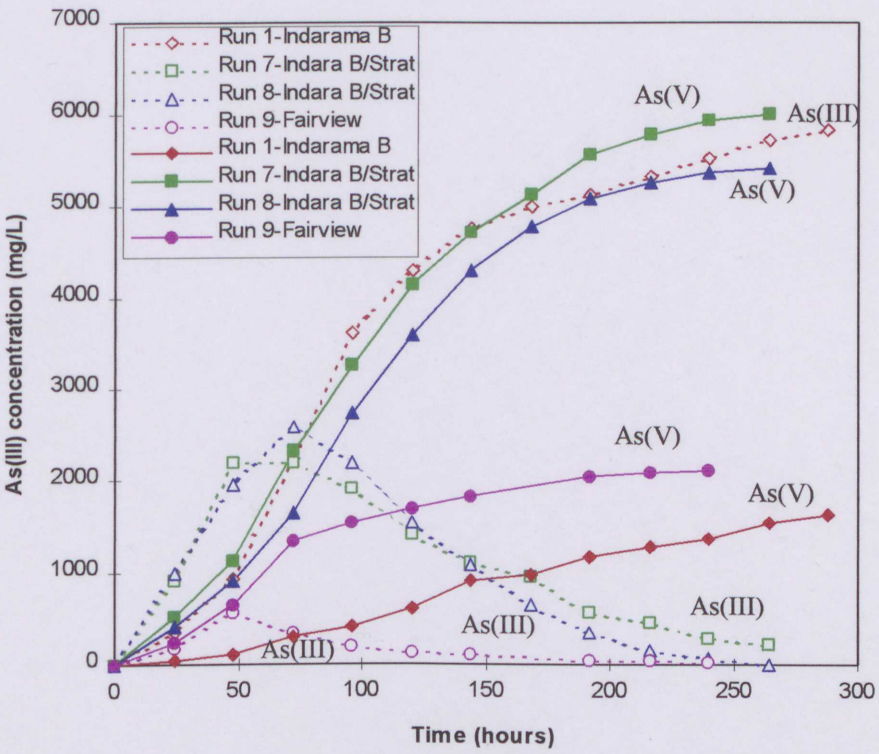


Figure 5.10: Variation in arsenic(III) and arsenic(V) concentrations of the bioleaching slurry for Runs 1 and 7-9 (see Table 5.2 for composition of solids).

of arsenic(III) in the bioleaching slurry of the Fairview concentrate did not exceed 50% of the leached arsenic at any point. Arsenic(III) reached its maximum proportion of 46% after 48 hours, corresponding to about 570 mg/L and this was also the maximum arsenic(III) concentration which was measured in the bioleaching slurry for this experiment (Run 9). The results from this run are comparable to those of Run 6 (the Olympias concentrate) in which the proportion of arsenic(III) never exceeded 50% of the leached arsenic at any point. Mineralogical compositions showed that these two concentrates had the highest ratios of pyrite to arsenopyrite (Table 5.1 and 5.2).

The rate of arsenopyrite leaching was almost the same for Runs 7 and 9, while more pyrite was leached for Run 9 compared to Run 7 (Figure 5.11). Figure 5.11 shows that arsenopyrite was leached faster than pyrite. The addition of more pyrite to the arsenopyrite-rich Indarama B concentrate not only improved the rate of oxidation of arsenic(III) to arsenic(V) but also increased the amount of pyrite leached as can be seen by comparison of Runs 1 and 7 (Figure 5.11). The rate of arsenopyrite dissolution was also increased.

Figure 5.12 shows the concentrations of iron(II) and iron(III) for Runs 1 and 7-9. Iron(II) concentrations show maxima in the first 72 hours and then drop thereafter (Figure 5.12). The maximum concentrations of iron(II) measured in the bioleaching slurry for Runs 7-9 were about 260 mg/L, 1090 mg/L and 900 mg/L respectively. These concentrations of iron(II) occurred at the same time when the proportion of arsenic(III) was highest in the bioleaching slurry (comparison of Figures 5.9 and 5.12). The iron(III) concentrations for the Runs 1 and 7-9 are also shown in Figure 5.12. From this figure it can be seen that different maximum concentrations of iron(III) were measured in the bioleaching slurry with Run 1 having the lowest value of iron(III) concentration (about 6410 mg/L) for the oxidation period considered here. However the same run had the highest concentration of arsenic(III) in the slurry. The maximum concentrations of iron(III) in the bioleaching slurry for Runs 7-9 were about 14100 mg/L, 13100 mg/L and 8240 mg/L. Although Run 9 had the lowest concentration of iron(III) compared with Runs 7 and 8, the rate of oxidation of arsenic(III) to arsenic(V) was faster than

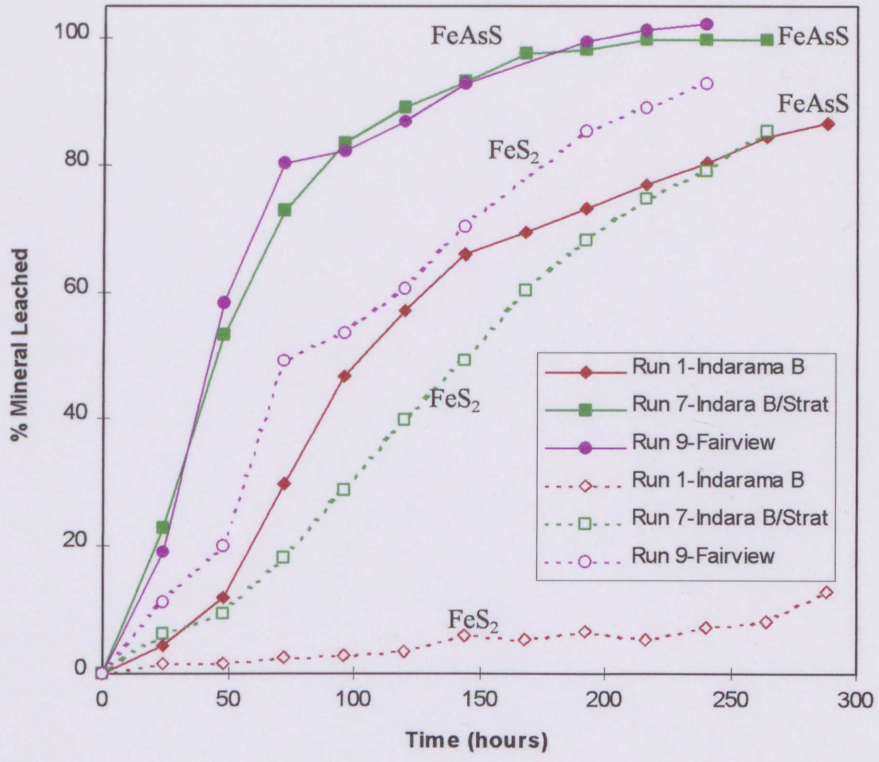


Figure 5.11: Plot of arsenopyrite and pyrite oxidation against time for Run 1, 7 and 9 (see Table 5.2 for composition of solids).

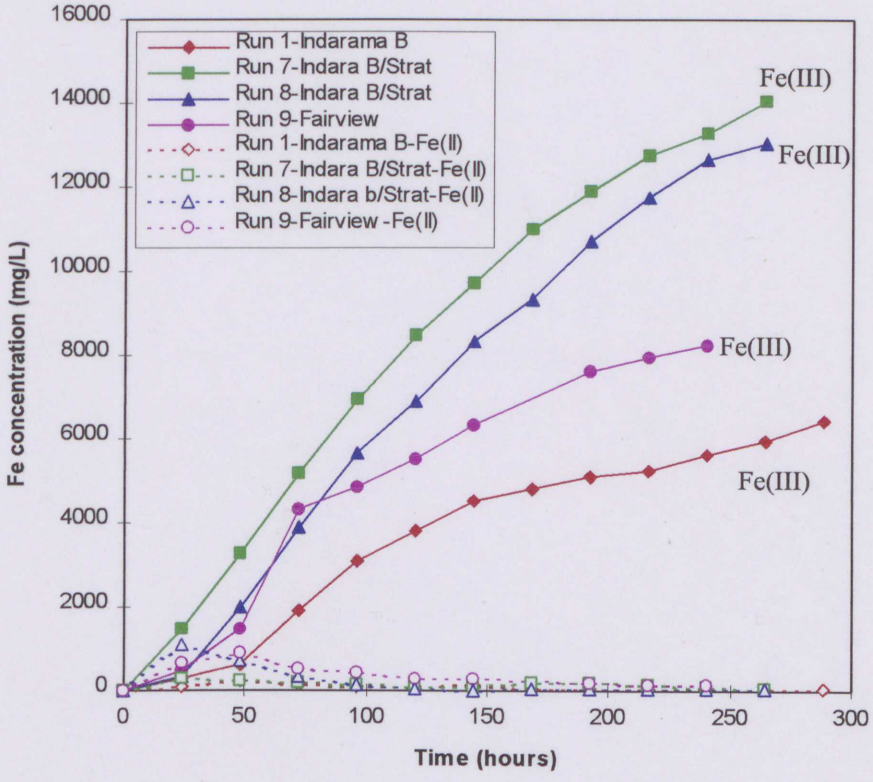


Figure 5.12: Concentrations of iron(II) and Fe(III) in the bioleaching slurry for Runs 1 and 7-9 (see Table 5.2 for composition of solids).

in the other two runs (Figure 5.9). The same figure also show that Run 7 had a slightly higher rate of arsenic(III) oxidation in the early stages than Run 8, but towards the end of the oxidation stage considered here arsenic(III) oxidation was faster in Run 8 than in Run 7 despite the fact that the latter had a slightly higher iron(III) concentration.

5.2.4 Effect ferric ions on the speciation of arsenic

Low ferric iron concentrations between 0.3 and 4.5 g/L were found by Kelly and Jones **[146]** to enhance biooxidation. High concentrations above 11 g/L were, however found to inhibit the bacteria and substrate oxidation. Collinet and Morin **[187]** studied the relative tolerance of *Thiobacillus ferrooxidans* and *Thiobacillus thiooxidans* to ferrous and ferric iron. These researchers found that both strains were inhibited by 10 g/L ferric iron, however *Thiobacillus thiooxidans* was found to have more tolerance to ferrous iron than *Thiobacillus ferrooxidans*. 20 g/L iron(II) was found to be toxic to *Thiobacillus ferrooxidans*, but 30 g/L iron(II) was necessary to impede the growth of *Thiobacillus thiooxidans*. Some researchers have successfully used bacterially-rich ferric sulphate with iron(III) concentrations of about 10 g/L to enhance the leaching of pyrite/arsenopyrite concentrates **[112, 121, 144, 188-189]**. The variation in the ferric iron tolerance of bacteria is likely to differ for different strains and also because of the adaptation of the culture.

The results described for the first runs above show that the amount of iron(III) in the bioleaching slurry plays an important role in the oxidation of arsenic(III) to arsenic(V) in addition to the ore compositions (mineralogical ratio of pyrite to arsenopyrite in the concentrates). The ore composition was also found to control the amount of iron(III) formed. It was then decided to add initial soluble iron(III) to some of the experiments to investigate the effect of the ferric iron on the speciation of arsenic during bacterial leaching. The mineralogical compositions and the origins of the concentrates which were used for this investigation are given in Table 5.3. In Runs 10-13 an initial dissolved iron(III) concentration of 2.4 g/L was used.

Figure 5.13 shows the percentage of arsenic extracted from the concentrates when in the presence of added dissolved iron(III). The iron(III) increased the rate of arsenopyrite leaching. The most significant improvement was shown by the Indarama B concentrate (Run 10). More than 96% arsenic extraction was achieved compared to only 86% when no initial dissolved iron(III) was added to the bioleaching slurry (comparison of Figure 5.1 and 5.13). The other concentrates used in Runs 11-13 also showed enhanced arsenic extractions as a result of the iron(III) additions.

Table 5.3: Compositions and origins of the concentrates used in Runs 10-13 to investigate the effect of iron(III) additions.

Run Number	Sample Origin	Sample I.D	wt % As	wt % Fe	Ratio FeS_2/FeAsS
Run 10	Indarama	B	17.28	26.55	0.78
Run 11	Indarama/Stratoni	M 1	12.48	31.47	1.76
Run 12	Riverlea	R	9.47	27.46	2.13
Run 13	Akbakai	A	13.09	30.39	1.56

Figures 5.13 also shows the percentage of arsenic(III) and Figure 5.4 shows the corresponding concentrations of arsenic(III) and arsenic(V) in mg/L of the bioleaching slurry for Runs 10-13. As previously observed in the first runs, arsenic(III) predominates in the bioleaching slurry in the initial stages of the leaching. The maximum percentage of arsenic(III) measured in Run 10 was 83% corresponding to about 3500 mg/L arsenic(III) and the maximum concentration of arsenic(III) in the bioleaching slurry was about 5210 mg/L. Oxidation of arsenic(III) to arsenic(V) occurred to a significant extent. At the end of the oxidation stage considered here, 26% (corresponding to about 2310 mg/L, Figures 5.13 and 5.14) of the solubilised arsenic remained in the bioleaching slurry as arsenic(III) compared to 78% (corresponding to about 5800 mg/L, Figures 5.1 and 5.2) when no initial iron(III) was supplemented to the run on the same concentrate. Runs 11-13 also showed some improvements in the oxidation rate of arsenic(III) compared to their respective runs in the previous section where no initial dissolved iron(III) was added to the bioleaching slurry. Run 12 showed

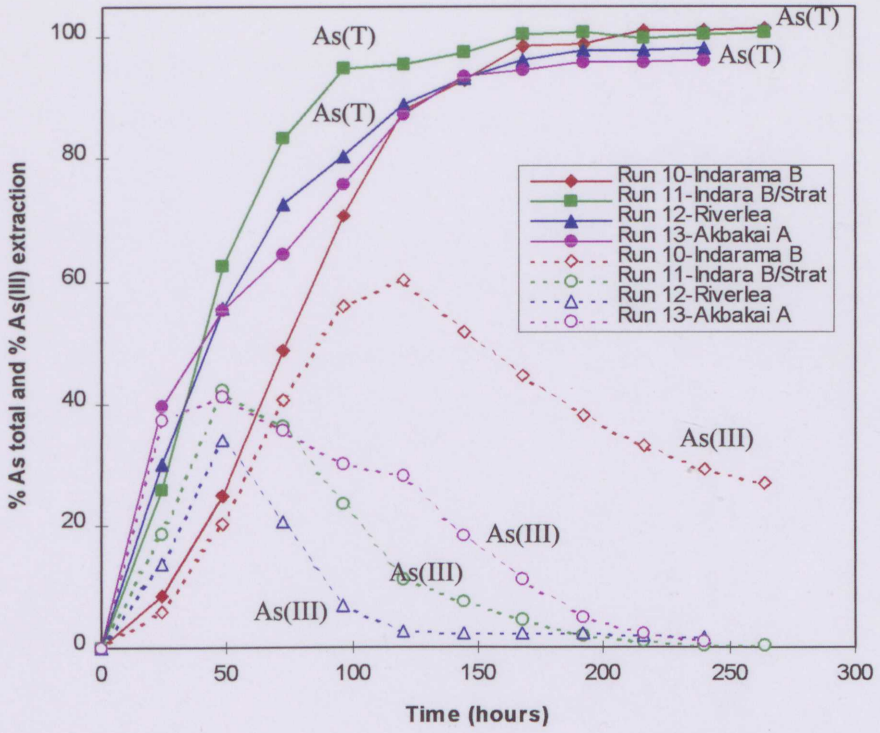


Figure 5.13: Percentage total arsenic extraction and percentage of arsenic(III) during bioleaching for Runs 10-13 (see Table 5.3 for compositions of solids).

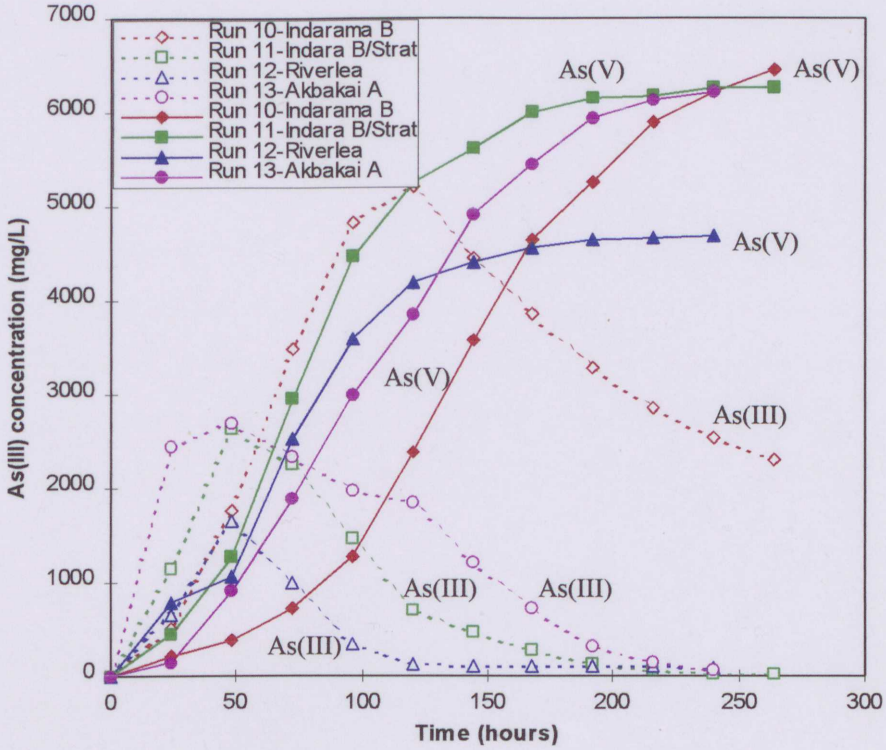


Figure 5.14: Variation in arsenic(III) and arsenic(V) concentrations of the bioleaching slurry for Runs 10-13 (see Table 5.3 for composition of solids).

a maximum arsenic(III) proportion of 61% corresponding to about 1650 mg/L (Figures 5.13 and 5.14) compared with 87% corresponding to about 1610 mg/L (Figures 5.1 and 5.2) when no initial iron(III) was used. Although the concentration of arsenic(III) in the bioleaching slurry seem to differ little, the rate of arsenic extraction and arsenic(III) oxidation differs significantly. The amount of arsenic(V) in the bioleaching slurry for Run 3 and Run 10 are about 240 mg/L and 1060 mg/L respectively after 48 hours. This showed that the rate of arsenic(III) oxidation was much faster when iron(III) was supplemented to the bioleaching slurry.

Figure 5.15 shows the amount of arsenopyrite and pyrite leached from the initial concentrates for Runs 10-13. The addition of initial iron(III) enhanced the solubilisation of arsenopyrite in the concentrates. It is important to note that the amount of pyrite leached for Run 10 increased by 9-fold after 264 hours when compared to Run 1 (Figure 5.11). The increased rate of pyrite leaching was also accompanied by an increase in the rate of arsenic(III) oxidation as shown by comparison of Figures 5.2 and 5.14 (Run 1).

The concentrations of iron(II) and iron(III) in the bioleaching slurry for Runs 10-13 are shown in Figure 5.16. The same trends as those observed in the previous runs are shown in this figure. The difference is that the peak concentrations of iron(II) was higher than in the corresponding runs where iron(III) was not added to the bioleaching slurry. The concentration of iron(II) shown in Figure 5.16 was a combination of the iron(II) from bacterial leaching of the pyrite and arsenopyrite and also the chemical reduction of the initial iron(III) added during the oxidation of arsenic(III) and leaching of arsenopyrite. The total iron(III) concentration in the bioleaching slurry was almost the same for Run 10 and Run 13 but Run 13 showed a better conversion rate of arsenic(III) to arsenic(V).

Table 5.4 shows the leaching conditions of some runs which were carried out on the Indarama C concentrate to further investigate the effect of iron(III). The above results suggest that additions of soluble iron(III) promote the oxidation of arsenic(III) and consequently it was decided to increase the amount of initial iron(III) in the slurry. The composition of the Indarama C is given in Table 5.1.

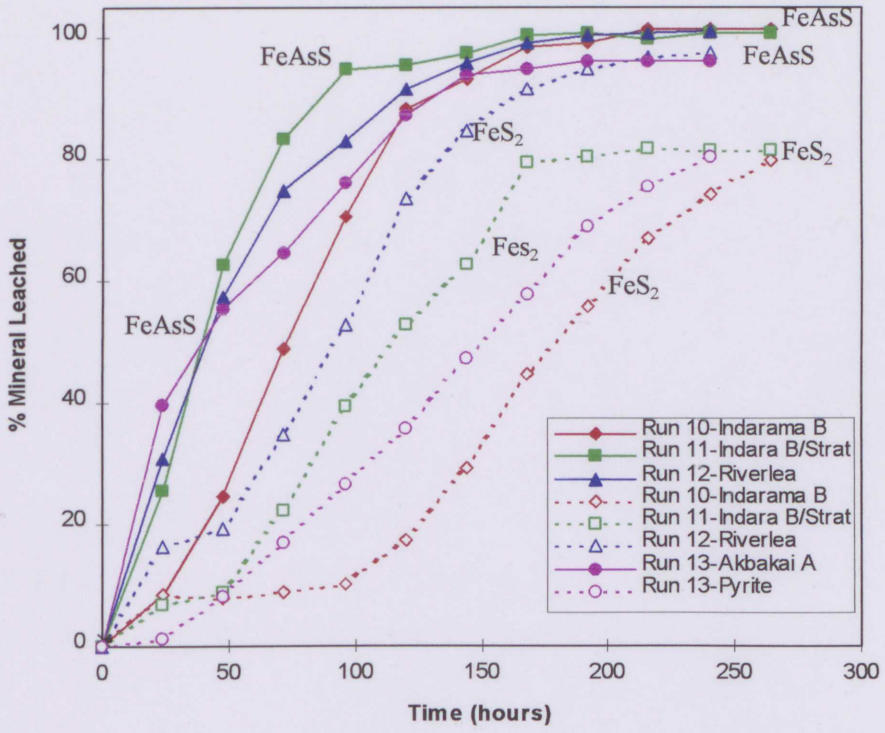


Figure 5.15: Plot of arsenopyrite and pyrite oxidation against time for Runs 10-13 (see Table 5.3 for composition of solids).

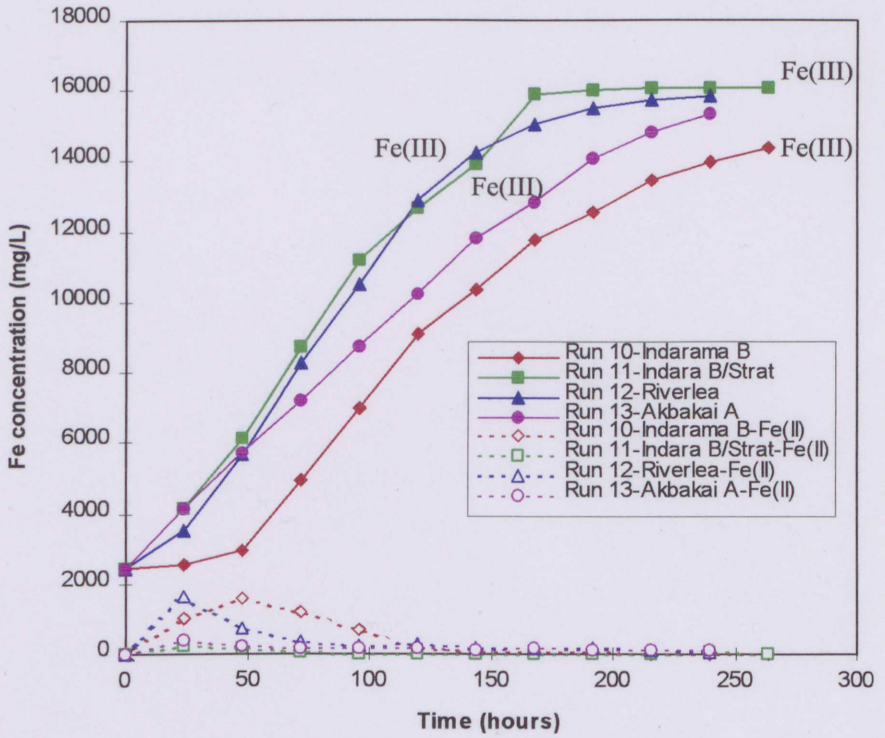


Figure 5.16: Concentrations of iron(II) and iron(III) in the bioleaching slurry for Runs 10-13 (see Table 5.3 for composition of solids).

Table 5.4: Leaching conditions used to further investigate the effect of initial iron(III) on the speciation of arsenic.

Run Number	Sample Location	Sample I.D	Initial Iron(III) concentration (g/L)
Run 2	Indarama	C	Nil
Run 14	Indarama	C	2.4
Run 15	Indarama	C	5.1
Run 16	Indarama	C	10.0

Figure 5.17 shows the variation of arsenic(III) percentage in the bioleaching slurry phase for Runs 2 and 14-16 and Figure 5.18 shows the corresponding concentrations of arsenic(III) in mg/L. While the extraction of arsenic remained high the oxidation of arsenic(III) to arsenic(V) was affected under the experimental conditions applied here. Addition of increased concentrations of iron(III) retarded the arsenic(III) oxidation rate. The results still showed the predominance of arsenic(III) in the bioleaching slurry in the early stages of leaching. At the end of 264 hours, about 2% (about 170 mg/L) remained in the bioleaching slurry phase as arsenic(III) for Run 14 while in Run 15 and 16 the percentages were 23% (about 1800 mg/L) and 28% (about 2170 mg/L) respectively. Figure 5.17 shows that there was a phase lag in attainment of the maximum arsenic(III) concentration as the amount of initial dissolved iron(III) was increased in the bioleaching slurry phase.

Calculation of the amount of pyrite leached after 264 hours show that 77% was leached in Run 14, 36% in Run 15 and 28% for Run 16. These results show a strong link between pyrite dissolution and the oxidation of arsenic(III). Although the concentrations of iron(III) in the leaching slurry in all the cases were very high (about 17700 mg/L for Run 14, 15100 mg/L for Run 15 and 18900 mg/L for Run 16), they did not affect the oxidation of arsenic(III) very much.

Table 5.5 shows the leaching conditions which were used to investigate the effect of recycling fractions of the iron and arsenic rich bioliquors from the previous runs.

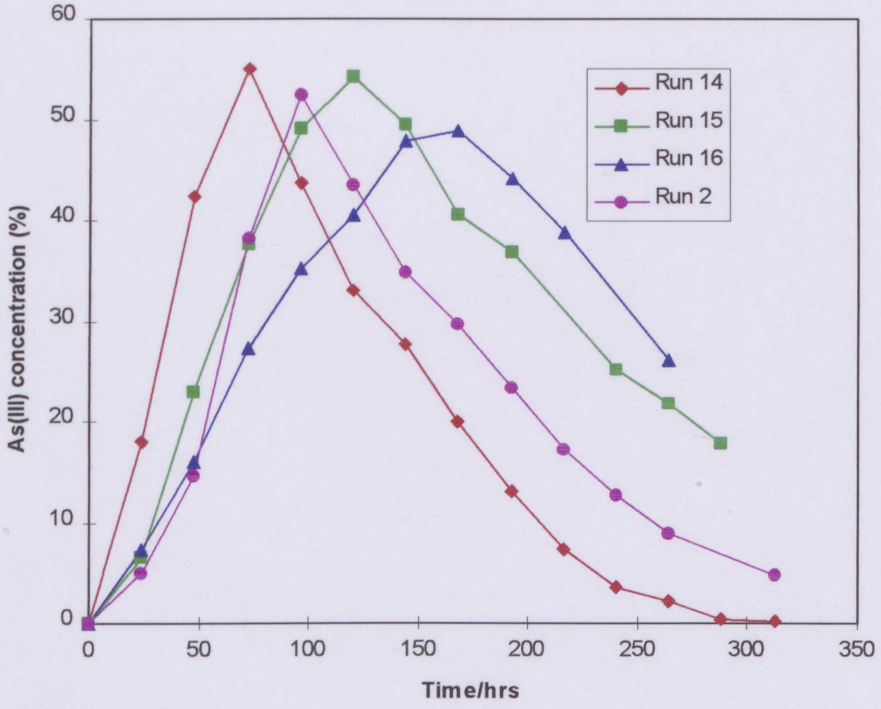


Figure 5.17: Variation in the percentage of arsenic(III) formed during bioleaching for Runs 14-16 (see Table 5.4 for compositions of solids).

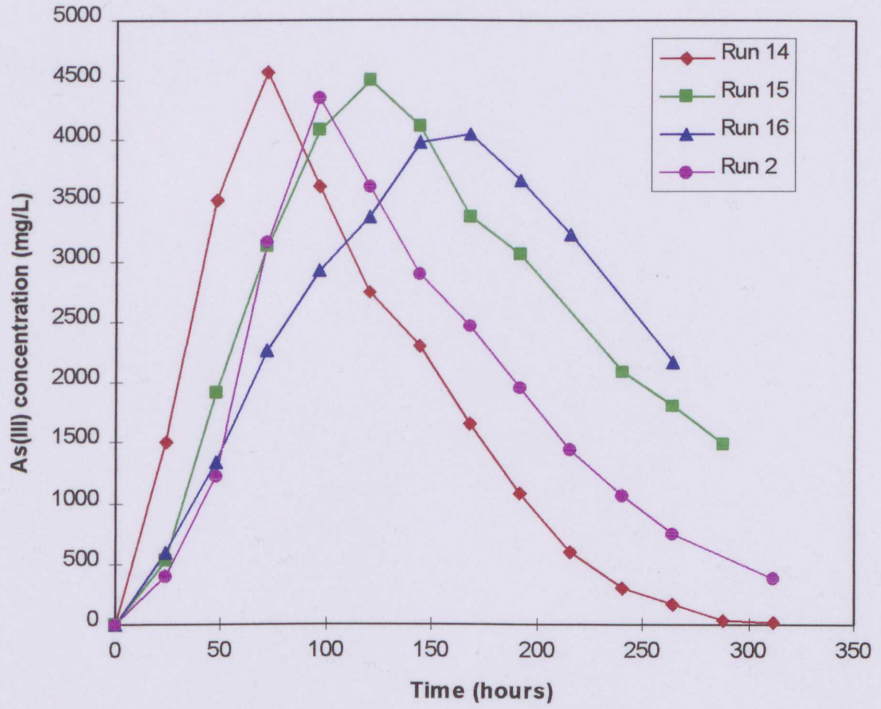


Figure 5.18: Variation in arsenic(III) concentrations of the bioleaching slurry for Runs 14-16 (see Table 5.4 for compositions of solids).

Recycling the bioleaching liquor from the previous run also retarded the oxidation of arsenic(III) as shown in Figures 5.19. These liquors contain bacterially generated iron(III) and arsenic mostly as arsenic(V) as shown in Table 5.5. When the same solution as the one used in Run 17 was used for the Akbakai D concentrate (Run 19) which contains less pyrite and arsenopyrite initially, the oxidation of arsenic(III) was improved slightly when compared with the results of Run 5 (Figure 5.4 and Figure 5.20).

Table 5.5: Leaching conditions used in experiments to investigate the effect of recycling the bioliquor.

Run Number	Sample origin	Sample I.D.	% (v/v) recycled sol.	Initial Fe g/L	Initial As g/L
Run 17	Indarama	C	20	4.6	1.8
Run 18	Indarama	C	30	6.1	3.1
Run 19	Akbakai	D	20	4.6	1.8

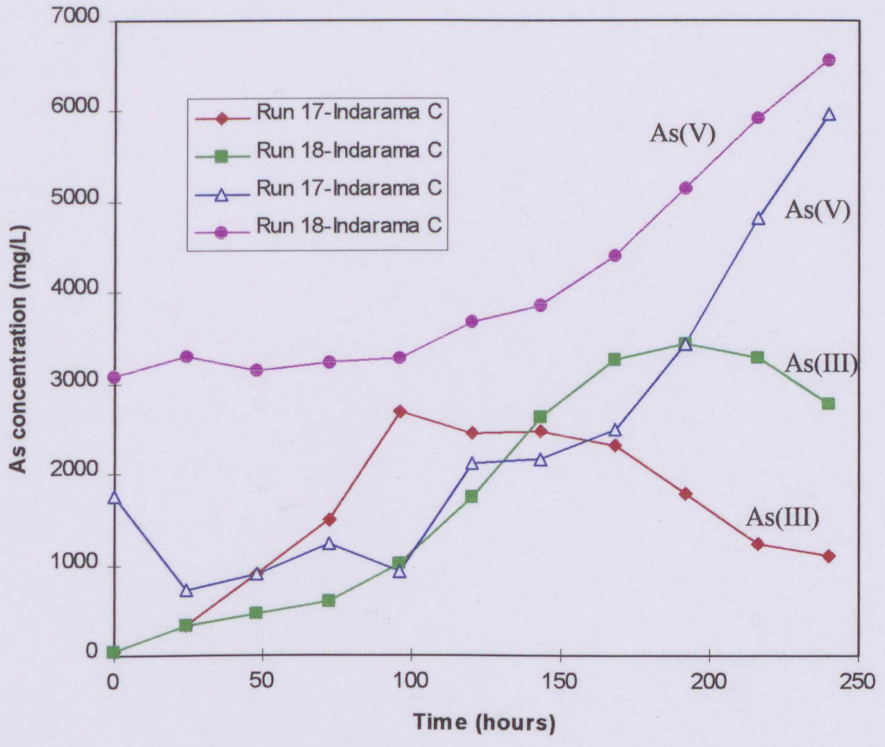


Figure 5.19: Speciation of arsenic in the bioleaching slurry with time for the Indarama C concentrate (see Table 5.5 for leaching conditions).

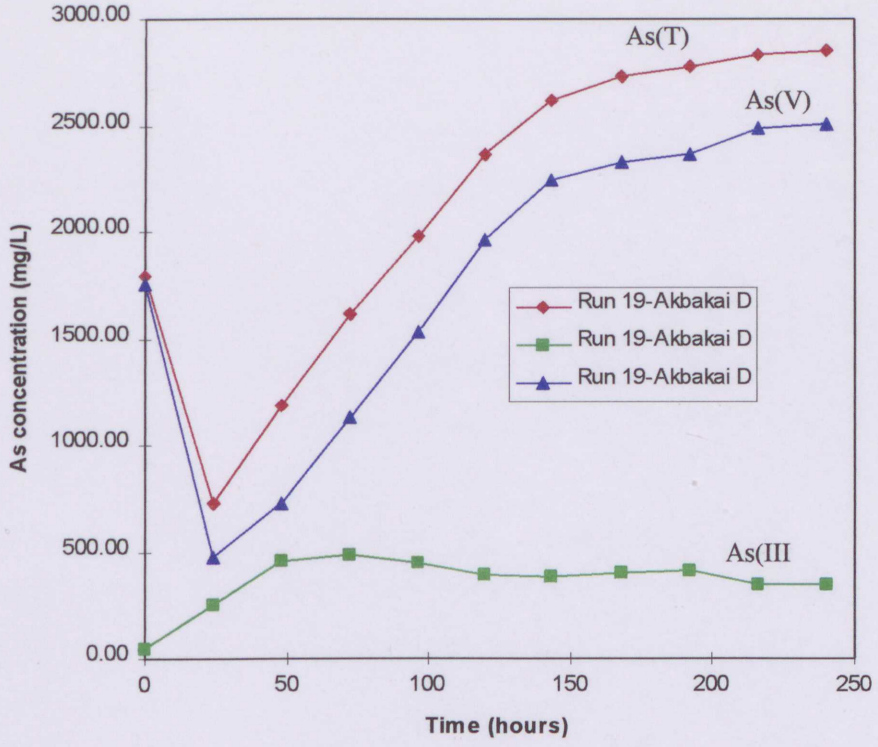


Figure 5.20: Speciation of arsenic in the bioleaching slurry with for the Akbakai D concentrate (see Table 5.5 for leaching conditions).

5.2.5 Effect of controlling pH

In the experiments above the pH of the bioleaching slurry was initially set at 1.8 and then left to drift freely to lower values as the oxidation of the minerals proceeded. Very low pH values were measured at the end of the oxidation stages (as low as 0.9). To investigate the effect of controlling the pH, lithium hydroxide was used for adjusting the pH daily before sampling. Lithium hydroxide was chosen to minimise the formation of jarosites. In the experiments on the effect of pH, samples taken for analysis were split and one part was acidified with concentrated hydrochloric acid in order to dissolve all the precipitates, while the other part was analysed without acidifying. This allowed a comparison of the amount of precipitation taking place as a result of pH control. No initial dissolved iron(III) was added in these experiments.

Figure 5.21 shows the speciation of arsenic during bacterial leaching with the pH being adjusted to 1.5 on a daily basis. The difference in concentrations of arsenic species between the curves in which the sample was acidified and the non-acidified sample

gives the amount of arsenic(III) and arsenic(V) in the precipitated solids. There was no major difference in the oxidation trends of arsenic(III) when the pH of the bioleaching slurry was controlled around 1.5. Arsenic(III) predominated in the bioleaching slurry, reaching its maximum concentrations of about 4970 mg/L for the acidified sample and 4420 mg/L for the non-acidified sample after 96 hours. The difference in the concentrations of arsenic(III) in the acidified sample and the non-acidified sample was very low throughout the oxidation period considered here. This meant that there was very little incorporation of arsenic(III) in the precipitated residues, most of it remained in solution. There was precipitation of arsenic(V) as shown by the difference in the concentrations of arsenic(V) and the total concentrations of arsenic. The precipitation became more pronounced after 120 hours. The overall extraction of arsenic was not much affected (about 98%) when compared with the experiments described above in which the pH of the leaching slurry was left to drift freely. There was a difference in the extent of arsenic oxidation, 7% of the solubilised arsenic remained in the bioleaching slurry as arsenic(III) while values of less than 2% were typical in most experiments where the pH was left to drop freely using the same concentrate. Calculation of the pyrite leached show that 53% pyrite was dissolved.

Figure 5.22 shows the speciation of arsenic with the pH being controlled around 1.8. The same trends as the ones shown in Figure 5.21 can be seen, however there was more precipitation and significant precipitation of the arsenate started earlier. The extent of arsenic(III) oxidation was not affected much, with 5% arsenic(III) remaining in the bioleaching slurry at the end of the oxidation period considered here, 65% of the pyrite was leached. A major deviation from the above trends was observed when the pH was controlled around 2.5 as shown in Figure 5.23. All the arsenic(V) formed was immediately precipitated and a significant amount of arsenic(III) was also incorporated into the precipitates. At the end of the oxidation stage 42% of the leached arsenic remained in the bioleaching slurry as arsenic(III). The extent of arsenic extraction was reduced (85% extraction after 312 hours). Less pyrite was leached (about 10%). The relationship between pyrite oxidation and extent of arsenic(III) leaching can be seen in these results.

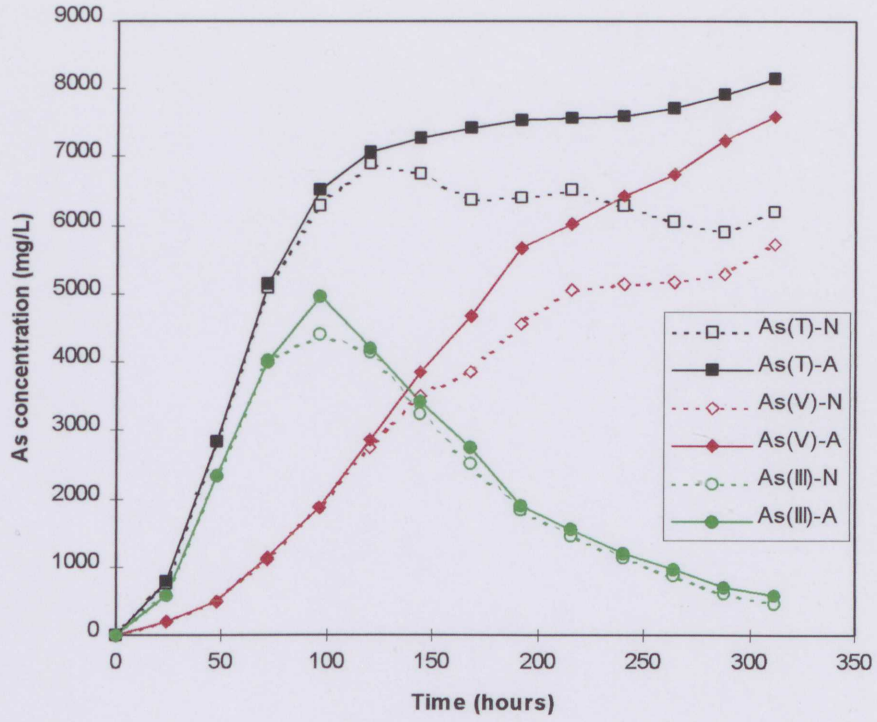


Figure 5.21: Speciation of arsenic in the bioleaching slurry with pH being controlled around 1.5. T= total, A = sample acidified before analysis, N = sample not acidified.

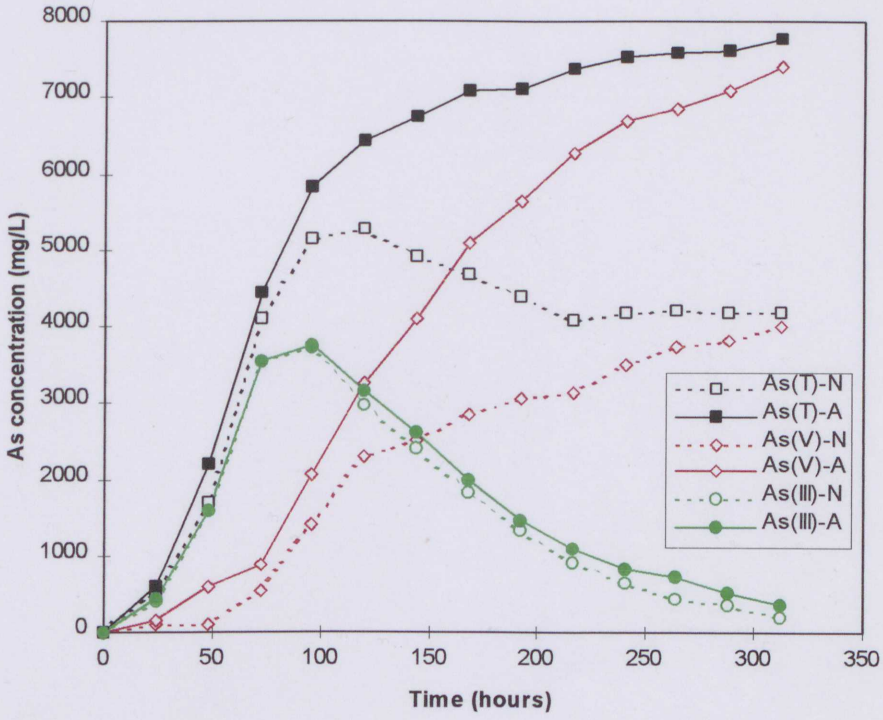


Figure 5.22: Speciation of arsenic in the bioleaching slurry with pH being controlled around 1.8. T= total, A = sample acidified before analysis, N = sample not acidified.

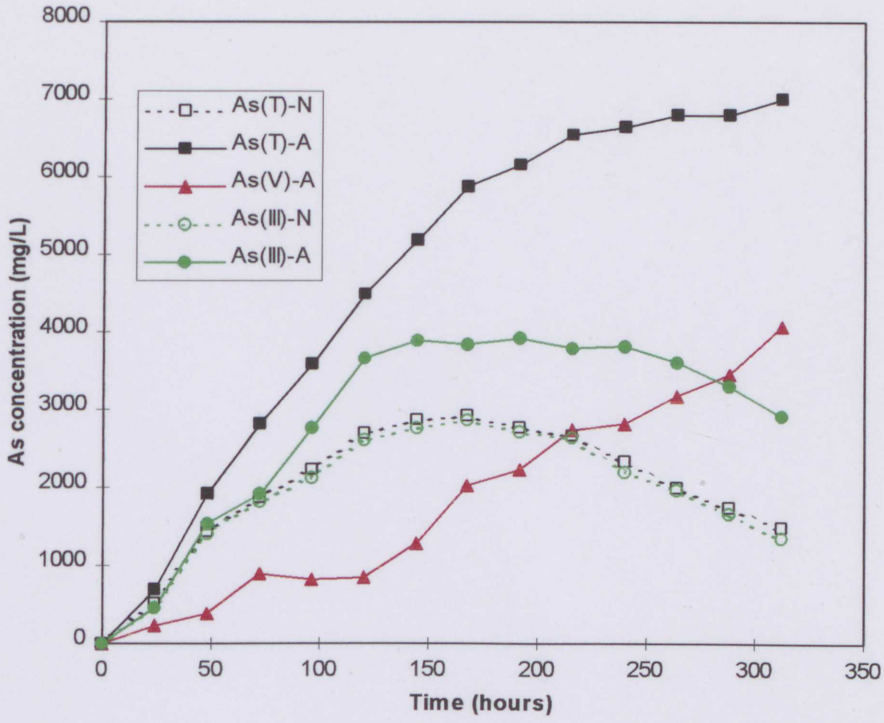


Figure 5.23: Speciation of arsenic in the bioleaching slurry with pH being controlled around 2.5. T= total, A = sample acidified before analysis, N = sample not acidified.

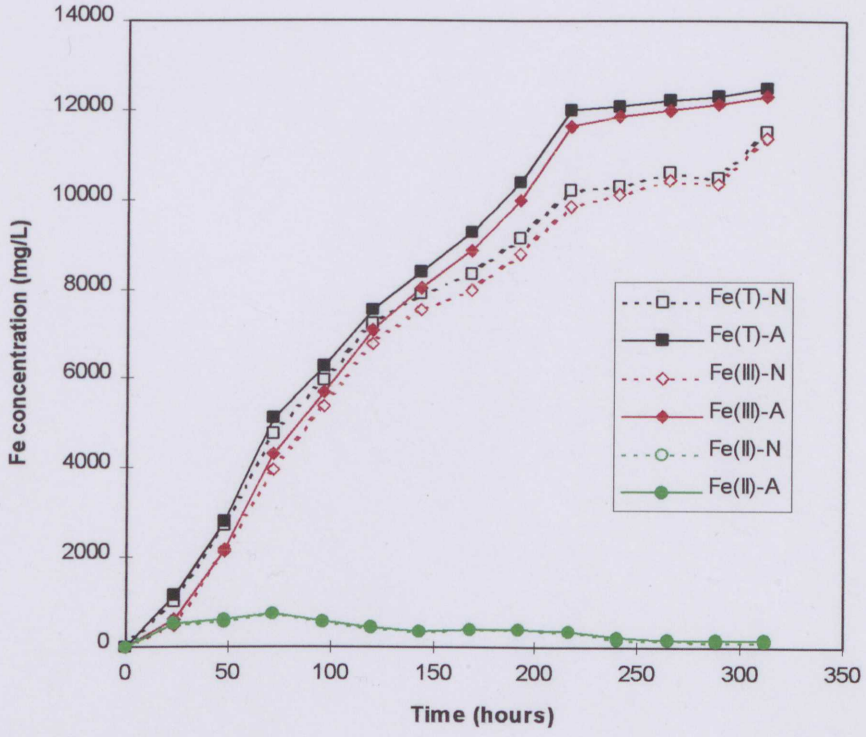


Figure 5.24: Speciation of iron in the bioleaching slurry with pH being controlled at around 1.5. T= total, A = sample acidified before analysis, N = sample not acidified.

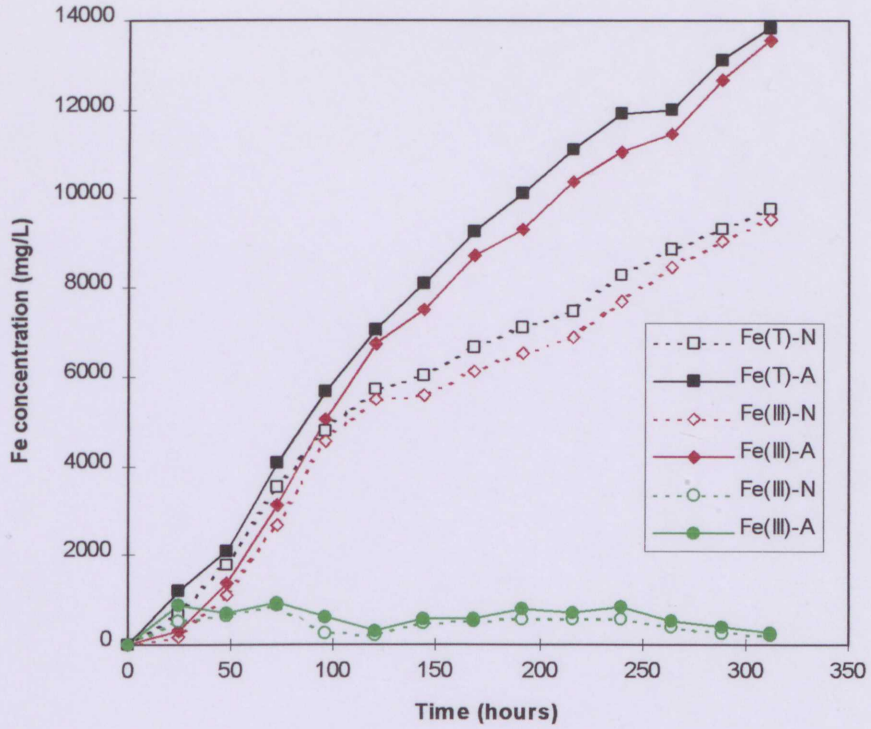


Figure 5.25: Speciation of iron in the bioleaching slurry with pH being controlled at around 1.8. T= total, A = sample acidified before analysis, N = sample not acidified.

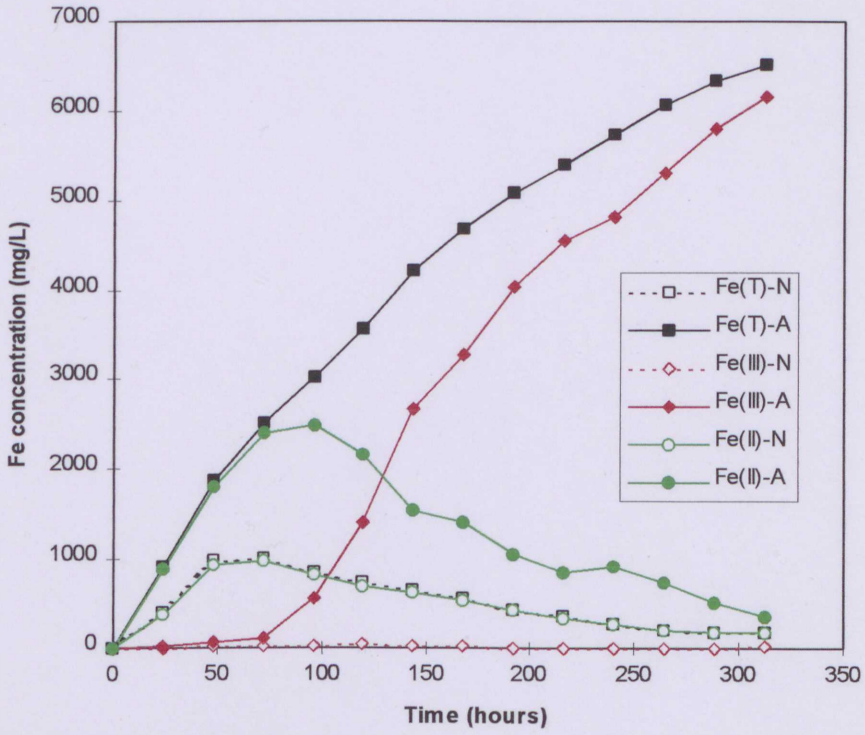


Figure 5.26: Speciation of iron in the bioleaching slurry with pH being controlled at around 2.5. T= total, A = sample acidified before analysis, N = sample not acidified.

Figures 5.24-26, show the speciation of iron for experiments carried out at pH 1.5, 1.8, and 2.5 successively. Figures 5.24 and 5.25 show that precipitation of iron(III) was following the same pattern as arsenic(V) precipitation (Figures 5.21 and 5.22). Figures 5.26 and 5.23 show that all the iron(III) and the arsenic(V) formed was immediately precipitated. The iron in solution was mainly iron(II).

5.2.6 Effect of pulp density

The effect of pulp density was investigated to check if the trends in the speciation of arsenic differed significantly with this variable. Tests were conducted at pulp densities of 5%, 10%, 15% and 20% solids (w/v) using the Fairview concentrate. Table 5.6 gives a summary of the runs and the pulp densities used. The composition of the Fairview concentrate is given in Table 5.2.

Figure 5.27 show the percentage of arsenic extracted from the initial concentrates at different pulp densities. Experimental runs for the pulp densities 5, 10 and 15 % achieved at least 96% arsenic extraction after 240 hours and Run 25 achieved 91% extraction. Although different levels of iron and arsenic were present in the bioleaching slurry, the extraction rate of arsenic remained almost the same for all the runs.

Table 5.6: Descriptions of the experimental runs at different pulp densities.

Run Number	Pulp Density Solids (w/v) %
Run 9	5
Run 23	10
Run 24	15
Run 25	20

The percentage of arsenic(III) in the bioleaching slurry and the corresponding concentrations in mg/L are given in Figures 5.27 and 5.28 respectively. For the pulp

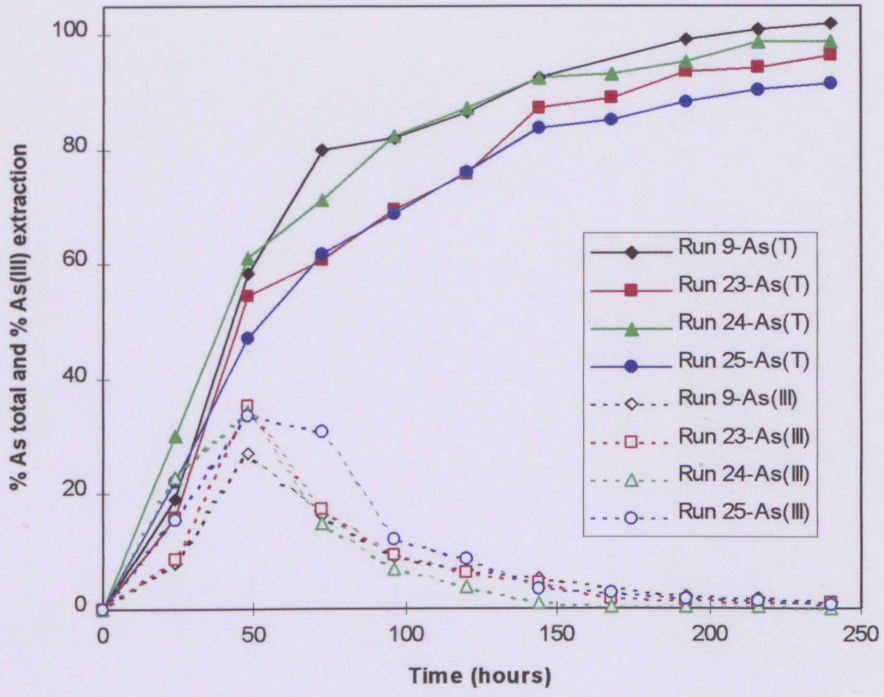


Figure 5.27: Percentage total arsenic extraction and percentage arsenic(III) during bioleaching for Runs 9 and 23-25 (see Table 5.6 for pulp densities).

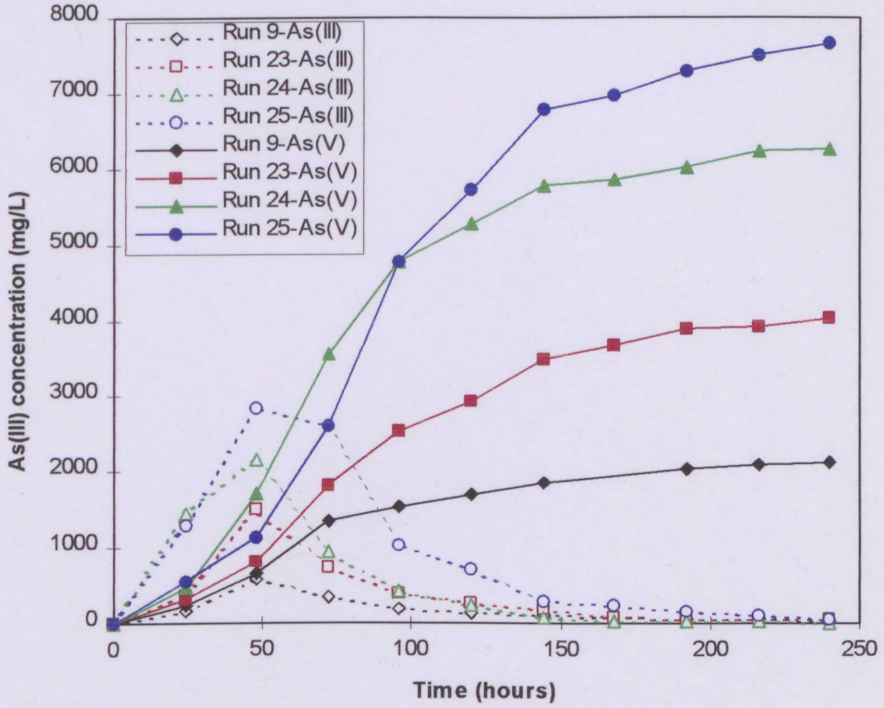


Figure 5.28: Variation in arsenic(III) and arsenic(V) concentrations of the bioleaching slurry for Runs 9 and 23-25 from Fairview mine (see Table 5.6 for pulp densities).

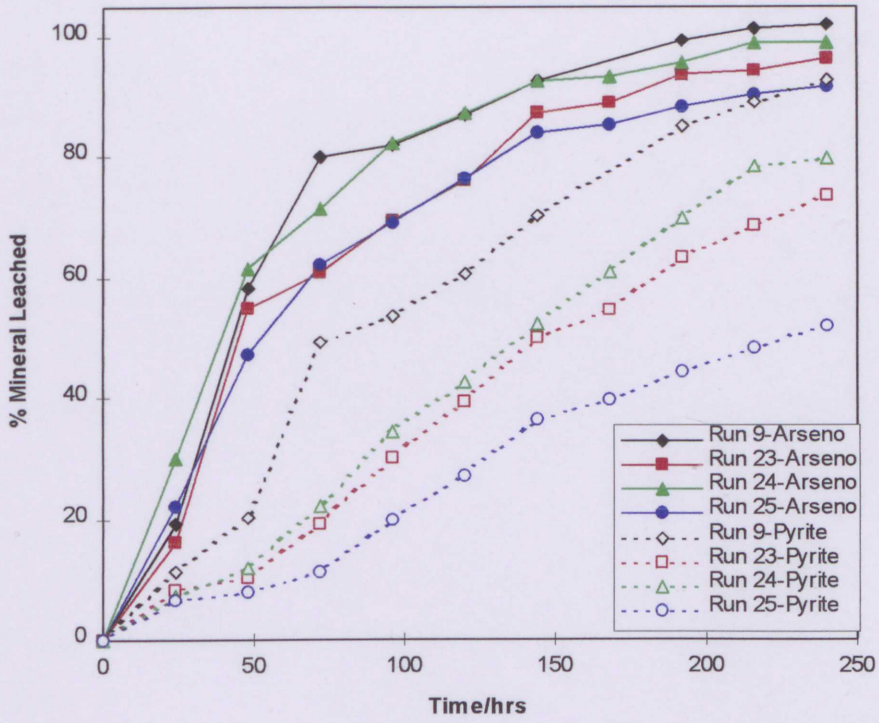


Figure 5.29: Plot of arsenopyrite and pyrite oxidation for Runs 9 and 23-25 (see Table 5.6 for pulp densities).

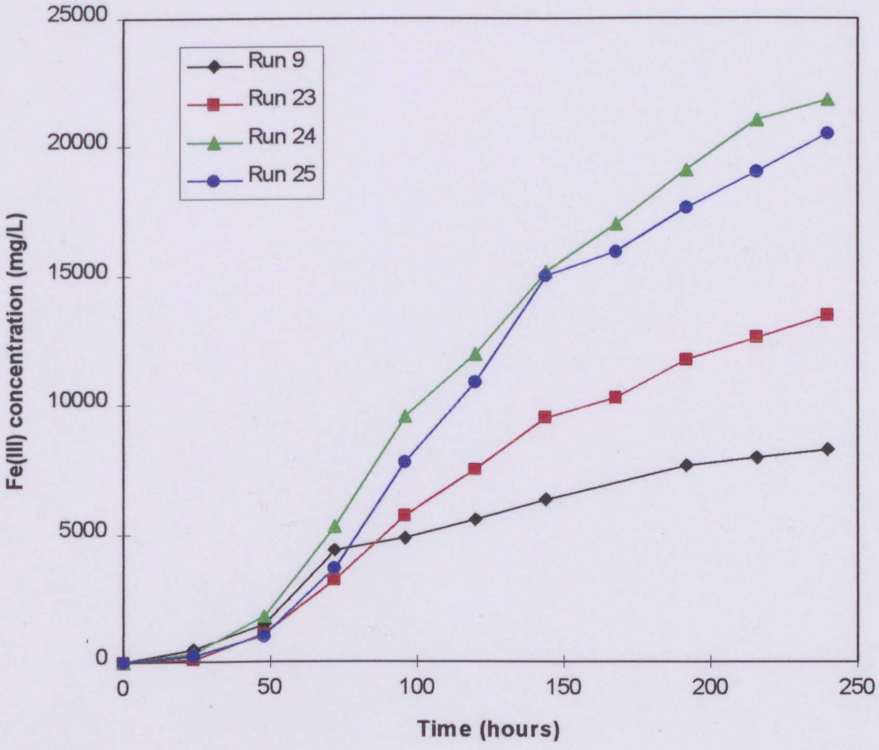


Figure 5.30: Concentrations of iron(III) in the bioleaching slurry for Runs 9 and 23-25 (see Table 5.6 for pulp densities).

densities considered arsenic(III) predominated in the bioleaching slurry in the early part of the leaching period. Increasing the pulp density also increased the maximum percentage of the proportion of arsenic(III) in the leaching slurry. At 5% pulp density the maximum proportion of arsenic(III) did not exceed 50% of the solubilised arsenic. At 10% pulp density the maximum percentage of arsenic(III) increased to 65% corresponding to about 1500 mg/L and this was the maximum amount of arsenic(III) measured in the bioleaching pulp. At 15% pulp density maximum proportion of arsenic(III) reached 76% (about 1440 mg/L) and at 20% pulp density it was 72% (about 2860 mg/L).

Less than 1% of the extracted arsenic remained in the bioleaching slurry as arsenic(III) at the end of 240 hours for Runs 23-25 and about 1.1% remained as arsenic(III) for Run 9 at 5% pulp density. Run 24 shows the fastest oxidation rate of arsenic(III). Calculation of the amount of pyrite leached also show some relationship between the extent of pyrite leached and the oxidation of arsenic(III) (Figure 5.29). The same figure also show that there was more selective attack on arsenopyrite at higher pulp densities when compared with 5% pulp density.

Figure 5.30 shows the concentrations of iron(III) in the bioleaching slurry. Different concentrations of iron(III) were measured during the leaching because of the difference in pulp densities which were used for the experiments. Although Run 24 and 25 show very high concentrations of iron(III) (about 21,8 g/L and 20,5 g/L respectively) when compared with Run 9 and 23 (about 8,2 g/L and 13,5 g/L respectively), the concentrations of iron(III) does not seem to be a limiting factor on the oxidation of arsenic(III) under the experimental conditions considered here.

5.2.8 Effect of stibnite

Stibnite was found to be one of the main minerals in one of the samples from the Indarama mine and also gudmundite which contains antimony was found to be associated with the gold in this sample. It was decided to investigate the influence of stibnite during bacterial leaching of pyrite/arsenopyrite concentrate from the Indarama

mine. Mixtures of arsenopyrite/pyrite/stibnite were prepared from the Indarama C concentrate and the Indarama 1 sample which was mainly composed of massive stibnite. The compositions of the different mixtures used in this experimental study are given in Table 5.7. The experiments were carried out at 5% pulp density (w/v).

Figure 5.31 shows the extraction of arsenic during bioleaching of the mixtures described in Table 5.7. There was no significant difference in the extraction rates for the first 96 hours. Runs 14, 26 and 27 show more than 94% arsenic extraction while that of Run 28 was reduced to about 87%.

The oxidation of arsenic(III) was not affected in Runs 14, although Runs 26 and 27 showed slightly more arsenic(III) remaining in the bioleaching slurry at the end of the oxidation period considered here as shown in Figures 5.31 and 5.32 (about 4% for Run 26 and 6% for Run 27). In Run 28 the oxidation of arsenic(III) was affected, more than 16% of the leached arsenic remained in the leaching slurry as arsenic(III). Calculation of the pyrite leached show that the least amount of pyrite was leached in this sample (about 50%) compared with more than 80% in the other three (Runs 14, 26 and 27). Figure 5.33 shows the concentrations of iron(III) which were measured during the runs described here. There was a variation in the amount of iron(III) due to the compositional differences of the feed concentrates. The levels of the

Table 5.7: Compositions of the arsenopyrite/pyrite/stibnite concentrates used in Runs 14 and 26-28.

Run Number	Sample I.D	wt % Fe	wt % As	wt % Sb
Run 14	Indarama C	36.79	16.60	0.49
Run 26	T	33.48	15.15	2.97
Run 27	S	30.17	13.69	5.44
Run 28	U	23.55	10.79	10.39

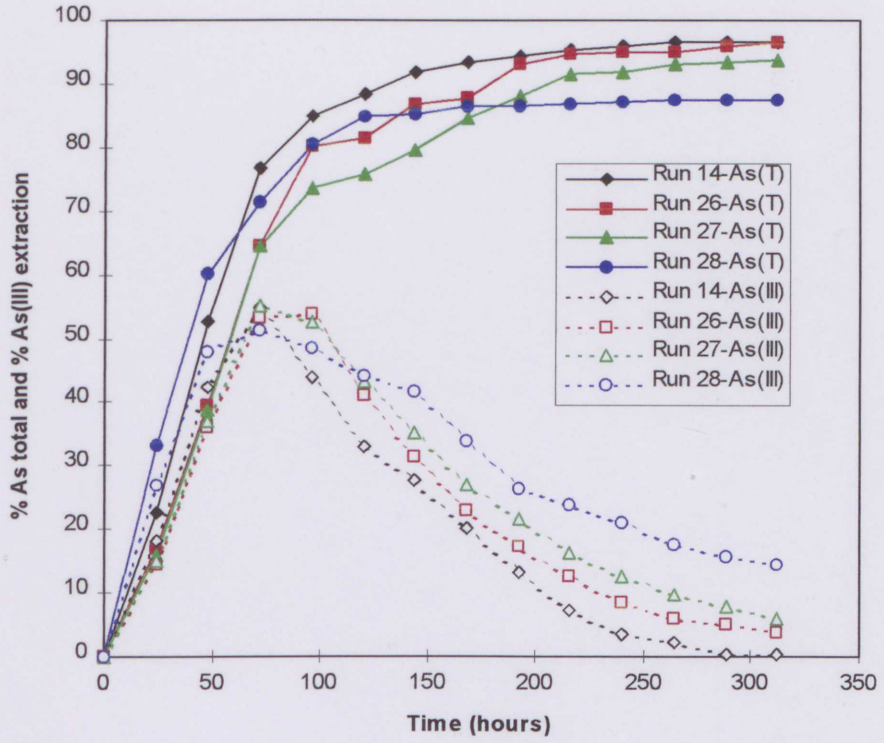


Figure 5.31: Percentage total arsenic extraction and percentage of arsenic(III) for Runs 14 and 26-27 (see Table 5.7 for compositions of solids).

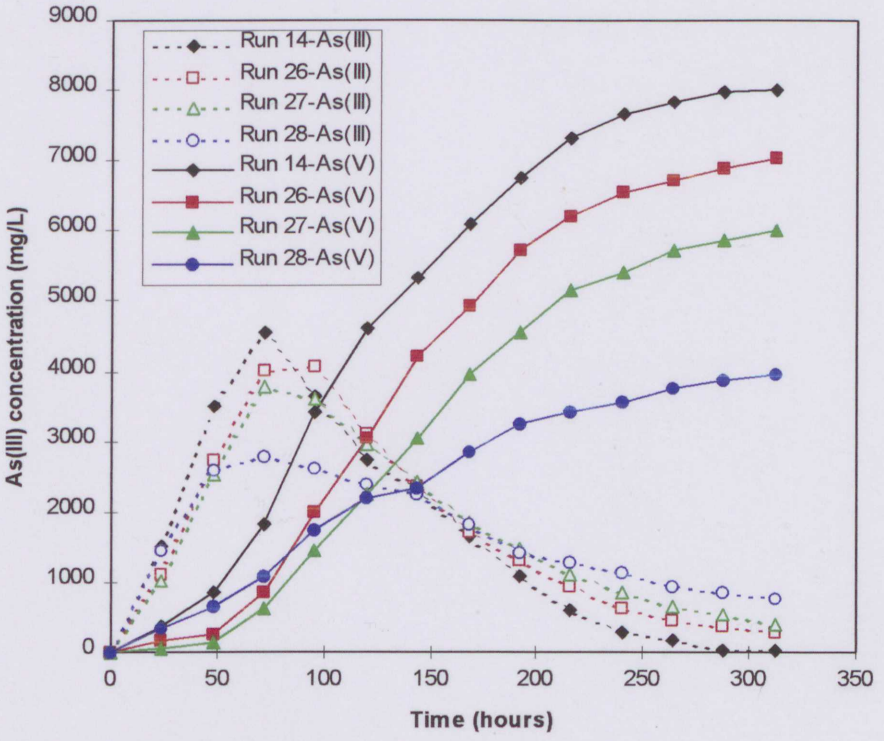


Figure 5.32: Variation in arsenic(III) and arsenic(V) concentrations of the bioleaching slurry for Runs 14 and 26-28 (see Table 5.7 for compositions of solids).

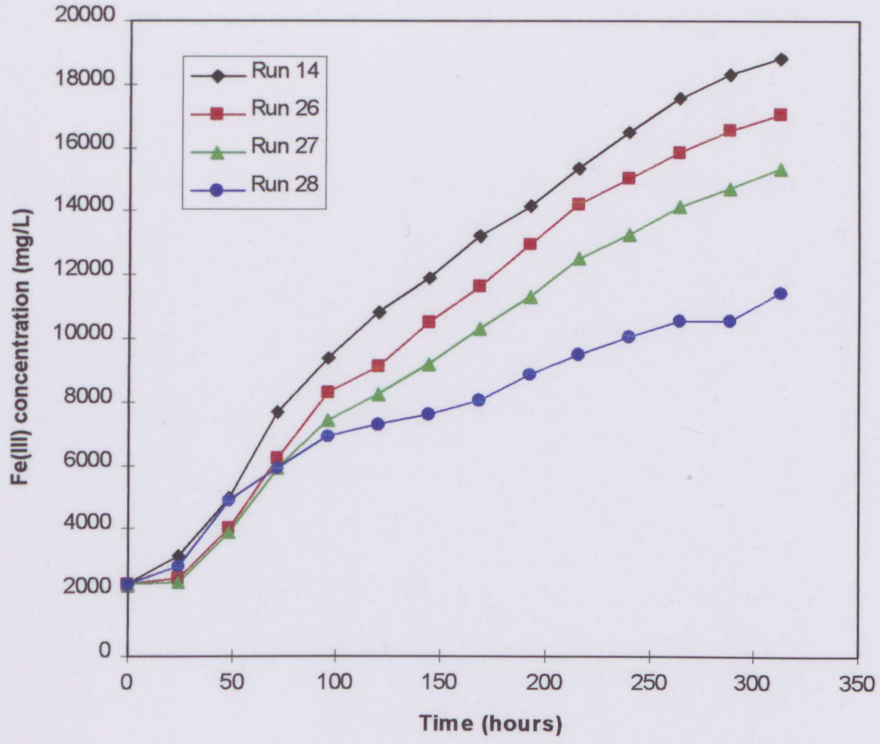


Figure 5.33: Concentrations of iron(III) in the bioleaching slurry for Runs 14 and 26-28 (see Table 5.7 for compositions of solids).

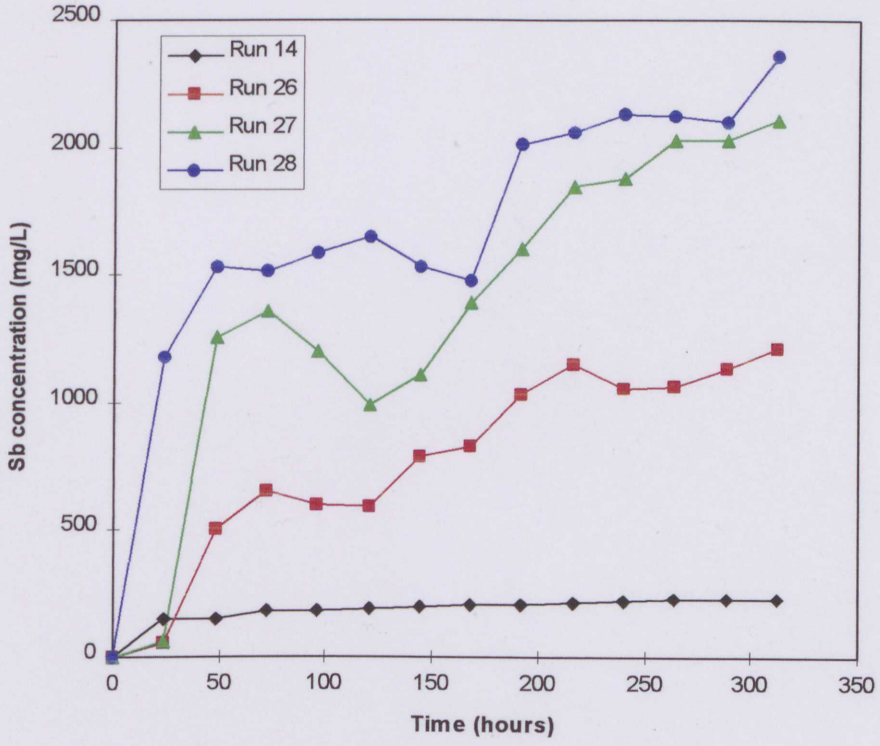


Figure 5.34: Concentrations of antimony in the bioleaching slurry for Runs 14 and 26-28 (see Table 5.7 for compositions of solids).

ferric ions should be enough to complete the oxidation of arsenic(III) basing this reasoning on the previous Runs which were carried in this study.

The concentrations of antimony in the bioleaching slurry are shown in Figure 5.34. Most of the antimony leached was immediately precipitated and there was a limit in the amount of antimony which remained in solution for Run 28. The maximum concentration of antimony which was measured in the leaching slurry was 2360 mg/L for Run 28, corresponding to about 45% of the initial amount of antimony in the sample. Microscopic examination of the residues showed that most of the stibnite was leached, however some of the antimony produced was hydrolysed resulting in only 45 % reporting in solution. The other runs show that more than 77% of the antimony was in solution. The precipitation of antimony in Run 28 also affected the oxidation of arsenic(III) and the pyrite leached from the sample.

5.2.8 Oxidation of As(III) synthetic solutions by Fe(III), pyrite and bacteria

In order to understand further the chemistry of oxidation of arsenic(III) during bacterial leaching, some experiments were devised which tried to separate the different factors involved in the leaching process. Arsenious oxide was used as a source of arsenic(III). This was dissolved in concentrated sodium hydroxide and then acidified to pH 1.8 using concentrated sulphuric acid. Concentrations of arsenic(III) in the range 1400-1500 mg/L were used in the starting solutions and a 5% pulp density was used for experiments which included pyrite. Table 5.8 shows the leaching conditions used in the experiments.

In order to check the influence of bacteria on the oxidation of arsenic(III) in the absence of the mineral substrates, ferrous sulphate was used as a source of energy for the bacteria (Figure 5.35, Run 30). The bacteria used in this experiment were grown on pyrite/arsenopyrite concentrate and were adapted to high concentrations of arsenic(more than 10 g/L). The concentration of arsenic(III) remained constant in the solution for the oxidation period considered here, however iron(II) was rapidly oxidised to iron(III) in about 120 hours. Run 31 in Figure 5.35 shows the results of the chemical reaction between ferric sulphate and arsenic(III) in the presence of pyrite. The reaction took

place to a significant extent oxidising more than half of the arsenic(III) which was initially present in the solution. In Run 29 pyrite was used as a source of energy for the bacteria and no soluble iron was added to the experiment. The oxidation of arsenic(III) proceeded to completion. The bacteria solubilised the pyrite generating the iron(III) which was needed for the oxidation of arsenic(III).

Table 5.8: Leaching conditions for the oxidation of arsenic(III) synthetic solutions.

Run Number	Initial Fe(III) g/L	Inocculum	Pyrite
Run 29	Nil	Yes	Yes
Run 30	9*	Yes	Nil
Run 31	9	Nil	Yes
Run 32	9	Nil	Nil
Run 33	6	Yes	Yes

* In Run 30 the concentration indicated is iron(II)

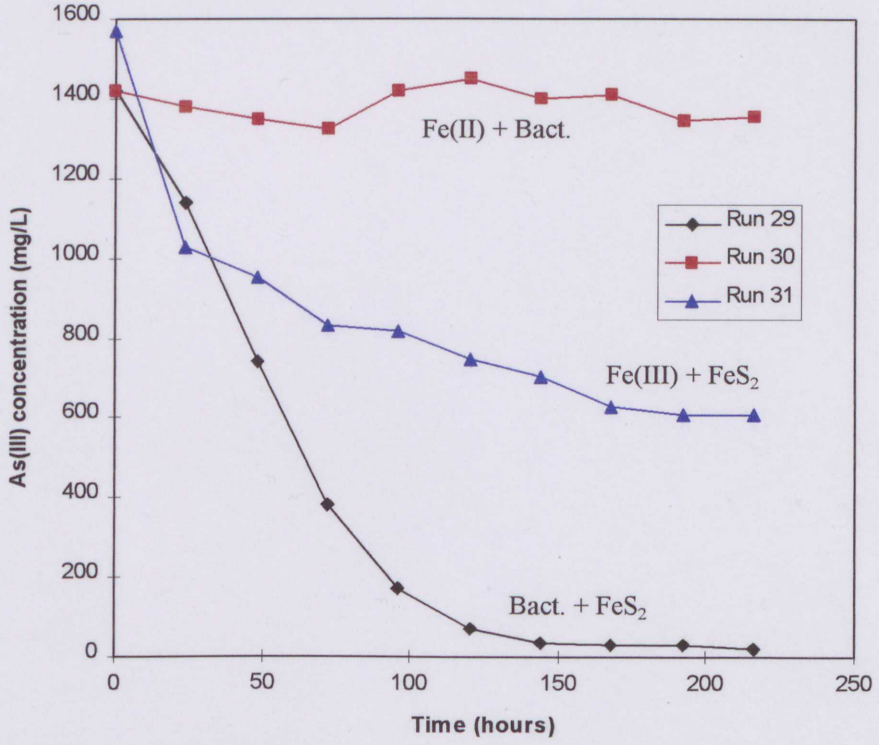


Figure 5.35: Oxidation of arsenic(III) under different leaching conditions as described in Table 5.8.

The reaction between iron(III) and arsenic(III) did not take place even when air was sparged in (Figure 5.36, Run 32) although thermodynamics predicts the feasibility of the oxidation under these conditions. The experiment was left to run for extended periods of time and still no reaction could be detected after three weeks. When arsenic(III) was added to a culture already growing on pyrite (6 days growing period) the oxidation of arsenic(III) proceeded much faster (Run 33, Figure 5.36) than the experiment which had only pyrite at the start (Run 29, Figure 5.35). The difference between Run 29 and 33 was that Run 33 had bacterially generated iron(III) at the start of the experiment and also the pyrite in this experiment had been partially leached.

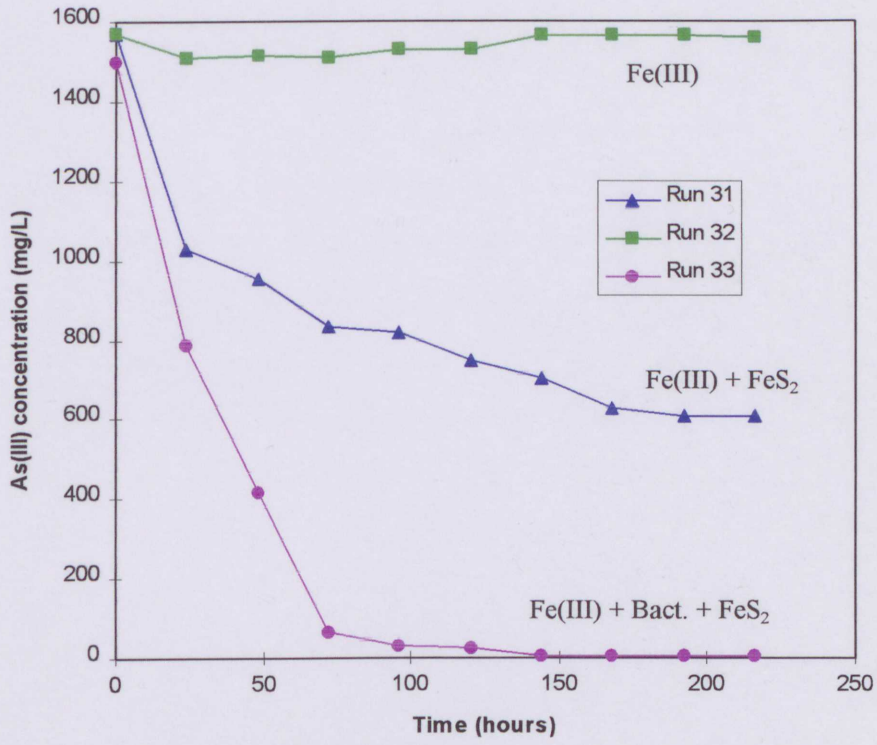


Figure 5.36: Oxidation of arsenic(III) under different leaching conditions as described in Table 5.8.

5.3 Discussion

5.3.1 Introduction

Many researchers have used mixed cultures of *Thiobacillus ferrooxidans, Thiobacillus thiooxidans* and *Leptosperillium ferrooxidans* to accelerate the dissolution of mineral sulphides, mainly pyrite and arsenopyrite, in order to release refractory gold

encapsulated in these sulphides. The assumption has been that bacterial leaching will produce environmentally acceptable residues which will be dominated by arsenic(V) because it forms stable salts. Despite this assumption, very few workers have actually measured the speciation of arsenic during bacterial leaching of arsenical ores. The discussion presented here compares the findings of the present study with the work already reported on the subject of arsenic speciation in bacterial oxidation of arsenical ores.

5.3.2 Bacterial leaching of different concentrates

Comparison of the speciation results during bacterial oxidation of arsenical concentrates from different ore deposits show some differences in the rate and extent of arsenic(III) oxidation for the leaching periods considered. This variation was found to be mainly attributable to the difference in mineralogical compositions of the concentrates, in particular the ratio of pyrite to arsenopyrite. The grade of the sulphide (proportion of pyrite and arsenopyrite in relation to the gangue minerals) was also found to play an important role on the extent and rate of arsenic(III) oxidation in bacterial leaching.

Bacterial leaching of concentrates with different ratios of pyrite and arsenopyrite have shown different speciation of arsenic characteristics (Figures 5.1-5.4). Arsenic(III) was found to predominate in bioleaching slurries in the initial stages of the oxidation period with the proportion of arsenic(III) exceeding 50% of the extracted arsenic at its maximum value. The predominance of arsenic(III) in the initial stages showed that bioleaching of arsenopyrite primarily releases arsenic(III) into the solution. The arsenic(III) produced is then oxidised to arsenic(V) and gradually decreases to low values in the bioleaching slurry. The Indarama B concentrate which contained the lowest ratio of pyrite to arsenopyrite (0.78) showed an ever increasing concentration of arsenic(III) as shown in Figure 5.2; however, examination of Figure 5.2 shows that the oxidation of arsenic(III) was taking place but at a very slow rate. There was accumulation of arsenic(III) in the reactor. Very high concentrations of arsenic(III) inhibit the activity of the bacteria resulting in the slowing down of the oxidation

process. Apart from its undesirable effects on the activity of the bacteria, arsenic(III) has severe environmental impacts due to the instability of the resulting residues **[16]**.

The results of Run 1 shown in Figures 5.1 and 5.2 (the Indarama B concentrate) are in agreement with those of Morin and Ollivier **[81]** in which they presented the results of pilot plant continuous testing using *Thiobacillus ferrooxidans* and *Thiobacillus thiooxidans* to bioleach two refractory gold concentrates with high arsenopyrite contents (pyrite to arsenopyrite ratios in the concentrates were 0.70 and 0.56). Very high dissolved arsenic concentrations were measured in the bioleaching slurry (about 13 g/L), predominantly arsenic(III). After 120 hours the culture slurry contained 86% arsenic(III) and 14% arsenic(V). Ewart **[99]** has criticised their work, citing the method of arsenic(III) analysis as a possible source of error leading to the high concentrations, Morin and Ollivier **[81]** did not mention whether they used the method of standard additions to eliminate matrix interferences during analysis of arsenic(III) by polarography. The results presented here (Figure 5.1 and 5.2, Run 1) showed that up to 78% of the arsenic in the bioleaching slurry was arsenic(III) and the method of standard additions was employed for the analysis of arsenic(III) by polarography. Furthermore the composition of the concentrate used for this work was very similar to the ones used by Morin and Ollivier **[81]** and therefore their results are consistent with the current findings. In the other concentrates studied here the oxidation of arsenic(III) proceeded to completion at different rates; this can be attributed to the presence of more pyrite in these concentrates which provided catalytic surfaces for the oxidation of arsenic(III). Pyrite was found to promote the oxidation of arsenic(III) to arsenic(V) during bacterial oxidation, the oxidation rate was accelerated by the presence of bacteria suggesting that the bacteria were continually exposing clean pyrite surfaces for the reaction. In a recent publication on the speciation of arsenic, Langhans et al., **[16]** reported bacterial leach solutions from their experiments containing 17 g/L arsenic comprising of 18 times as much arsenic(III) as arsenic(V). This high arsenic(III) can be attributed to the composition of the ore which was used. Although no composition of the ore in terms of pyrite to arsenopyrite was given in this instance, the chemical composition of the ore shows that there was more arsenopyrite than pyrite in the ore. The ore contained 8.7

wt% Fe, 6.2 wt% As and 3.5 wt% S which gives a theoretical ratio of pyrite to arsenopyrite of 0.25. The grade of the concentrate could also have played a part in the low oxidation of arsenic(III).

5.3.3 Effect of concentrate grade

This study has shown that the sulphide grade also plays an important role in the speciation of arsenic. Figure 5.3 and 5.4 (Run 4 and 5) show the speciation characteristics of two concentrates produced from the same material (Akbakai). The concentrate used in Run 4 (Akbakai A concentrate) was produced by upgrading the concentrate used in Run 5 (Akbakai D concentrate) by cleaner flotation. Mineralogical calculations show that the concentrate used in Run 4 had a pyrite to arsenopyrite ratio of 1.56 while that for Run 5 was 1.89. It was expected that the rate of oxidation of arsenic(III) in Run 5 (Akbakai D concentrate) would be faster than that for Run 4 (Akbakai A concentrate); however the reverse was found to be the case. This can be explained in terms of the grade of the concentrate, the Akbakai D concentrate contains more gangue phases than the Akbakai A concentrate, which means there was a smaller amount of pyrite surfaces available in the former to catalyse the oxidation of arsenic(III) and also to produce ferric ions which take part in the oxidation of arsenic(III). Run 4 showed almost complete oxidation of arsenic(III) in the bioleaching slurry while Run 5 still contained up to 36 % as arsenic(III) (Figures 5.3 and 5.4). The Indarama B and C concentrates were also from the same deposit but differed significantly in their pyrite to arsenopyrite ratio and consequently the extent of arsenic(III) oxidation during bacterial leaching. These results showed that a change in the mineralogy of the ore within the same deposit can lead to completely different arsenic speciation behaviour during bacterial oxidation pretreatment, also the flotation practice may also have an influence on this behaviour.

5.3.4 Oxidation of iron(II) in the presence of arsenic(III)

The analysis of ferrous and ferric ions in the bioleaching slurry show that the oxidation of iron(II) was taking place even in situations where the concentrations of arsenic(III) was very high (Figures 5.7 and 5.8). The oxidation of iron(II) in the presence of

arsenic(III) shows that the bacterial strain was well adapted to the high concentrations of arsenic possibly through natural selection or plasmid-borne resistance as suggested by Silver et al., **[190]**. The strain used by Morin and Ollivier **[20, 81,]** was also able to oxidise iron(II) in the presence of high concentrations of arsenic(III). Typical leach solutions from their study had the following composition: 10.8 g/L arsenic(III), 1.7 g/L arsenic(V), 2.9 g/L iron(II) and 9.5 g/L iron(III) **[20]**.

The redox potentials of the bioleaching slurry measured by Morin and Ollivier **[20, 81]** were typically more than 790 mV versus standard hydrogen electrode potential, but nevertheless high concentrations of arsenic(III) in the leaching slurry were measured. Stronger oxidising conditions were observed in this study during bioleaching of the Indarama B concentrate in the stirred flasks, where the E_h rose to approximately 800 mV (Appendix Three). Again, the oxidation of arsenic(III) remained slow and from these observations it can be concluded that the redox potential does not give any indication of the oxidation of arsenic(III) to arsenic(V), however it does give a good indication of the activity of the bacteria i.e. the oxidation of iron(II) to iron(III).

When the concentrations of arsenic(III) started dropping in the bioleaching slurry the concentrations of iron(III) was also increasing at the same time (comparison of Figures 5.2 and 5.4 with Figures 5.7 and 5.8). The increase in iron(III) and simultaneous decrease in arsenic(III) concentrations in the bioleaching slurry may be compatible with the suggestion that the oxidation of arsenic(III) is carried out by iron(III) to give the less toxic arsenic(V). A comparison of the calculated redox potentials at pH 1.5 show that the redox couples Fe(III)/Fe(II) and As(V)/As(III) have potentials 0.67 V and 0.47 V respectively. While iron(III) should be able to oxidise arsenic(III) it is difficult to predict the kinetics of the oxidation from thermodynamic data. Barrett et al., **[105, 156]** have studied this reaction up to 70°C and have found no evidence for the reaction taking place in the time period and experimental conditions of their work. Further evidence for the slow kinetics of this reaction under the conditions used in bioleaching will be presented later in this discussion.

5.3.5 The effect of pyrite leaching on the oxidation of arsenic(III)

There was a relationship between pyrite leached and the oxidation of arsenic(III) in the bioleaching slurry (Figures 5.5 and 5.6). The Indarama B concentrate (Run 1) had the least amount of pyrite leached (about 13%) at the end of the oxidation stage considered here and at the same time it had the highest concentration of arsenic(III) in the bioleaching slurry. This high concentration of arsenic(III) can be interpreted in terms of ore composition, there was less pyrite in this ore to provide enough catalytic surfaces for the oxidation to take place. Furthermore the high concentration of toxic arsenic(III) seemed to have inhibited the leaching of pyrite which means there was not much increase in the surface area of the pyrite as was evidenced by examination of the bacterially leached residues. The leaching of pyrite also provided more iron(III) ions which are also essential in the oxidation of arsenic(III).

Significant leaching of pyrite took place when more than 60 % of the arsenopyrite had been leached in most experiments and at this point there was a decrease of arsenic(III) concentrations in the bioleaching slurry. This may be due to the increased availability of fresh pyrite surfaces to catalyse the oxidation of arsenic(III) as more pyrite was being leached. The rate and extent of pyrite dissolution was much faster for Run 2 and 3 (Figure 5.5) than for Run 1, and this was also reflected in the oxidation of arsenic(III) in the bioleaching slurry (Figures 5.1 and 5.2). The Akbakai D concentrate showed a high rate of pyrite leaching but a lower oxidation rate of arsenic(III). This has much to do with the grade of the concentrate which was used in this experiment, there was not enough arsenopyrite which serves as an easy source of energy for the bacteria, this could have led to the faster oxidation of the available pyrite. Because there was a high proportion of the gangue phase in this concentrate the availability of pyrite surfaces to catalyse the oxidation of arsenic(III) was a limiting factor in this case. Although it looked as if less pyrite was leached in Run 6 compared with Run 4 (Figure 5.6), this concentrate had more pyrite and it contained less gangue minerals compared with the concentrate used in the latter run (Chapter Four, Table 4.2).

Addition of pyrite to the Indarama B concentrate in order to change its composition in terms of pyrite to arsenopyrite improved the oxidation of arsenic(III) to arsenic(V) as shown by the concentration profiles of the runs presented in Figures 5.9 and 5.10. The addition of pyrite to the Indarama B concentrate also increased the rate of arsenic extraction (Figure 5.9). This was probably a result of the oxidation of arsenic(III) to the less toxic arsenic(V) due to the availability of pyrite surfaces. The increased oxidation of arsenic(III) in the mixtures was also reflected by an increase in the amount of pyrite leached from the initial samples (Figure 5.11), demonstrating the importance of clean pyrite catalytic surfaces during the oxidation of arsenic(III). The Fairview concentrate shows the fastest rate of arsenic(III) oxidation when compared with the mixtures used. This was in accordance with the predictions made by examining its mineralogical composition. This concentrate contained more pyrite compared to the mixtures (M1 and M2) consequently there were more catalytic surfaces available for the oxidation of arsenic(III). Although there was less iron(III) in solution for the Fairview concentrate compared with the mixtures (M1 and M2), the Fairview concentrate showed a better conversion of arsenic(III) to arsenic(V) due to the amount pyrite in the ore. These results show that the oxidation of arsenic(III) was mainly influenced by the pyrite content of the concentrates.

5.3.6 The effect of iron(III) additions

The arsenic oxidation rate of the Indarama B concentrate was improved by supplementing the bioleaching slurry with an initial iron(III) concentration of 2.4 g/L (Figure 5.13, Run 10). There was also an improvement in the oxidation of arsenic(III) to arsenic(V) (Figures 5.13 and 5.14). This improvement may be explained by the fact that the iron(III) added chemically accelerated the oxidation of arsenopyrite which is an easier source of energy for the bacteria, and when most of the arsenopyrite was leached the bacteria started attacking the pyrite exposing clean surfaces for the oxidation of arsenic(III) (Figure 5.15). However the oxidation did not go to completion in the time period which was considered, a fact which can be attributed to the initial composition of pyrite in the concentrate. There was less pyrite in the concentrate and the depletion of pyrite as a result of bacterial leaching might have limited arsenic(III) oxidation.

Langhans et al., **[16]** found that arsenic(III) remained stable in the bioleach slurry for the ore they used even with iron:arsenic ratio in solution as high as 6:1. This showed that the chemical oxidation of arsenic(III) to arsenic(V) by the ferric ions cannot be used to account for the formation of arsenic(V) in the bioleaching slurry and their results are consistent with the speciation studies reported here. The chemical oxidation of arsenic(III) by iron(III):

$$As(III) + 2Fe(III) = As(V) + 2Fe(II) \qquad (5.1)$$

is kinetically restricted. Ewart **[99]** proposed that such reactions are usually slow, either because a third order reaction is required (if a two electron reaction occurs) or to a third order reaction leading to the formation of some intermediate species like arsenic(IV) which would make the completion of the reaction very difficult.

Figures 5.17 and 5.18 show the concentrations of arsenic(III) when the initial dissolved iron(III) concentrations were increased during bacterial oxidation of the Indarama C concentrate. Higher concentrations of initial iron(III) did not show positive results, instead the oxidation of arsenic(III) was retarded under the experimental conditions used. There was much precipitation in the early stages of the leaching process and as a result protecting most of the pyrite from bacterial attack, this in turn limited the clean catalytic surfaces available for the oxidation of arsenic(III).

Recycling of the bioleaching solution containing ferric sulphate and arsenic(V) was found not to have a positive effect on either leaching rate or oxidation of arsenic(III) as shown in Figure 5.19. This was possibly due to nutrient deficiency and also the high concentrations of the iron(III) and arsenic(V) promoted precipitation in the early stages of the leaching process and as a result this could have protected the pyrite whose surface has been found to play a vital role in the oxidation of arsenic(III). Spencer et al., **[90]** have found that recycling of up to 50% of the slurry from the final biooxidation stage had an inhibitory effect on the oxidation kinetics and Breed et al., **[157]** have shown that the addition of a mixed culture of *Thiobacillus ferrooxidans* and

Leptospirillum ferrooxidans to a slurry containing arsenic(V) resulted in both lag phase and a reduced rate of bacterial oxidation. These results and the current findings show that arsenic(V) is also toxic to the bacterial cultures used in mineral sulphide leaching although it has been shown that arsenic(III) is more toxic than arsenic(V) by a number of researchers **[90, 93, 99, 105, 157]**. The results showed that the use of very high initial ferric iron promoted precipitation in the early stages of leaching and as a result retard the subsequent oxidation of arsenic(III). Although some researchers have successfully used bacterially-rich ferric sulphate to bioleach pyrite/arsenopyrite concentrates **[112, 144, 188-189]**, they did not report the speciation of arsenic in their work which makes it difficult to know whether the oxidation of arsenic(III) went to completion.

5.3.7 Effect of controlling pH

Lithium hydroxide was used to control the pH of the bioleaching slurry in some experiments (Figures 5.21-5.26, Runs 20-22) because it has been shown that lithium does not form jarosites **[191]**. It was found that most of the arsenic(III) remained in solution during bacterial leaching at pH 1.5 and 1.8, however a significant amount of arsenic(V) was found to precipitate when a concentration higher than 4 g/L arsenic (total) was in the bioleaching slurry (Figures 5.21 and 5.22). The arsenic(V) possibly precipitated according to the simplified equation:

$$2H_3AsO_4(aq) + Fe_2(SO_4)_3(aq) + 2nH_2O(l) = 2FeAsO_4.nH_2O(s) + 3H_2SO_4(aq) \qquad (5.2)$$

Figure 5.23 shows that at pH 2.5 all the arsenic(V) formed was immediately precipitated and some arsenic(III) was also incorporated into the precipitates. This is not desirable because the solids which contain arsenic(III) are very unstable. There was precipitation of arsenic(V) for experiments carried out at pH 1.5 and 1.8 but the oxidation of arsenic(III) was not affected to the same extent as at pH 2.5, possibly because the precipitation started at a later stage when the bacteria had already attached to the pyrite surface and as a result the leaching of pyrite was not inhibited. Because of the low pH (pH 1.5 and 1.8) not all the arsenic(V) formed was immediately precipitated which means the surfaces of the pyrite were not covered by precipitates to the same extent as at

pH 2.5. There was more pyrite which was leached at pH 1.5 and 1.8 suggesting that clean catalytic surfaces were continually being exposed for the oxidation of arsenic(III). In contrast to the above observation the experiment carried out at pH 2.5 showed that there was precipitation right from the start of the experiment. Less than 11% pyrite was leached showing the effects of immediate precipitation on pyrite leaching and arsenic(III) oxidation. Results from this experiment are consistent with results from other runs in which precipitation was observed to take place in the early stages of leaching (Figure 5.19). It has also been reported **[191]** that *Thiobacillus ferrooxidans* cells adsorbed to pyrite surfaces serve as nucleation sites for jarosite formation which tends to have two negative effects: jarosites destroy the cells as they grow, and form a layer on the pyrite surface changing the leaching mechanism from convective to pore diffusion, thus slowing down the pyrite dissolution. The current study has demonstrated that there is a strong link between pyrite leaching and the oxidation of arsenic(III) in bacterial oxidation of pyrite/arsenopyrite concentrates. The bacteria attached to the pyrite may have served as nucleation sites for the precipitates and thus preventing the oxidation of arsenic(III) on the pyrite surfaces in some experiments where significant precipitation was observed in the early stages.

5.3.8 Effect of pulp density and stibnite

Bioleaching of the Fairview concentrate at different pulp densities did not show any significant deviation in the trends of arsenic(III) oxidation. At 20% pulp density the extent of arsenic extraction was slightly lower than for the other pulp densities (Figure 5.27). This may have been due to the shear forces affecting the bacterial activity and hence the leaching process. Figure 5.29 shows different leaching rates of pyrite for the different pulp densities, however this is not reflected in the oxidation rates of arsenic(III) because of different amounts of pyrite initially added to the experiments at varying pulp densities. While the least amount of pyrite was leached at 20% pulp density, because of the quantity of pyrite which was added to this experiment, the availability of clean pyrite surfaces for the oxidation of arsenic(III) matched that at lower pulp densities.

The bioleaching of stibnite has been reported to be a feasible process, however this work has shown that while at lower concentrations the antimony remained in solution, higher concentrations of antimony hydrolyse and precipitate. At lower concentration stibnite was found not to interfere with the oxidation of arsenic(III) and leaching of pyrite (Figures 5.31 and 5.32). At more than 10 wt% antimony in the initial sample, however the hydrolysis of antimony affected the leaching of pyrite and consequently the rate and extent of arsenic(III) oxidation (Run 28, Figures 5.31 and 5.32). The precipitates may have coated the pyrite surfaces preventing the bacterial activity. Figure 5.34 shows that the concentration of dissolved antimony in the slurry was limited to less than 2.4 g/L.

5.3.9 Oxidation of arsenic(III) during bacterial leaching

These results show the importance of ore composition in terms of pyrite to arsenopyrite ratio on the speciation of arsenic in the bioleaching of pyrite/arsenopyrite concentrates and they demonstrate that pyrite and bacteria play an important catalytic role in the oxidation of arsenic(III) to arsenic(V). Furthermore a strong link between pyrite leaching and arsenic(III) oxidation has been shown. Similar conclusions were reached by Barrett et al., **[105]** who showed that in the presence of moderately thermophilic bacteria (*M4*) the oxidation of arsenic(III) to arsenic(V) was catalysed by pyrite. The same effect of pyrite has been shown here using a mixed culture dominated by *Thiobacillus ferrooxidans* with ores of different proportions of pyrite to arsenopyrite.

In experiments in which a synthetic arsenic(III) solution was oxidised under different conditions, it was shown that there was no reaction between ferric sulphate and arsenic(III) even in the presence of sparged air (Figure 5.36, Run 32). This eliminated the chemical oxidation of arsenic(III) by bacterially generated ferric sulphate or the possibility of dissolved oxygen in the bioleaching slurry carrying out the oxidation of arsenic(III) according to the equations below, as claimed by some researchers **[90, 106, 112, 192]**:

$$2HAsO_2 + O_2 + 2H_2O = 2H_3AsO_4 \qquad (5.3)$$

$$HAsO_2 + Fe_2(SO_4)_3 + 2H_2O = H_3AsO_4 + 2FeSO_4 + H_2SO_4 \quad (5.4)$$

Neither could bacteria, well adapted to arsenic, oxidise arsenic(III) when inoculated into a solution containing ferrous sulphate (Figure 5.35, Run 29). However the bacteria did oxidise all the ferrous to ferric ions (about 9 g/L) in about 120 hours. This experiment showed that the main reaction taking place in the bulk solution during bacterial leaching is the oxidation of ferrous to ferric ions. Barrett et al., **[105]** suggested that the rate of oxidation of arsenic(III) in the presence of pyrite and bacteria may have been accelerated by iron(III) complexing with ligands released by the cells during metabolism, and that the redox potential of the resulting complex was sufficiently enhanced to allow the oxidation to arsenic(III) to occur. In the experiment in which ferrous sulphate was used to supply the energy for the bacteria (Run 29, Figure 5.35), metabolism of the cells was ensured. However the ferric ions generated and the possible ligands released by the cells failed to facilitate the oxidation of arsenic(III).

The chemical oxidation of arsenic(III) by iron(III) in the presence of pyrite was initially rapid and then the reaction slowed down (Figure 5.35, Run 31). The reaction might have slowed due to the depletion of the iron(III) which was being reduced to iron(II). Furthermore there were no bacteria present to regenerate the iron(III) and also the deterioration of the pyrite surface might have contributed to this slow down. In another experiment in which pyrite was used as a source of energy for the bacteria without initial soluble iron(III), the oxidation of arsenic(III) started immediately and went to completion (Figure 5.35, Run 29). In this experiment, the bacteria generated the ferric ions which were in turn used in the oxidation of arsenic(III). The oxidation went to completion because the bacteria kept on exposing clean pyrite surfaces as evidenced by the surface morphology of the leached pyrite residues (Chapter Six refers). When arsenic(III) was added to a culture after six days of growing on pyrite the oxidation of arsenic(III) was much faster than the one which had only pyrite at the start of the reaction (Figure 5.36, Run 33). The oxidation was faster in this reaction because the pyrite surfaces were already exposed and clean and there was more iron(III) in solution to immediately start the oxidation reaction on the pyrite surfaces. Furthermore the

surface area of pyrite had been increased compared with freshly added pyrite in the other experiment.

The primary role of the bacteria was to provide the ferric ions by oxidising iron(II) generated either by bacterial leaching of pyrite or chemical oxidation of arsenic(III) by ferric ions on the pyrite surface. However complex reactions which directly involve bacterial cells, iron(III) and pyrite surfaces cannot be ruled out as a possibility for the enhanced oxidation of arsenic(III). The bacteria which attach to the mineral surface may have a direct involvement in the oxidation of arsenic(III) via the pyrite surfaces. It is also possible that when arsenic(III) is adsorbed on the pyrite surfaces, the resulting complex may have a lower oxidation potential such that oxidation becomes feasible under the conditions used in bioleaching. These results on the oxidation of arsenic(III) in the presence of bacteria and pyrite are consistent with Ewart's findings using a mixed culture of *Moderately thermophilic* bacteria **[99]**.

The speciation studies reported here have shown that arsenic is primarily leached from arsenopyrite as arsenic(III). In fact arsenic(III) predominated over arsenic(V) in the initial stages of bacterial leaching of pyrite/arsenopyrite concentrates. Because of these trends the biological oxidation of arsenopyrite to produce arsenic(V) directly was considered to be insignificant under the conditions used in these experiments. This is in contrast to Iglesias and Carranza's **[116]** proposition that the arsenic(V) in bioleaching of arsenopyrite is due to the direct formation of arsenic acid when arsenopyrite is leached. Cassity and Pesic **[191]** used *Thiobacillus ferrooxidans* to leach a pyrite/arsenopyrite concentrate (9.90 wt% As, 18.60 wt% Fe, 9.26 wt% S). Similar trends to the current findings were observed in which arsenic(III) increased in the leach solution, reaching a maximum and then being oxidised to arsenic(V). They also found that the bacteria oxidised a synthetic solution of arsenic(III) in the presence of the leached ore. However they attributed the oxidation of arsenic(III) to arsenic(V) to chemical oxidation by ferric ions and bacterial cells as suggested by some researchers **[112, 193]**. The composition of the ore they used showed that there was more pyrite than arsenopyrite (pyrite to arsenopyrite ratio = 1.12) to catalyse the oxidation of

arsenic(III) to arsenic(V). The oxidation of arsenic(III) by bacteria in the presence of leached residues was probably due to the pyrite that remained in the residues which catalysed the reaction.

Dew **[93]** reported the concentrations of arsenic(III) in the primary bioreactors for the BIOX commercial plants. In the primary reactors the arsenic(III) concentration for the Fairview concentrate remained below 500 mg/L. In case of biooxidation of the Sao Bento concentrate 3-6 g/L arsenic(III) were measured in solution. The difference in the arsenic(III) species remaining in solution can be explained in terms of ore composition. The Sao Bento concentrate contained 10.1% pyrite and 26.9% arsenopyrite therefore according to the results of this study, it is expected that arsenic(III) will dominate in the bioleaching slurry because of there being a low amount of pyrite surfaces available to catalyse arsenic oxidation. Furthermore the concentrate contained 26.7% pyrrhotite which can act as an easy source of energy for the bacteria in preference to pyrite. Dew **[93]** explained the high concentration of arsenic(III) as a result of the low redox potential. However the results of this study have shown that the redox potential of the bioleaching slurry does not give any indication of the dominant oxidation state of arsenic.

The mineralogical composition has been found to be the main factor that controls the speciation of arsenic in bacterial oxidation. Bacteria alone were found to be unable to oxidise arsenic(III) to arsenic(V), however they were found to be able to catalyse this reaction in the presence of pyrite. Wakao et al., **[168]** reported that *Thiobacillus ferrooxidans* were unable to oxidise arsenic(III). This was probably due to the fact that the bacteria used were not well adapted to arsenic and there was no pyrite to catalyse the oxidation. Some soil organisms have been found to directly oxidise arsenite to arsenate **[169]**. Wakao et al., **[168]** isolated an acidophilic bacteria from a pyritic acid mine drainage (optimum growth pH = 3-4) which could directly oxidise arsenite to arsenate. However these bacteria could not oxidise ferrous iron or elemental sulphur as a sole source of energy and could not derive the energy for chemoautotrophic growth from arsenite oxidation. Evidence has been provided for the mineral leaching

archaebacterium *Sulpholobus acidocaldarius* strain BC to have the ability to oxidise arsenite to arsenate **[155]**.

5.3.10 Mechanisms of bacterial leaching of pyrite and arsenopyrite

The mechanisms of bacterial oxidation of pyrite and arsenopyrite are far form simple because of the various reactions which take place in the reaction vessel during bioleaching. Speciation studies help to identify some of the intermediate prdoducts during bioleaching of these minerals which are not usually encountered in the final products. Iron(II) and arsenic(III) were found to predominate in the bioleaching slurry in the early stages of bacterial leaching suggesting that they are the primary products in the decomposition of pyrite and arsenopyrite. The oxidation of arsenic(III) was found to dominate in the later stages when the leaching of most of the arsenopyrite had taken place. The results presented in this chapter also allow for a better elucidation of the bacterial leaching mechanisms of pyrite and arsenopyrite. Although the concept of direct and indirect mechanism is still being used by some authors, the results of the current study do not support these mechanisms. Instead they do support the mechanistic conclusions which were first reached by Barrett et al., **[104]** which divided the bacterial oxidation into primary and secondary processes. According to the results the primary and secondary processes during bacterial oxidation of pyrite/arsenopyrite concentrates were found to be best represented by the equations below:

Primary processes

$$2FeS_2 + 7O_2 + 2H_2O \xrightarrow{\text{Bacteria/iron(III)}} 2FeSO_4 + 2H_2SO_4 \qquad (5.5)$$

$$4FeAsS + 11O_2 + 2H_2O \xrightarrow{\text{Bacteria/iron(III)}} 4\,FeSO_4 + 4HAsO_2 \qquad (5.6)$$

Secondary processes

$$4FeSO_4 + 2H_2SO_4 + O_2 \xrightarrow{\text{Bacteria}} 2Fe_2(SO_4)_3 + 2H_2O \qquad (5.7)$$

$$HAsO_2 + Fe_2(SO_4)_3 + 2H_2O \xrightarrow[\text{Pyrite}]{\text{Bacteria}} H_3AsO_4 + H_2SO_4 + 2FeSO_4 \qquad (5.8)$$

It is important to monitor the concentration of arsenic(III) in the bioleaching pulp because its accumulation is deleterious to both the bacteria and the environment. It is also possible that different strains of bacteria used in commercial bacterial leaching plants may have different effect on the oxidation rate of arsenic(III) to arsenic(V).

CHAPTER SIX

MINERALOGICAL CHANGES AND ENVIRONMENTAL STABILITY OF BACTERIAL OXIDATION RESIDUES

6.1 Introduction

The success of bacterial oxidation technology is based on the ability of the naturally occurring bacteria to break down the mineral sulphides that contain valuable metals and to use these minerals as an energy source to sustain the growth of the culture. The precious metals remain in the oxidised residues and can be recovered in a conventional CIP/CIL or other chemical leaching step. Biooxidation has been reported to be selective for gold rich areas of the sulphides **[194-195]**. Because of the selective oxidation of the gold-rich areas it is often argued that the slow kinetics of this process can be compensated by this fact. However it is important to have a balance between gold liberation and the long term environmental acceptability of the arsenical residues produced by this process which can be classified into two categories:

(a) arsenical sludges from the neutralisation of the acidic bioliquors and

(b) solid biooxidation residues

Most data in the literature on bacterial leaching applications to arsenical ores refer mainly to the stability of neutralised sludges from acidic bioliquors, while information on the stability of solid bioresidues and cyanidation tailings is very limited. As a result of the mineralogical changes which take place in the bioreactors, the environmental suitability of the resulting residues should be evaluated in relation to the chemistry of bacterial attack and the mineralogy of the feed concentrate.

6.2 Gold liberation

Some of the residues from bacterial oxidation were subjected to cyanidation to assess the extent of gold liberation. Figures 6.1-6.3 show the gold recovery curves obtained for commercial flotation concentrates from the Indarama, the Riverlea and the Akbakai mines respectively. The concentrates were biooxidised to different levels and gold recoveries were measured by cyanide leaching. The point at zero percent arsenic extraction represents the gold recovery from the unoxidised material.

A direct relationship between gold dissolution and arsenic removal is evident for the Indarama and the Riverlea concentrates. The relationship is not so pronounced on the Akbakai concentrate as this concentrate was not very refractory according to the mineralogical observations. More than 90 % maximum gold recoveries were achieved

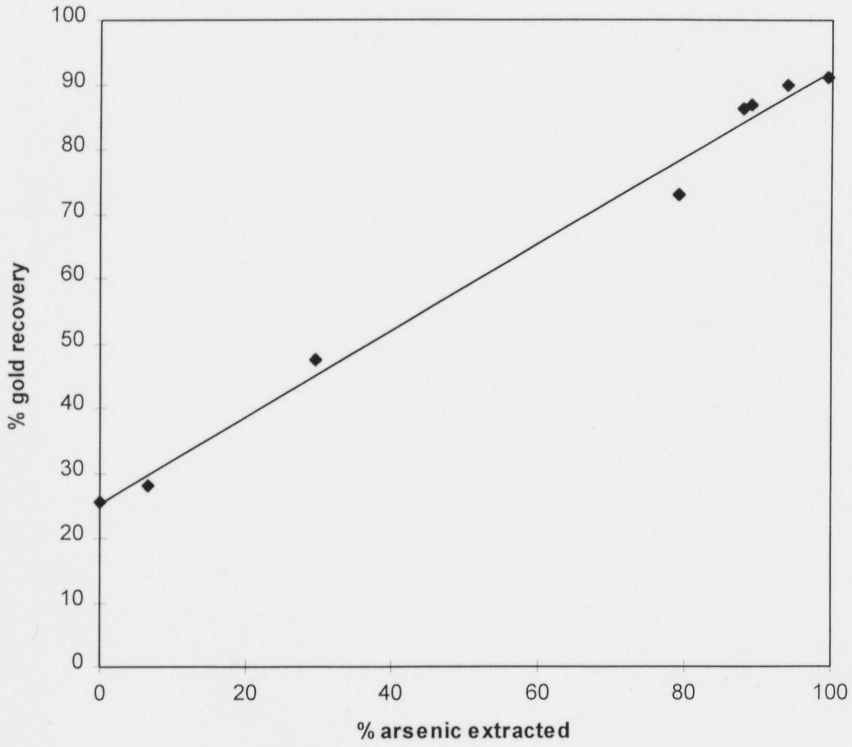


Figure 6.1: Gold release versus arsenic extraction during bacterial oxidation of the Indarama C concentrate.

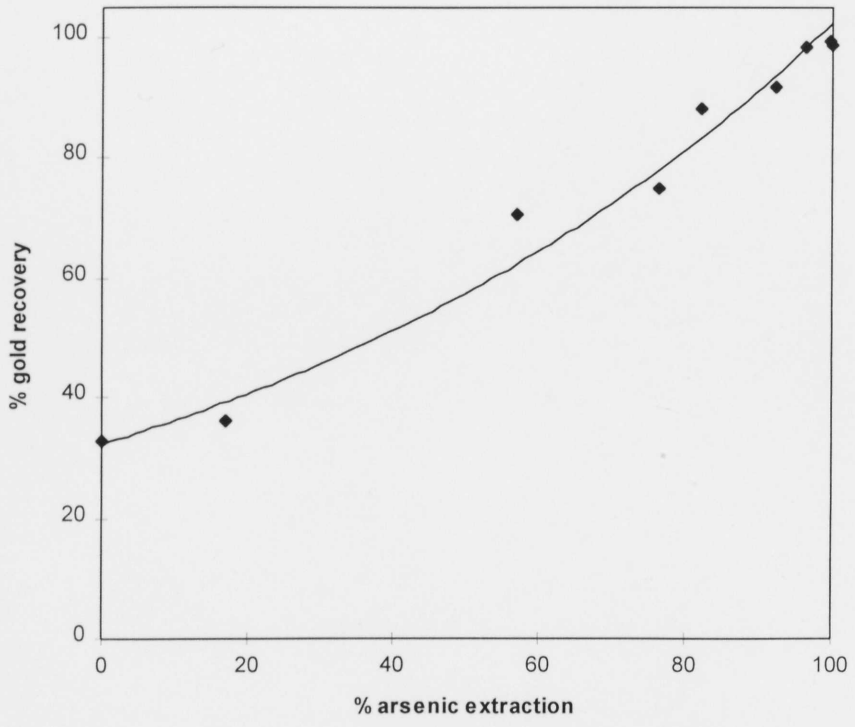


Figure 6.2: Gold release versus arsenic extraction during bacterial oxidation of the Riverlea concentrate.

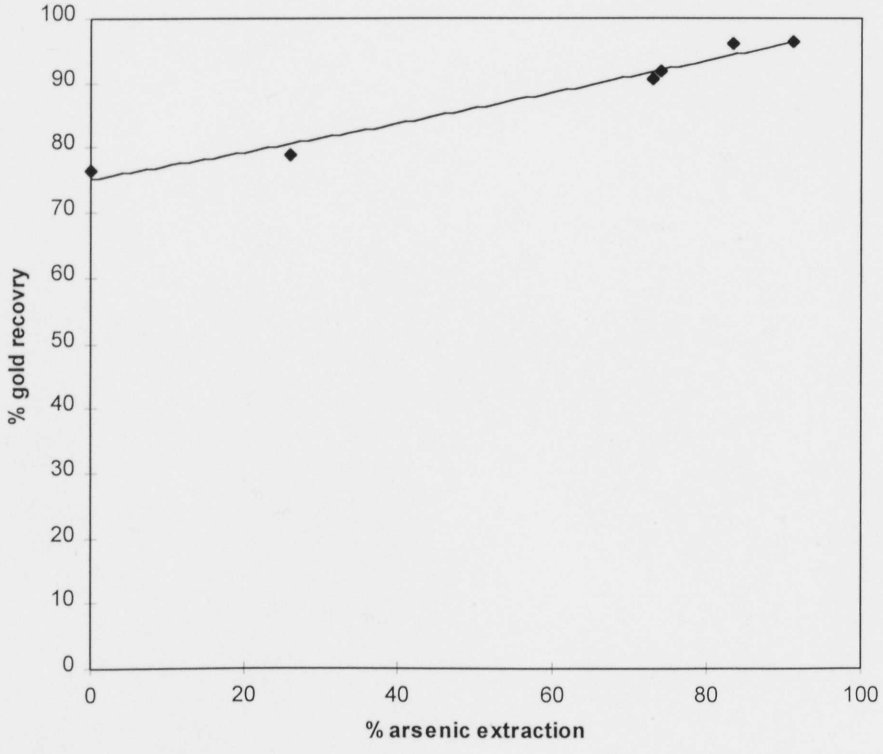


Figure 6.3: Gold release versus arsenic extraction during bacterial oxidation of the Akbakai D concentrate.

after pre-treatment. The gold recoveries for the Fairview and the Olympias concentrates are given in the literature **[140, 181]**.

6.3 Microscopic examination of the biooxidation residues

The arsenopyrite crystals were oxidised more rapidly than the pyrite crystals during the same period of time. Observation of the biooxidation residues showed that the arsenopyrite crystals were completely degraded while the pyrite crystals showed pitting on the surface and dissolution channels along the contacts and arsenic rich zones. Some gold-rich sulphides were also found to be areas of preferential attack and therefore releasing most of the gold in the early stages of leaching. Figures 6.4 shows a gold grain as observed under the optical microscope in the bacterial oxidation residues.

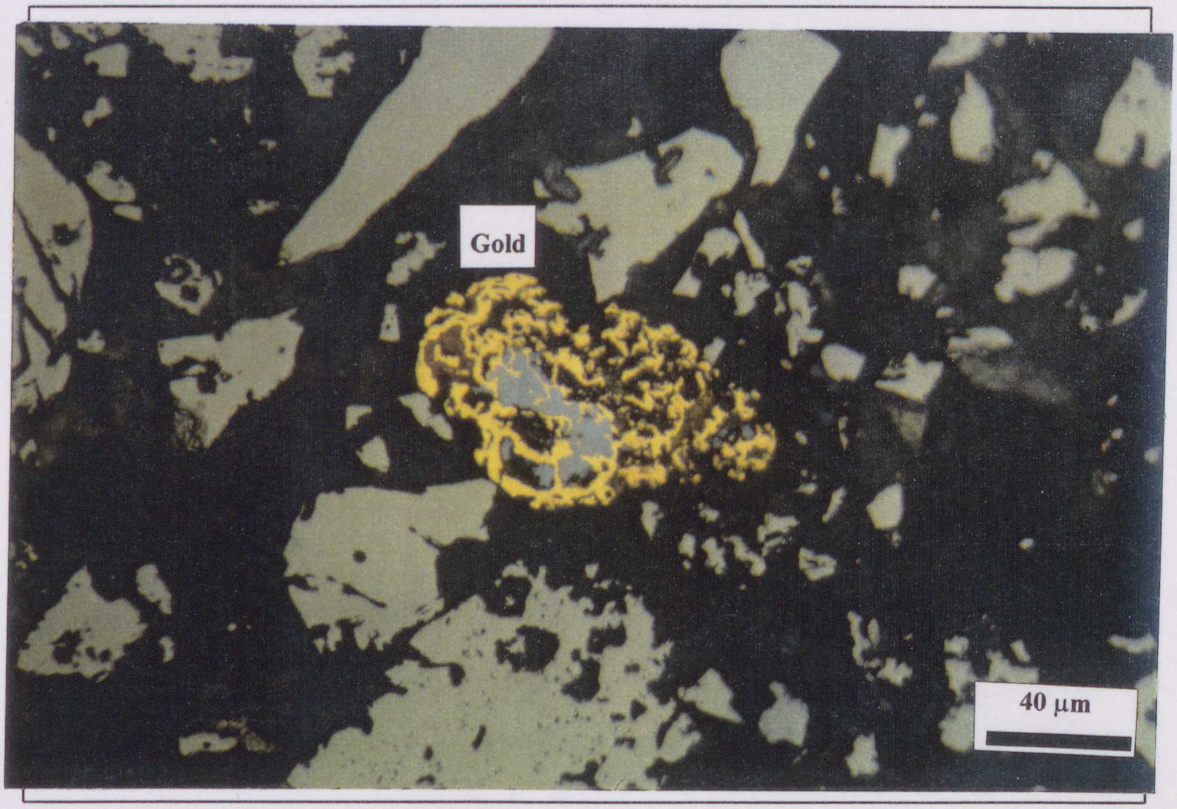


Figure 6.4: Optical microscopy photomicrograph showing a gold grain which has been liberated from an antimony sulphide particle (Indarama).

It is evident that arsenopyrite crystals were rapidly and preferentially attacked as shown in Figure 6.5. The arsenopyrite showed some dissolution pores and channels whilst

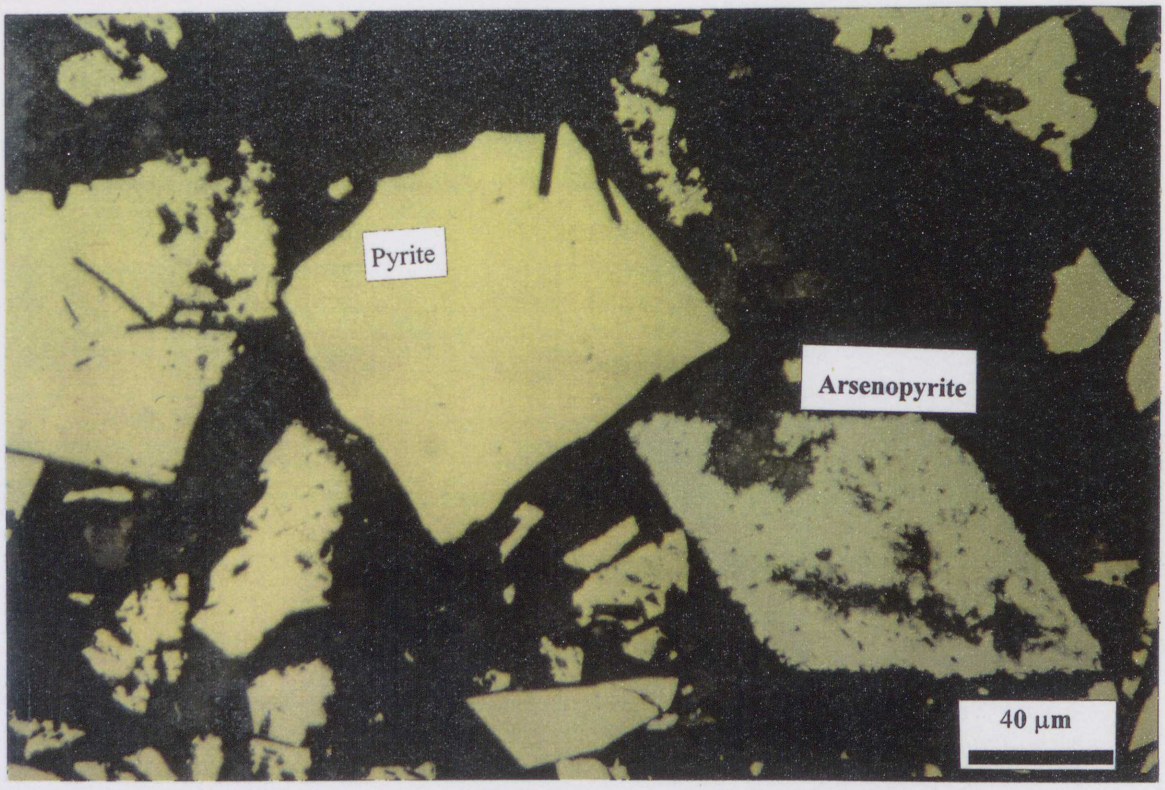


Figure 6.5: Optical microscopy photomicrograph showing preferential attack of the arsenopyrite crystal in relation to pyrite (Riverlea).

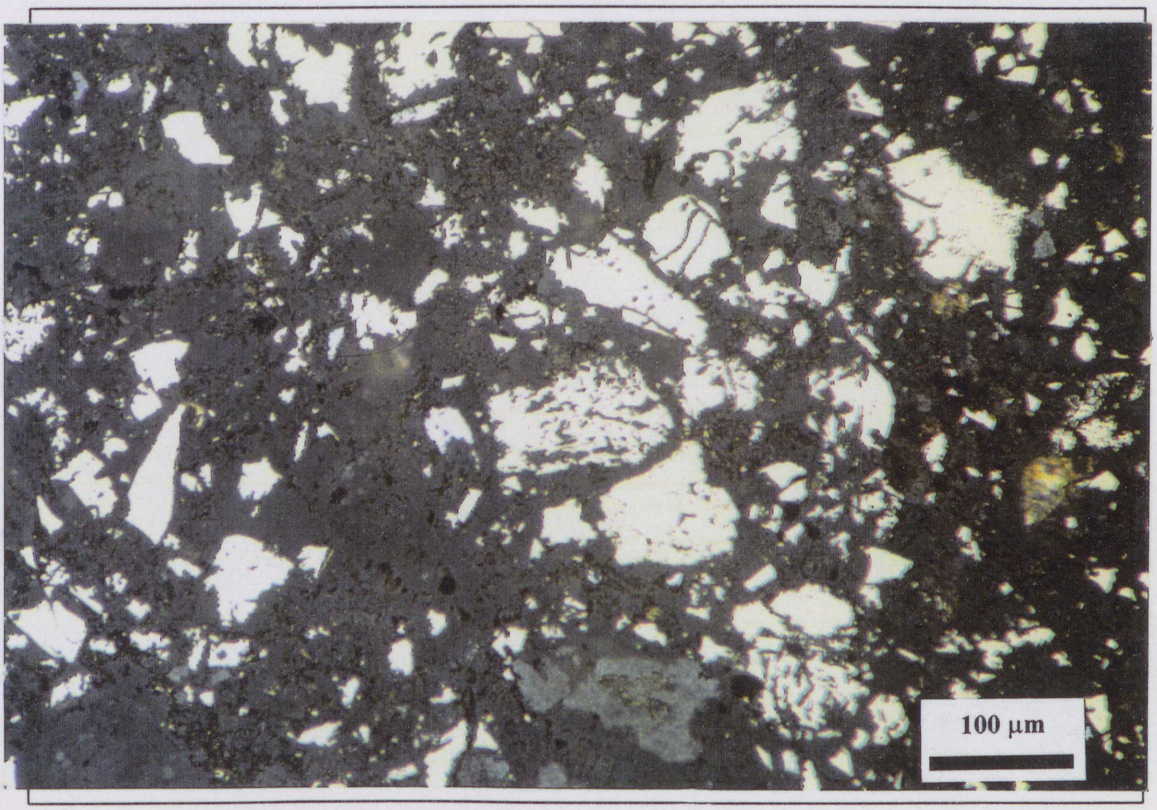


Figure 6.6: Optical microscopy photomicrograph showing penetrating pore on the pyrite crystals (Indarama).

some of the pyrite was still unreacted. Polished sections of the residues showed that some of the pores penetrated through the pyrite crystals as shown in Figure 6.6.

Figure 6.7 shows pyrite and arsenopyrite crystals in the concentrate before bioleaching. Figures 6.8-6.16 show scanning electron microscopy photomicrographs of the bacterial oxidation residues.

The arsenopyrite crystals were completely porous after 8 days of attack as shown in Figures 6.8 and 6.9. The pyrite resisted the attack resulting in the development of pores and dissolution channels in the areas of weakness such as arsenic rich and contact zones. Extensive preferential oxidation of arsenic rich zones were observed on zoned arsenopyrite and pyrite crystals. Pits and dissolution channels were clearly distinguished as shown in Figures 6.10-6.13. The dissolution pits on the arsenopyrite were mainly cylindrical and at times the shape could not be seen because they merged. The pyrite crystals showed

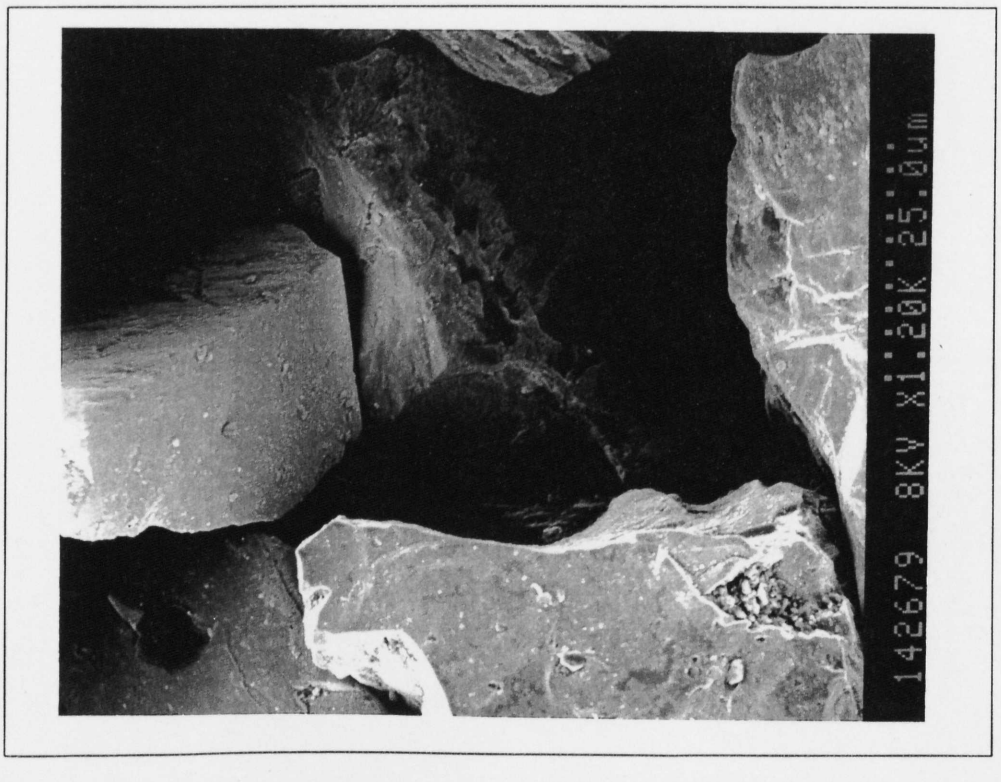


Figure 6.7: Secondary electron image showing pyrite and arsenopyrite crystals before bacterial oxidation.

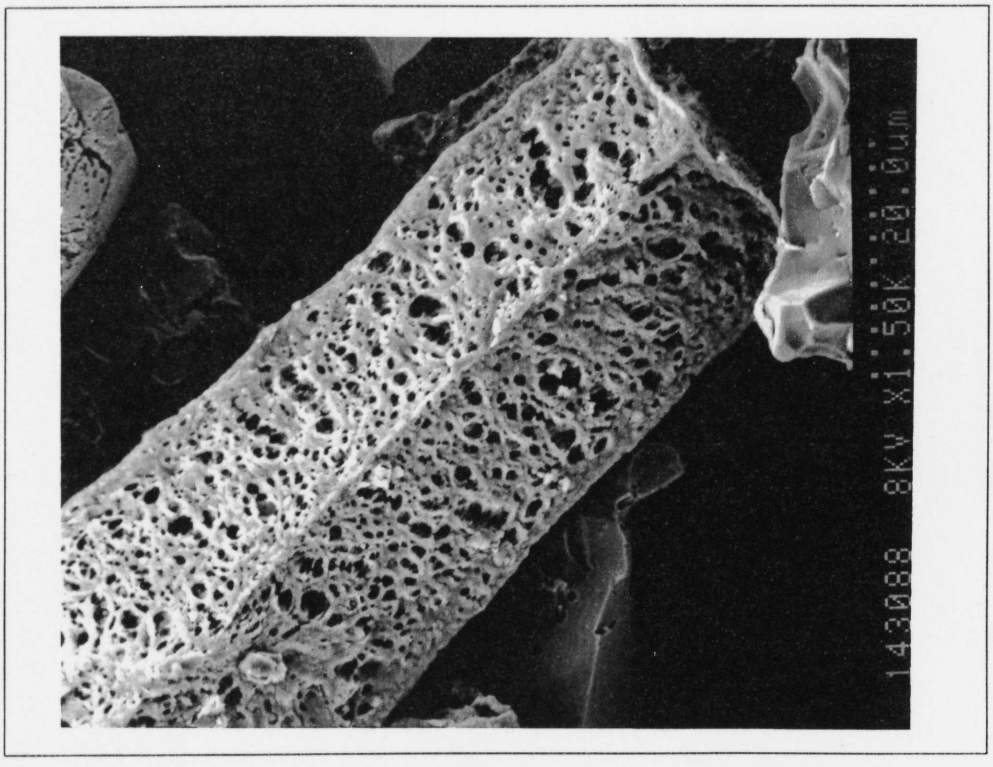


Figure 6.8: Secondary electron image of an arsenopyrite crystal after 7 days of bioleaching (the Indarama C concentrate).

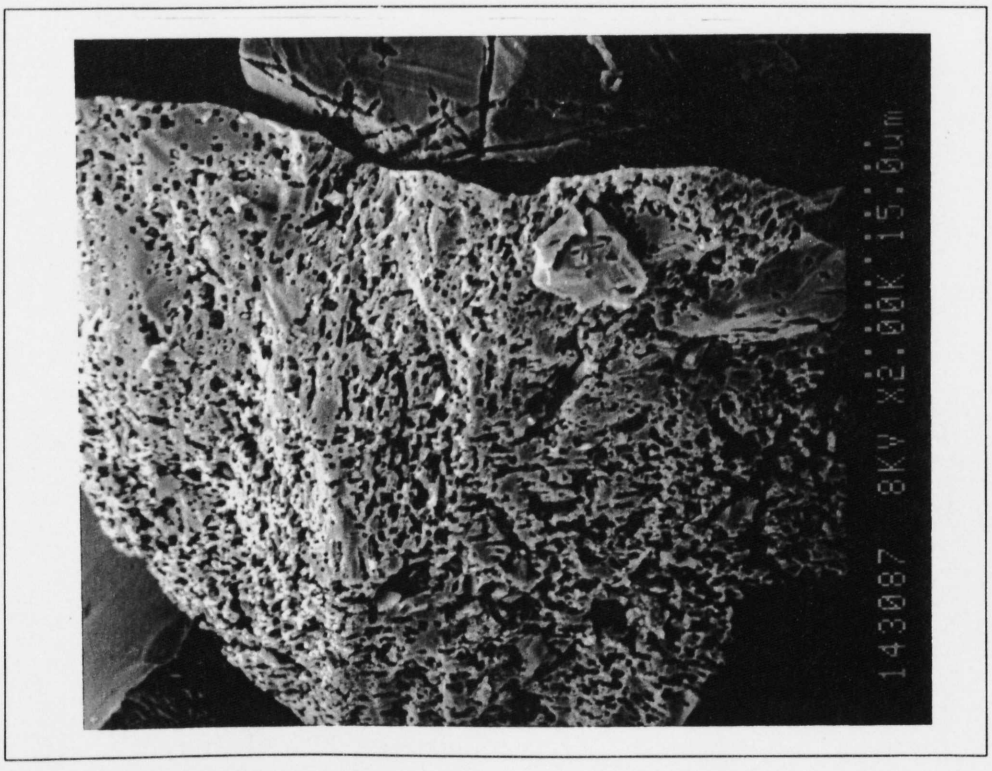


Figure 6.9: Secondary electron image of an arsenopyrite grain after 8 days of bacterial attack (the Indarama C concentrate).

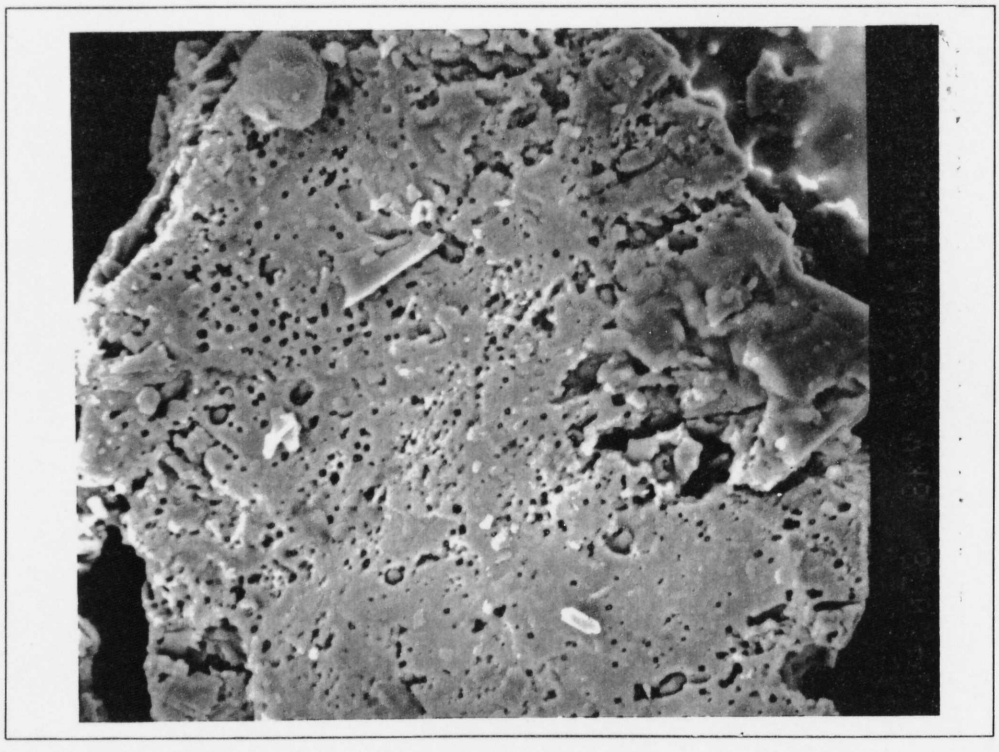


Figure 6.10: Secondary electron image of a pyrite crystal after 11 days of bacterial attack (the Akbakai concentrate).

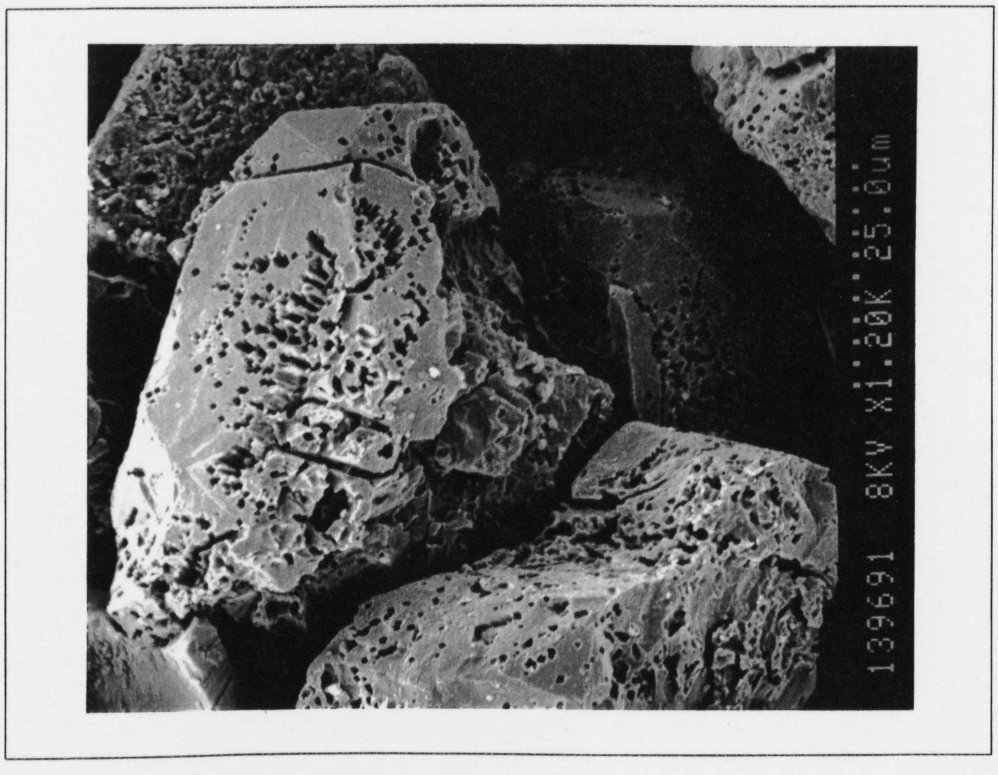


Figure 6.11: Secondary electron image of pyrite grains after 11 days of bacterial attack (the Indarama C concentrate).

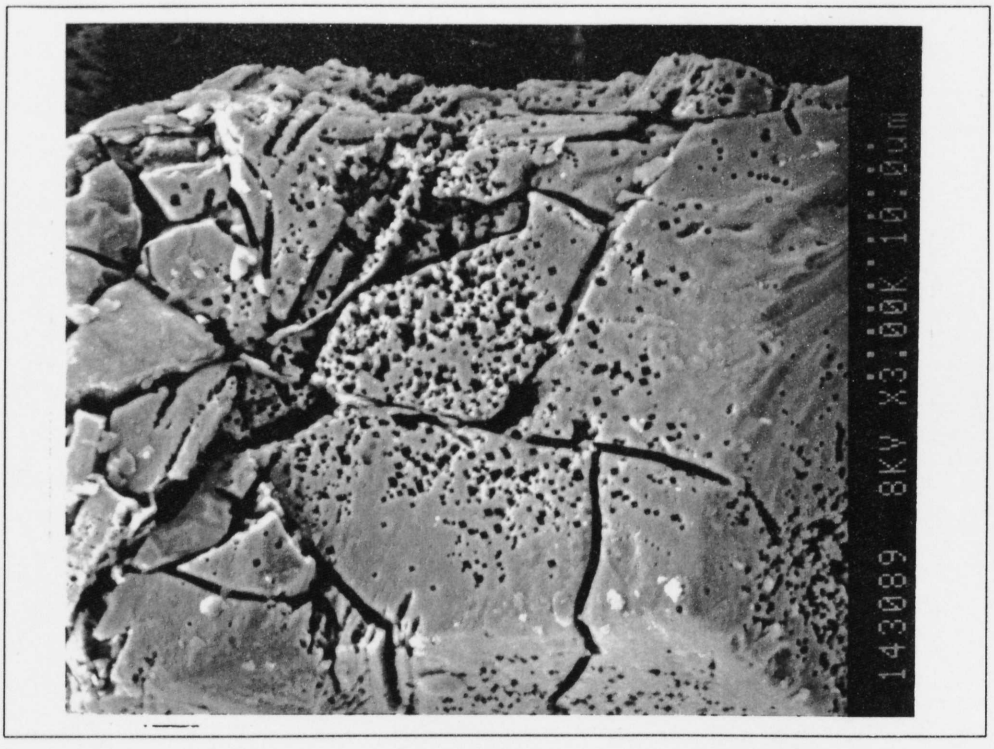


Figure 6.12: Secondary electron image of a pyrite crystal after 12 days of bacterial attack (the Indarama concentrate).

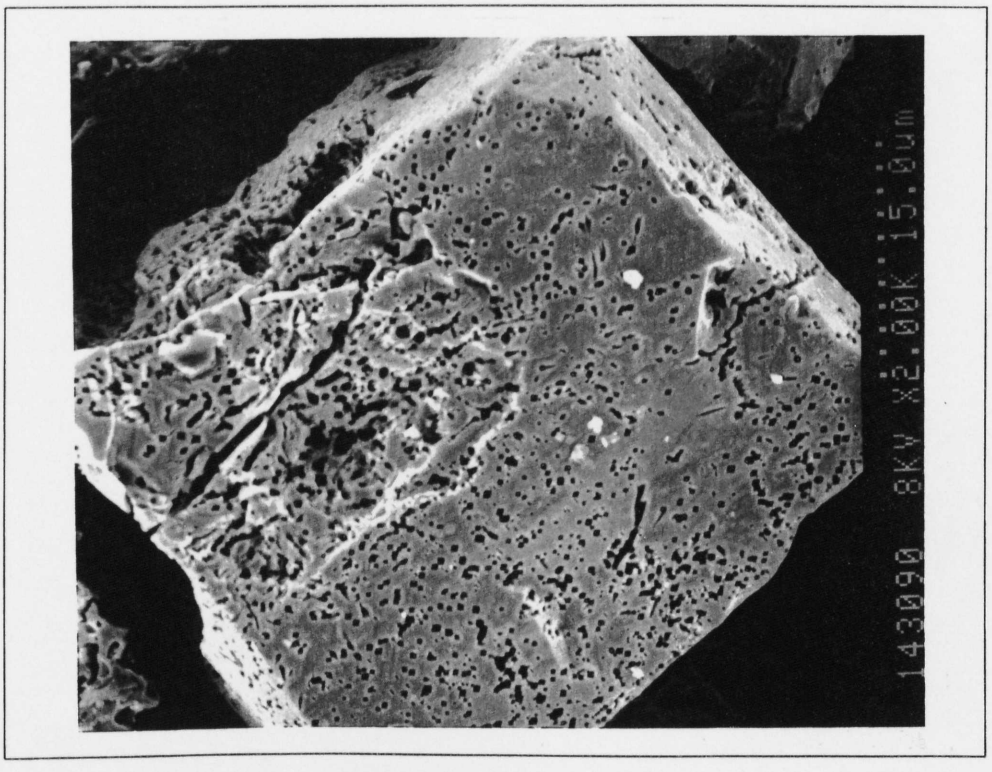


Figure 6.13: Secondary electron image of a pyrite grain after 13 days of bacterial attack (the Indarama C concentrate).

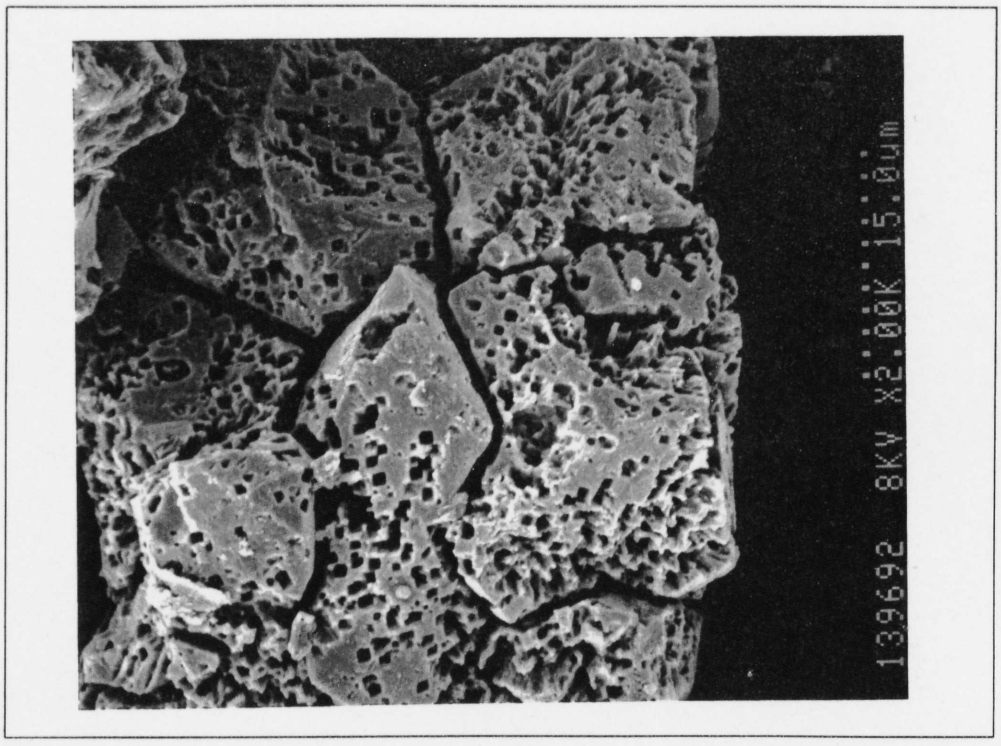


Figure 6.14: Secondary electron image of a pyrite crystal after 10 days of bacterial attack (the Olympias concentrate).

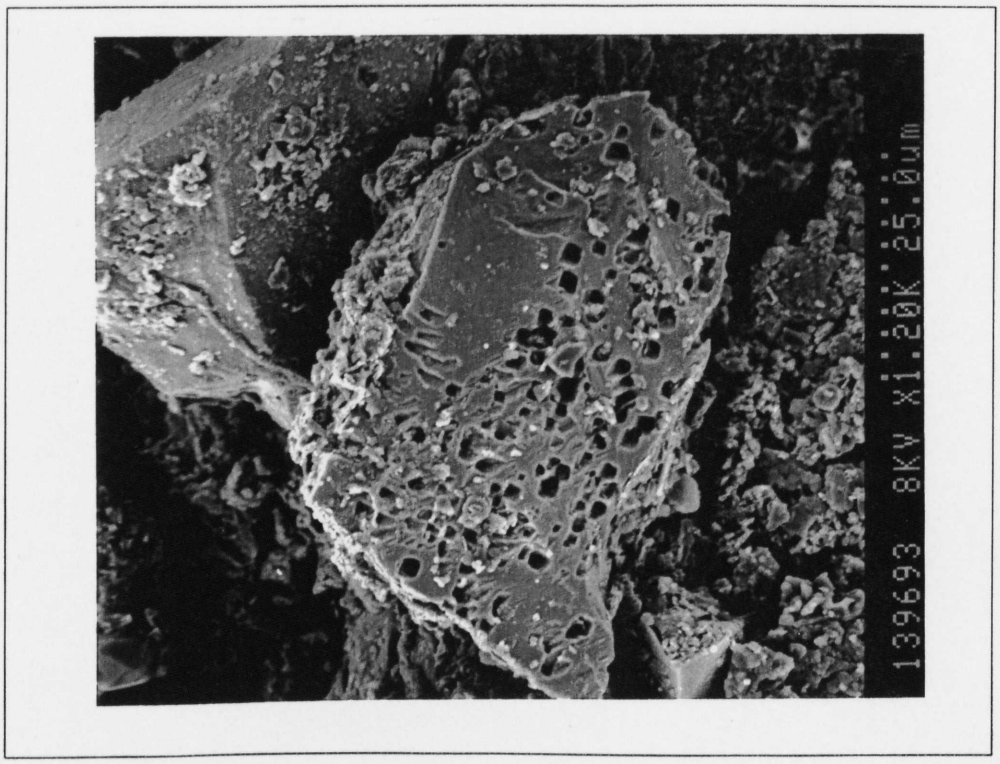


Figure 6.15: Secondary electron image of a pyrite grain after 13 days of bacterial attack (the Riverlea concentrate).

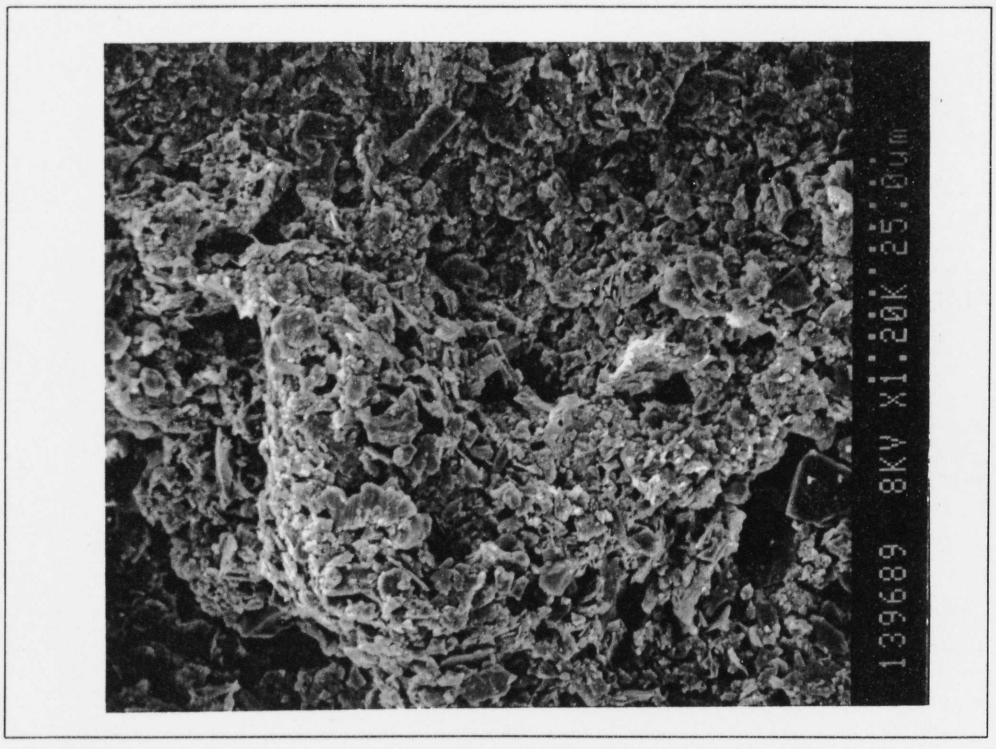


Figure 6.16: Secondary electron image of the residues after 14 days of bacterial attack (the Riverlea concentrate).

mainly hexagonal dissolution pits and also cylindrical corrosion patterns. The density of corrosion patterns was much higher on the arsenopyrite than the pyrite (comparison of Figures 6.8-6.9 with Figures 6.10-6.15. After about 12 days most of the pyrite was leached and all the structures were completely destroyed as shown in Figure 6.16.

6.4 Environmental stability of biooxidation residues

The biooxidation residues were subjected to the standard United States Environmental Protection Agency Toxicity Characteristic Leach Procedure (US EPA TCLP) test to evaluate their environmental disposal solubility. The EPA TCLP test does not give any information about the long-term stability of the residue but it rather gives an indication of the solubility of the residues. Therefore the word stable refers to the solubility criteria of the EPA test which is at the moment accepted to be a measure of the requirements for disposal of the waste residues. The feed concentrates were also subjected to the same test in order to provide a reference point. Table 6.1 shows the EPA TCLP test results on the concentrates before bacterial oxidation. All the concentrates showed that the pyrite and arsenopyrite were stable as far as arsenic was concerned. They all showed soluble

arsenic concentrations of less than 5 mg/L which is the maximum limit of the soluble arsenic in a stable residue according to the TCLP test criteria.

Table 6.1: EPA test results for the feed concentrates.

Sample Origin	Sample I.D	As mg/L
Indarama mine	B	2.3
Indarama mine	C	1.3
Akbakai mine	D	0.5
Riverlea mine	R	0.9
Olympias mine	O	1.2
Fairview mine	F	1.0

Table 6.2 shows the EPA test results of the biooxidation residues from different concentrates and mixtures used. In some of the EPA filtrates the concentrations of arsenic(III) was measured and it was noted that the majority of the soluble arsenic was in the +3 oxidation state (As^{3+}). For the tests 1-18 the pH of the bioleaching slurry was not controlled and for tests 19-21 the pH values were adjusted to 1.5, 1.8 and 2.5 respectively on a daily basis. When the pH of the leaching slurry was left the drift to lower values (range 0.9 to 1.3) the amount of arsenic precipitated in solids was found to be limited and in most cases it accounted for less than 1 % in the residues. EPA TCLP test of the residues from the Indarama B concentrate showed the highest concentration of soluble arsenic (about 112 mg/L total arsenic, with 91 mg/L being arsenic(III)) and this concentrate had the highest proportion of arsenic(III) in the bioleaching slurry at the end of bacterial oxidation stage. When pyrite was added to the Indarama B concentrate the resulting residues from bacterial leaching of the mixtures passed the EPA TCLP test (less than 5 mg/L soluble arsenic). Oxidation of arsenic(III) to arsenic(V) also went to completion. Residues from bacterial oxidation experiments in which the pH was controlled around 2.5 were highly unstable showing an arsenic concentration of more than 88 mg/L (Indarama (21), Table 6.2). The slurry of this experiment had a significant concentration of arsenic(III) at the end of the oxidation stage which was considered

Table 6.2: EPA test results of the biooxidation residues (see Appendix Three, Table A3.2.4 for composition of concentrates before bioleaching).

Sample origin	Run number	% As in solids	Soluble solids in residue			EPA As mg/L	EPA As(III) mg/L
			% As	%Fe	Fe/As[M]		
Olympias	34	0.88	0.42	0.80	2.50	0.53	-
Akbakai	13	0.27	0.23	0.43	2.57	1.50	-
Fairview	9	0.32	0.18	0.43	3.13	1.65	-
Akbakai	5	0.39	0.36	0.63	2.38	1.73	-
Inda/Stra	11	1.88	1.02	2.03	2.66	2.22	-
Riverlea	3	0.65	0.56	3.01	7.35	2.73	-
Olympias	6	4.63	0.10	0.12	1.61	3.00	-
Indarama	2	0.92	0.85	2.22	3.52	3.98	-
Riverlea	12	0.51	0.41	2.63	8.65	4.03	-
Inda/Stra	8	0.70	0.69	1.21	2.35	4.08	-
Inda/Stra	7	0.91	0.74	1.13	2.05	4.43	-
Indarama	14	0.81	0.64	1.66	3.49	4.65	-
Riverlea	35	0.83	0.38	2.54	8.82	4.72	-
Indarama	26	0.80	0.64	1.73	3.60	8.12	-
Indarama	15	0.96	0.72	1.78	3.34	13.60	8.21
Indarama	17	2.54	1.29	1.60	1.66	15.00	11.14
Indarama	16	1.12	0.46	1.05	3.09	16.90	10.67
Indarama	21	13.83	12.10	13.66	1.51	24.40	17.97
Indarama	20	7.72	6.86	7.37	1.44	28.90	18.15
Indarama	10	1.64	1.21	10.12	1.82	45.90	33.23
Indarama	22	12.00	10.05	13.14	1.75	88.50	72.35

here. Solubility tests of partially leached pyrite and arsenopyrite showed that the arsenic was unstable as shown in Table 6.3. Arsenic stability was only achieved when there was almost complete conversion of arsenic(III) to arsenic(V) during bacterial oxidation. The

molar ratio of iron:arsenic ranged from 1.4 to about 8.6. However there was no correlation between the molar ration of iron to arsenic and the stability of the residues. Soluble solids in Table 6.2 refers to the oxidised precipitates of iron and arsenic in the biooxidation residues which was soluble in 5M HCl as described in Chapter Three (section 3.7). In Table 6.3 the percentage arsenic extraction is the amount of arsenic which was leached from the original sample during bacterial oxidation at the time when the experiment was stopped.

Table 6.3: EPA test results of some of the biooxidation residues with significant partially leached arsenopyrite.

Sample origin	Run number	% As Extraction	EPA As (mg/L)	EPA As(III) (mg/L)
Indarama C	36	59.9	53.7	44.3
Indarama C	37	68.9	67.4	59.9
Akbakai D	38	63.7	18.8	16.2
Riverlea	39	53.0	43.5	37.5
Riverlea	40	80.3	28.0	21.3

The residues from bacterial oxidation normally pass through the cyanidation step to recover the gold before disposal. Stability tests which were carried out on the cyanidation residues showed that there was no improvement with regard to arsenic stability. EPA TCLP test results on some of the cyanidation tailings are shown in Table 6.4. It can be seen that the arsenic solubilities in the cyanide tailings are similar to those of their respective biooxidation residues. No improvement was seen on the unstable residues instead the concentration of soluble arsenic tend to increase slightly. Similar observations to those shown in Table 6.4 were also made by other researchers who tested the stability of the bioresidues in their work **[16, 19]**. Adam et al., **[19]** found that the soluble arsenic in the EPA TCLP tests were dominated by arsenic(III), although speciation studies of some soluble solids in the biooxidation residues showed that arsenic(V) and iron(III) were the dominant species in most of the samples. The Indarama B showed almost an equal amount of arsenic(III) and arsenic(V) in the soluble

solids. The iron(II) and arsenic(III) which was detected in the soluble solids was mainly attributed to partially reacted pyrite and arsenopyrite grains. These species were probably from the intermediate products of the dissolution mechanisms of arsenopyrite and pyrite since it was shown that the leaching of these minerals primarily produce iron(II) and arsenic(III).

Table 6.4: EPA test results on cyanidation tailings.

Sample Origin	Run number	EPA before cyanidation As (mg/L)	EPA after cyanadation As (mg/L)
Indarama B	1	112.3	146.5
Indarama C	16	15.3	34.9
Riverlea R	35	3.6	2.1
Riverlea R	41	8.5	9.2
Akbakai A	13	2.8	1.6
Akbakai D	5	4.9	5.7

Due to the limited quantities of the precipitated iron-arsenic compounds associated with the solid residues during bacterial oxidation, they were not identified by XRD. However when the pH was controlled during bioleaching more than 6 wt% arsenic was precipitated. Characterisation of these precipitates using XRD showed that they were amorphous. The concentrates used were not purely composed of pyrite and arsenopyrite, carbonates were also identified during mineralogical examination. Because of the multicomponent nature of the concentrates and coexistence of unreacted pyrite and arsenopyrite, the iron-arsenic oxidised products were not clearly identified on the scanning electron microprobe and thus no attempt was made to describe these products with a specific chemical formula.

6.5 Discussion

Optical and scanning electron microscopic examination of the residues revealed interesting textures in the partially leached mineral grains. Penetrating pores were typically of the order 2-5 μm in diameter were common features on both pyrite and arsenopyrite grains (Figures 6.1-6.16). These pores were at times at right angles and occasionally hexagonally-shaped indicating that they were following crystallographic planes or lines of weakness in the crystal structure, such as dislocations, inclusions or fractures introduced during crushing and grinding. Similar observations were made by Southwood and Southwood **[196]** who examined polished sections of partially leached biooxidation residues. They proposed that the pores represented sites of accelerated chemical and bacterial attack at dislocations in sulphide lattice were the weaker chemical bonding provides easily obtained energy for the bacteria. Monroy-Fenandez at al., **[134]** observed that bacterial oxidation of arsenopyrite was accelerated as a consequence of direct oxidation by the adhering bacteria and the indirect chemical oxidation by iron(III) ions generated simultaneously by free bacteria. However they suggested that the isotropic distribution of the corrosion patterns on the mineral surfaces suggest that the electrochemical oxidation process is dominant. The existence of the porous structure on the pyrite particles is related to the accelerated oxidation of arsenic(III) to arsenic(V) during bacterial oxidation (Chapter Five refers) in the present study. The opening up of the pyrite surfaces through these pores provides a greater surface area for the oxidation of arsenic(III). This oxidation reaction was found to take place only in the presence of pyrite as catalyst. Furthermore since these pores are active dissolution sites, clean pyrite surfaces are continually exposed avoiding the deterioration of the reaction surfaces.

The composition of arsenopyrite and pyrite played a very important role in determining areas of preferential attack. Microprobe analysis of mounted concentrate grains which have been exposed to an actively growing culture in the pachuca showed that areas enriched in arsenic in arsenopyrite were attacked first and the same was true with pyrite (arsenian pyrite) as observed under the microscope. The arsenopyrite and pyrite were preferentially attacked on sites representing structural deviations in the crystal lattice.

These deviations include contacts between zones, inclusions of other minerals or elements, dislocations and cracks. Some dislocations and cracks are also introduced during mineral processing especially crushing and grinding. As a result most of the submicroscopic gold is assumed to be liberated during the initials stages of oxidation before achieving a complete sulphide breakdown. Preferential attack on gold-rich sites was also evident on the polished sections of the partially leached biooxidation residues (Figure 6.4). From these observations together with the cyanidation tests, it was shown that most of the refractory gold associated with the sulphides was released before complete sulphide dissolution is achieved.

Another common feature seen during examination of the residues was the preferential attack of arsenopyrite compared with pyrite (Figure 6.5) and arsenic-rich areas in pyrite particles. It was concluded that arsenopyrite was an easier source of energy for the bacteria possibly due to the weaker bonding in its structure. Furthermore it is well documented in the literature that during leaching of mixed minerals exhibiting different rest potentials, galvanic interaction occurs, significantly enhancing the leaching process **[197-199]**. Galvanic contact between different conducting or semi-conducting minerals leads to the less noble acting as anodes by nature of electrochemical relativity. Therefore in the presence of pyrite, arsenopyrite will be leached at a faster rate **[200]**. The possibility of galvanic interaction contributing towards the preferential dissolution of arsenopyrite cannot be ruled out and the fact that the bacteria attach to the minerals and cause localised attack could have accelerated the galvanic dissolution. In order to demonstrate the selectivity of arsenopyrite versus pyrite oxidation Texiachou et al. **[140]** defined the selectivity index (S.I):

$$S.I. = (\%\ FeAsS_{oxidised}/\%\ FeS_{2\ oxidised})/(\%\ FeAsS_{feed}/FeS_{2\ feed})$$

and showed that the selectivity index increased with increasing pulp density during bacterial oxidation. However this can be expected because at higher pulp density more arsenopyrite will be available for the energy of the bacteria and this can delay dissolution of pyrite.

The stability of the arsenical residues was found to be mainly controlled by the extent of arsenic(III) to arsenic(V) oxidation during bacterial leaching. This was in turn controlled by the mineralogical composition of the feed concentrate (ratio of pyrite to arsenopyrite). Bacterial oxidation residues from the highly arsenical concentrates where the oxidation of arsenic(III) to arsenic(V) was not completed showed high values during EPA TCLP tests. This was mainly attributed to the incorporation of the arsenite in the soluble solids. The presence of the arsenite ions was also attributed to the dissolution intermediate products on the surfaces of the partially leached arsenopyrite. It was shown that bacterial oxidation of arsenopyrite primarily produce arsenic(III) and it is most likely that these products contained arsenic(III). Similar conclusions were reached by Adam et al., **[19]** who examined the stability of bacterial oxidation residues emanating from a highly arsenical concentrate. These researchers went on to releach the unstable bacterial oxidation residues in bacterially-rich ferric sulphate in an attempt to stabilise the residues, however they found that there was no improvement as far as arsenic stability was concerned. According to the present results this can be expected because ferric sulphate alone was found not to be able to oxidise arsenic(III) to arsenic(V) during bacterial leaching. A releach of these unstable residues with some bacteria and pyrite added as well could have been the solution towards stabilising them. The unstable arsenic(III) could have been oxidised to arsenic(V) on the pyrite surfaces.

The final bioresidues in which the conversion of arsenic(III) to arsenic(V) was not completed during bacterial leaching did not pass the EPA TCLP test before or after cyanidation. This study has shown that it is critical to remove as much arsenic as possible and oxidise it to arsenic(V) during biooxidation to minimise the amount of arsenic(III) reporting to the residues. The addition of pyrite to highly arsenical concentrates also resulted in stability of the resulting residues because pyrite promoted the oxidation of arsenic(III) to arsenic(V). Despite the limited content of the arsenic(III) in the soluble solids in the residues, arsenic(III) was the key factor dictating the solubility of the residues since it accounted for the majority of the measured soluble arsenic in the EPA TCLP tests. There was no correlation between Fe/As ratio of the soluble solids and the solubility of the residues in some cases. This may have been due

to the presence of calcium in the concentrates which can also combine with the arsenate to form calcium arsenate compounds. Based on the results from this work and other reported work **[16, 19]**, it is concluded that in case of refractory gold ores where the gold is preferentially associated with arsenopyrite, the separation of pyrite from arsenopyrite during beneficiation of the ore (selective flotation of arsenopyrite) has to be carefully considered in terms of process environmental performance if bacterial oxidation is to be employed as the pre-treatment method to liberate the gold. Furthermore supplementing highly arsenopyrite concentrates with pyrite should be considered during bacterial oxidation of these concentrates in order to produce environmentally acceptable residues. The precipitated bacterial oxidation residues were found to be amorphous by XRD analysis. This is in agreement with other researchers who have also found that the bacterial oxidation residues are amorphous **[16, 19, 201]**, however these results are in disagreement with other reports on characterisation of bacterial oxidation residues in which crystalline scorodite was identified **[202-203]**. While several XRD peaks which matched scorodite were identified by Carlson et al., **[203]**, they based their conclusions on only one characterisation technique. It is possible that due to the multicomponent nature of the reaction products during bacterial oxidation which includes unreacted sulphides and elemental sulphur, there might be peak overlaps. On the other hand Cruz et al., **[202]** used only two peaks on the XRD pattern which corresponded to scorodite as evidence for the formation of scorodite during bacterial leaching. The infrared spectra of their residues did not match typical spectra for scorodite which have been demonstrated by Swash and Monhemius **[22-24]** during hydrothermal precipitation of arsenical compounds. It is possible that both crystalline and amorphous products can be produced during bacterial leaching, however because of the limited amount of the crystalline products it is very difficult to characterise them and draw clear conclusions as regards their proper chemical formulae. Current findings showed that bacterial oxidation precipitates in the residues were amorphous, if crystalline products were present, probably their concentrations were too little to be detected.

CHAPTER SEVEN

GENERAL DISCUSSION AND CONCLUSIONS

7.1 General discussion

The growth in the processing of refractory gold particularly where arsenopyritic ores are involved has led to increasing environmental pressure. The acceptability of bacterial oxidation processes will depend on the long term stability of the arsenical residues emanating from the leaching of arsenopyrite in the ores. Although increased gold recovery can lead to economical justification of any flowsheet, it is the environmental issues that are the driving forces behind the development of alternative flowsheets.

A significant improvement in the understanding of the relationship between mineralogies of different ores and the subsequent oxidation of arsenic(III) during bacterial leaching has been achieved. Furthermore the stability of the residues resulting from the bacterial oxidation process has been related to the mineralogy of the ores. This information will help in understanding the processes of interest in the bioreactor in order to produce residues which are safe for environmental disposal. A comparative study of arsenic speciation during bacterial oxidation of refractory gold ranging from high to low arsenopyrite content has been carried out. A correlation was found to exist between pyrite leaching and the rate and extent of arsenic(III) oxidation during the bacterial leaching process. The ratio of pyrite to arsenopyrite was demonstrated to be the key factor in the oxidation of arsenic(III) to arsenic(V). More pyrite in the concentrate was found to promote the oxidation of arsenic(III) because pyrite provided catalytic surfaces

for the oxidation reaction. Arsenopyrite was found to be leached more easily than pyrite, providing an easy source of energy (iron(II)) for the bacteria and as a result there was selective oxidation of arsenopyrite and once the arsenopyrite was depleted the bacteria started attacking pyrite to significant extent. The attack of pyrite increased the surface area and hence the rate of arsenic(III) oxidation as was demonstrated by the examination of the surfaces of the partially leached pyrite grains. Conditions in the bioleaching slurry which can lead to the fast depletion of arsenopyrite will lead to bacteria attacking the pyrite in the early stages and hence promoting the oxidation of arsenic(III).

The variation in the mineralogy of the same deposit was found to produce concentrates with completely different speciation behaviour during bacterial leaching (the Indarama concentrates). The grade of the sulphide was also found to affect the oxidation of arsenic(III) during bacterial oxidation (the Akbakai concentrates). For consistency in the oxidation of arsenic(III) during biooxidation it was found necessary to control the pyrite grade of the sulphide concentrate, in particular the ratio of pyrite to arsenopyrite and the amount of the gangue phases in the concentrate. The flotation practice should be carefully controlled in order to eliminate the gangue phases reporting to the concentrate, this will also limit the volume of materials requiring processing increasing the output of the plant. Production of dilute concentrates may lead to pyrite surface area being the limiting factor on the oxidation of arsenic(III) to arsenic(V) (the Akbakai concentrates).

The addition of pyrite to aid the oxidation of arsenic(III) during bacterial oxidation should be considered especially in cases where high arsenopyrite content concentrates are being processed. The addition of pyrite was found to promote the oxidation of arsenic(III) to arsenic(V) during bacterial oxidation because pyrite provided the catalytic surfaces and the ferric ions leading to stable residues.

The composition of pyrite and arsenopyrite was found to play an important role in determining areas of preferential attack. In general arsenopyrite was preferentially attacked compared with pyrite. However arsenic-rich areas of pyrite crystals were also leached at the same time as arsenopyrite. Structural defects of the crystal lattice which

includes inclusions of other minerals or elements, dislocations and cracks introduced during mineral processing techniques such as crushing and grinding were also areas of preferential attack. Because of these structural defects, gold liberation is normally achieved without total sulphide distruction. The fact that arsenopyrite is attacked first is good for the environment and gold liberation in the process especially where most of the gold is associated with the arsenopyrite.

The stability of bacterial oxidation residues was found to be dictated by the mineralogical composition and the solution chemistry during bacterial oxidation. Complete oxidation of arsenic(III) to arsenic(V) was found necessary to produce environmentally stable residues. Arsenic(III) dominated in the soluble arsenic after the EPA TCLP tests of the unstable residues. Partial oxidation of arsenopyrite grains was also found to produce unstable residues possibly as a result of the intermediate products formed during arsenopyrite leaching which were assumed to contain mainly arsenic(III). This conclusion was reached after observing that bacterial leaching of arsenopyrite primarily produced arsenic(III). Total extraction of arsenic and complete oxidation of arsenic(III) was necessary for the production of environmental stable residues. The bioleaching of pyrite was adversely affected by precipitation in the early stages and this led to more arsenic(III) reporting in the bioleaching slurry at the end of the oxidation stages which were considered here.

The use of lime to neutralise the residues from biooxidation can lead to the formation of calcium arsenate, which is stable in the presence of excess lime, however when the calcium arsenate is exposed to the atmospheric air and acidic conditions it can react with the carbon dioxide in the air **[22]** according to the following equation:

$$Ca_3(AsO_4)_2 + 3CO_2 + 4OH^- = 3CaCO_3 + 2HAsO_4^{2-} + H_2O \qquad (7.1)$$

releasing the arsenic into the environment. Although the precipitates in the residues from bacterial oxidation were amorphous, operating at pH less than 1.3 resulted in most of the arsenic remaining in the solution. This can be one of the advantages of bacterial

oxidation, even if the long-term stability of the amorphous residues is questionable, the process remains an option for environmental considerations by operating at low pH. The resulting biooxidation liquors can be treated by a process such as hydrothermal precipitation to produce stable crystalline scorodite and type-2 compounds as was demonstrated by Swash and Monhemius **[22-25]**. However the costs of incorporating an autoclave for the treatment of bioliquors has to be evaluated against alternative processes such as pressure oxidation. Despite all these advances in the treatment of arsenical residues, the long term stability of the residues still remains a question to be resolved. Scorodite may be a long term stable compound because of the known stability of naturally occurring scorodite, however there is no natural analogue of type-2 compound and further tests on its long term stability should be continued.

7.2 Conclusions

7.2.1. A significant improvement in understanding the relationship between mineralogies of different ores and the subsequent speciation of arsenic during bacterial oxidation of the resulting concentrates has been achieved. Furthermore an understanding of the important factors and reactions responsible for the oxidation of arsenic(III) during bacterial leaching has been demonstrated.

7.2.2. The results have shown the importance of the pyrite to arsenopyrite ratio in relation to the oxidation of arsenic(III) during bacterial oxidation. Bacterial oxidation of a concentrate dominated by arsenopyrite showed that 78 % of the solubilised arsenic reported in the bioleaching slurry as arsenic(III). The addition of pyrite to this ore to alter its composition promoted the oxidation of arsenic(III) to arsenic(V). The oxidation of arsenic(III) was found to be catalysed by pyrite surfaces and bacteria in the presence of iron(III). The results have shown that chemical oxidation of arsenic(III) by iron(III) did not occur under the experimental conditions which were used here, however the oxidation of arsenic(III) took place to a significant extent in the presence of pyrite and iron(III) only, in the absence of bacteria.

7.2.3. The presence of bacteria was found to accelerate the oxidation of arsenic(III) and as a result it was concluded that bacteria may be directly involved in the oxidation of arsenic(III) via the pyrite surfaces, in addition to providing clean catalytic pyrite surfaces and regenerating the iron(III). Furthermore a strong dependence of pyrite leaching and arsenic(III) oxidation was demonstrated. Bioleaching conditions which did not favour the leaching of pyrite were also found to result in more arsenic(III) reporting in the bioleaching slurry at the end of the oxidation stages.

7.2.4. The sulphide grade was also found to affect the rate of arsenic(III) oxidation. Pyrite surfaces were found to be the limiting factor on the rate and extent of arsenic(III) oxidation when a low grade concentrate was subjected to bacterial oxidation as was shown by the speciation behaviour of the Akbakai concentrates.

7.2.5. Based on the speciation studies reported in this study, bacterial leaching of pyrite/arsenopyrite concentrates were shown to primarily produce arsenic(III). The primary and secondary processes during bacterial oxidation are best represented by the following equations:

Primary processes

$$2FeS_2 + 7O_2 + 2H_2O \xrightarrow{\text{Bacteria/iron(III)}} 2FeSO_4 + 2H_2SO_4 \qquad (5.5)$$

$$4FeAsS + 11O_2 + 2H_2O \xrightarrow{\text{Bacteria/iron(III)}} 4FeSO_4 + 4HAsO_2 \qquad (5.6)$$

Secondary processes

$$4FeSO_4 + 2H_2SO_4 + O_2 \xrightarrow{\text{Bacteria}} 2Fe_2(SO_4)_3 + 2H_2O \qquad (5.7)$$

$$HAsO_2 + Fe_2(SO_4)_3 + 2H_2O \xrightarrow[\text{Pyrite}]{\text{Bacteria}} H_3AsO_4 + H_2SO_4 + 2FeSO_4 \qquad (5.8)$$

$$2H_3AsO_4 + Fe_2(SO_4)_3 + nH_2O = 2FeAsO_4.nH_2O(s) + 3H_2SO_4 \quad (5.9)$$
(amorphous)

7.2.6. Mineralogical observations showed that gold-bearing arsenopyrite was usually depleted in arsenic with respect to its stoichiometric composition, but there was no correlation between gold and iron content. In pyrite crystals gold was usually associated with areas enriched in arsenic. Microscopic examination of partially bioleached pyrite and arsenopyrite particles revealed pores and dissolution channels on their surfaces. There was preferential oxidation of arsenopyrite, however both minerals were preferentially attacked on sites representing structural imperfections in the crystal lattice. These deviations include contact between zones, inclusions of other minerals or elements, dislocations and cracks introduced during crushing and grinding. The porous structure of pyrite surfaces was compatible with the hypothesis that the bioleaching of pyrite provides clean catalytic surfaces and an increased surface area for the oxidation of arsenic(III) during the bacterial oxidation process.

7.2.7. The environmental stability of bacterial oxidation residues emanating from leaching of pyrite/arsenopyrite was found to be directly related to the mineralogical composition of the feed concentrate, in particular the ratio of pyrite to arsenopyrite and also to the extent of arsenic extraction and oxidation. More pyrite in the concentrates promoted the formation of stable residues because of the complete oxidation of arsenic(III) to arsenic(V) oxidation during bacterial oxidation stage. Partially leached arsenopyrite was found to produce unstable residues due to the oxidised precipitates on the surfaces of the unreacted minerals which were dominated by arsenic(III).

7.2.8. The precipitated compounds were found to be amorphous, however operating at a pH less than 1.3 was found to limit the amount of arsenical precipitates reporting to the solids. Keeping the dissolved arsenic in solution by operating at a lower pH is one of the ways of meeting the environmental standards in the

solid residues from bacterial oxidation processes of arsenical concentrates. The arsenic in solution may be stabilised by other proven methods such as hydrothermal precipitation **[22-25]**.

7.3 Further work

7.3.1 It is possible that the use of different strains of bacteria used in mineral leaching may lead to different rates of arsenic(III) oxidation. A comparative study of the speciation behaviour of arsenical ores using different strains will be a substantial exercise.

7.3.2 The use of pure mixtures of pyrite and arsenopyrite during bacterial oxidation experiments may lead to better characterisation of bacterial oxidation precipitates.

7.3.3 More work is required on the resistance mechanism of bacteria used in mineral leaching towards arsenic species. Genetic engineering may offer some solutions to this problem.

7.3.4 Further work is required to understand the preferential attack of arsenopyrite during bacterial oxidation. The contribution of galvanic mechanisms towards selective leaching of arsenopyrite has to be evaluated.

CHAPTER EIGHT

REFERENCES

1. Fraser, K. S., Walton, R. H. and Wells, J. A. (1991) Processing of refractory gold ores. *Minerals Engineering,* **4** *(7-11),* 1029-1041.

2. Petruck, W. (1989) Recent progress in mineralogical investigations related to gold recovery. *CIM. Bulletin,* **82** *(931),* 37-39.

3. Monhemius, A.J. (1994) The processing of gold ores. Annual Review 1994, *Irish Association for Economic Geology*, 39-46.

4. Pershagen, G. (1983) The epidemiology of human arsenic exposure. *In: Biological and Environmental Effects of Arsenic*, (Ed.) Fowler, B.A., Elsevier Science Publishers B.V. 199-232.

5. Roberts, W.L. Rapp, G.R. Jr. and Weber, J. (1974) *Encyclopedia of minerals*. Van Nostrand, New York.

6. Broadhurst, J.L. (1994) Neutralisation of arsenic bearing BIOX liquors. *Mineral Engineering,* **7**, *(8),* 1029-1038.

7. Olliver, P., Toromanoff, P. and Marion, D. (1990) Gold liberation and environmental aspects of bio-oxidation treatment of refractory gold ores. *In: Gold '90,* Salt Lake City, 477-485.

8. Robins, R.G., Huang, J.C.Y., Nishimura, T. and Khoe, G.H. (1988) The adsorption of arsenate ion by ferric hydroxide. In: *Arsenic Metallurgy, Fundamentals and Applications,* eds. Reddy R.G., Hendrix, J.L. and Queneau P.B., AIME, 99-111.

9. Barter, J. Carter, A.J., Holder, N.H.M, Miller, D.M. and van Aswegen, P.C. (1992) Design and commissioning of a 40 tonne per day flotation concentrate bio-

oxidation treatment plant at the Harbour Lights mine. *Extractive Metallurgy of Gold and Base Metals*, Kalgoorlie, 113-119.

10. van Aswegen, P. C., Marais, H. J. and Haines, A. K. (1991) Design and operation of a commercial biooxidation plant at Fairview. *Northern Mineral Magazine,* **6** *(6),* 1-12.

11. Emett, M.T. and Khoe, G. H. (1993) Environmental stability of arsenical bearing hydrous iron oxide. *Proceedings of EPD Congress 1994*, ed. Warren, G.W., TMS Annual Conference, 153-165.

12. Harris, G.B. and Monette, S. (1988) The stability of arsenic bearing residues. In: *Arsenic Metallurgy, Fundamentals and Applications,* eds. Reddy R.G., Hendrix, J.L. and Queneau P.B., AIME, 469-487.

13. van Aswegan, P. C., and Haines, A. K. (1988) Bacteria enhance gold recovery. *International Mining,* **5** *(5),* 19-23.

14. Stefanakis, M. and Kontopoulos, A. (1988) Production of environmentally acceptable arsenites-arsenates from solid arsenic trioxide. In: *Arsenic Metallurgy, Fundamentals and Applications,* eds. Reddy R.G., Hendrix, J.L. and Queneau P.B., AIME, 287-303.

15. Barrett, J. Hughes, M.N., Islam, A.N. and Simons, C. (1991) The nature and stability of precipitated solids from arsenopyrite bio-oxidation effluents. *Proceedings of the Randol Gold Forum,* Cairns, 179-183.

16. Langhans, D., Lord, A., Lampshire, D., Burbank, A. and Baglin, E. (1995) Biooxidation of an arsenic bearing refractory gold ore. *Minerals Engineering*, **8** (1/2), 147-158.

17. U.S. EPA, (1986) *Toxicity characteristic leaching procedure*. US Register, **51**, Appendix I, 216.

18. U.S. EPA, (1980) *Characteristic of EP toxicity*. US Federal Register, **45**, paragraph 261.24, 98.

19. Adam, K., Komnitsas, C., Papassiopi, N.L., Kontopoulos, A., Pooley, F.D. and Tidy, N.P. (1994) Stability of arsenical bacterial oxidation products. *Hydrometallurgy '94 Conference,* Cambridge, IMM, 291-311.

20. Olliver, P. and Morin, D. (1990) Bioleaching of sulfide concentrates and ores: study of refractory gold and non-ferrous base metals. In: *Randol Gold Forum 90*, Squaw Valley, 93-99.

21. Hackl, R.P. (1990) Stability of arsenical tailings from the Salmita Bioleach Pilot Project. *Randol '90*, 101-106.

22. Swash, P.M. (1996) The hydrothermal precipitation of arsenical solids in the Ca-Fe-AsO_4-SO_4 system at elevated temperatures. *Ph.D. Thesis*, Imperial College, University of London.

23. Swash, P. and Monhemius, A.J. (1994) Hydrothermal precipitation from aqueous solutions containing iron(III), arsenate and sulphate. *Hydrometallurgy '94*, IMM, Cambridge, 178-190.

24. Swash, P. and Monhemius, A.J. (1995) Synthesis, characterisation and solubility testing of solids in the Ca-Fe-AsO_4 system. *Conference on Mining and the Environment*, Sudbury, Ontario, 17-28.

25. Swash, P. and Monhemius, A.J. (1995) The disposal of arsenical wastes: technologies and environmental considerations. *International Minerals and Metals Technology*, 121-125.

26. Robins, R.G. and Jayaweera, L.D. (1992) Arsenic in gold processing. *Mineral Processing and Extractive Metallurgy Review,* **9**, 255-275.

27. Harris, G.B. and Monette, S. (1989)The disposal of arsenical solids. *Productivity and Technology in Metallurgical Industries*, TMS-AIME Joint Symposium, 1-18.

28. Cabri, L. J., Chryssoulis, S. L., De Villiers, J. P. R., Laflamme, J. H. G. and Buseck, P. R. (1989)The nature of "invisible" gold in arsenopyrite. *Canadian Mineralogist,* **27**, 353-362.

29. Kingston, G.A. (1992) Mineralogy in evaluation of ore deposits. *The Geological Society,* 47-59.

30. JHA M. C. (1987) Refractoriness of certain gold ores to cyanidation: probable causes and possible solutions. *Mineral Processing and Extractive Metallurgy Review,* **2** *(4),*331-352.

31. Chryssoulis, S.L. and Cabri, L.J. (1990) Significance of gold mineralogical balances in mineral processing. *Trans. Inst. Min. Metall.*, **99**, C1-C10.

32. Gasparrini, C. (1983) The mineralogy of gold and it's significance in metal extraction. *C.I.M. Bulletin,* **76**, *(851),* 144-153.

33. Henley, K.J. (1983) A combined mineralogical/metallurgical approach to determining the nature and location of gold in ores and mill products. *Minerals Engineering,* **2** *(4),* 459-470.

34. Pooley, F.D. (1987) Use of bacteria to enhance recovery of gold from refractory ores. *MINPREP 87, International Symposium Innovative Plant and Processes for Mineral Engineering*, 23-41.

35. Swash, P.M. (1988) A mineralogical investigation of refractory gold ores and their beneficiation, with special reference to arsenical ores. *Journal of the South African Inst. Min. Metall.*, **88** *(5),* 173-180.

36. Adam, K., Prevosteau, J. M., Kontopoulos, A., Stefanakis, M. and Errington, M. (1990) Applications of process mineralogy on the treatment of Olympias pyrite concentrate. In: *Gold '90,* ed. Hausen, D. M., Halbe, D. N., Petersen, E. U. And Tafuri, W. J., Society for Mining, Metallurgy and Exploration, 341-351.

37. Cathelinau, H., Boiron, M.C., Holliger, Ph. and Marion, Ph. (1988) Gold-rich arsenopyrite: crystal chemistry, gold location and state, physical and chemical conditions of crystallisation. *Bicentennial Gold, Extended Abstracts, Oral Programme,* 235-240.

38. Marion, P., Holliger, P., Boiron, M.C. ,Cathelineau, M., and Wagner, F.E. (1991) New improvement in the characterisation of refractory gold in pyrite: An electron microprobe, Mössbauer spectrometry and ion probe study. *Brazil Gold '91,* 389-395.

39. Wells, J. D. and Mullens, T. E. (1973) Gold-bearing arsenian pyrite determined by Microprobe analysis, Cortez and Carlin gold mines, Nevada. *Economic Geology,* **89**, 187-201.

40. Henley, K.J. (1975) Gold ore mineralogy and its relation to metallurgical treatment. *Mineral Science Engineering,* **7**, (4), 289-312.

41. Feather, C.E. and Koen, G.M. (1973) The significance of mineralogical and surface characteristics of gold grains in the recovery process. *Journal of the South African Institution of Mining and Metallurgy.* **73** *(7),* 223-234.

42. Harris, D. C. (1990) The mineralogy of gold and it's relevance to gold recoveries. *Mineral. Deposita* **25** *[suppl],* S3-S7.

43. Lorenzen, L. and Van Deventer, J. S. J. (1992) The mineralogical identification of refractory gold ores by means of selective decomposition of minerals. *Extractive Metallurgy of Gold and Base Metals*, Kalgoorlie, 171-176.

44. Lorenzen, L. and van Deventer, J.S.J. (1992) The mechanism of leaching of gold from refractory ores. *Minerals Engineering*, **5** (10-12), 1377-1387.

45. Lorenzen, L. and van Deventer, J.S.J. (1992) Electrochemical interaction between gold and its associated minerals during cyanidation. *Hydrometallurgy*, **30**, 177-194.

46. Henley, K. J. (1992) A review of recent developments in the process mineralogy of gold. *Extractive Metallurgy of Gold and Base Metals,* Kalgoorlie, 177-194.

47. Jones, M.P. and Gavrilovic, J. (1968) Automatic searching unit for quantitative location of rare phases by electron probe X-ray microanalysis. *Trans. Inst. Min. Metall.*, **77**, B137-B143.

48. Jones, M.P. and Cheung, T.S. (1988) Automatic method for finding gold grains in ores and mill products. *In: Asian Mining '88,* 73-81.

49. McDonald, K. J. and Sparrow, G. J. (1992) Automated location of gold in samples from Australian Concentrators. *Extractive Metallurgy of Gold and Base Metals,* Kalgoorlie, 195-201.

50. Corrans, I. J. and Angove, J. E. (1991) Ultrafine milling for the recovery of refractory gold. *Mineral Engineering,* **4,** 763-776.

51. Reed, S.J.B. (1990) Recent developments in geochemical microanalysis. *Chemical Geology,* **83**, 1-9.

52. Freeman, H.D., Hartley, J.N. and Wick, O.J. (1981) Scanning Electron Microscope and Microprobe analysis of refractory gold ores and process implications of the analysis. In: *Process Mineralogy in Metal Extraction,* AIME, Mineral Exploration and Energy Materials, 305-323.

53. Cabri, L. J., Campbell, J. L., Laflamme, J. H. G., Maxwell, R. G. L., Leigh, R. G. and Scott, J. D. (1985) Proton-Microprobe analysis of trace elements in sulphides from some massive sulphides deposits. *Canadian Mineralogist,* **23**, 133-148.

54. Graham, J., Just, J. and Nguyen, G. (1988) Electron beam techniques in gold mineralogy: exploration and processing. In: *Randol Perth Gold International Conference,* 137-140.

55. Gasparrini, C. (1980) The role of ore microscope in the mining industry. *CMI. Bulletin,* **73** *(815),* 73-85.

56. Johanson, Bo. and Kojonen, K. (1991)Ore mineralogy of gold occurrences in the late Achean Ilomantsi greenstone belt, eastern Finland. *Brazil Gold '91,*183-186.

57. Arrowsmith, P. (1987) Laser ablation of solids for elemental analysis by inductively coupled plasma mass spectrometry. *Analytical Chemistry,* **59**, 1437-1444.

58. Coles, B.J., Gleeson, S.A., Wilkinson, J.J. and Ramsey, M.H. (1995) Improved detection limits for transient signal analysis of fluid inclusions by inductively coupled plasma atomic emission spectrometry using correlated background correction. *Analyst,* **120**, 1421-1425.

59. Ramsey, M.H., Coles, B.J. and Wilkinson, J.J. (1992) Single fluid inclusion analysis by laser ablation inductively coupled plasma atomic emission

spectrometry: Quantification and validation. *Journal of Analytical Atomic Spectrometry,* **7**, 587-593.

60. Rankin, A.H., Ramsey, M.H., Coles, B., Van Langevelde, F. and Thomas, C.R. (1992) The composition of hypersaline, iron-rich granitic fluids based on laser-ICP and Synchrotron-XRF microprobe analysis of individual fluid inclusions in topaz, Mole granite, eastern Australia. *Geochemica et Cosmochimica Acta,* **56**, 67-79.

61. Musket, J.L. (1994) A mineralogical study of the gold mineralisation of the Lady Lina property, Gwanda greenstone belt, Zimbabwe. *Msc Thesis*. Department of Geology, Imperial College, University of London.

62. Middleton, A. (1989) An assessment of the potential of laser ablation for gold and trace elements analysis of pyrite. *Msc Thesis*, Department of Geology, Imperial College, University of London.

63. Wagner, F.E. Marion, Ph. and Regnard, J.R. (1986) Mössbauer study of the chemical state of gold in ores. *In: Gold 100, Proceedings of the International Conference on Gold,* **2**, SAIMM, 435-443.

64. Shuey, R.T. (1975) Semiconducting ore minerals. *Developments in Economic Geology*, **4**, 205-311.

65. Smith, F.G. (1942) Variation in the properties of pyrite. *American Mineralogist*, **27**, 1-19.

66. Kullerud, G. and Yoder, H.S. (1959) Pyrite stability relation in the Fe-S system. *Economic Geology*, **54**, 533-572.

67. Fleischer, M. (1955) Minor elements in some sulphide minerals. *Economic Geology*, 50th Anniversary Vol., 970-1024.

68. Beurger, M.J. (1936) The symmetry and crystal structure of the minerals of the arsenopyrite group. *Zeitschr. Kristallographie*, **95**, 83-113.

69. Hurlbut, C.S. Jr., and Klein, C. (1977) *Manual of Mineralogy* (after James D. Dana) 19th Edition, John Wiley & Sons, 238.

70. Kretschmar, U. and Scott, D.S. (1976) Phase relations involving arsenopyrite in the system Fe-As-S and their application. *Canadian Mineralogist*, **14**, 364-386.

71. Clark, A.C. (1960) The Fe-As-S system: phase relations and applications. *Economic Geology*, **55** (7), 1346-1363.

72. Genkin, A.D., Cabri, L.J., Bortnikov, N.S., McMahon, G., Stanley, C.J., Wagner, F.E., Friedl, J., Safonov, Y.G. and Gamyanin, G.N. (1997) Geology and

characteristics of gold mineralization in four Siberian gold deposits, Russia. *Global Exploration of Heap Leachable Gold Deposits* ed. Hausen, D.M., The Minerals, Metals & Materials Society, 129-140.

73. Henley, K.J. (1988) The metallurgical aspect of gold ore mineralogy, or 'what every exploration Geologist should know about gold ore treatment'. *Bicentennial Gold 88,* Melbourne, 533-535.

74. Henley, K.J. and Steveson, B.G. (1979) Determination of distribution of gold and silver in ores and mill products. *Trans. Inst. Min. Metall.,* C215-C219.

75. Komnitsas, C. and Pooley, F.D. (1989) Mineralogical characteristics and treatment of refractory gold ores. *Minerals Engineering,* **2** *(4),* 449-457.

76. Kontopoulos, A. and Stefanakis, M. (1989) Process selection for the Olympias refractory concentrate. *In: Precious metals '89,* Minerals, Metals and Materials Society, 179-209.

77. Dew, D., Miller, D.M. and van Aswegen, P.C. (1993) GENMIN's commercialisation of bacterial oxidation process for the treatment of refractory gold concentrates. In: *Randol Gold Forum Beaver Creek*, 229-237.

78. Emmett, R. C., Klepper, R. P., Sitarski, J. T. and Luinstra, L. W. (1990) Operation of a bio-oxidation pilot plant on a refractory gold concentrate. *In: Gold '90,* Salt Lake City, 487-492.

79. Holmes, D. S. (1988) Biotechnology in the mining and metal processing industries: challenges and opportunities. *Minerals and Metallurgical Processing*, 49-56.

80. Griffin, E. A. and Luinstra, L. (1990) Bioreactor scale-up: practical considerations for biologically assisted gold recovery. *In: Biohydrometallurgy '89.* ed. Salley, R. G. L. and Wichlacz, P. L. Canmet, Ottawa, 221-230.

81. Morin, D. and Ollivier, P. (1990) Pilot practice of continuous biooxidation of a gold refractory sulphide concentrate with a high As content. *In: Biohydrometallurgy '89,* ed. Salley, R. G. L. and Wichlacz, P. L. Canmet, Ottawa, 563-576.

82. Spencer, P. A., Budden, J. R. and Rhodes, M. K. (1991) Bacterial oxidation technology-a viable process for refractory gold ores and base metal recovery. *Mineral Engineering,* **4** *(7-11),* 1143-1152.

83. Budden, J. R. and Bunyard, M. (1994) Pilot plant testwork and engineering design of the BacTech bacterial oxidation plant at the Youanmi Mine. *Biomine '94*, Australian Mineral Foundation, 4.1-4.8.

84. Gormely, L. S. and Branion, R. M. R. (1990) Engineering design of microbiological leaching reactors. *In: Biohydrometallurgy '89*, ed. Salley, R. G. L. and Wichlacz, P. L., 499-518.

85. Nicholson, M. H., Smith, G. R., Stewart, R. J., Kock, F. W. and Marais, H. J. (1994) Design and commissioning of the Ashanti's Sansu BIOX plant. *Biomine '94*, Australian Mineral Foundation, 2.1-2.8.

86. Haines, A. K. and van Aswegan, P. C. (1990) Process and engineering challenges in the treatment of refractory gold ores. *International Deep Mining Conference: Innovations in Metallurgical Plants,* Johannesberg, SAIMM, 103-110.

87. McCready, R. G. L. (1988) Progress in the bacterial leaching of metals in Canada. In: *Biohydrometallurgy Proceedings of the International Symposium Warwick 1987*, ed. Norris, R. P. and Kelly, D. P., 177-195.

88. Kelly, D.P., Norris, P.R. and Brierley, C.L. (1979) Microbiological methods for the extraction and recovery of metals. *Microbiology Technology: Current State, Future Prospects*. Eds. Bull, A.T., Ellwood, D.C. and Ratledge, C., Academic Press, London, S.G.M. Symposium 29, 267-308.

89. Kulpa, C. F., Mjoli, N. and Roskey, M. T. (1986) Comparison of iron and sulphur oxidation in *Thiobacillus ferrooxidans*: Inhibition of iron oxidation by growth on sulphur. *Biotechnology and Bioengineering Symposium, (16),* 289-295.

90. Spencer, P. A., Budden, J.R. and Barrett, J. (1991) Pilot plant bio-oxidation of gold bearing arsenopyrite concentrates. *Trans. Inst. Min. Metall.,* ***100****,* C21-C24.

91. Rawling, D. E. and Woods, D. R. (1995) Development of improved biomining bacteria. *Bioextraction and Biodeterioration of Metals,* 63-84.

92. Helle, U. and Onken, U. (1988) Continuous bacterial leaching of a pyritic flotation concentrate by mixed cultures. In: *Biohydrometallurgy Proceeding of the International Symposium Warwick 1987,* ed. Norris, D. P. and Kelly, R. P., 61-75.

93. Dew, D.W. (1995) Comparison of performance for continuous bio-oxidation of refractory gold ore flotation concentrates. In: *Biohydrometallurgy Processing*, University of Chile, eds. Vargas, T., Jerez, J.V. and Toledo, H., 239-251.

94. Le Roux, N.W., Wakerley, D.S. and Perry, V.F. (1978) Leaching of minerals using other bacteria other than T*hiobacilli. In: Metallurgical Applications of Bacterial Leaching and Related Microbiological Phenomena*, eds. Murr, L.E., Torma, A.E. and Brierley, J.A. London, New York: Academic Press, 167-191.

95. Brierley, C.L. (1978) Bacterial leaching. CRC *Critical Reviews of Microbiology,* **5**.

96. Norris, P. R. (1990) Factors affecting bacterial mineral oxidation: the example of carbon dioxide in the context of bacteria diversity. *In: Biohydrometallurgy '89,* ed. Salley, R. G. L. and Wichlacz, P. L., Canmet, Ottawa, 3- 14.

97. Jordan, M.A., McGinnes and Phillips, C.V. (1996) Acidophilic bacteria-their potential mining and environment applications. *Mineral Engineering,* **9**, *(2),* 169-181.

98. Brierley, J.A. and Lockwood, S.J. (1977) The occurrence of a thermophilic iron oxidising bacteria in a copper leaching system. *FEMS Microbiological Letters,* **2**, 163-165.

99. Ewart, D.K. (1990) Studies on a moderately thermophilic mixed culture of bacteria and its application to the biooxidation of gold-bearing minerals. *Ph.D. Thesis*. King's College, University of London.

100. Karaivako, G.I., Golovacheva, R.S., Tzaplina, T.A. and Vartanjan, N.S. (1988) Thermophilic bacteria of the genus *Sulfobacillus*. In: *Biohydrometallurgy Proceeding of the International Symposium Warwick 1987,* eds. Norris, P.R and Kelly, D.P. Science and Technology Letters, Kew, Surrey, 29-41.

101. Brierley, J.A. and Brierley, C.L. (1978) Microbial leaching of copper at ambient and elevated temperatures. *In: Metallurgical Applications of Bacterial Leaching and Related Microbiological Phenomena*, eds. Murr, L.E., Torma, A.E. and Brierley, J.A. London, New York: Academic Press, 477-490.

102. Lawrence, R. W. and Marchant, P. B. (1988) Comparison of Mesophilic and Thermophilic oxidation systems for the treatment of refractory gold ores and concentrates. In: *Biohydrometallurgy Proceedings of the International Symposium Warwick 1987,* ed. Norris, D. P. and Kelly, R. P., 359-374.

103. Barrett, J. Hughes, M.N., Karaivaiko, G.I. and Spencer, P.A. (1993*) Metal Extraction by Bacterial Oxidation of Minerals*. Ellis Horwood.

104. Barrett, J. (1993) Key stages in the bacteria oxidation mechanism of pyrite and arsenopyrite. *In: Randol Gold Forum Beaver Creek* , 239-242.

105. Barrett, J., Ewart, D. K., Hughes, M. N., Nobar, A. M. and Poole, R. K. (1990) The oxidation of arsenic in arsenopyrite: the toxicity of As(III) to a moderately thermophilic mixed culture. In*: Biohydrometallurgy '89,* ed Salley, R. G. L. and Wichlacz, P. L., Canmet, Ottawa, 49-57.

106. Yongzhu, Z., Yiyuan, L., Tiancong, Z. And Rongqing, Q. (1992) Bio-oxidation of two arsenical refractory gold concentrates and gold cyanidation. *Extractive Metallurgy of Gold and Base Metals,* Kalgoolie, 345-348.

107. Khoe, G.H. and Robins, R.G. (1988) *Journal of Chemical Society Dalton Trans.* 2015.

108. Latimer, W.L. (1955) *Oxidation Potentials*. Prentice Hall.

109. Cservenyak, I. (1994) Electrochemical reduction of pyrite in acidic aqueous electrolytes. Ph.D. Thesis, Imperial College, University of London.

110. Vink, B.W. (1996) Stability relations of antimony and arsenic compounds in the light of revised and extended E_h-pH diagrams. *Chemical Geology,* **130**, 21-30.

111. Komnitsas, C. And Pooley, F. D. (1994) Oxidation of arsenopyrite in bacterial ferric solution. *Hydrometallurgy '94*, IMM, Cambridge, 361-367.

112. Shrestha, G. N. (1988) Microbial pretreatment of refractory gold ores. *Asian Mining '88'*, London, IMM, 179-187.

113. Hiskey, J.B. and Sachez, V. (1988) An electrochemical study of the surface oxidation of arsenopyrite in alkaline media. In: *Arsenic Metallurgy, Fundamentals and Applications*, Reddy, R.G., Hendrix, J.L. and Queneau, P.B. (eds), AIME, 59-75.

114. Kondos, P. and Demopoulos, G.P. (1987) Arsenic speciation in oxidative acid leaching systems. In: *Separation Processes in Hydrometallurgy* (ed) Davies, D.A., Ellis Horwood.

115. Bhatti, T. M., Bigham, J. M., Carlson, L. and Tuovinen, O. L. (1993) Mineral products of pyhrrotite oxidation by *Thiobacillus ferrooxidans. Applied and Environmental Microbiology,* **59** *(6),* 1984-1990.

116. Iglesias, N. and Carranza, F. (1994) Refractory gold bearing ores: a review of treatment methods and recent advances in biotechnological techniques. *Hydrometallurgy,* **34** *(3),* 383-395.

117. Baldi, F., Clark, T., Pollack, S. S. and Olson, G. J. (1992) Leaching of pyrites of various reactivities by *Thiobacillus ferrooxidans. Applied and Environmental Microbiology,* **58** *(6),* 1853-1856.

118. Marais, H. J. (1990) Bacterial oxidation of arseno-pyritic refractory gold ore: Barberton Mines' answer to pollution. *In: International Deep Mining Conference,* Johannesberg, SAIMM,**1** *(S10),* 1990, 125-129.

119. Morin, D. (1995) Bacterial leaching of refractory sulphide gold ores. *Bioextraction and Biodeterioration of Metals,* 25-62.

120. Murthy, D. S. R. (1990) Microbial enhanced thiourea leaching of gold and silver from lead-zinc sulphide tailings. *Hydrometallurgy,* **25**, 51-60.

121. Pooley, F. D., Shrestha, G. N., Errington, M. T. and Gibbs, H. E. (1987) The separate generator concept applied to bacterial leaching of auriferous minerals. *Separation Processes in Hydrometallurgy,* ed. Davies, G. A., 60-67.

122. Veglio, F., Nardini, A., Toro, L., Ulbaldini, S. and Abbruzzese, C. (1995) Process development for the bio-oxidation of pyrrhotite for gold recovery by cyanidation. In: *Biohydrometallurgy Processing*, University of Chile, eds. Vargas, T., Jerez, J.V. and Toledo, H., 369-378.

123. Acevedo,F., Cacciuttolo, M. A. and Gentina, J. C. (1988) Comparative performance of stirred and pachuca tanks in the bioleaching of a copper concentrate. In: *Biohydrometallurgy Proceeding of the International Symposium Warwick 1987,* ed. Norris, D. P. and Kelly, R. P., 385-394.

124. Hoffman, W. , Batterham, R. and Conochie, D. (1993) A novel , low energy bioreactor for refractory gold ores. *In: Randol Gold Forum Beaver Creek,* 243-245.

125. Rossi, G. (1990) *Biohydrometallurgy*. McGraw-Hill.

126. Bailey, A. D. and Hanford, G. S. (1994) Oxygen mass transfer limitation of batch bio-oxidation at high solids concentration. *Minerals Engineering,* **7** *(2-3),* 293-303.

127. Liu, M. S., Branion, R. M. R. and Duncan, D. W. (1988) Oxygen transfer to *Thiobacillus* cultures. In: *Biohydrometallurgy Proceedings of the International Symposium Warwick 1987,* ed. Norris, R. P. and Kelly, D. P., 375-384.

128. Bailey, J.E. and Ollis, D.F. (1987) *Biochemical Engineering Fundamentals*. 2nd edition, McGraw-Hill, Singapore.

129. Braddock, J. F., Loung, H. V. and Brown, E. J. (1984) Growth kinetics of *Thiobacillus ferrooxidans* isolated from Arsenic Mine Drainage. *Applied and Environmental Microbiology,* **48** *(1),* 48-55.

130. Pronk, J. T., Liem, K., Bos, P. and Kuenen, J. G. (1991) Energy transduction by anaerobic ferric iron respiration in *Thiobacillus ferrooxidans*. *Applied and Environmental Microbiology,* **57** *(7),* 2063-2068.

131. Silverman, M. P. and Lundgren, D. G. (1959) Studies on the chemoautotrophic iron bacterium *Thiobacillus ferrooxidans*. 1. An improved medium and harvesting procedure for securing high cell yields. *Journal of Bacteriology,* **77**, 642-647.

132. Sugio, T., White, J. L., Shute, E., Choate, D. and Blake, R. (1992) Existence of a hydrogen sulphide: Ferric ion oxidoreductase in iron-oxidising bacteria. *Applied and Environmental Microbiology,* **58** *(1),* 431-433.

133. Tuovinen, O.H. and Kelly, D.P. (1973) Studies on the growth of *Thiobacillus ferrooxidans*. I. Use of membrane filters and ferrous iron agar to determine viable numbers, and comparison with $^{14}CO_2$ fixation and iron oxidation as measures of growth. *Archiv fur Mikrobiologie,* **88**, 285-298.

134. Monroy-Fernandez, M.G., Mustin, C., de Donato, P., Berthelin, J. and Marion, P. (1995) Bacterial behaviour and evolution of surface oxidised phases during arsenopyrite oxidation *Thiobacillus ferrooxidans*. In: *Biohydrometallurgy Processing*, University of Chile, eds. Vargas, T., Jerez, J.V. and Toledo, H., 57-66.

135. Natarajan, K. A. (1988) Electrochemical aspects of bioleaching multisulphide minerals. *Minerals and Metallurgical Processing*, 61-65.

136. Atkins, P.W. (1982) *Physical Chemistry*. 2nd edn, 355.

137. Barrett, J. and Hughes M.N. (1993) The mechanism of bacterial oxidation of arsenopyrite-pyrite mixtures: the identification of plant control parameters. *Minerals Engineering*, **6** (8-10), 969-975.

138. Ingledew, W.J. (1986) Ferrous iron oxidation by *Thiobacillus ferrooxidans*. *Biotechnology and Bioengineering Symposium, (16),* 23-33.

139. Panin, V.V., Karavaiko, G.I. and Pol'kin, S.I. (1985) Mechanism and kinetics of bacterial oxidation of sulphide minerals. *Biotechnology of Metals*, Karavaiko, G.I. and Groudev, S.N. (eds), Centre for International Projects, Moscow, 197-215.

140. Taxiarchou, M., Adam, K. and Kontopoulos, A. (1994) Bacterial oxidation conditions for gold extraction from Olympias refractory arsenical pyrite. *Hydrometallurgy*, **36**, 169-185.

141. Adam, K., Stefanakis, M. and Kontopoulos, A. (1989) Bacterial oxidation of the Olympias arsenical pyrite. In: *Biotechnology in Mineral and Metal Processing*, SME, 131-138.

142. Demopoulos, G.P. and Papangelakis, V.G. (1989) Recent advances in refractory gold processing. *CMI Bulletin*, **82** (931), 85-91.

143. Komnitsas, K., Xenidis, A. and Adam, K. (1995) Oxidation of pyrite and arsenopyrite in sulphidic spoils in Lavrion. *Minerals Engineering*, **8** (12), 1443-1454.

144. Komnitsas, C. and Pooley, F. D. (1990) Bacterial oxidation of an arsenical gold sulphide concentrate from Olympias , Greece. *Minerals Engineering,* **3** *(3/4),* 295-306.

145. Lindström, E.B. and Sehlin, H.M. (1989) Toxicity of arsenic compounds to the sulphur-dependent archaebacterium *Sulfolobus*. *Biohydrometallurgy-89*, Jackson Hall, July 1989, Salley, J., McCready, R.G.L and Wilchlacz, P.L. (eds), 59.

146. Kelly, D.P. and Jones, C.A. (1978) Factors affecting metabolism and ferrous iron oxidation in suspensions and batch cultures of *Thiobacillus ferrooxidans*: Relevance to ferric iron leach solutions regeneration. In: *Metallurgical Applications of Bacterial Leaching and Related Microbial Phenomena,* Academic Press, New York, 11-44.

147. Shrestha, G.N. (1983) Practical applications of bacterial leaching of mineral sulphides. *Ph.D. Thesis*, University of Wales.

148. Sand, W., Gehrke, T., Jozsa, P.G. and Schippers, A. (1997) Novel mechanism for bioleaching of metal sulphides. *International Biohydrometallurgy Symposium IBS97-Biomine 97*, Australian Mineral Foundation, QP2.1-QP2.10.

149. Norris, R.P. and Kelley, D.P. (1978) Dissolution of pyrite (FeS_2) by pure and mixed cultures of some acidophilic bacteria. *FEMS Microbiological Letters,* **4**, 143-146.

150. Rosen, B.P., Weigel, U., Karkaria, C. and Gangola, P. (1988) Molecular characterisation of an anion pump. *Journal of Biological Chemistry,* **263**, 3067-3070.

151. Silver, S. et al. (1981) Inducible plasmid-determined resistance to arsenate, arsenite, and antimony(III) in Escherichia coli and Staphyococcus aureus. *Journal of Bacteriology,* **146**, *(3),* 983-996.

152. Silver, S., Nucifora, G., Chu, L. and Misra, T.K. (1989) Bacterial resistance ATPases: primary pumps for exporting toxic cations and anions. *Trends in Biochemical Science,* **14**, 76-80.

153. Trevors, J.T., Oddie, K.M. and Belliveau, B.H. (1985) Metal resistance in bacteria. *FEMS Microbiology Reviews*, **32**, 39-54.

154. Angle, J.S. and Chaney, R.L. (1989) Cadmium resistance screening in nitrilotriacetate-buffered minimal media. *Applied Environmental Microbiology*, **55** (8) 2101-2104.

155. Sehlin, M.H. and Lindsrom, E.B. Oxidation and reduction of arsenic by *Sulfolobus acidocaldarius* strain BC. *FEMS Microbiology Letters*, **93**, 87-92.

156. Barrett, J. Ewart, D.K., Hughes, M.N. and Poole, R.K. (1992) Chemical and biological pathways in bacterial oxidation of arsenopyrite. *FEMS Microbiology Reviews,* **11**, 57-62.

157. Breed, A.W., Glatz, A., Hansford, G.S. and Harrison, S.T.L. (1996) The effect of As(III) and As(V) on the batch bioleaching of a pyrite-arsenopyrite concentrate. *Minerals Engineering*, **9** (12), 1235-1252.

158. Tuvionen, O.H., Niemela, S.I. and Gyllenberg, H.G. (1971) Tolerance of Thiobacillus ferrooxidans to some metals. *Antonie van Leeuwenhoek*, **37**, 489-496.

159. Coddington, K. (1986) A review of arsenicals in biology. *Toxicological and Environmental Chemistry*, **11**, 281.

160. Aposhian, H.V. and Aposhian, M.M. (1989) Newer developments in arsenic toxicity. *Journal of the American College of Toxicology*, **8** (7), 1297.

161. Silver, S. and Nakahara, H. (1983) Bacterial resistance to arsenical compounds. *Arsenic: Industrial Biomedical Environmental Perspectives*, Lederer, W.H. and Fensterheim, R.J. (eds), Van Nostrand Reinhold, New York, 190.

162. Cullen, W.R. and Reimer, K.J. (1989) Arsenic speciation in the environment. *Chemical Reviews*, **89** (4), 713.

163. Willsky, G.R. and Malamy, M.H. (1980) Effect of arsenate on inorganic phosphate transport in *Escherichia coli. Journal of Bacteriology*, **144** (1), 366-374.

164. Breed, A.W., Harrison, S.T.L. and Hansford G.S. (1997) The bioleaching of a pyrite-arsenopyrite flotation concentrate in a continuous bioleaching mini-plant. Steady-state operation and behaviour during periods without aeration and agitation. *International Biohydrometallurgy Symposium IBS97-Biomine 97*, Australian Mineral Foundation, M8.3.1-M8.3.10.

165. Ahohen, I. and Tuovenon, O. H. (1990) Catalytic effect of silver in microbiological of finely ground chalcopyrite-containing ore material in shaking flasks. *Hydrometallurgy,* **24**, 219-236.

166. Ballester, A., Gonzalez, F., Balaquez, M. L., Gomez, C. and Mier, J.L. (1992) The use of catalytic ions in bioleaching. *Hydrometallurgy,* **29**, 145-160.

167. Mier, J.L., Ballester, A., Blazquez, M. L., Gonzalez, F. and Munoz, J. A. (1995) Influence of metallic ions in the bioleaching of chalcopyrite by *Sulfolobus BC*: Experiments using pneumatically stirred reactors and massive samples. *Minerals Engineering,* **8** *(9),* 949-965.

168. Wakao, N., Koyatsu, H., Komai, Y., Shimokawara, H., Sakurai, Y. and Shiota, H. (1988) Microbial oxidation of arsenite and occurrence of arsenite-oxidising bacteria in acid mine water from a sulphur-pyrite mine. *Geomicrobiology Journal*, **6**, 11-24.

169. Phillips, S.E. and Taylor, M.L. (1976) Oxidation of arsenite to arsenate by *Alcaligenes faecalis*. *Applied and Environmental Microbiology*, **32** (3), 392-399.

170. Lindström, E.B., Gunneriusson, E. and Tuvinen, O.H. (1992) Bacterial oxidation of refractory sulphide ores for gold recovery. *Critical Reviews in Biotechnology*, **12** (1/2), 133.

171. Nicolau, C. and Raimond, J. (1983)Procedure for the enrichment the resistance to arsenite and arsenate of Thiobacillus ferrooxidans. *S. African Patent No. 833709.* as cited by Breed et al. (1996) The effect of As(III) and As(V) on the batch bioleaching of a pyrite-arsenopyrite concentrate. *Minerals Engineering*, **9** (12), 1235-1252.

172. Attia, Y. A. and Elzeky, M. (1991) Effect of bacteria adaptation and solution replacement on bioleaching of sulphidic gold ores. *Minerals and Metallurgical Processing, **8** (3),* 122-127.

173. Spencer, P. A., Budden, J. R. and Sneyd, R. (1990) Use of a moderately thermophilic culture for the treatment of refractory arsenopyrite concentrate. In: *Biohydrometallurgy '89,* ed. Salley, R. G. L. and Wichlacz, P. L., Canmet, Ottawa, 231-242.

174a. Vogel, A.I. (1989) *Vogel's Textbook of Quantitative Chemical Analysis.* 5th edition, Longman Scientific and Technical.

174b. Bond, A.M. (1980) *Modern Polarographic Methods in Analytical Chemistry.* Marcel Dekker Inc., New York.

175. Model 384 Polarographic analyzer operating and service manual (1981), *EG & G Applied Research*, USA.

176. Buchholz, P., Friedrich, G. and Herzig, P. (1990) Gold-antimony mineralisation in the Zimbabwe craton: the Indarama mine at Kwekwe and the Belingwe Star mine at Mberengwa, 345-376.

177. Foster, R.P., Fisher, N.J. Porter, C.W. Fabiani, W.M.B. and Carter, A.H.C. (1991) The tectonic and magmatic of Archean lode-gold mineralization in the Midlands greenstone belt, Zimbabwe. *Brazil Gold '91*, 359-366.

178. Buchanan, D.L. *Private communication.*

179. Nicolaou, M. and Kokonis, D. (1980) Geology and development of the Olympias mine, Eastern Chalkidiki, Macedonia, Greece. *In: Complex Sulphide Ores*, ed. Jones, M.J., IMM Conference Proceedings, 260-270.

180. Wiggert, B.S.A., Brink, W.C.J. and Vorster, M.A. (1986) The Fairview gold mine, Barberton greenstone belt. *Mineral Deposits of Southern Africa*, Geol. Soc. S.Afr., Johannesburg, 170-178.

181. Claassen, R. (1991) The effect of mineralogy on the bacterial oxidation of refractory gold-bearing sulphides from a Berberton deposit. *Bacterial Oxidation Colloquium,* SAIMM, 1-19.

182. Aylmore, M.G. and Graham, J. (1992) A mineralogical approach to auriferous arsenopyrite. *Extractive Metallurgy of Gold and Base Metals*, Kalgoorlie, 203-210.

183. Robinson, P.C. (1983) Mineralogy and treatment of refractory gold from the Porgera deposit, Papua New Guinea. *Trans. Inst. Min. Metall.*, **92**, C83-C89.

184. Castroviejo, R. (1990) Gold ores related to shear zones, West Santa Comba-Fervenza area (Galicia, NW Spain): A mineralogical study. *Mineralium Deposita*, **25** [Suppl], S42-S52.

185. Hausen, D.M. (1981) Process mineralogy of auriferous pyritic ores. *Process Mineralogy in Metal Extraction,* AIME, Mineral Exploration and Energy Materials, 271-289.

186. Mandl, M., Matulovà, P. and Docekalova, H. (1992) Migration of arsenic(III) during bacterial oxidation of arsenopyrite in chalcopyrite concentrate by *Thiobacillus ferrooxidans*. *Applied Microbiology Biotechnology*, **38**, 429-431.

187. Collinet, M.N. and Morin, D. (1990) Characterisation of arsenopyrite oxidising *Thiobacillus*. Tolerance to arsenite, arsenate, ferrous and ferric iron. *Antonie van Leeuwenhoek*, **57**, 237-244.

188. Komnitsas, C and Pooley, F. D. (1994) Bacterial oxidation of an auroferrous arsenical concentrate. *Hydrometallurgy '94*, Cambridge, IMM, 351-359.

189. Komnitsas, C. and Pooley, F. D. (1991) Optimisation of the bacterial oxidation of an arsenical gold sulphide concentrate from Olympias, Greece. *Minerals Engineering,* **4** *(12),* 1297-1303.

190. Silver, S. and Keach, D. (1982) Energy-dependent arsenate efflux: the mechanism of plasmid-mediated resistance. *Proc. Natl. Acad. Sci. USA*, **79**, 6114-6118.

191. Cassity, W.D. and Pesic, B. (1994) Interaction of *Thiobacillus ferrooxidans* with arsenite, arsenate and arsenopyrite. *New Remediation Technology in the Changing Environmental Arena*, 223-228.

192. Frenay, J. (1997) Bioleaching of cobalt arsenides. In: *Hydrometallurgy and Refining of Nickel and Cobalt*, 27th Annual Hydrometallurgical Meeting of CIM, **1**, 111-116.

193. Torma, A.E. and Oolman, T. (1992) Bioliberation of gold. *International Materials Reviews*, **37** (4), 187-193.

194. Miller, D.M. and Hansford, G.S. (1992) Batch biooxidation of a gold-bearing pyrite-arsenopyrite concentrate. *Minerals Engineering*, **5** (6), 613-629.

195. Hansford, G.S. and Chapman, J.T. (1992) Batch and continuous biooxidation kinetics of a refractory gold-bearing pyrite concentrate. *Minerals Engineering*, **5** (6), 597-612.

196. Southwood, M.J. and Southwood, A.J. (1985) Mineralogical observations of the bacterial leaching of auriferrous pyrite: a new mathematical model and implications for the release of gold. *Fundamental and Applied Biohydrometallurgy, Proc. 6th Int. Symp. on Biohydrometallurgy*, Vancouver. Eds. Lawrence, R.W., Branion, R.M.R. and Ebner, H.G., Elesvier, Amsterdam, 263-275.

197. Mehta, A.P. and Murr, L.E. (1983) Fundamental studies of the contribution of galvanic interaction to acid-bacterial leaching of mixed metal sulphides, *Hydrometallurgy*, **9**, 235-256.

198. Attia, Y. A. and El-zeky, M. (1990) Effects of galvanic interactions of sulphides on extraction of precious metals from refractory complex sulphides by bioleaching. *International Journal of Mineral Processing*, **30**, 90-111.

199. Natarajan, K. A. (1992) Bioleaching of sulphides under applied potentials. *Hydrometallurgy*, **29**, 161-172.

200. Atkins, A.S. (1978) Studies on the bacterial oxidation of sulphide minerals (pyrite) in the presence of bacteria. *Metallurgical Applications of bacterial Leaching and Related Microbiological Phenomena*, eds. Murr, L.E., Torma, A.E. and Brierley, Academic Press, New York, 403-425.

201. Fernandez, M.G.M., Mustin, C., de Donato, P., Barres, O., Morin, P. and Berthelin, J. (1995) Occurrences at mineral-bacteria interface during oxidation of arsenopyrite by *Thiobacillus ferrooxidans*. *Biotechnology and Bioengineering*, **46**, 13-21.

202. Cruz, R., Lázaro, I., Rodríguez, J.M., Monroy, M. and González, I. (1997) Surface characterisation of arsenopyrite in acidic medium by triangular scan voltammetry on carbon paste electrodes. *Hydrometallurgy*, **46**, 303-319.

203. Carlson, L., Lindström, E.B., Hallberg, K.B. and Tuovinen, O.H. (1992) Solid-phase products of bacterial oxidation of arsenical pyrite. *Applied and Environmental Microbiology*, **58** (3), 1046-1049.

204. Lazer, M.J., Southwood, M.J. and Southwood, A.J. (1986) The release of refractory gold from sulphide minerals during bacterial leaching. *Gold 100*, **2**, 287-297.

205. Bailey, A.D. (1993) An assessment of oxygen availability, iron build-up and the relative significance of free and attached bacteria, as factors affecting bio-oxidation of refractory gold-bearing sulphides at high solids concentrations. *Ph.D. Thesis*, University of Cape Town.

206. Bruynesteyn, A., Hackl, R.P. and Wright, F. (1986) The BIOTANK leach process. *Extractive Metallurgy of Gold*. SAIMM, Johannesburg, **2**, 353-365.

207. Novick, R.P. and Roth, C. (1968) Plasmid-linked resistance to inorganic salts in Staphylococcus aureus. *Journal of Bacteriology*, **95** (4), 1335.

208. Hanford, G. S. and Drossou, M. (1988) A propagating-pore model for the batch bioleach kinetics of refractory gold-bearing pyrite. In: *Biohydrometallurgy Proceedings of the International Symposium Warwick 1987*, eds. Norris, R. P. and Kelly, D. P., 345-358.

209. Bailey, A.D. and Hansford, G.S. (1993) Factors affecting bio-oxidation of sulphide minerals at high concentration of solids: A review. *Biotechnology and Bioengineering*, **42,** 1164-1174.

210. Bakken, B.M., Hochella, JR., M.F., Marshall, A.F. and Turner, A.M. (1989) High-resolution microscopy of gold in unoxidised ore from the Carlin mine, Nevada. *Economic Geology*, **84**, 171-179.

211. Gasparrini, E. (1976) The energy-dispersive spectrometer attached to the electron microprobe: a new tool of investigation for the Earth Scientist. *Minerals Science Engineering*, **8** (1), 3-22.

212. Bonnemaison, M. and Marcoux, E. Auriferous mineralization in some shear-zones: A three-stage model of metallogenesis. *Mineralium Deposita*, **25**, 96-104.

213. Ubaldini, S., Verglió, F., Toro, L. and Abbruzzese, C. (1997) Biooxidation of arsenopyrite to improve gold cyanidation: study of some parameters and comparison with grinding. *International Journal of Mineral Processing*, **52**, 65-80.

214. Pinches, A. (1972) The use of microorganisms for the recovery of the metals from mineral materials. *Ph.D. Thesis*, University College Cardiff, Wales.

215. Jordan, M.A. (1993) The oxidation of base metal sulphides and pyritic gold concentrates with particular reference to mechanism and preferential release of ferrous iron. *Ph.D. Thesis*, Camborne School of Mines, University of Exeter.

216. Hansford, G.S. and Bailey, A.D. (1992) The logistic equation for modelling bacterial oxidation kinetics. *Minerals Engineering*, **5** (10-12), 1355-1364.

217. Pinches, A., Chapman, J.T., te Riele, W.A.M. and van Steden, M. (1988) The performance of bacterial leach reactors for the pre-oxidation of refractory gold-bearing sulphide concentrates. In: *Biohydrometallurgy Proceedings of the International Symposium Warwick 1987*, Science and Technology Letters, Kew, UK, 329-344.

218. Dempsey, P., Human, P., Pinches, A. and Neale, J.W. (1990) Bacterial oxidation of Vaal Reefs. International Deep Mining Conference: *Innovations in Metallurgical Plants*, Johannesburg, SAIMM.

219. Das, A., Modak, J.M. and Natarajan, K.A. (1997) Studies on multi-metal ion tolerance of *Thiobacillus ferrooxidans. Minerals Engineering*, **10** (7), 743-749.

220. Mandl, M. and Vyskovsky, M. (1994) Kinetics of arsenic(III) oxidation by iron(III) catalysed by pyrite in the presence of *Thiobacillus ferrooxidans. Biotechnology Letters*, **16** (11), 1199-1204.

221. Rosen, B.P., Hsu, C.M., Karkara, C.E., Owolabi, J.B. and Tisa L.S. (1990) Molecular analysis of an ATP-dependent anion pump. *Phil. Trans. R. Soc. Lond. B*, **326**, 455-463.

222. Bruhn, D.F. and Roberto, F.F. (1993) Maintenance and expression of enteric arsenic resistance genes in *Acidiphilium*. Biohydrometallurgy Technology, Torma, A.E. (ed), *Mineral, Metals and Materials Society*, Warrendale, **2**, 745.

223. Ji., G. and Silver, S. (1992) Reduction of arsenate to arsenite by the ArsC proten of the arsenic resistance operon of Staphylococcus aureus plasmid pI258. *Proc. Natl. Acad. Sci. USA*, **89**, 9474-9478.

224. Rosenstein, R., Peschel, A., Wieland, B. and Gotz, F. (1992) Expression and regulation of antimonite, arsenite and arsenate resistance operon of *Staphylococcus xylosus* plasmid pSX267. *American Society for Microbiology*, **174** (11), 3676-3683.

225. Mobley. H.L.T. and Rosen, B.P. (1982) Enegetics of plasmid-mediated resistance in *Escherichia coli. Proc. Natl. Acad. Sci. USA*, **79**, 6119-6122.

226. Beattie, M.J.V. and Poling, G.W. (1987) A study of the surface oxidation of arsenopyrite using cyclic voltammetry. *International Journal of Mineral Processing*, **20**, 87-108.

227. Schrenk, M.O., Edwards, K.J., Goodman, R.M., Hamers, R.J. and Banfield, J.F. (1998) Distribution of *Thiobacillus ferrooxidans* and *Leptosperillum ferrooxidans*: Implications for generation of acid mine drainage. *Science*, **279**, 1519-1521.

APPENDICES

A1.1: APPENDIX ONE: ANALYTICAL METHODS

Standard methods used for decomposition of concentrates and residues

A1.1.1: Ashing with magnesium nitrate

Analytes: As, Sb, Bi.

Sample types: soils, rocks, stream sediments

Procedure

1. Weigh 0.100-0.250 (± 0.001) g sample into 50 mL beakers, using a top pan balance.
2. Add 1.0 mL saturated magnesium nitrate solution from a mini bottle dispenser.
3. Place the beakers in a furnace set at a temperature of 450°C and leave for 6 hours.
4. After 6 hours switch off the furnace and allow it to cool to room temperature before removing the beakers.
5. Add 5 mL conc. HCl from an Oxford dispenser and leave for 10 minutes, cover beakers with clingfilm.
6. Place on rocking machine and leave overnight.
7. Remove clingfilm and add 5 mL freshly prepared 0.2% KI solution using an Oxford dispenser and again cover with clingfilm. Swirl gently and leave for 0.5 hours.
8. Decant into a number of test tubes without rinsing.

A1.1.2: Hydrobromic acid and bromine attack

Analytes: Gold

Sample types: Rocks, soils, stream sediments, mineral concentrates

Procedure

The mineral concentrates were ignited at 650°C in a furnace

1. Weigh 8.000g sample into screw capped culture tubes.
2. Add 16 mL of HBr/Br_2 solution (15 mL HBr and 1 mL Br_2) using a 25 mL measuring cylinder and leave for 10-15 minutes.
3. Cap tubes firmly and shake for 15 minutes on a shaking machine.
4. Add 16 mL of water and 10 mL of MIBK using a 10 mL pipette. Shake on the machine for a further 2 minutes.
5. Centrifuge at 600 rpm for 5 minutes.

6. Transfer the MIBK with a pasteur pipette to tubes containing 25 mL of 0.1N HBr. Shake for 15 minutes by hand.
7. Transfer MIBK into centrifuge tubes or centrifuge it if needed.
8. Atomise MIBK layer directly against matching calibrators.
9. The solutions were analysed on AAS and ICP-AES.

A1.1.3: Sulphur oxidation

Procedure

1. Weigh out accurately 1.000 g of sample into a dry 400 mL beaker.
2. Add 10 mL of bromine-carbon tetrachloride solution (1 mL Br_2 and 9 mL CCl_4) and cover with a clock glass.
3. Allow to stand on a cold bath in the fume cupboard for 15-20 minutes, with occasional shaking of the beaker.
4. Add 15 mL of concentrated nitric acid down the side of the beaker and allow to stand for another 15-20 minutes, shaking occasionally.
5. Heat the covered beaker below 100°C, on a thick asbestos board over a steam bath until all action has ceased and most of the bromine has been expelled.
6. Raise the clock glass cover using glass riders (U-shaped glass rods) and evaporate to dryness.
7. Add 10 mL of concentrated hydrochloric acid, mix, and evaporate again to eliminate most of the nitric acid.
8. Place the beaker in the oven at 95-100°C in order to dehydrate any silica which may be present.
9. Add 5 mL concentrated hydrochloric acid and allow to stand for a few minute.
10. Add 20 mL of distilled water and keep the solution warm on a hot plate. Filter the solution and make up to 250 mL in a standard volumetric flask.

A2.1: APPENDIX TWO: CALCULATIONS

A2.1.1: Arsenopyrite and pyrite oxidation during bacterial oxidation

Assumptions

(I) All the arsenic was assumed to be coming from arsenopyrite.

(II) The concentrates were considered to consist of stoichiomertic arsenopyrite (FeAsS) and pyrite (FeS_2).

(III) The measured iron concentration was assumed to be from pyrite and arsenopyrite only.

Example

Molecular mass of arsenopyrite = M_a g

Molecular mass of pyrite = M_p g

Molecular mass of arsenic = C g

Molecular mass of iron = D g

Initial mass of the concentrate at the start of the experiment = A g

Percentage of arsenic in the intial concentrate = a %

Percentage of iron in the intial concentrate = b %

Initial amount of arsenic in the concentrate = (aA/100) g

= E g

Initial amount of arsenopyrite = [(aA/100)/C] x M_a g

= (E/C) x M_a g

= F g

Amount of iron in arsenopyrite = {[(aA/100)/C] x M_a} x (D/M_a) g

= F x (D/M_a) g

= G g

Initial amount of iron in the concentrate = (bA/100) g

= H g

Initial amount of iron from pyrite = (H - G) g

= I g

Initial amount of pyrite = I x (M_p/D) g

= J g

Percentage of arsenopyrite in the concentrate = {(G/A) x 100} %

Percentage of pyrite in the concentrate = {(J/A) x 100} %

The approximate percentages of arsenopyrite and pyrite oxidised during bacterial leaching were calculated by using the concentrations of arsenic and iron at any given point following the same procedure as above.

A.2.1.2: Gold recovery

$$\% \text{ Gold Recovery} = \frac{(\text{Solution Volume (L)} \times \text{Assay (mg/L)}) \times 100}{\text{Sample Weight (g)} \times \text{Sample Assay (g/t)}}$$

A3.1: APPENDIX THREE: EXPERIMENTAL DATA

The data obtained during the various experiments as part of this thesis are presented in this appendix.

A3.1.1: Mineralogical data

Below is a description of the locations and sketch diagrams within the Indarama mine where the samples were collected. The samples were named Indarama 1 to Indarama 5. In the sketches below, the exact points where the samples were collected are labelled by a black box and *IN*.

Indarama 1 and Indarama 2.

These samples were collected on 5-level drive east.

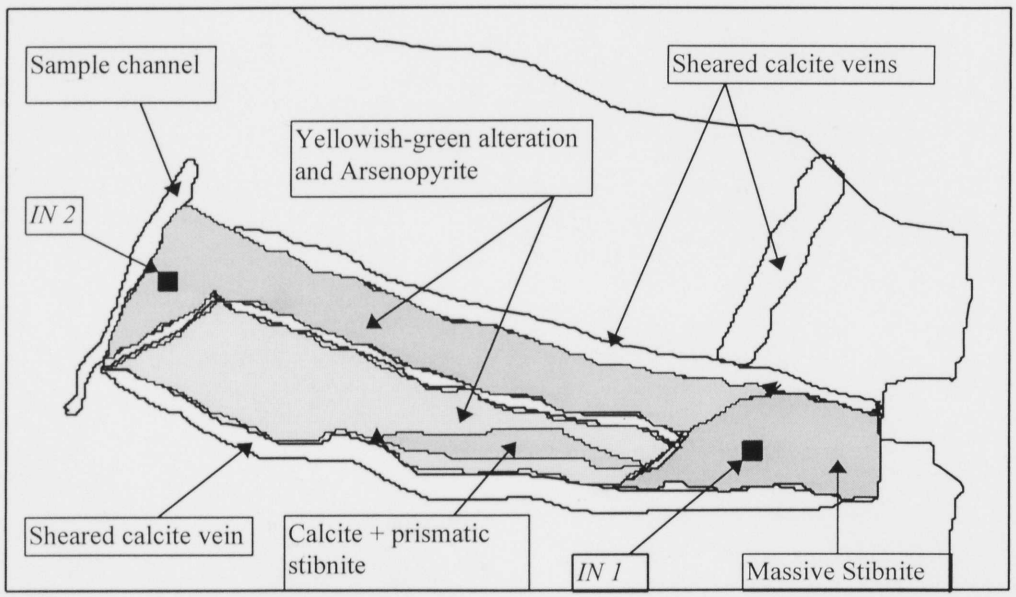


Figure A.3.1: Section looking south 5-level haulage drive east. The reef striking east-west and dipping to the north. Scale = 1:25cm.

Indarama3

This sample was collected on 5-level drive south (Figure A3.2).

Indarama 4

This sample was collected on 11-level drive north (Figure A3.3).

Indarama 5

This sample was collected on 10-level stope north (Figure A3.4).

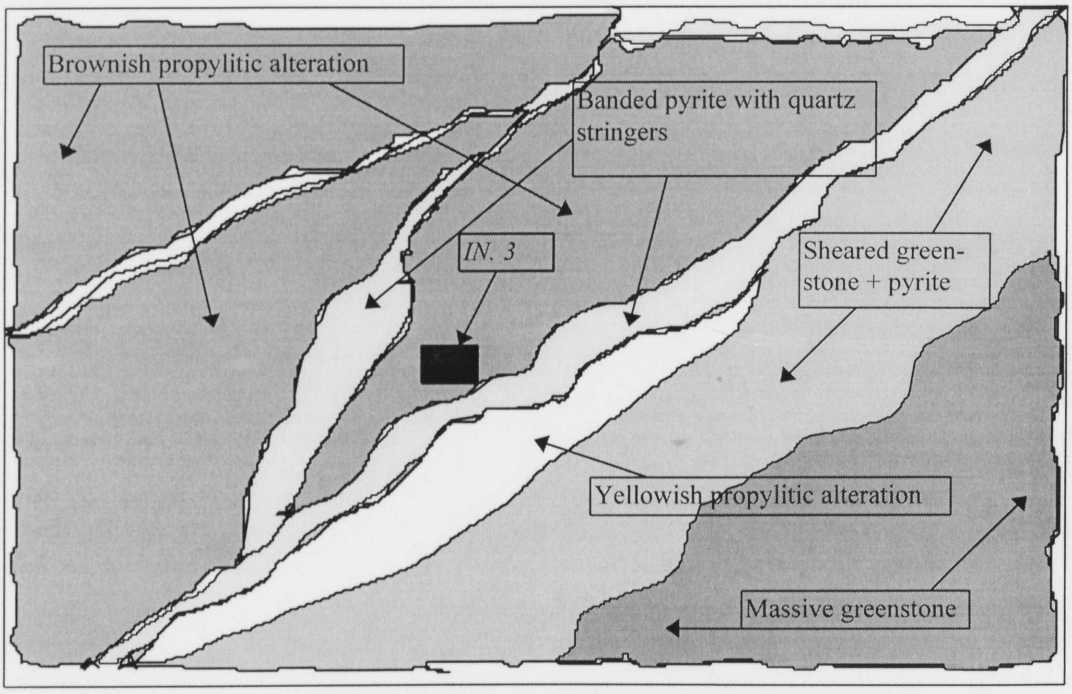


Figure A3.2: Section looking west 5-level drive south. The reef has a normal dip (IN 3 sample location). Scale = 1:25cm.

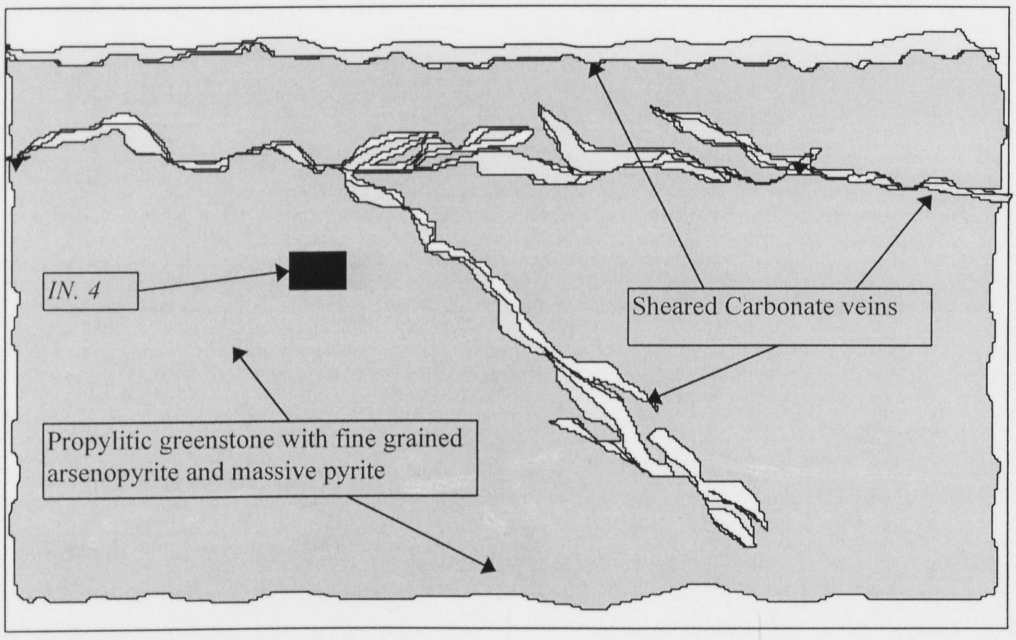


Figure A3.3: Face looking west 11-level drive north (IN 4 sample location). Scale = 1:25cm.

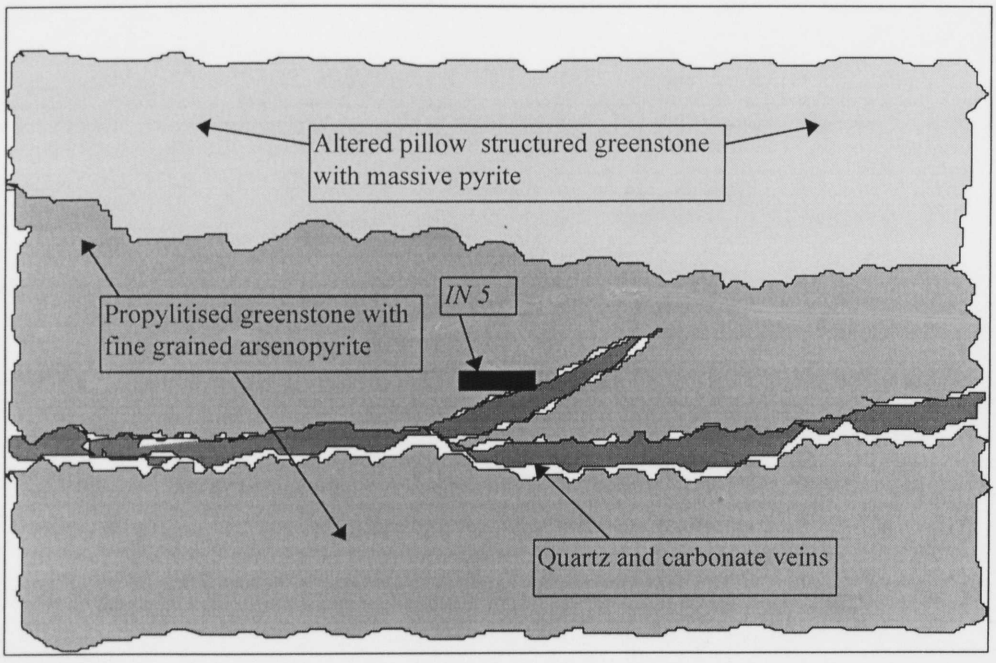


Figure A3.4: Face looking north (Stope 10-level-IN 5 sample location). Scale = 1:25cm.

Microprobe analysis of minerals in the Indarama Gold deposit.

Table A3.1.1: Microprobe analysis of some of the arsenopyrites in the Indarama deposit (wt %)

S	Fe	Co	Ni	Cu	As	Au	Total
50.66	45.55	0.00	0.06	0.00	1.67	0.00	97.95
50.49	45.77	0.06	0.08	0.08	2.59	0.00	99.08
22.25	34.73	0.12	0.22	0.03	35.65	0.05	93.16
22.54	35.68	0.05	0.11	0.11	41.67	0.00	100.22
22.60	35.36	0.19	0.15	0.00	40.90	0.07	99.85
23.58	36.08	0.24	0.28	0.00	39.47	0.04	100.03
23.64	35.51	0.22	0.43	0.11	39.16	0.00	99.61
39.78	41.76	0.10	0.06	0.09	19.26	0.01	101.07
49.39	45.13	0.00	0.07	0.09	4.05	0.00	98.72
49.30	45.36	0.02	0.00	0.04	3.87	0.01	98.62
20.22	34.47	0.04	0.06	0.06	44.12	0.00	99.08
20.84	34.78	0.06	0.16	0.00	43.49	0.00	99.32
20.55	34.74	0.13	0.06	0.10	43.16	0.07	98.90
22.57	35.77	0.05	0.05	0.09	41.06	0.00	99.65
10.16	17.26	0.02	0.01	0.02	22.96	0.00	50.56
20.70	34.14	0.01	0.11	0.08	42.14	0.00	97.23
20.75	34.70	0.10	0.23	0.00	43.83	0.08	99.89
31.98	38.41	0.06	0.04	0.11	28.83	0.00	99.51
51.86	46.05	0.03	0.00	0.00	1.06	0.01	99.03
19.89	34.40	0.06	0.26	0.01	45.53	0.00	100.38

19.88	35.16	0.05	0.18	0.21	45.52	0.00	101.07
19.59	34.94	0.10	0.19	0.11	45.80	0.02	100.93
19.81	34.97	0.02	0.28	0.05	45.35	0.02	100.59
20.55	34.92	0.01	0.18	0.00	44.25	0.05	100.18
20.94	35.53	0.05	0.05	0.06	43.10	0.00	100.46
20.31	35.02	0.11	0.01	0.00	44.97	0.39	100.91
20.64	35.14	0.05	0.01	0.14	44.16	0.03	100.61
20.72	35.20	0.04	0.11	0.05	43.35	0.02	100.22
20.84	34.86	0.00	0.00	0.05	43.04	0.00	99.35
19.75	33.19	0.05	0.08	0.09	45.57	0.00	98.78
19.56	33.91	0.04	0.16	0.00	43.58	0.08	97.32
20.04	34.69	0.09	0.06	0.00	45.11	0.00	100.03
19.78	34.82	0.00	0.15	0.00	44.74	0.03	99.51
20.09	35.15	0.07	0.07	0.00	45.45	0.00	100.84
20.04	34.85	0.00	0.09	0.04	45.53	0.08	100.66
19.93	34.42	0.10	0.19	0.04	45.10	0.02	99.86
19.94	34.71	0.17	0.21	0.00	45.08	0.00	100.11
20.14	33.56	0.46	0.50	0.06	44.69	0.02	99.51
19.92	32.91	0.25	0.34	0.06	42.38	0.00	95.91
21.56	34.63	0.00	0.17	0.01	43.24	0.02	99.72
21.28	35.15	0.07	0.05	0.10	43.93	0.10	100.66
21.92	35.72	0.03	0.01	0.00	42.76	0.07	100.65
21.71	35.67	0.00	0.07	0.00	42.69	0.07	100.40
21.88	36.09	0.00	0.00	0.05	42.74	0.25	101.13
21.53	35.71	0.04	0.04	0.09	43.23	0.09	100.90
21.87	35.28	0.07	0.00	0.06	42.33	0.09	99.86
21.55	35.53	0.07	0.00	0.08	43.48	0.19	101.06
21.90	35.71	0.07	0.03	0.05	42.66	0.24	100.72
20.95	34.76	0.03	0.05	0.07	43.26	0.01	99.29
21.09	35.34	0.06	0.00	0.06	43.58	0.00	100.30
21.42	36.01	0.05	0.06	0.05	43.46	0.02	101.35
20.94	34.91	0.01	0.00	0.00	43.92	0.00	99.89
20.67	34.69	0.00	0.00	0.12	43.11	0.00	98.62
21.64	35.30	0.03	0.00	0.10	43.60	0.00	100.81
21.53	35.42	0.07	0.12	0.00	43.74	0.00	101.12
21.64	34.96	0.01	0.02	0.06	42.35	0.00	99.24
20.97	34.85	0.07	0.02	0.00	43.68	0.00	99.65
21.12	35.18	0.08	0.14	0.00	43.64	0.00	100.19
21.07	35.23	0.11	0.11	0.01	43.06	0.08	99.77
21.85	35.32	0.04	0.06	0.03	42.80	0.09	100.29
20.87	34.63	0.09	0.08	0.00	43.42	0.04	99.17
20.79	35.06	0.00	0.05	0.11	43.18	0.01	99.40
21.35	35.47	0.10	0.00	0.00	43.84	0.02	100.86
21.17	35.28	0.04	0.07	0.02	43.74	0.10	100.52
20.91	35.73	0.04	0.06	0.06	44.00	0.01	100.92
20.95	35.65	0.09	0.06	0.06	44.23	0.14	101.32

21.53	35.56	0.00	0.03	0.09	43.15	0.02	100.62
21.13	35.30	0.00	0.03	0.13	44.03	0.00	100.64
21.39	35.75	0.06	0.00	0.00	43.99	0.00	101.25
21.82	35.18	0.09	0.01	0.10	43.11	0.09	100.39
22.15	35.99	0.00	0.11	0.00	42.80	0.06	101.21
21.42	34.11	0.54	0.31	0.19	41.05	0.00	97.81
21.98	34.85	0.14	0.41	0.14	40.43	0.11	98.19
21.57	33.06	0.77	1.31	0.13	43.56	0.02	100.60
21.32	33.85	0.36	0.62	0.76	42.86	0.00	100.49
21.97	34.14	0.78	0.55	0.03	43.05	0.04	100.81
21.25	34.56	0.04	0.00	0.06	41.35	0.01	97.32
22.15	35.37	0.02	0.02	0.00	42.54	0.02	100.30
21.83	34.85	0.21	0.11	0.07	42.30	0.06	99.63
22.24	35.52	0.02	0.08	0.00	42.27	0.00	100.40
21.97	20.99	0.12	0.20	5.09	27.37	0.16	97.27
21.01	35.06	0.03	0.00	0.00	43.65	0.00	99.98
21.15	36.00	0.07	0.07	0.00	44.52	0.06	101.95
21.03	35.25	0.02	0.04	0.17	44.00	0.06	100.78
21.15	35.51	0.02	0.00	0.02	43.83	0.00	100.53
21.05	35.25	0.06	0.29	0.06	43.88	0.00	100.76
20.97	35.53	0.00	0.11	0.14	44.62	0.00	101.48
20.53	35.46	0.10	0.07	0.03	45.06	0.00	101.32
20.47	35.19	0.08	0.02	0.00	45.06	0.10	101.02
22.47	36.11	0.10	0.00	0.00	42.49	0.04	101.30
21.53	35.80	0.00	0.00	0.07	44.09	0.00	101.73
20.81	35.30	0.05	0.23	0.03	45.03	0.02	101.52
21.43	35.76	0.05	0.00	0.10	44.05	0.02	101.43
21.87	35.11	0.07	0.10	0.00	43.14	0.03	100.43
22.62	35.97	0.05	0.05	0.00	42.21	0.08	101.01
22.48	35.94	0.08	0.03	0.00	42.53	0.02	101.11
21.93	35.90	0.06	0.00	0.07	42.88	0.00	101.28
22.06	34.39	0.02	0.00	0.06	40.66	0.00	97.48
21.15	34.97	0.03	0.00	0.09	44.21	0.05	100.50
21.24	35.64	0.07	0.07	0.00	43.95	0.08	101.04
20.62	34.46	0.02	0.04	0.07	43.75	0.02	99.08
21.04	35.18	0.03	0.00	0.02	44.54	0.00	100.87
20.82	34.84	0.01	0.08	0.01	44.41	0.01	100.16
20.85	35.24	0.00	0.08	0.09	44.60	0.03	100.99
20.84	34.91	0.13	0.09	0.02	43.59	0.00	99.72
21.11	34.35	0.05	0.04	0.03	43.63	0.00	99.20
23.29	36.17	0.02	0.08	0.06	40.43	0.00	101.02
23.51	37.24	0.03	0.08	0.12	40.31	0.05	102.10
24.34	36.60	0.08	0.02	0.13	39.94	0.00	101.83
24.63	37.11	0.06	0.01	0.00	38.87	0.00	101.19
23.20	36.00	0.14	0.18	0.06	41.46	0.00	101.52
22.95	36.41	0.03	0.07	0.00	41.60	0.00	101.37

21.44	35.94	0.11	0.07	0.00	43.85	0.01	101.59
20.96	34.84	0.18	0.27	0.04	44.49	0.03	100.92
21.46	35.02	0.05	0.00	0.00	43.82	0.10	100.69
21.95	35.02	0.00	0.00	0.00	42.82	0.00	100.13
21.02	34.89	0.00	0.03	0.00	42.46	0.00	98.64
21.22	35.15	0.00	0.00	0.09	43.65	0.00	100.43
21.32	35.36	0.00	0.05	0.00	43.45	0.02	100.68
20.98	35.06	0.01	0.00	0.00	44.99	0.05	101.26
20.41	34.89	0.11	0.00	0.02	45.08	0.03	100.70
20.64	35.02	0.07	0.00	0.10	45.52	0.00	101.35
20.67	34.16	0.09	0.00	0.01	44.80	0.02	99.98
22.06	34.61	0.07	0.30	0.18	41.91	0.02	99.66
22.08	34.77	0.13	0.70	0.01	41.73	0.00	100.90
22.57	35.93	0.09	0.31	0.06	42.29	0.00	101.80
21.63	35.88	0.11	0.28	0.13	43.30	0.13	101.61
23.75	36.41	0.08	0.07	0.01	39.70	0.05	100.60
23.50	36.32	0.00	0.15	0.08	41.03	0.07	101.66
23.18	35.72	0.00	0.21	0.01	41.32	0.01	100.81
22.04	35.52	0.07	0.03	0.00	42.23	0.00	100.25
20.93	34.01	0.34	1.04	0.09	44.68	0.09	101.17
20.92	33.69	0.47	0.98	0.10	44.68	0.00	100.95
20.75	34.52	0.16	0.63	0.05	44.44	0.00	100.66
20.56	35.10	0.06	0.18	0.01	44.94	0.05	100.98
21.36	35.86	0.03	0.02	0.00	43.71	0.00	101.33
20.70	35.24	0.00	0.05	0.01	44.06	0.09	100.27
21.33	35.80	0.07	0.01	0.03	43.05	0.08	100.73
22.58	36.03	0.00	0.07	0.07	42.62	0.07	101.97
21.23	35.74	0.02	0.00	0.00	44.34	0.00	101.35
21.17	35.63	0.02	0.03	0.00	44.01	0.00	100.98
21.61	35.43	0.09	0.03	0.09	43.64	0.00	100.92
20.87	35.21	0.00	0.05	0.19	44.68	0.01	101.06
20.77	35.34	0.10	0.08	0.00	44.63	0.18	101.11
20.97	35.33	0.05	0.17	0.09	44.65	0.14	101.41
20.92	34.83	0.05	0.03	0.00	43.05	0.03	98.92
20.76	35.30	0.09	0.00	0.00	44.64	0.06	100.91
21.38	35.17	0.00	0.03	0.05	43.10	0.08	99.80
20.64	34.36	0.05	0.06	0.00	42.68	0.05	97.99
20.38	33.68	0.08	0.00	0.12	44.32	0.11	98.73
2.94	5.28	0.00	0.04	0.00	9.54	0.00	17.83
21.26	35.47	0.01	0.00	0.00	44.04	0.00	100.86
21.61	35.78	0.07	0.00	0.03	43.58	0.09	101.15
21.98	35.49	0.00	0.05	0.00	42.82	0.00	100.34
21.66	35.75	0.07	0.02	0.00	43.97	0.02	101.62
21.24	35.29	0.00	0.00	0.08	44.07	0.00	100.70
21.61	35.68	0.02	0.09	0.10	43.94	0.00	101.47
21.16	36.07	0.00	0.04	0.00	44.52	0.00	101.89

21.38	35.90	0.07	0.00	0.02	44.33	0.08	101.78
20.97	34.61	0.07	0.02	0.00	42.02	0.00	97.69
21.87	22.85	0.14	0.10	2.66	27.27	0.12	99.49
20.88	34.54	0.21	0.11	0.00	43.72	0.16	100.11
19.99	34.47	0.12	0.06	0.08	42.72	0.07	97.81
21.53	34.84	0.17	0.12	0.00	41.59	0.09	99.58
20.85	34.47	0.07	0.08	0.00	44.24	0.16	99.92
19.79	33.23	0.24	0.09	0.09	41.44	0.06	95.67
19.96	34.24	0.39	0.13	0.06	42.55	0.00	97.53
20.75	35.34	0.10	0.00	0.01	44.70	0.01	101.20
20.79	34.92	0.02	0.00	0.12	44.49	0.04	100.79
23.15	35.94	0.04	0.00	0.04	41.78	0.10	101.11
23.22	36.06	0.00	0.00	0.00	41.26	0.05	100.69
22.47	35.69	0.08	0.00	0.01	40.84	0.01	99.38
23.01	36.68	0.00	0.00	0.06	41.88	0.00	101.76
22.58	36.29	0.07	0.00	0.00	41.87	0.00	100.95
22.62	36.22	0.00	0.00	0.04	42.14	0.00	101.03
22.58	35.54	0.09	0.02	0.02	42.39	0.04	100.67
21.13	35.30	0.02	0.11	0.04	43.91	0.02	100.61
19.96	32.99	0.02	0.18	0.15	41.69	0.00	95.20
20.54	34.15	0.06	0.11	0.09	42.99	0.07	98.20
21.69	36.08	0.03	0.08	0.00	43.51	0.00	101.50
21.72	36.68	0.09	0.07	0.00	43.92	0.08	102.70
22.49	36.97	0.08	0.15	0.11	43.17	0.00	103.02
21.89	36.36	0.10	0.05	0.10	44.07	0.00	102.87
21.32	33.07	0.18	0.08	0.08	40.60	0.06	101.78

Table A3.1.2: Microprobe analysis of some pyrites from the Indarama deposit (wt %).

Fe	S	Co	Ni	Cu	As	Au	Total
46.19	51.66	0.00	0.05	0.02	0.31	0.00	98.28
46.88	52.95	0.06	0.03	0.03	0.10	0.00	100.23
46.97	52.68	0.06	0.00	0.05	0.08	0.00	99.85
46.46	52.56	0.00	0.00	0.00	0.05	0.03	99.21
47.15	52.56	0.06	0.04	0.00	0.07	0.00	99.95
46.82	52.60	0.13	0.05	0.08	0.19	0.04	100.11
47.11	52.53	0.05	0.00	0.07	0.17	0.00	100.03
47.31	52.68	0.10	0.00	0.00	0.07	0.00	100.43
47.00	52.53	0.05	0.00	0.00	0.08	0.00	99.73
47.00	52.26	0.04	0.00	0.07	0.53	0.00	99.89
45.59	50.72	0.08	0.08	0.00	1.68	0.00	98.16
46.90	51.93	0.05	0.00	0.05	1.23	0.00	100.19
46.96	52.80	0.00	0.02	0.03	0.05	0.00	100.15
47.00	52.79	0.06	0.05	0.03	0.03	0.00	100.26
46.56	52.37	0.02	0.01	0.04	0.04	0.00	99.06
47.10	52.70	0.04	0.00	0.00	0.06	0.04	99.98

47.02	52.92	0.07	0.00	0.03	0.05	0.02	100.25
46.31	51.78	0.04	0.00	0.00	0.22	0.05	98.59
46.56	52.81	0.01	0.01	0.00	0.28	0.00	99.98
46.83	51.75	0.02	0.03	0.12	1.01	0.00	99.96
46.18	52.23	0.03	0.03	0.00	0.65	0.00	99.15
46.76	51.59	0.10	0.01	0.02	1.44	0.00	100.02
45.96	51.62	0.05	0.00	0.00	1.23	0.00	99.05
46.63	51.56	0.00	0.00	0.08	1.29	0.00	99.71
46.14	51.32	0.08	0.07	0.00	1.63	0.00	99.36
46.50	51.59	0.01	0.00	0.08	1.49	0.00	99.70
46.27	51.37	0.00	0.01	0.01	1.72	0.00	99.55
46.57	51.40	0.07	0.07	0.01	1.70	0.02	100.13
45.85	51.15	0.09	0.09	0.03	1.50	0.00	98.92
46.90	51.45	0.12	0.00	0.13	1.52	0.00	100.33
46.73	52.63	0.06	0.18	0.00	0.06	0.00	99.81
46.29	52.04	0.11	0.19	0.35	0.02	0.00	99.22
46.61	52.30	0.20	0.09	0.27	0.00	0.00	99.48
44.38	51.08	0.39	0.17	2.20	0.05	0.00	100.13
45.85	52.69	0.23	0.33	0.12	0.05	0.00	99.59
46.06	53.10	0.44	0.31	0.03	0.03	0.00	100.23
45.78	52.14	0.28	0.17	0.12	0.02	0.03	98.73
47.73	53.58	0.30	0.23	0.14	0.04	0.00	102.08
47.69	53.26	0.30	0.37	0.00	0.07	0.00	101.90
45.15	51.73	0.05	0.59	0.01	0.12	0.03	97.76
46.04	52.49	0.10	0.70	0.19	0.05	0.04	99.75
46.06	52.27	0.09	0.64	0.30	0.07	0.00	99.68
45.93	52.27	0.06	0.35	0.13	0.07	0.01	99.03
45.89	52.17	0.06	0.32	0.62	0.00	0.00	99.09
45.71	51.83	0.02	0.33	0.37	0.09	0.00	98.46
46.11	52.23	0.06	0.29	0.46	0.02	0.01	99.31
45.84	52.50	0.06	0.53	0.10	0.06	0.06	99.28
45.40	52.39	0.00	0.96	0.00	0.03	0.00	98.78
45.44	52.68	0.15	1.16	0.12	0.04	0.00	99.67
46.16	52.24	0.12	0.22	0.01	0.05	0.04	99.05
45.85	51.96	0.66	0.02	0.08	0.05	0.00	98.67
46.04	52.24	0.85	0.04	0.00	0.05	0.02	99.37
46.16	52.20	0.34	0.00	0.00	0.06	0.00	99.19
46.01	52.43	0.60	0.00	0.09	0.06	0.00	99.30
45.61	52.23	0.72	0.05	0.14	0.03	0.00	98.94
45.64	52.02	0.73	0.00	0.00	0.04	0.00	98.85
45.89	52.27	0.51	0.02	0.00	0.02	0.00	98.79
45.89	52.14	0.90	0.01	0.10	0.07	0.00	99.49
46.24	52.22	0.61	0.09	0.00	0.02	0.00	99.36
45.99	52.04	0.29	0.00	0.00	0.02	0.05	98.64
46.16	52.15	0.10	0.37	0.09	0.07	0.00	99.02
45.40	52.15	0.04	0.98	0.00	0.12	0.04	98.86

46.45	52.10	0.06	0.27	0.00	0.02	0.05	99.31
45.90	52.04	0.00	0.22	0.11	0.07	0.00	98.50
45.67	52.50	0.00	0.40	0.01	0.10	0.01	98.72
45.05	51.86	0.07	1.27	0.06	0.31	0.04	98.79
45.10	50.78	0.08	0.73	0.00	0.31	0.08	97.43
46.05	52.04	0.14	0.62	0.12	0.39	0.00	99.51
45.73	51.80	0.00	0.44	0.00	0.25	0.10	98.45
45.98	52.14	0.15	0.50	0.00	0.33	0.04	99.15
46.11	51.94	0.00	0.33	0.04	0.31	0.00	98.98
45.93	52.06	0.11	0.35	0.05	0.31	0.00	98.88
46.06	51.98	0.11	0.32	0.00	0.03	0.02	98.64
46.35	52.06	0.05	0.10	0.12	0.07	0.00	98.81
46.45	52.20	0.15	0.14	0.12	0.08	0.00	99.22
45.88	51.90	0.02	0.01	0.15	0.10	0.00	98.43
46.78	52.29	0.03	0.08	0.02	0.04	0.00	99.37
46.26	52.07	0.00	0.00	0.06	0.09	0.04	98.58
46.23	51.98	0.07	0.00	0.04	0.06	0.00	98.63
46.71	52.37	0.04	0.00	0.04	0.05	0.00	99.34
46.98	52.09	0.06	0.04	0.00	0.09	0.00	99.55
46.33	52.14	0.06	0.01	0.07	0.04	0.00	99.10
46.57	52.18	0.00	0.09	0.00	0.06	0.01	99.03
46.23	52.17	0.01	0.00	0.05	0.07	0.00	98.66
46.58	52.29	0.08	0.02	0.00	0.07	0.03	99.13
46.80	52.06	0.07	0.02	0.00	0.10	0.05	99.41
46.52	52.02	0.03	0.00	0.01	0.27	0.00	99.05
46.24	51.58	0.07	0.00	0.01	0.31	0.01	98.40
43.35	46.03	0.23	0.00	0.04	0.12	0.05	90.13
46.04	52.12	0.26	0.13	0.12	0.37	0.00	99.23
43.17	47.21	0.43	0.07	0.00	0.13	0.00	91.14
46.10	51.69	0.59	0.08	0.13	0.20	0.00	98.83
46.31	52.24	0.91	0.04	0.12	0.31	0.00	100.03
46.52	51.93	0.22	0.01	0.00	0.10	0.06	99.21
46.55	51.78	0.11	0.00	0.09	0.94	0.07	99.63
46.16	51.49	0.00	0.00	0.00	0.54	0.00	98.38
46.51	52.33	0.11	0.00	0.06	0.44	0.03	99.59
46.11	52.85	0.07	0.01	0.00	0.59	0.00	99.95
46.93	52.96	0.04	0.03	0.07	0.20	0.06	100.52
46.56	52.79	0.00	0.00	0.00	0.49	0.00	100.10
46.03	51.75	0.00	0.00	0.07	1.87	0.00	99.81
46.57	52.00	0.00	0.04	0.00	1.38	0.00	100.13
46.57	52.60	0.06	0.05	0.00	0.41	0.02	99.95
46.25	52.13	0.00	0.05	0.08	0.44	0.01	99.07
45.53	50.49	0.00	0.01	0.17	2.25	0.04	98.72
45.79	50.78	0.00	0.01	0.00	2.40	0.10	99.13
46.24	51.86	0.02	0.03	0.12	1.19	0.00	99.63
46.32	51.70	0.02	0.00	0.08	1.21	0.04	99.36

45.70	49.93	0.12	0.06	0.00	3.47	0.00	99.67
45.62	50.57	0.00	0.07	0.07	2.66	0.04	99.16
43.49	47.17	0.00	0.40	0.00	4.71	0.00	96.05
45.83	51.09	0.06	0.09	0.00	2.29	0.02	99.64
46.23	51.03	0.00	0.09	0.01	1.89	0.01	99.55
45.83	51.24	0.02	0.00	0.06	2.40	0.05	99.78
45.88	50.80	0.06	0.00	0.07	2.38	0.00	99.24
46.47	51.64	0.04	0.03	0.00	1.25	0.00	99.64
46.48	52.03	0.07	0.00	0.00	1.23	0.02	100.04
46.05	51.61	0.08	0.06	0.11	1.66	0.06	99.76
45.50	50.87	0.00	0.11	0.01	2.47	0.00	99.35
46.13	51.42	0.05	0.07	0.08	1.99	0.00	100.10
46.14	51.87	0.00	0.00	0.04	1.65	0.01	99.70
46.18	51.73	0.00	0.10	0.00	1.71	0.00	99.83
46.12	51.56	0.05	0.17	0.11	1.70	0.00	99.79
45.95	50.89	0.10	0.00	0.00	2.11	0.04	99.18
46.68	52.99	0.11	0.05	0.10	0.06	0.00	100.20
46.98	52.91	0.01	0.00	0.02	0.14	0.00	100.15
46.97	53.20	0.00	0.06	0.00	0.04	0.00	100.48
47.04	53.02	0.02	0.05	0.03	0.56	0.02	100.88
46.55	52.68	0.02	0.05	0.00	0.70	0.00	100.16
46.86	52.75	0.04	0.00	0.01	1.09	0.00	100.86
46.67	52.70	0.05	0.00	0.01	0.79	0.00	100.55
46.58	52.55	0.01	0.00	0.00	0.95	0.00	100.10
42.14	45.66	0.11	0.00	0.00	0.84	0.01	88.93
41.90	41.54	0.06	0.00	0.03	2.48	0.06	86.69
46.02	51.81	0.03	0.09	0.00	1.67	0.01	99.92
45.55	52.42	0.12	0.00	0.00	0.07	0.02	98.36
46.03	52.83	0.00	0.00	0.00	0.16	0.06	99.33
47.01	53.23	0.01	0.00	0.04	0.09	0.00	100.50
46.98	53.76	0.03	0.00	0.00	0.07	0.00	100.88
47.13	53.37	0.03	0.04	0.05	0.06	0.01	100.82
46.80	53.33	0.05	0.00	0.05	0.05	0.00	100.42
46.85	53.89	0.09	0.10	0.00	0.07	0.01	101.14
46.91	53.18	0.02	0.00	0.00	0.07	0.00	100.20

Table A3.1.3: Microprobe analysis of some minerals from the Indarama deposit (wt %).

Mineral	% Fe	% As	% S	% Sb	% Cu	% Zn	% Au	Total
Gudmundite	26.4	-	15.1	62.6	-	-	-	104.1
Gudmundite	26.4	-	15.0	62.0	-	-	-	103.4
Gudmundite	26.6	-	15.1	61.2	-	-	-	102.8
Gudmundite	26.5	-	15.1	62.9	-	-	-	104.5
Gudmundite	26.7	-	15.2	57.9	-	-	-	99.7
Gudmundite	26.4	-	15.0	57.1	-	-	-	98.5
Gudmundite	26.5	-	15.0	56.4	-	-	-	97.9

Gudmundite	26.3	-	15.0	56.6	-	-	-	97.8
Native gold	-	-	-	-	-	-	101.7	101.7
Native gold	-	-	-	-	-	-	101.9	101.9
Native gold	-	-	-	-	-	-	98.8	98.8
Native gold	-	-	-	-	-	-	102.3	102.3
Native gold	-	-	-	-	-	-	102.2	102.2
Native gold	-	-	-	-	-	-	98.4	98.4
Aurostibite	-	-	-	57.6	-	-	43.6	101.2
-	14.6	1.0	31.4	23.0	30.3	-	-	100.2
-	14.4	0.8	38.3	-	-	47.1	-	100.6
-	4.2	1.0	24.1	28.1	36.7	3.1	-	97.1
-	4.2	0.9	24.1	28.3	37.1	2.9	-	97.5
-	3.5	-	31.9	-	1.0	60.4	-	97.2
Arsenopyrite	31.3	41.3	20.1	3.8	3.0	-	-	99.5
Arsenopyrite	22.8	31.3	21.7	12.0	14.4	0.9	-	103.1

Table A3.1.4: Laser ablation results of some of the arsenopyrites in the Indarama deposit (calculated wt %).

Analysis Number	wt % As	wt % Fe	wt % S	Atomic% As	Au (ppm)
1	50.89	32.60	16.45	36.84	600
2	52.95	30.84	16.15	38.33	604
3	51.14	31.88	16.91	37.02	679
4	54.41	30.07	19.46	39.39	646
5	52.02	30.77	17.15	37.66	608
6	49.79	31.89	18.35	36.04	602
7	54.76	28.90	16.29	39.64	452
8	55.82	28.20	15.95	40.41	395
9	51.85	30.84	17.26	37.53	408
10	48.83	32.08	19.05	35.35	435
11	56.06	28.29	15.63	40.58	253
12	50.96	30.29	18.21	36.89	402
13	48.62	32.43	18.88	35.20	682
14	51.27	31.63	17.03	37.12	712
15	50.51	31.47	17.93	36.56	827
16	52.57	29.81	17.54	38.06	413
17	51.57	30.28	18.10	37.33	474
18	51.00	30.21	18.75	36.92	344
19	50.22	30.59	19.13	36.35	558
20	51.07	30.69	18.21	36.97	284
21	50.48	31.01	18.47	36.54	337
22	51.28	30.60	18.09	37.12	297
23	51.62	32.71	15.62	37.37	538
24	53.12	30.64	16.17	38.45	676
25	54.18	29.50	16.28	39.22	344

26	51.32	30.56	18.08	37.15	412
27	52.35	31.16	16.45	37.90	336
28	50.98	30.59	18.40	36.91	386
29	54.68	28.47	16.78	39.58	726
30	52.78	30.36	16.79	38.21	682

Table A3.1.5: Micrprobe analysis of some arsenopyrites and pyrites from the Riverlea deposit (wt %).

S	Fe	Cu	As	Ag	Sb	Au	Total
52.46	47.07	0.11	2.13	0.02	0.00	0.01	101.81
52.72	47.25	0.04	1.92	0.01	0.04	0.03	102.01
44.71	33.55	12.94	1.64	0.00	8.48	0.00	101.31
52.54	46.91	0.00	1.86	0.09	0.00	0.01	101.42
52.20	46.87	0.00	1.92	0.07	0.01	0.00	101.08
52.58	46.88	0.02	1.54	0.00	0.04	0.07	101.12
52.95	46.73	0.02	1.48	0.00	0.03	0.00	101.22
53.38	47.06	0.06	1.30	0.00	0.08	0.04	101.92
52.97	46.98	0.00	1.29	0.00	0.00	0.00	101.24
52.93	46.68	0.11	1.55	0.00	0.03	0.01	101.32
23.34	36.41	0.00	40.95	0.10	0.47	0.01	101.27
22.97	36.45	0.03	41.87	0.00	0.25	0.00	101.58
23.72	37.17	0.07	40.88	0.00	0.43	0.03	102.30
23.38	36.40	0.00	41.13	0.00	0.43	0.05	101.39
23.64	36.68	0.00	40.92	0.00	0.37	0.00	101.61
23.55	36.79	0.07	40.88	0.00	0.39	0.00	101.67
22.98	36.54	0.00	41.21	0.00	0.38	0.06	101.18
23.61	36.54	0.00	40.99	0.09	0.40	0.00	101.64
23.31	36.38	0.00	41.60	0.00	0.42	0.00	101.71
23.09	36.60	0.05	41.63	0.00	0.34	0.00	101.71
53.46	47.02	0.00	1.17	0.00	0.02	0.00	101.68
53.51	46.92	0.00	1.23	0.01	0.10	0.00	101.76
53.18	47.05	0.04	1.21	0.00	0.07	0.02	101.57
52.88	46.65	0.03	1.30	0.00	0.01	0.00	100.87
50.91	44.03	2.32	1.49	0.02	1.70	0.05	100.53
25.61	7.58	37.93	0.82	0.11	28.45	0.00	100.51
53.40	47.33	0.00	0.88	0.10	0.03	0.01	101.75
53.17	46.94	0.02	1.34	0.00	0.01	0.04	101.52
53.04	47.08	0.00	1.03	0.00	0.03	0.00	101.19
53.47	46.84	0.05	1.09	0.00	0.02	0.00	101.47
23.27	35.93	0.00	41.47	0.00	0.13	0.07	100.87
21.82	35.58	0.00	43.36	0.02	0.07	0.03	100.88
21.26	34.37	0.06	41.27	0.00	0.14	0.06	97.16
21.94	36.13	0.00	43.54	0.00	0.10	0.05	101.76
21.19	34.36	0.00	41.31	0.03	0.13	0.08	97.10
22.86	35.99	0.10	41.43	0.00	0.22	0.05	100.65

21.88	36.06	0.04	43.68	0.00	0.00	0.21	101.87
21.46	35.72	0.03	43.94	0.00	0.19	0.05	101.39
52.81	46.67	0.00	1.27	0.03	0.00	0.00	100.79
53.22	47.30	0.00	1.32	0.00	0.06	0.02	101.93
53.24	46.94	0.02	1.30	0.00	0.04	0.01	101.54
52.99	46.74	0.00	1.44	0.09	0.00	0.00	101.26
53.18	46.97	0.09	1.17	0.00	0.00	0.05	101.47
53.23	46.86	0.04	1.49	0.00	0.00	0.00	101.62
53.03	47.55	0.00	1.42	0.00	0.00	0.00	102.00
53.06	47.46	0.00	1.42	0.00	0.01	0.00	101.96
52.88	47.31	0.02	1.51	0.00	0.01	0.00	101.74
52.91	47.11	0.00	1.56	0.00	0.00	0.09	101.67

Table A3.1.6: Microprobe analysis of the Riverlea pyrites (wt %).

Fe	S	Co	Ni	Cu	As	Au	Total
47.02	52.54	0.09	0.01	0.00	1.64	0.05	101.36
46.84	52.52	0.04	0.00	0.05	1.93	0.00	101.55
46.96	52.26	0.04	0.00	0.09	1.93	0.00	101.31
46.77	52.60	0.10	0.04	0.00	1.89	0.04	101.63
46.83	52.10	0.00	0.02	0.02	2.07	0.00	101.26
46.50	52.17	0.00	0.02	0.04	2.24	0.06	101.42
46.97	52.70	0.07	0.07	0.01	1.78	0.00	101.67
46.46	51.75	0.10	0.08	0.00	2.66	0.07	101.40
47.05	52.04	0.07	0.06	0.05	2.14	0.00	101.76
46.23	51.55	0.00	0.06	0.00	2.22	0.01	100.17
46.48	52.65	0.07	0.20	0.00	2.21	0.02	101.62
47.16	51.99	0.11	0.11	0.06	2.15	0.07	101.73
46.72	52.46	0.07	0.08	0.00	2.15	0.00	101.70
47.05	51.95	0.11	0.00	0.00	1.93	0.10	101.16
47.08	52.21	0.00	0.00	0.00	2.23	0.00	101.82
46.71	52.64	0.05	0.00	0.09	1.60	0.00	101.28
46.86	52.46	0.01	0.04	0.02	1.91	0.00	101.60
47.11	52.65	0.11	0.05	0.05	1.83	0.01	102.03
47.19	52.66	0.01	0.00	0.07	1.73	0.00	101.89
46.70	51.84	0.00	0.00	0.10	1.81	0.00	100.63
46.66	52.00	0.06	0.06	0.06	2.53	0.00	101.59
46.55	51.95	0.05	0.06	0.10	2.14	0.00	101.15
46.47	52.02	0.00	0.00	0.00	2.14	0.00	100.95
46.85	52.71	0.02	0.00	0.00	1.83	0.00	101.64
46.23	52.52	0.00	0.01	0.00	1.98	0.00	100.97
46.48	52.55	0.00	0.11	0.03	1.95	0.02	101.31
40.01	45.51	0.09	0.07	0.07	1.47	0.00	87.33
47.38	52.56	0.06	0.03	0.03	1.89	0.00	102.04
47.06	52.73	0.04	0.00	0.08	1.78	0.00	102.05
46.13	51.28	0.02	0.00	0.03	1.55	0.00	99.14

47.87	54.36	0.07	0.77	0.00	0.07	0.00	100.44
43.19	44.30	0.07	0.10	0.00	1.05	0.01	103.44
47.31	53.68	0.05	0.00	0.06	0.03	0.00	100.38
45.67	52.87	0.65	0.46	0.12	0.28	0.01	101.17
46.76	53.11	0.21	0.72	0.00	0.10	0.00	100.34
46.41	53.51	0.19	0.53	0.01	0.01	0.04	101.21
47.03	52.17	0.11	0.00	0.00	1.75	0.00	101.16
47.19	52.19	0.06	0.05	0.10	1.86	0.00	101.18
46.78	52.16	0.00	0.00	0.00	1.78	0.00	101.51
46.96	52.58	0.07	0.00	0.00	1.54	0.00	100.91
47.23	52.84	0.09	0.00	0.00	1.62	0.02	101.44
46.02	51.12	0.09	0.00	0.13	2.19	0.03	101.80
47.08	51.91	0.05	0.00	0.00	2.19	0.00	99.80
47.12	52.55	0.05	0.00	0.10	1.57	0.09	101.41
45.72	50.25	0.08	0.00	0.14	2.60	0.00	101.53
45.48	50.99	0.17	0.03	0.17	0.00	0.00	98.88
46.78	52.66	0.10	0.14	0.00	0.09	0.02	97.16
46.63	53.02	0.16	0.22	0.00	0.05	0.00	100.07
46.85	52.53	0.15	0.03	0.12	0.00	0.00	100.27
46.97	53.17	0.12	0.03	0.01	0.02	0.00	99.94
46.84	52.79	0.04	0.04	0.12	0.00	0.00	100.49
46.00	51.53	0.04	0.02	0.09	0.00	0.05	100.11
46.85	52.96	0.09	0.00	0.00	0.00	0.01	98.03
46.88	52.35	0.10	0.13	0.06	0.01	0.01	100.05
47.18	52.76	0.06	0.12	0.12	0.02	0.00	99.65
46.59	51.57	0.05	0.04	0.10	1.54	0.05	100.35
47.19	52.64	0.05	0.00	0.00	0.76	0.02	100.05
46.93	52.64	0.00	0.00	0.02	0.64	0.00	100.92
46.65	52.10	0.00	0.00	0.00	1.70	0.00	100.62
46.98	52.10	0.06	0.00	0.00	2.01	0.01	100.72
46.50	51.99	0.09	0.04	0.00	1.98	0.00	101.23
46.85	51.96	0.10	0.00	0.17	1.89	0.01	100.66
46.71	51.61	0.00	0.00	0.00	2.11	0.00	101.17
47.27	51.76	0.07	0.05	0.06	1.90	0.00	100.73
46.56	51.52	0.03	0.00	0.11	2.30	0.00	101.24
47.00	52.84	0.00	0.04	0.03	0.07	0.04	100.86
47.51	52.55	0.00	0.01	0.04	0.04	0.04	100.29
47.73	53.16	0.01	0.04	0.05	0.04	0.03	100.31
47.68	53.09	0.05	0.00	0.00	0.06	0.05	101.32
47.32	53.12	0.07	0.00	0.00	0.06	0.02	101.02
47.56	53.11	0.13	0.12	0.00	0.05	0.05	100.69
47.70	53.13	0.00	0.00	0.00	0.03	0.00	101.25
47.33	52.60	0.00	0.05	0.04	0.06	0.00	101.00
47.41	52.71	0.02	0.09	0.00	0.04	0.00	100.20
47.37	52.57	0.00	0.00	0.00	0.09	0.00	100.61
46.66	52.05	0.11	0.03	0.00	1.55	0.00	100.38

46.76	51.73	0.11	0.02	0.00	1.55	0.00	100.51
47.39	52.47	0.01	0.03	0.01	1.44	0.06	100.35
46.72	51.77	0.03	0.10	0.00	1.57	0.01	101.63
41.44	45.58	0.07	0.12	0.00	1.43	0.00	100.23
46.81	51.59	0.03	0.04	0.01	1.54	0.08	88.74
46.80	51.65	0.04	0.06	0.05	1.39	0.01	100.10
46.92	51.95	0.04	0.11	0.10	0.14	0.04	100.27
46.66	51.53	0.05	0.05	0.00	1.59	0.04	99.37
46.48	51.97	0.00	0.01	0.01	1.09	0.00	100.15
46.38	51.14	0.05	0.08	0.04	2.31	0.00	99.80
46.71	51.39	0.00	0.00	0.13	1.98	0.03	100.18
46.52	50.91	0.05	0.00	0.01	1.85	0.00	100.32
46.57	51.14	0.06	0.01	0.00	2.28	0.08	99.70
46.43	51.06	0.07	0.00	0.00	2.29	0.04	100.28
47.03	51.25	0.06	0.00	0.01	2.19	0.00	100.08
46.77	51.90	0.07	0.01	0.00	1.05	0.00	100.62
46.90	52.09	0.00	0.00	0.06	0.39	0.03	99.91
47.11	52.06	0.04	0.05	0.00	0.48	0.06	99.75
47.12	52.40	0.04	0.00	0.02	0.17	0.00	99.85
46.85	52.30	0.09	0.13	0.00	0.06	0.00	99.82
46.66	52.00	0.15	0.06	0.02	0.07	0.04	99.63
47.21	52.04	0.06	0.01	0.00	0.02	0.00	99.06
47.04	52.12	0.08	0.04	0.00	0.00	0.01	99.52
46.74	51.91	0.17	0.20	0.00	0.12	0.00	99.62
46.70	52.21	0.05	0.02	0.00	0.07	0.05	99.72
46.97	52.21	0.00	0.01	0.05	0.05	0.00	99.48
47.10	52.40	0.03	0.05	0.08	0.01	0.03	99.42
47.34	51.87	0.00	0.00	0.00	0.02	0.01	99.73
47.12	52.50	0.00	0.09	0.09	0.04	0.00	99.41
46.02	51.22	0.05	0.00	0.00	0.12	0.00	100.07
45.98	50.99	0.04	0.03	0.06	0.14	0.00	97.61
46.66	51.36	0.00	0.05	0.00	0.07	0.04	97.34
46.55	50.94	0.03	0.13	0.00	0.23	0.01	98.44
46.49	51.17	0.04	0.00	0.07	0.12	0.01	98.02
46.37	51.06	0.09	0.07	0.06	0.14	0.04	98.32
45.91	50.69	0.04	0.11	0.09	0.15	0.02	98.09
45.91	50.67	0.04	0.08	0.06	0.13	0.00	97.21
45.68	50.94	0.12	0.05	0.01	0.14	0.00	97.12
46.99	51.24	0.05	0.01	0.00	0.08	0.00	97.07
45.63	50.59	0.03	0.02	0.03	0.40	0.05	98.49
46.50	51.73	0.01	0.12	0.06	0.07	0.00	97.11
46.50	51.74	0.12	0.01	0.09	0.06	0.00	98.67
46.74	51.47	0.07	0.05	0.00	0.06	0.02	99.01
46.68	51.77	0.11	0.05	0.16	0.02	0.00	98.40
46.10	51.45	0.06	0.15	0.07	0.11	0.00	98.96
45.51	50.75	0.12	0.14	0.10	0.19	0.00	98.02

46.00	51.03	0.00	0.02	0.00	0.08	0.03	97.24
46.01	51.19	0.04	0.08	0.00	0.15	0.00	97.20
43.71	48.18	0.08	0.09	0.09	0.16	0.02	97.68
46.56	51.52	0.03	0.00	0.00	1.41	0.00	92.35
46.79	51.45	0.06	0.00	0.02	1.45	0.00	99.71
46.30	51.22	0.15	0.05	0.00	1.55	0.00	100.07
47.07	51.47	0.07	0.06	0.16	1.64	0.01	99.52
47.14	51.55	0.01	0.08	0.00	1.60	0.00	100.58
46.83	51.38	0.01	0.00	0.04	1.81	0.00	100.51
47.02	51.28	0.01	0.00	0.00	1.65	0.00	100.08
46.78	51.40	0.04	0.09	0.06	1.67	0.03	100.19
46.84	51.52	0.01	0.00	0.00	1.58	0.02	100.19
46.10	50.97	0.01	0.06	0.00	2.07	0.05	100.20
41.56	49.01	0.83	0.62	2.55	2.23	0.01	99.29
42.30	49.00	0.71	0.73	1.92	2.08	0.00	98.70
44.85	50.79	0.37	0.40	0.40	0.91	0.00	98.32
43.51	49.40	0.63	0.52	1.16	1.71	0.00	98.40
41.44	48.63	0.64	0.59	2.84	1.95	0.00	97.83
44.80	49.99	0.29	0.16	0.32	0.57	0.00	98.32
41.13	48.29	0.59	0.66	3.09	2.07	0.00	96.87
43.31	49.98	0.64	0.53	1.27	1.71	0.05	98.35
43.87	49.93	0.52	0.57	0.86	1.34	0.02	98.68
46.22	51.43	0.17	0.32	0.00	0.43	0.06	98.25
46.39	51.99	0.20	0.16	0.00	0.24	0.00	99.05
46.93	52.30	0.24	0.22	0.00	0.14	0.00	99.27

Table A3.1.7: Microprobe analysis of some of the pyrite and arsenopyrite minerals of the Akbakai deposit (wt%).

Pyrite				Arsenopyrite			
Fe	As	S	Total	Fe	As	S	Total
46.64	1.80	51.53	99.97	36.15	43.12	20.72	99.99
47.13	1.09	51.78	100.00	34.52	46.07	19.33	99.92
47.40	0.87	51.73	100.00	36.64	41.79	21.54	99.97
46.78	0.97	52.22	99.97	35.52	45.26	19.20	99.98
47.05	1.46	51.48	99.99	35.37	45.39	19.21	99.97
46.55	1.51	51.91	99.97	35.73	44.37	19.90	100.00
47.33	0.52	52.13	99.98	36.41	43.11	20.48	100.00
47.18	1.83	51.00	100.01	36.44	41.12	19.41	96.97
47.20	0.59	52.20	99.99	35.63	43.76	20.56	99.95
47.15	0.85	52.00	100.00	35.26	45.23	19.23	99.72
47.14	0.59	52.27	100.00	36.14	42.18	21.66	99.98
47.19	0.97	51.84	100.00	36.01	42.25	21.74	100.00
56.59	5.20	38.18	99.97	38.40	43.17	17.78	99.35
47.05	1.12	51.83	100.00	33.37	46.23	19.96	99.56
47.47	1.06	51.45	99.98	35.91	43.75	20.33	99.99

47.06	0.98	51.96	100.00	35.72	44.01	20.25	99.98
46.75	0.76	52.47	99.98	35.37	44.70	19.89	99.96
47.01	1.66	51.33	100.00	35.07	44.69	20.27	100.03
46.51	2.31	51.18	100.00	35.74	44.29	19.95	99.98
47.04	0.90	52.06	100.00	36.45	43.82	19.74	100.01
46.89	2.05	51.05	99.99	35.93	44.05	20.01	99.99
47.17	1.44	51.40	100.01	35.30	44.99	19.71	100.00
47.51	0.77	51.73	100.01	35.38	45.11	19.48	99.97
46.62	1.14	52.20	99.96	35.09	45.20	19.71	100.00
46.81	0.73	52.42	99.96	35.85	43.38	20.69	99.92
46.96	1.73	51.31	100.00	35.88	42.95	21.16	99.99
47.34	1.08	51.55	99.97	35.37	44.53	20.03	99.93
47.08	0.78	52.14	100.00	35.21	43.67	21.06	99.94
47.18	0.95	51.87	100.00	36.20	42.38	21.42	100.00
47.45	1.64	50.91	100.00	35.69	42.22	22.08	99.99
47.20	1.82	50.98	100.00	35.22	44.76	20.01	99.99
46.82	0.98	52.21	100.01	34.59	45.22	20.19	100.00
47.34	0.78	51.88	100.00	36.35	42.83	20.82	100.00
47.18	0.89	51.91	99.98	36.07	42.97	20.93	99.97
47.84	1.10	51.05	99.99	35.64	44.27	20.09	100.00

A3.2: Results of biooxidation of different concentrates

The concentrations of iron, arsenic and dissolved oxygen (DO_2) are in mg/L in all the runs. The redox potential (E_h) is quoted against the standard hydrogen electrode. The pulp density used was 5 % (w/v) unless otherwise stated.

Run 1: Material: Indarama 2 concentrate

Time (hrs)	Total Fe	Fe(II)	Fe(III)	Total As	As(III)	As(V)	pH	E_h	DO_2
24	382	100.9	281.5	382	347.7	34.6	2.07	711	6.72
48	872	257.0	615.4	1026	927.6	98.7	2.10	706	6.07
72	2071	153.0	1918.4	2556	2250.0	306.3	2.13	717	3.63
96	3191	97.3	3094.1	4026	3621.3	405.0	1.83	728	3.84
120	3911	106.8	3804.6	4906	4299.3	607.0	1.93	755	5.40
144	4631	126.9	4504.5	5666	4759.1	907.2	1.88	767	5.50
168	4841	41.5	4799.9	5976	4989.3	987.0	1.80	771	5.53
192	5161	44.5	5116.9	6296	5122.1	1174.2	1.79	777	5.56
216	5299	38.3	5261.1	6616	5323.0	1293.4	1.81	801	5.56
240	5651	52.8	5598.6	6906	5525.1	1381.2	1.73	803	5.28
264	5981	51.8	5929.6	7266	5715.1	1551.2	1.70	804	5.58
288	6461	48.6	6412.8	7456	5813.5	1642.8	1.67	795	5.28

Run 2: Indarama 1 concentrate

Time (hrs)	Total Fe	Fe(II)	Fe(III)	Total As	As(III)	As(V)	pH	E_h	DO_2
24	490	413.4	76.7	478	404.6	73.4	1.81	677	4.63
48	1160	659.9	500.1	1350	1217.3	132.7	1.90	692	4.09
72	2710	1026.6	1683.4	3370	3167.7	202.3	1.96	715	3.22
96	4180	469.0	3711.0	4970	4353.6	616.4	1.76	755	3.46
120	5000	231.8	4768.3	5210	3620.5	1589.5	1.51	791	3.48
144	6510	258.0	6252.0	5720	2890.1	2829.9	1.35	802	2.43
168	7920	294.0	7626.1	6300	2462.6	3837.4	1.26	812	1.83
192	9850	218.1	9631.9	7240	1945.9	5294.1	1.16	817	1.94
216	11800	208.1	11591.9	7970	1436.1	6533.9	1.12	832	2.13
240	12900	203.6	12696.4	8120	1054.6	7065.4	1.06	842	2.16
264	13900	180.1	13720.0	8140	746.6	7393.4	1.04	857	2.60
312	15100	170.2	14929.8	8150	387.7	7762.3	1.01	872	3.11

Run 3: Riverlea concentrate

Time (hrs)	Total Fe	Fe(II)	Fe(III)	Total As	As(III)	As(V)	pH	E_h	DO_2
24	690	294.5	395.5	560	362.8	197.3	1.77	717	5.25
48	1770	479.1	1290.9	1850	1612.4	237.6	1.87	769	3.95
72	2680	295.6	2384.4	2220	1352.4	867.6	1.59	821	1.50
96	4100	210.4	3889.6	2510	853.8	1656.2	1.44	827	2.64
120	6130	192.8	5937.2	3300	495.1	2804.9	1.34	871	3.28
144	7530	207.1	7322.9	3800	446.6	3353.4	1.24	897	3.28
168	8930	184.0	8746.0	4200	394.1	3805.9	1.20	917	2.70
192	10400	188.4	10211.6	4570	293.5	4276.5	1.14	941	2.26
216	11400	192.0	11208.0	4685	233.6	4451.4	1.13	949	2.22
240	12000	183.8	11816.2	4690	180.0	4510.0	1.09	948	3.16
264	12600	175.3	12424.7	4690	125.9	4564.1	1.11	948	4.05
312	13000	171.0	12829.0	4695	94.5	4600.5	1.10	952	4.41

Run 4: Akbakai 2 concentrate

Time (hrs)	Total Fe	Fe(II)	Fe(III)	Total As	As(III)	As(V)	pH	E_h	DO_2
24	2084	373.2	1710.9	2596	2446.6	149.6	1.80	741	3.72
48	3534	245.9	3288.1	3616	2692.6	923.6	1.56	789	2.66
72	4934	163.9	4770.1	4226	2341.9	1884.3	1.35	802	1.63
96	6464	142.1	6322.0	4966	1974.4	2991.8	1.26	818	1.60
120	7954	158.5	7795.5	5706	1851.3	3854.9	1.17	832	1.62
144	9454	91.6	9362.5	6126	1203.8	4922.4	1.12	852	1.83
168	10584	156.8	10427.2	6186	729.7	5456.5	1.07	867	2.62
192	11784	113.0	11671.0	6266	323.0	5943.2	1.03	898	3.08
216	12484	91.6	12392.4	6272	146.8	6125.4	0.98	909	3.12
240	12984	98.9	12885.1	6286	70.4	6215.8	0.98	914	4.32

Run 5: Akbakai 1 concentrate

Time (hrs)	Total Fe	Fe(II)	Fe(III)	Total As	As(III)	As(V)	pH	E_h	DO_2
24	1688	16.7	1671.3	364	108.3	255.6	1.85	703	5.09
48	2468	14.2	2453.9	748	257.8	490.1	1.75	829	4.98
72	3278	10.5	3267.5	1297	582.1	714.8	1.65	851	3.02
96	3798	23.0	3775.1	1767	828.3	938.6	1.51	862	2.23
120	3998	20.0	3978.0	1877	842.5	1034.4	1.48	869	5.39
144	4198	22.4	4175.6	1977	878.0	1098.9	1.47	878	6.16
168	4388	20.5	4367.5	2017	872.6	1144.3	1.46	879	6.38
192	4388	20.4	4367.6	2017	855.1	1161.8	1.44	879	6.78
216	4458	26.7	4431.3	2027	762.2	1264.7	1.42	907	6.77
240	4462	20.9	4397.2	2029	733.5	1295.4	1.41	909	6.84

Run 6: Olympius concentrate

Time (hrs)	Total Fe	Fe(II)	Fe(III)	Total As	As(III)	As(V)	pH	E_h
24	1150	383.7	766.3	650	304.4	345.6	1.63	772
48	2860	251.4	2608.6	1600	666.3	933.7	1.52	787
72	4400	202.8	4197.2	2210	682.0	1528.0	1.38	797
96	5840	153.7	5686.3	2710	632.0	2078.0	1.29	803
120	7210	189.0	7021.0	3080	512.9	2567.1	1.22	810
144	8530	195.2	8334.8	3370	343.0	3027.0	1.16	819
168	9640	114.8	9525.2	3560	230.5	3329.5	1.14	830
192	10800	196.6	10603.4	3690	141.2	3548.8	1.07	838
216	11600	185.2	11414.8	3695	49.2	3645.8	1.10	842
240	12600	140.7	12459.4	3710	9.8	3700.2	1.04	854
264	13800	130.2	13669.8	3810	4.3	3805.7	1.02	868

Run 7: Indarama/Stratoni mixture-M1

Time (hrs)	Total Fe	Fe(II)	Fe(III)	Total As	As(III)	As(V)	pH	E_h	DO_2
24	1760	290.9	1469.2	1420	905.9	514.1	1.90	729	2.32
48	3520	255.9	3264.1	3320	2192.6	1127.4	1.85	752	1.83
72	5400	210.0	5190.0	4540	2210.9	2329.1	1.64	791	1.66
96	7070	123.9	6946.1	5200	1926.3	3273.7	1.46	821	1.76
120	8550	72.6	8477.4	5550	1416.4	4133.6	1.31	830	1.46
144	9790	89.9	9700.1	5810	1106.2	4703.9	1.22	834	1.51
168	11200	212.8	10987.2	6090	956.4	5133.6	1.14	854	2.47
192	12100	196.2	11903.8	6130	569.8	5560.2	1.07	862	3.04
216	12900	124.3	12775.7	6220	449.8	5770.2	1.04	866	4.11
240	13400	92.1	13308.0	6221	289.7	5931.3	1.03	882	4.36
264	14100	46.4	14053.6	6225	224.2	6000.8	1.03	884	5.06

Run 8: Indarama 2/Stratoni concentrates mixture-M 2

Time (hrs)	Total Fe	Fe(II)	Fe(III)	Total As	As(III)	As(V)	pH	E_h	DO_2
24	1440	1086.6	353.4	1420	1002.6	417.8	1.71	716	2.98
48	2700	704.2	1995.8	2870	1960.8	909.7	1.71	739	2.20
72	4230	315.1	3914.9	4240	2589.0	1651.4	1.60	770	1.60
96	5780	126.8	5653.2	4960	2206.0	2754.4	1.42	802	1.28
120	6990	65.1	6924.9	5140	1537.9	3602.5	1.28	819	1.38
144	8380	23.0	8357.0	5390	1088.8	4301.6	1.20	834	1.61
168	9380	52.1	9327.9	5419	652.0	4767.1	1.13	837	1.63
192	10780	48.0	10732.1	5420	349.4	5070.6	1.07	853	2.01
216	11780	36.4	11743.6	5422	160.1	5261.9	1.03	866	2.62
240	12680	30.0	12650.0	5424	55.6	5368.4	1.01	880	3.22
264	13080	32.3	13047.7	5427	8.7	5418.3	0.98	887	3.65

Run 9: Fairview concentrate

Time (hrs)	Total Fe	Fe(II)	Fe(III)	Total As	As(III)	As(V)	pH	E_h
24	1120	649.2	470.8	401	165.3	235.7	1.82	793
48	2390	897.0	1493.0	1230	574.2	655.8	1.78	798
72	4880	547.0	4333.0	1690	342.2	1347.8	1.57	820
96	5250	405.5	4844.5	1730	191.1	1538.9	1.49	839
120	5810	305.3	5504.7	1830	139.8	1690.2	1.47	860
144	6600	283.5	6316.5	1950	107.5	1842.5	1.44	869
192	7810	196.4	7613.6	2090	47.1	2042.9	1.44	887
216	8120	164.2	7955.9	2130	39.7	2090.4	1.42	898
240	8400	165.2	8234.8	2150	24.9	2125.1	1.41	902

Run 10: Indarama 2 concentrate

Time (hrs)	Total Fe	Fe(II)	Fe(III)	Total As	As(III)	As(V)	pH	E_h	DO_2
24	1140	1002.4	137.6	737	517.8	219.6	1.84	678	5.52
48	2120	1599.2	520.9	2134	1760.6	373.8	1.80	700	3.12
72	3750	1217.3	2532.7	4224	3495.6	728.8	1.81	722	1.87
96	5240	669.0	4571.0	6094	4828.4	1266.0	1.77	743	1.76
120	6840	175.6	6664.4	7594	5208.6	2385.8	1.62	789	2.45
144	7980	58.6	7921.5	8024	4454.8	3569.6	1.46	818	2.85
168	9380	43.8	9336.2	8494	3849.5	4644.9	1.34	840	2.90
192	10180	33.8	10146.2	8544	3281.8	5262.6	1.28	852	3.24
216	11080	27.9	11052.2	8734	2847.5	5886.9	1.23	867	3.74
240	11580	23.5	11556.5	8744	2521.3	6223.1	1.15	874	4.53
264	11980	22.1	11957.9	8749	2305.7	6443.7	1.01	883	5.43

Run 11: Indarama 2/Stratoni concentrates mixture-M 1

Time (hrs)	Total Fe	Fe(II)	Fe(III)	Total As	As(III)	As(V)	pH	E_h	DO_2
24	1960	240.2	1719.8	1605	1157.5	447.9	1.78	720	3.80
48	3880	171.3	3708.7	3905	2629.8	1275.6	1.79	762	2.09
72	6340	33.9	6306.1	5205	2258.0	2947.4	1.45	825	1.45
96	8780	17.0	8763.0	5925	1461.7	4463.7	1.27	882	1.17
120	10280	22.4	10257.6	5955	697.4	5258.0	1.16	914	1.74
144	11480	13.0	11467.0	6085	466.8	5618.6	1.13	935	3.70
168	13480	20.5	13459.5	6275	275.7	5999.7	1.11	935	3.84
192	13580	2.0	13578.0	6285	129.5	6155.9	1.08	939	4.52
216	13680	5.5	13674.5	6225	65.7	6159.7	1.07	946	5.17
240	13684	42.7	13641.3	6276	19.7	6256.6	1.06	946	5.36
264	13687	15.4	13671.6	6280	18.4	6261.4	1.02	952	5.80

Run 12: Riverlea concentrate

Time (hrs)	Total Fe	Fe(II)	Fe(III)	Total As	As(III)	As(V)	pH	E_h	DO_2
24	2780	1667.1	1112.9	1459	668.3	790.3	1.67	715	4.35
48	4010	734.8	3275.2	2709	1652.6	1056.0	1.66	761	2.91
72	6170	313.8	5856.2	3529	994.7	2533.9	1.41	806	1.67
96	8320	222.4	8097.6	3919	330.1	3588.5	1.24	844	1.60
120	10720	278.6	10441.4	4319	120.1	4198.5	1.15	910	3.00
144	12020	196.9	11823.1	4529	116.0	4412.6	1.08	920	3.32
168	12820	178.7	12641.3	4679	115.4	4563.2	1.07	924	3.75
192	13220	159.4	13060.6	4749	113.0	4635.6	1.04	934	4.13
216	13420	119.1	13300.9	4759	102.1	4656.5	1.03	930	4.42
240	13520	83.4	13436.6	4769	78.8	4689.8	1.03	929	5.18

Run 13: Akbakai 2 concentrate

Time (hrs)	Total Fe	Fe(II)	Fe(III)	Total As	As(III)	As(V)	pH	E_h	DO_2
24	1250	1187.9	62.1	1127	701.1	425.7	1.64	740	3.72
48	2640	729.6	1910.4	2777	2087.6	689.3	1.61	744	2.66
72	4180	651.4	3528.6	4477	3391.9	1084.9	1.58	762	2.63
96	5530	531.2	4998.8	5557	3646.1	1910.8	1.45	793	2.60
120	6770	297.4	6472.6	5987	2950.2	3036.6	1.30	813	2.62
144	7900	232.7	7667.3	6167	2228.1	3938.7	1.20	822	1.83
168	9000	279.9	8720.1	6257	1461.1	4795.7	1.12	835	1.62
192	10000	189.6	9810.4	6317	995.9	5320.9	1.10	843	1.08
216	11100	188.2	10911.8	6367	628.7	5738.1	1.17	852	3.12
240	11900	166.0	11734.0	6367	359.2	6007.6	1.17	862	4.32
264	12600	150.3	12449.7	6387	220.9	6166.0	1.17	870	5.26

Run 14: Indarama 1 concentrate

Time (hrs)	Total Fe	Fe(II)	Fe(III)	Total As	As(III)	As(V)	pH	E_h	DO_2
24	2280	1386.1	893.9	1862	1499.7	362.3	1.78	714	4.28
48	4250	1560.2	2689.8	4362	3516.6	845.4	1.85	717	2.69
72	6130	708.8	5421.2	6382	4563.5	1818.5	1.72	749	2.08
96	7550	430.0	7120.1	7062	3633.6	3428.4	1.45	781	1.73
120	8820	270.0	8550.0	7342	2740.4	4601.6	1.32	798	1.63
144	9820	241.3	9578.7	7612	2298.6	5313.4	1.22	802	1.81
168	11120	205.7	10914.3	7762	1656.6	6105.4	1.20	820	1.67
192	12020	180.4	11839.6	7822	1079.9	6742.1	1.17	822	2.66
216	13220	142.4	13077.6	7922	601.0	7321.0	1.08	842	2.54
240	14320	140.2	14179.8	7952	298.5	7653.5	1.04	875	2.64
264	15420	126.9	15293.1	8002	173.1	7828.9	1.02	908	2.77
288	16120	122.3	15997.7	8010	29.0	7981.0	0.93	918	3.17
312	16620	88.1	16531.9	8022	19.6	8002.5	0.92	933	4.42

Run 15: Indarama 1 concentrate

Time (hrs)	Total Fe	Fe(II)	Fe(III)	Total As	As(III)	As(V)	pH	E_h
24	830	1812.0	4108.0	701	538.0	163.0	1.82	720
48	2340	1762.3	5667.7	2354	1913.7	440.3	1.85	725
72	3550	1730.3	6909.7	3974	3121.2	852.8	1.79	726
96	4810	1208.1	8691.9	5484	4084.2	1399.8	1.73	742
120	6010	732.0	10368.1	6594	4504.3	2089.7	1.60	761
144	7110	474.3	11725.7	7204	4115.7	3088.3	1.50	779
168	8010	419.8	12680.2	7464	3372.4	4091.6	1.40	787
192	8910	415.2	13584.8	7774	3064.9	4709.2	1.36	788
240	9710	239.8	14560.2	7782	2080.2	5701.8	1.26	803
264	10310	327.3	15072.7	7814	1802.1	6011.9	1.22	802
288	11010	263.9	15836.1	7974	1485.9	6488.1	1.21	806

Run 16: Indarama 1 concentrate

Time (hrs)	Total Fe	Fe(II)	Fe(III)	Total As	As(III)	As(V)	pH	E_h
24	730	3390.3	7309.1	732	601.5	130.5	1.47	717
48	1330	3382.3	7917.0	1646	1335.5	310.5	1.52	709
72	2330	3446.6	8853.4	2746	2270.1	475.9	1.63	715
96	3330	3114.1	10186.0	3866	2931.6	934.4	1.64	722
120	4530	2194.7	12305.4	5046	3374.0	1672.0	1.60	734
144	5230	1463.8	13736.2	5936	3983.7	1952.3	1.50	752
168	6030	864.4	15135.7	6646	4062.6	2583.4	1.48	766
192	7230	547.0	16653.0	7206	3671.8	3534.2	1.43	785
216	8130	354.2	17745.5	7536	3221.2	4314.8	1.38	812
264	9130	235.9	18864.1	7706	2165.1	5540.9	1.26	817

Run 17: Indarama 1 concentrate

Time (hrs)	Total Fe	Fe(II)	Fe(III)	Total As	As(III)	As(V)	pH	E_h	DO_2
24	3070	371.5	2698.5	1060	335.2	724.8	1.61	727	4.50
48	3830	269.8	3560.2	1800	897.9	902.1	1.73	750	1.22
72	4740	457.6	4282.3	2730	1489.4	1240.6	1.76	753	1.40
96	5260	535.3	4724.8	3620	2690.2	929.8	1.84	750	1.35
120	5960	239.8	5720.2	4540	2433.5	2106.5	1.82	779	1.41
143	6520	102.0	6418.0	4630	2465.7	2164.3	1.62	788	1.42
168	7440	35.1	7405.0	4790	2300.4	2489.6	1.48	812	1.44
192	8660	46.4	8613.6	5210	1782.8	3427.2	1.37	826	2.69
216	10500	15.1	10484.2	6040	1226.3	4813.7	1.29	834	2.41
240	12200	19.4	12180.6	7060	1099.1	5960.9	1.21	850	3.38

Run 18: Indarama 1 concentrate

Time (hrs)	Total Fe	Fe(II)	Fe(III)	Total As	As(III)	As(V)	pH	E_h	DO_2
24	8640	1837.3	6802.7	3630	326.5	3303.5	1.52	701	6.54
48	8500	1574.3	6925.8	3620	465.9	3154.1	1.50	701	6.61
72	8670	832.1	7837.9	3830	602.6	3227.4	1.55	707	5.66
96	8820	687.0	8133.0	4300	1018.2	3281.8	1.57	728	3.65
120	9910	544.9	9365.1	5400	1732.6	3667.4	1.55	734	2.83
143	10800	526.9	10273.1	6480	2627.4	3852.6	1.55	744	2.44
168	11800	335.5	11464.5	7660	3249.2	4410.8	1.52	759	2.43
192	12900	282.4	12617.6	8570	3428.4	5141.6	1.49	772	2.01
216	14000	191.0	13809.0	9210	3290.4	5919.6	1.36	784	2.69
240	14500	143.3	14356.7	9320	2770.3	6549.7	1.30	789	2.36

Run 19: Akbakai 2 concentrate

Time (hrs)	Total Fe	Fe(II)	Fe(III)	Total As	As(III)	As(V)	pH	E_h	DO_2
24	2500	204.9	2295.1	731	254.6	476.4	1.85	752	5.17
48	3150	19.3	3130.8	1190	460.4	729.6	1.73	839	2.21
72	4090	11.2	4078.8	1620	488.3	1131.7	1.65	879	1.77
96	5000	13.2	4986.9	1980	449.5	1530.5	1.56	901	2.73
120	5820	8.9	5811.1	2360	393.5	1966.5	1.50	912	4.24
143	6300	3.3	6296.7	2620	380.7	2239.3	1.48	917	5.50
168	6550	1.4	6548.7	2730	400.5	2329.5	1.47	925	5.84
192	6690	4.2	6685.8	2780	412.7	2367.3	1.45	937	6.23
216	6820	5.2	6814.8	2830	345.5	2484.5	1.44	942	6.35
240	6900	0.0	6900.0	2850	349.9	2500.1	1.44	944	6.68

Run 20: Indarama 1 concentrate, pH = 1.5

Time (hrs)	Total Fe	Fe(II)	Fe(III)	Total As	As(III)	As(V)	pH	E_h
24	1160	523.8	636.2	787	587.9	199.1	1.53	707
48	2800	605.5	2194.5	2848	2343.9	504.2	1.61	728
72	5110	774.0	4336.0	5150	4021.8	1128.2	1.56	750
96	6280	587.0	5693.0	6520	4968.2	1872.9	1.51	775
120	7550	456.2	7093.8	7060	4208.6	2851.4	1.38	785
144	8360	356.5	8003.5	7270	3411.2	3858.8	1.35	792
168	9260	396.4	8863.6	7410	2734.9	4675.2	1.34	810
192	10400	391.9	10008.1	7550	1894.9	5655.1	1.34	812
216	12000	354.4	11645.6	7580	1562.9	6017.1	1.41	812
240	12100	222.0	11878.0	7610	1194.4	6415.7	1.41	810
264	12200	196.0	12004.0	7710	962.4	6747.6	1.45	812
288	12300	184.0	12116.0	7930	694.1	7235.9	1.41	812
312	12500	174.0	12326.0	8160	571.1	7588.9	1.44	816

Run 20: indarama 1 concentrate, pH = 1.5

Time (hrs)	Total Fe	Fe(II)	Fe(III)	Total As	As(III)	As(V)	pH	E_h
24	1030	519.2	510.8	771	577.3	193.7	1.53	707
48	2740	600.0	2140.0	2820	2335.7	484.3	1.61	728
72	4750	763.0	3987.0	5090	3990.6	1099.4	1.56	750
96	5980	574.5	5405.5	6290	4421.2	1868.8	1.51	775
120	7210	423.7	6786.3	6910	4156.9	2753.1	1.38	785
144	7890	346.4	7543.6	6760	3253.7	3506.3	1.35	792
168	8350	382.6	7967.4	6380	2510.0	3870.0	1.34	810
192	9150	379.2	8770.8	6410	1855.0	4555.0	1.34	812
216	10200	344.0	9856.0	6520	1456.9	5063.1	1.41	812
240	10300	185.0	10115.0	6280	1130.0	5150.0	1.41	810
264	10600	166.0	10434.0	6040	871.5	5168.5	1.45	812
288	10500	154.0	10346.0	5900	601.6	5298.4	1.41	812
312	11500	143.0	11357.0	6200	479.5	5720.5	1.44	816

Run 21: Indarama 1, pH = 1.8

Time (hrs)	Total Fe	Fe(II)	Fe(III)	Total As	As(III)	As(V)	pH	E_h
24	1190	891.5	298.5	598	437.2	160.8	1.93	692
48	2120	720.6	1399.4	2198	1603.0	595.1	2.03	718
72	4070	940.7	3129.3	4450	3567.0	883.0	2.01	720
96	5690	644.0	5046.0	5840	3776.8	2063.2	1.80	776
120	7070	313.5	6756.5	6440	3166.2	3273.8	1.66	779
144	8090	597.6	7492.4	6740	2623.9	4116.1	1.64	806
168	9280	567.6	8712.4	7080	1988.7	5091.3	1.63	813
192	10100	803.8	9296.2	7110	1457.8	5652.3	1.66	817
216	11100	702.9	10397.1	7370	1103.7	6266.3	1.72	815
240	11900	839.1	11060.9	7530	845.7	6684.3	1.72	815
264	12000	532.0	11468.0	7580	733.4	6846.6	1.73	823
288	13100	421.3	12678.7	7600	518.1	7081.9	1.73	823
312	13800	253.7	13546.3	7770	378.8	7391.2	1.75	824

Run 21: Indarama 1 concentrate, pH = 1.8

Time (hrs)	Total Fe	Fe(II)	Fe(III)	Total As	As(III)	As(V)	pH	E_h
24	684	526.3	157.7	538	428.6	109.4	1.93	692
48	1770	673.4	1096.6	1700	1595.2	104.8	2.03	718
72	3540	872.5	2667.5	4100	3550.0	550.0	2.01	720
96	4790	248.0	4542.0	5150	3746.2	1403.8	1.80	776
120	5720	221.9	5498.1	5270	2972.6	2297.4	1.66	779
144	6060	470.0	5590.0	4910	2396.3	2513.7	1.64	806
168	6680	544.3	6135.8	4670	1828.1	2841.9	1.63	813
192	7110	596.6	6513.4	4390	1322.6	3067.4	1.66	817
216	7470	586.7	6883.3	4070	920.3	3149.7	1.72	815
240	8270	581.3	7688.8	4170	656.7	3513.3	1.72	815
264	8840	401.0	8439.0	4200	450.1	3749.9	1.73	823
288	9290	256.0	9034.0	4180	353.2	3826.8	1.73	823
312	9750	211.9	9538.1	4190	196.2	3993.8	1.75	824

Run 22: Indarama 1, pH = 2.5

Time (hrs)	Total Fe	Fe(II)	Fe(III)	Total As	As(III)	As(V)	pH	E_h
24	913	888.0	25.0	688	467.2	220.8	2.64	672
48	1880	1813.0	67.0	1930	1537.6	392.4	2.65	655
72	2520	2403.2	116.8	2830	1935.4	894.6	2.34	698
96	3040	2485.9	554.1	3600	2779.8	820.2	2.29	695
120	3560	2154.2	1405.8	4500	3654.6	845.4	2.34	703
144	4220	1543.8	2676.2	5170	3895.8	1274.2	2.36	711
168	4680	1405.6	3274.4	5870	3838.2	2031.8	2.24	722
192	5080	1039.5	4040.5	6150	3925.1	2224.9	2.21	736
216	5390	841.2	4548.8	6530	3797.9	2732.1	2.21	746
240	5740	920.8	4819.2	6650	3831.5	2818.5	2.36	756
264	6060	745.0	5315.0	6790	3607.3	3182.7	2.19	759
288	6330	523.0	5807.0	6790	3317.6	3472.4	2.16	765
312	6500	352.0	6148.0	7010	2923.6	4086.4	2.15	774

Run 22: Indarama 1, pH = 2.5

Time (hrs)	Total Fe	Fe(II)	Fe(III)	Total As	As(III)	As(V)	pH	E_h
24	399	388.0	11.0	504	450.0	54.1	2.64	672
48	973	943.6	29.5	1440	1397.5	42.5	2.65	655
72	998	976.6	21.4	1870	1825.0	45.0	2.34	698
96	850	830.1	20.0	2223	2126.8	96.3	2.29	695
120	738	698.0	40.0	2690	2619.0	71.0	2.34	703
144	639	614.9	24.1	2870	2773.5	96.5	2.36	711
168	548	530.0	18.0	2930	2863.0	67.0	2.24	722
192	423	419.5	3.5	2770	2729.0	41.0	2.21	736
216	353	343.7	9.3	2670	2641.0	29.0	2.21	746
240	271	268.4	2.6	2330	2194.0	136.0	2.36	756
264	200	195.1	4.9	2010	1984.0	26.0	2.19	759
288	185	178.3	6.8	1740	1674.0	66.0	2.16	765
312	188	176.0	12.0	1490	1364.0	126.0	2.15	774

Run 23: Fairview concentrate, pulp density (w/v) = 10 %

Time (hrs)	Total Fe	Fe(II)	Fe(III)	Total As	As(III)	As(V)	pH	E_h
24	1720	1667.4	52.6	679	370.2	308.8	1.91	719
48	3220	2119.1	1100.9	2310	1501.6	808.4	1.92	776
72	4750	1552.1	3197.9	2570	739.5	1830.5	1.59	814
96	6590	894.8	5695.2	2930	402.4	2527.6	1.47	829
120	8170	744.3	7425.7	3200	258.9	2941.1	1.41	844
144	10100	634.6	9465.4	3680	188.1	3491.9	1.38	866
168	10800	575.1	10224.9	3750	72.4	3677.6	1.34	867
192	12200	485.9	11714.1	3940	58.5	3881.5	1.28	869
216	13000	425.2	12574.8	3970	49.3	3920.7	1.26	880
240	13800	384.0	13416.0	4060	40.4	4019.7	1.24	872

Run 24: Fairview concentrate, pulp density (w/v) = 15 %

Time (hrs)	Total Fe	Fe(II)	Fe(III)	Total As	As(III)	As(V)	pH	E_h
24	3060	2720.0	340.0	1910	1443.8	466.3	2.16	697
48	5490	3716.7	1773.3	3880	2176.5	1703.5	1.75	763
72	8280	2964.7	5315.3	4510	946.5	3563.5	1.43	785
96	11500	1961.8	9538.2	5210	430.9	4779.1	1.31	819
120	13500	1535.5	11964.5	5520	249.1	5270.9	1.29	819
144	15900	764.2	15135.8	5850	75.8	5774.3	1.22	852
168	17800	824.6	16975.4	5900	27.7	5872.3	1.20	862
192	19900	766.4	19133.6	6040	28.1	6011.9	1.16	872
216	21900	837.4	21062.6	6260	20.8	6239.2	1.12	872
240	22200	380.1	21819.9	6261	0.0	6261.0	1.11	886

Run 25: Fairview concentrate, pulp density (w/v) = 20 %

Time (hrs)	Total Fe	Fe(II)	Fe(III)	Total As	As(III)	As(V)	pH	E_h
24	3370	3112.5	257.5	1870	1306.7	563.3	2.35	668
48	5290	4258.3	1031.7	3990	2860.9	1129.1	1.95	726
72	7190	3518.8	3671.2	5230	2623.8	2606.2	1.63	752
96	10200	2411.9	7788.1	5820	1031.4	4788.6	1.36	806
120	12800	1912.8	10887.2	6440	719.4	5720.6	1.35	806
144	16000	985.5	15014.5	7080	283.7	6796.3	1.25	807
168	17000	1114.8	15885.2	7190	232.7	6957.3	1.18	796
192	18600	997.3	17602.7	7440	146.2	7293.8	1.16	804
216	19900	915.2	18984.9	7620	117.5	7502.5	1.15	811
240	21000	539.5	20460.6	7720	62.1	7657.9	1.14	813

Run 26: Indarama 1 concentrate

Time (hrs)	Total Fe	Fe(II)	Fe(III)	Total As	As(III)	As(V)	pH	E_h	DO_2
24	1780	1600.8	179.2	1285	1104.1	180.5	1.69	694	2.16
48	3170	1438.5	1731.5	2985	2730.1	254.5	1.82	712	1.79
72	4700	723.5	3976.5	4895	4028.5	866.2	1.76	741	1.26
96	6210	219.3	5990.8	6075	4079.0	1995.6	1.56	783	1.11
120	6980	112.6	6867.4	6165	3110.1	3054.5	1.40	812	1.11
144	8300	79.3	8220.7	6585	2371.6	4213.0	1.27	825	1.08
168	9400	48.6	9351.4	6655	1722.8	4931.8	1.22	834	1.28
192	10700	36.4	10663.6	7055	1317.3	5737.3	1.12	847	2.04
216	12000	53.6	11946.4	7165	941.5	6223.1	1.09	847	2.32
240	12800	33.9	12766.1	7185	633.0	6551.6	1.05	864	2.35
264	13600	25.3	13574.7	7185	452.2	6732.4	1.00	874	3.45
288	14300	39.6	14260.5	7265	370.1	6894.5	0.96	892	4.62
312	14800	39.2	14760.8	7325	294.1	7030.5	0.94	898	5.12

Run 27: Indarama 1 concentrate

Time (hrs)	Total Fe	Fe(II)	Fe(III)	Total As	As(III)	As(V)	pH	E_h	DO_2
24	1150	1080.4	69.6	1084.6	1036.6	48.0	1.75	711	3.25
48	2700	1063.9	1636.1	2664.6	2522.5	142.1	1.82	725	2.16
72	4130	494.2	3635.8	4414.6	3788.1	626.5	1.87	749	1.93
96	5250	101.9	5148.1	5054.6	3610.1	1444.5	1.63	798	2.72
120	6010	44.0	5966.0	5204.6	2958.8	2245.8	1.50	830	2.71
144	6940	36.6	6903.4	5454.6	2411.6	3043.0	1.38	833	2.72
168	8100	36.2	8063.9	5794.6	1847.1	3947.5	1.28	839	2.26
192	9100	37.0	9063.0	6024.6	1481.2	4543.4	1.22	829	1.76
216	10300	44.9	10255.1	6274.6	1119.2	5155.4	1.17	843	2.24
240	11000	37.8	10962.2	6284.6	864.8	5419.8	1.11	863	2.93
264	11900	40.0	11860.0	6384.6	668.7	5715.9	1.07	870	3.71
288	12500	35.8	12464.3	6396.6	529.1	5867.5	1.03	880	4.15
312	13100	44.6	13055.4	6424.6	411.5	6013.1	1.03	890	4.96

Run 28: Indarama 1 concentrate

Time (hrs)	Total Fe	Fe(II)	Fe(III)	Total As	As(III)	As(V)	pH	E_h	DO_2
24	1900	1341.4	558.6	1793	1458.4	335.0	1.79	719	1.60
48	3210	557.1	2652.9	3243	2580.1	663.3	1.78	770	2.71
72	3970	361.0	3609.0	3853	2778.4	1075.0	1.63	810	3.73
96	4900	283.7	4616.3	4343	2619.4	1724.0	1.53	834	4.33
120	5300	270.3	5029.7	4583	2385.4	2198.0	1.43	840	4.35
144	5520	195.8	5324.2	4593	2253.9	2339.6	1.39	845	4.32
168	5920	134.9	5785.1	4663	1822.9	2840.5	1.32	852	4.24
192	6770	180.0	6590.0	4673	1422.6	3250.8	1.30	863	4.42
216	7310	106.4	7203.6	4685	1281.4	3404.0	1.28	866	4.36
240	7840	77.3	7762.7	4698	1141.5	3556.9	1.24	890	4.56
264	8340	76.7	8263.3	4713	951.3	3762.1	1.20	890	4.91
288	8440	234.4	8205.6	4723	847.3	3876.1	1.17	901	5.12
312	9340	198.8	9141.3	4725	770.3	3955.1	1.16	904	5.36

Run 29: Solution of As(III)

Time (hrs)	Total Fe	Fe(II)	Fe(III)	Total As	As(III)	As(V)	pH	E_h
24	1330	389.0	941.0	1970	1136.3	833.8	1.71	737
48	1960	415.7	1544.3	1970	741.8	1228.3	1.53	756
72	2720	432.9	2287.1	1980	382.8	1597.2	1.43	772
96	3650	389.7	3260.3	2050	168.6	1881.4	1.35	785
120	4550	363.3	4186.7	2040	68.4	1971.6	1.30	797
144	5450	493.9	4956.1	2040	36.0	2004.0	1.26	809
168	6440	290.2	6149.8	2060	29.7	2030.3	1.19	824
192	7290	268.5	7021.5	2060	28.5	2031.5	1.17	825
216	8450	232.1	8217.9	2100	20.6	2079.5	1.15	826

Run 30: Solution of As(III)

Time (hrs)	Total Fe	As(III)	pH	E_h
24	9230	1380.0	1.91	697
48	9230	1350.0	1.83	765
72	9230	1326.0	1.74	878
96	9230	1420.0	1.71	878
120	9230	1449.0	1.65	876
144	9230	1401.8	1.60	887
168	9230	1410.8	1.59	890
192	9230	1341.8	1.57	895
216	9230	1352.0	1.53	892

Run 31: Solution of As(III)

Time (hrs)	Total Fe	Fe(II)	Fe(III)	Total As	As(III)	As(V)	pH	E_h
24	8910	3485.3	5424.7	1970	1030.5	939.5	1.53	693
48	9020	4131.8	4888.2	1980	951.0	1029.0	1.59	687
72	8960	4469.4	4490.6	1960	831.8	1128.3	1.46	677
96	9030	4720.3	4309.7	1960	815.3	1144.8	1.46	671
120	9090	4874.0	4216.0	1970	747.2	1222.9	1.32	674
144	9040	5112.0	3928.0	1950	704.1	1245.9	1.34	668
168	8770	6532.6	2237.4	1890	624.6	1265.4	1.34	662
192	8960	7239.6	1720.4	1910	608.6	1301.4	1.33	660
216	8820	7224.5	1595.6	1870	607.0	1263.0	1.34	662

Run 32: Solution of As(III)

Time (hrs)	Total Fe	As(III)	pH	E_h
24	9070	1509.6	1.69	879
48	9070	1512.8	1.46	871
72	9070	1511.3	1.71	875
96	9070	1528.3	1.70	876
120	9070	1530.0	1.52	875
144	9070	1563.0	1.54	871
168	9070	1566.0	1.57	873
192	9070	1563.0	1.54	875
216	9070	1560.8	1.53	873

Run 33: Solution of As(III)

Time (hrs)	Total Fe	Fe(II)	Fe(III)	Total As	As(III)	As(V)	pH	E_h
24	7520	313.8	7206.2	2770	786.8	1983.3	1.24	783
48	8490	289.1	8200.9	2730	416.5	2313.5	1.12	812
72	9350	278.4	9071.6	2760	64.3	2695.7	1.08	821
96	10200	276.6	9923.4	2730	28.6	2701.4	1.03	840
120	10900	270.5	10629.5	2720	24.9	2695.1	0.99	842
144	11900	260.3	11639.7	2780	7.2	2772.8	0.96	847
168	12100	255.2	11844.8	2700	6.3	2693.8	0.95	848
192	13200	246.3	12953.7	2720	5.5	2714.5	0.92	854
216	13800	231.8	13568.2	2720	4.8	2715.3	0.90	860

Table A3.2.1: Chemical analysis of some of the soluble solids in the biooxidation residues.

Sample Location	wt % Fe	wt % As	wt % S	Fe [M]	As [M]	Molar Ratio Fe/As
Indarama	1.66	0.64	0.24	12.10	3.47	3.49
Indarama	2.22	0.85	0.42	16.03	4.55	3.52
Indarama	1.78	0.72	0.28	12.36	3.70	3.34
Indarama	1.05	0.46	0.14	7.38	2.39	3.09
Indarama	1.60	1.29	0.21	11.82	7.11	1.66
Indarama	1.65	1.21	0.13	12.70	6.98	1.82
Indarama	1.73	0.64	0.19	12.50	3.47	3.60
Riverlea	3.06	0.56	0.17	21.67	2.95	7.35
Riverlea	2.55	0.39	0.12	20.59	2.34	8.82
Riverlea	2.64	0.41	0.09	19.16	2.22	8.65
Akbakai	0.63	0.36	0.31	4.83	2.03	2.38
Akbakai	0.42	0.18	0.25	3.06	0.98	3.13
Akbakai	0.44	0.23	0.24	3.67	1.43	2.57
Inda/Str	1.13	0.74	0.51	7.84	3.83	2.05
Indara/Strat	2.03	1.02	0.30	15.11	5.67	2.66
Indara/Strat	1.21	0.69	0.33	8.67	3.68	2.35
Olympias	0.12	0.10	0.18	1.00	0.62	1.61
Olympias	0.80	0.43	0.44	6.52	2.60	2.50
Indarama	7.37	6.86	1.19	56.05	38.84	1.44
Indarama	13.66	12.10	1.89	97.41	64.33	1.51
Indarama	13.14	10.05	2.02	96.16	54.86	1.75

Table A3.2.2: Chemical analysis of some of the biooxidation residues

Sample Location	wt % Fe	wt % As
Indarama	21.82	0.81
Indarama	12.30	0.92
Indarama	30.95	0.46
Indarama	31.47	1.12
Indarama	30.66	2.54
Indarama	34.10	10.12
Indarama	17.71	0.80
Riverlea	4.85	0.45
Riverlea	11.16	0.83
Riverlea	5.67	0.51
Akbakai	7.01	0.39
Akbakai	10.89	0.32
Akbakai	12.32	0.27
Inda/Str	13.93	0.91

Indara/Strat	13.36	1.88
Indara/Strat	21.34	0.50
Olympias	39.23	4.63
Olympias	34.43	0.89
Indarama	26.98	7.72
Indarama	27.86	13.83
Indarama	31.84	12.00

Table A3.2.3: EPA test results of some of the biooxidation residues. The concentrations are quoted in mg/L.

Location	Ca	Fe	As	S	Sb
Akbakai	1.69	0.60	1.65	46.00	0.70
Indarama	1.95	5.30	7.22	96.80	1.22
Indarama	1.93	0.85	6.65	62.10	3.93
Indarama	2.63	4.80	3.98	133.00	2.08
Indarama	1.77	3.00	45.90	50.00	3.93
Riverlea	0.92		2.73	42.00	0.76
Riverlea	0.91	0.13	5.72	55.80	0.75
Riverlea	1.25		5.03	31.10	0.72
Akbakai	1.79	0.83	1.50	52.90	0.63
Akbakai	2.12	0.63	1.73	47.90	0.62
Indarama	2.97	0.33	16.90	34.20	4.62
Olympias	1.49	0.25	13.60	36.70	3.95
Olympias	1.78	3.65	3.00	41.40	0.16
Inda/Stra	5.09	0.45	6.08	50.00	1.44
Inda/Stra	174.00	1.03	6.43	169.00	2.21
Olympias	0.98	5.43	0.53	77.60	0.58
Indarama	1.60	0.85	15.00	62.40	2.50
Indarama	1.55	2.58	8.12	70.50	1.93
Indarama	6.61	2.73	28.90	108.00	1.83
Indarama	2.06	4.95	24.40	127.00	0.66
Indarama	4.33	2.83	88.50	134.00	0.43

Table A3.2.4: Composition of the concentrates used in the different runs subjeted to the EPA TCLP tests.

Sample Origin	Run Number	Wt % As	Wt % Fe	Ratio FeS_2/FeAsS
Indarama	2	16.60	36.79	1.45
Riverlea	3	9.47	27.46	2.13
Akbakai	5	4.07	10.48	1.89
Olympias	6	7.96	38.84	4.09
Indara/Strat	7	12.48	31.47	1.76
Indara/Strat	8	10.88	33.11	2.27
Fairview	9	4.22	17.80	3.43

Indarama	10	17.28	26.55	0.78
Indara/Strat	11	12.48	31.47	1.76
Riverlea	12	9.47	27.46	2.13
Akbakai	13	13.09	30.39	1.56
Indarama	14	16.60	36.79	1.45
Indarama	15	16.60	36.79	1.45
Indarama	16	16.60	36.79	1.45
Indarama	17	16.60	36.79	1.45
Indarama	20	16.60	36.79	1.45
Indarama	21	16.60	36.79	1.45
Indarama	22	16.60	36.79	1.45
Indarama	26	16.60	36.79	1.45
Olympias	34	7.96	38.84	4.09
Riverlea	35	9.47	27.46	2.13